IAEA-TECDOC-1281

Natural circulation data and methods for advanced water cooled nuclear power plant designs

*Proceedings of a Technical Committee meeting
held in Vienna, 18–21 July 2000*

INTERNATIONAL ATOMIC ENERGY AGENCY

April 2002

NATURAL CIRCULATION DATA AND METHODS FOR
ADVANCED WATER COOLED NUCLEAR POWER PLANT DESIGNS
IAEA, VIENNA, 2002
IAEA-TECDOC-1281
ISSN 1011–4289

FOREWORD

An Advisory Group Meeting (AGM) on Development of a Strategic Plan for an International R&D Project on Innovative Nuclear Fuel Cycles and Power Plants was held in Vienna, 11–14 October 1999. The AGM recommended that the IAEA consider certain candidate projects in support of the development of innovative nuclear power technology, one of which was natural circulation systems.

As a result, a Technical Committee Meeting (TCM) on Natural Circulation Data and Methods for Innovative Nuclear Power Plant Design was held in Vienna from 18 to 21 July 2000 and organized according to the recommendations of the AGM. The objectives of the TCM were to assess the current base of experimental data and the applicability of current methodologies for computing natural convection phenomena in innovative reactor designs, and to develop perspectives on needed improvements in models and supporting experimental data.

This TECDOC provides the papers presented and summarizes the discussions. While the planned scope of the TCM included all types of reactor designs, the meeting participants and papers addressed only light and heavy water reactor designs. The papers and discussion addressed both evolutionary and innovative designs. The TECDOC title reflects the actual scope of the meeting and materials provided herein.

In addition to their participation in the TCM, N. Fil (Gidropress, Russian Federation), F. D'Auria (University of Pisa, Italy), E. Hicken (FZJ, Germany) and J. Vihavainen (LIC Technical Laboratory, Finland) contributed to the drafting of Sections 1 through 5 of this publication. The IAEA staff members responsible for this publication were J. Kendall, Yang-Eun Kim and J. Cleveland of the Division of Nuclear Power.

EDITORIAL NOTE

CONTENTS

1. INTRODUCTION

The complex set of physical phenomena that occur in a gravity environment when a geometrically distinct heat sink and heat source are connected by a fluid flow path can be identified as natural circulation (NC). No external sources of mechanical energy for the fluid motion are involved when NC is established. In a number of publications, including textbooks, the term natural convection is used as a synonym of NC. Within the present context, natural convection is used to identify the phenomena that occur when a heat source is put in contact with a fluid. Therefore, natural convection characterizes a heat transfer regime that constitutes a subset of NC phenomena.

This report provides the presented papers and summarizes the discussions at an IAEA Technical Committee Meeting (TCM) on Natural Circulation Data and Methods for Innovative Nuclear Power Plant Design. While the planned scope of the TCM involved all types of reactor designs (light water reactors, heavy water reactors, gas-cooled reactors and liquid metal-cooled reactors), the meeting participants and papers addressed only light water reactors (LWRs) and heavy water reactors (HWRs). Furthermore, the papers and discussion addressed both evolutionary and innovative water cooled reactors, as defined by the IAEA[1].

NC principles are of fundamental interest to the designers of nuclear power plant systems and components. Making reference to the existing water cooled reactors, the consideration of NC is brought to the design of the layout of the primary circuit. The core is located at a lower elevation with respect to the steam generators and the feed-water inlet location, in the cases of pressurized and boiling water reactors, respectively. In all of the adopted geometrical configurations, NC allows the removal of the decay heat produced by the core, should the forced circulation driven by centrifugal pumps become unavailable. Furthermore, NC is the working mode for the secondary side of most steam generators in existing pressurized heavy and light water reactors. It is essential as well for the core cooling in the unlikely event of loss of primary coolant.

Reactors based on natural circulation during normal operation (e.g. the Dodewaard Reactor in the Netherlands and the VK-50 in Russia) operated for an extended period of time. Most boiling water reactors can operate in the natural circulation mode for power levels below about 40 per cent of full power. Some newly developed designs are based on natural circulation core cooling for normal operation and on the use of the natural convection heat transfer for some safety systems. Reliance on natural circulation can result in simplified systems, reduced costs and — most importantly — a very high safety level.

The accomplishment of the objectives of achieving a high safety level and reducing the cost through the reliance on NC mechanisms, requires a thorough understanding of those mechanisms. Natural circulation systems are usually characterized by smaller driving forces with respect to the systems that use an external source of energy for the fluid motion. For instance, pressure drops caused by vertical bends and siphons in a given piping system, or heat losses to environment are a secondary design consideration when a pump is installed and drives the flow. On the contrary, a significant influence upon the overall system performance may be expected due to the same pressure drops and thermal power release to the environment when natural circulation produces the coolant flow. Therefore, the level of knowledge for the thermal-hydraulic phenomena for the specific geometric conditions and governing heat

---

[1] IAEA-TECDOC-936, Terms for Describing New, Advanced Nuclear Power Plants.

transfer conditions should be deeper when NC is involved. In addition, the lower driving forces for natural circulation systems might lead to quite large equipment for which the role of 3D phenomena is essentially increased.

Within nuclear technology the renewed interest in NC is a consequence of the above, in combination with the potential for cost savings from increased use of NC mechanisms in plant designs. Relevant experiments directed to the characterization of NC have been carried out in the past because of the importance of the related mechanisms for the safety of existing reactors. Similarly, thermal-hydraulic system codes have been qualified through the comparison of predicted results and experimental data. The quality of recorded experimental data and the precision level of the available system codes, or the expected uncertainty in these predictions, are generally evaluated as satisfactory for the needs of the current reactors. However, the exigencies posed by the more extensive use of the NC in the design of evolutionary and innovative water cooled reactors require a re-evaluation of the experimental data and of the code capabilities considering the new phenomena and conditions involved.

Recent activities completed under the IAEA umbrella, e.g. Refs [1–8], and by other institutions, such as the U.S. Nuclear Regulatory Commission (U.S. NRC) [9], the OECD/NEA/CSNI (Organization for Economic Cooperation and Development/Nuclear Energy Agency/Committee on the Safety of Nuclear Installations), Refs [10–13], and the EC (European Commission), Refs [14–16], show the importance of the subject and constitute the basis for future activities in the area of NC. Potential future international activities could be directed toward:

(a) identification of still unresolved issues from evolutionary and innovative water reactor designs, and

(b) enhancing the quality levels of the available computational tools and experimental databases in relation to design needs.

This report provides an overview of the current state of the art of natural circulation data and methods, and discusses potential benefits of an integrated future effort directed toward the achievement of the two aforementioned objectives. The main attention in this report is paid to the design basis accident phenomena; severe accident issues are considered briefly in their relation to the protection of the containment as the last safety barrier.

2. NATURAL CIRCULATION SYSTEMS IN NEW DESIGNS

2.1. THE ROLE OF NATURAL CIRCULATION SYSTEMS

The role of the natural circulation systems should be considered in the general context of implementation of passive safety systems[2] into new nuclear power plant designs. It may be noted that many systems and equipment proposed in future reactor concepts include natural circulation phenomena as the main mechanism that determines the passivity of the fulfilment of a designated function. Naturally driven systems have been used in the existing reactors both to remove the core heat under normal operation conditions including full power operation (like the Russian boiling water reactor VK-50 or the Dodewaard reactor in the Netherlands) and to fulfil some safety functions (like the passive part of the emergency core cooling system

---

[2] IAEA-TECDOC-626 : Safety Related Terms For Advanced Nuclear Plants.

in PWRs). So, there is a good technical basis and some operational experience to use passive systems in new reactor concepts.

With respect to plant safety, application of passive systems/components is intended to simplify the safety systems and to improve their reliability, to mitigate the effect of human errors and equipment failures, and to provide increased time to enable the operators to prevent or mitigate severe accidents. Natural circulation systems typically do not require or accommodate repair or maintenance work during power operation.Therefore, a reduced number of safety system trains may be needed to perform the designated safety function with the required reliability. An IAEA conference [1] included discussions on the safety of future plants, and noted that the use of passive safety systems is a desirable method of achieving simplification and increasing the reliability of the performance of essential safety functions, and should be used wherever appropriate.

However, natural circulation systems have their own advantages and drawbacks in comparison with forced flow systems, both in the areas of plant safety and plant economics. Passivity itself does not mean that a natural circulation system should be automatically considered as more reliable with regard to fulfilment of the designated safety function. Therefore a reasonable balance of traditional systems and new passive means is adopted in many future reactor concepts as a possible way to improve safety and public acceptability of nuclear power, and at the same time to keep nuclear power competitive with conventional power technologies. Many considerations govern this balance and define the final design decision, such as:

(a) Application of passive systems should reduce the number of components, and yield design simplification, so that the number and complexities of safety actions can be reduced;
(b) Passive means should be taken, to the extent possible, from similar ones having operational experience at power plants or elsewhere, so that the efforts needed to demonstrate the reliability and licensability are not too large;
(c) Passive systems actuation should be more reliable than for an active system providing the same function; otherwise the increase of the system reliability projected by implementation of the passive system may be lost;
(d) Passive systems should eliminate the need for short-term operator actions during accidents
(e) Passive systems should minimise dependence upon off-site power, moving parts, and control system actions for normal operation as well as during design basis and beyond design basis accidents;
(f) Passive systems should reduce the construction, operation and maintenance costs.

The main drawbacks of natural circulation systems include lower driving forces and less possibility to alter the course of an accident if something undesirable happens (i.e. less operational flexibility). In particular, in certain conditions where forceful or rapid actions are required, active systems may be more suitable to carry out certain safety functions. Also, load follow operation may be limited in the reactors based on natural circulation of the primary coolant. Therefore, in some new reactor designs originally designed for natural circulation, forced circulation flow (by pumps) has been introduced to allow for a better load follow capability and to increase the reactor rated power. Scaling for natural circulation systems is more difficult than for active systems. Therefore usage of experimental or operational data obtained for a system with a size that differs from that of the system being designed may not

be appropriate. Due to low driving forces, the operation of a natural circulation system may be adversely affected by small variations in thermal-hydraulic conditions. The lower driving forces might also lead to quite large equipment, and this factor may reduce the cost savings projected from elimination or downsizing of active components. Besides, larger components may cause additional difficulties in seismic qualification on some plant sites.

The design decisions with regard to balancing active/passive features may also depend upon the functions assigned to the given system. In particular, the system having an important role in the mitigation of severe accident consequences that is located in a potentially contaminated area (e.g. the part of the containment cooling system which is located inside the containment) could be designed to be as passive as reasonably achievable. This is because of the difficulty or even impossibility of access to such areas and because passive components may not require maintenance even during long-term operation.

All the above aspects are being taken into account by nuclear power plant designers, and as a result, both novel and more or less proven passive systems and features are proposed in many new designs [2]. Some designs have only added a few passive components to the traditional systems. Some other designs make use of the passive systems/components and natural circulation phenomena for power production in normal operation, or to fulfil a number of safety functions, intended to prevent severe accidents and mitigate their consequences.

2.2. REACTOR CONCEPTS BASED ON NATURAL CIRCULATION

In some designs, natural circulation in the primary circuit is being used as the core heat removal mechanism under normal operation conditions including full power operation. Generally, due to low driving forces of natural circulation this mechanism is being utilized for relatively small to medium size reactors. Some examples of the reactor concepts based on natural circulation of the primary coolant over the full range of the normal power operation are given below. Most of these concepts make use of passive systems also to ensure or to back up some safety functions.

HSBWR (Japan): The HSBWR [2] is a BWR design of up to of 600 MW(e). The HSBWR adopts natural circulation of primary coolant and passive safety systems to improve the economy, maintainability, and reliability by system simplification. In this reactor concept pumped re-circulation systems are eliminated in order to reduce the number of components driven by external force. A riser of 9 m height is installed above the core in order to increase the driving force for natural circulation. The 3.7 m length of the fuel assemblies, with an active length of 3.1 m, is determined by the objective of avoiding seismic resonance between the fuel bundles and the reactor building, independent of the conditions of the ground on which it is constructed. Elimination of the steam separators results in a reduced flow resistance in the primary circuit, thereby providing an increased natural circulation flow rate.

The power density of the reactor core is typically lower in a natural circulation reactor than in a forced circulation reactor, but the lower power density allows a longer continuous operation. The short heated length of the fuel and the low power density provide good thermal-hydraulic characteristics. With the 8×8 type fuel assembly selected, the power density is 34.2 kW/L; the number of fuel assemblies is 708, and the equivalent core diameter is 4.65 m. The uranium enrichment of the refuelling batch, at equilibrium, is 3.6%, and the average fuel burn-up is 39 GWd/t for operation cycles of 23 months.

SBWR (USA): The simplified boiling water reactor (SBWR) [2] is a 600 MW(e) design. It is based on natural circulation, with a nominal core power output of 2000 MW(th), and incorporates a number of innovative features to achieve plant simplifications. Among others, it includes introduction of passive safety systems, instead of or as supplement to the traditional active safety systems. The core configuration consists of 732 bundles — 648 interior bundles and 84 peripheral bundles. The core power density is 41.5 kW/L.

Reactivity control is maintained by movement of control rods and by burnable poisons in the fuel. The reactor pressure vessel (RPV) is a vertical, cylindrical pressure vessel, with a removable top head, and head flanges, seals and bolting, and with venturi-shaped flow restrictors in the steam outlet nozzles. The RPV is 6 m in diameter, with a wall thickness of about 158 mm with cladding, and 24.5 m tall from the inside of the bottom head to the inside of the top head. The RPV height permits natural circulation driving forces to produce sufficient core coolant flow by increasing the internal flow path length.

The large RPV volume provides a large amount of water above the core, which translates directly into a much longer period of time before core uncovery can occur as a result of loss of feed water flow or a loss-of-coolant-accident (LOCA). This gives an extended period of time during which automatic systems or plant operators can re-establish reactor inventory control using any other systems capable of injecting water into the reactor. The large RPV volume also reduces the reactor pressurization rate that develops when the reactor is suddenly isolated from the normal heat sink, which eventually leads to actuation of the safety-relief valves.

AHWR (India): The 235 MW(e) Indian Advanced Heavy Water Reactor (AHWR) [3] is a vertical, pressure tube type, boiling light water cooled, heavy water moderated reactor. The reactor core is designed for use of thorium-based fuel, and for achieving a slightly negative void coefficient of reactivity. The AHWR incorporates several passive safety systems. These include core heat removal through natural circulation, direct injection of emergency core coolant system (ECCS) water into the core, passive systems for containment cooling and isolation, gravity driven water pool (GDWP) to facilitate core decay heat removal and containment cooling for three days without invoking any active systems or operator action.

During normal reactor operation, the full reactor power is removed by natural circulation. The necessary flow rate is achieved by locating the steam drums at a suitable height above the centre of the core, taking the advantage of reactor building height. By eliminating nuclear grade primary circulating pumps, their prime movers, associated valves, instrumentation, power supply and control system, the plant is made simpler, less expensive, and easier to maintain as compared to options involving forced circulation in the primary coolant circuit. The above factors also lead to considerable enhancement of system safety and reliability since pump-failure related transients have beeneliminated by design.

CAREM (Argentina): CAREM [22,23] is an innovative 100 MW(e) PWR reactor design with an integrated self-pressurized primary system through which the coolant circulation is achieved by natural circulation. The CAREM design incorporates several passive safety systems. The entire primary system including the core, steam generators, primary coolant and steam dome are contained inside a single pressure vessel. The strong negative temperature coefficient of reactivity enhances the self-controlling features.. The reactor is practically self-controlled and need for control rod movement is minimized. In order to keep a strong negative temperature coefficient of reactivity during the whole operational cycle, it is necessary not to

utilize soluble boron for burnup compensation. Reactivity compensation for burnup is obtained with burnable poisons, i.e. gadolinium oxide dispersed in the uranium di-oxide fuel.

Water enters the core from the lower plenum. After being heated the coolant exits the core and flows up through the riser to the upper dome. In the upper part, water leaves the riser through lateral windows to the external region. Then it flows down through modular steam generators, decreasing its enthalpy by giving up heat to the water in the steam generator. Finally, the coolant exits the steam generators and flows down through the down-comer to the lower plenum, closing the circuit.

CAREM uses once-through straight tube steam generators. Twelve steam generators are arranged in an annular array inside the pressure vessel above the core. The primary side coolant flows through the inside of the tubes, and the secondary side water flows across the outside of the tubes. A shell and two tube plates form the barrier between primary and secondary circuits.

AST-500 (Russia): The 500 MW(th) reactor design is intended to generate low temperature heat for district heating and hot water supply to cities. AST-500 is a pressurized water reactor with integral layout of the primary components and natural circulation of the primary side coolant. Features of the AST-500 reactor include natural circulation of the coolant under reduced working parameters and specific features of the integral reactor, such as a built-in steam-gas pressurizer, in-reactor heat exchangers for emergency heat removal, and an external guard vessel.

V-500 SKDI (Russia): V-500 SKDI (500 MW(e)) [23] is a light water integral reactor design with natural circulation of the coolant in a vessel with a diameter less than 5 m. The core and the steam generators are contained within the steel pressure vessel. The core has 121 shroudless fuel assemblies having 18 control rod clusters.Thirty six fuel assemblies have burnable poison rods. The hot coolant moves from the core through the riser and upper shroud windows into the steam generators located in the downcomer. The coolant flows due to the difference in coolant densities in the downcomer and riser. The pressurizer is connected, by two pipelines, to the reactor pressure vessel and the water clean up system.

NHR-200 (China): NHR-200 [23] is a design for providing heat for district heating, industrial processes and seawater desalination. The reactor power is 200 MW(th). The reactor core is located at the bottom of the reactor pressure vessel (RPV). The system pressure is maintained by N_2 and steam. The reactor vessel is cylindrical. The RPV is 4.8 m in diameter, 14 m in height, and 197 tons in weight. The guard vessel consists of a cylindrical portion with a diameter of 5m and an upper cone portion with maximum 7 m in diameter. The guard vessel is 15.1 m in height and 233 tons in weight.

The core is cooled by natural circulation in the range from full power operation to residual heat removal. There is a long riser on the core outlet to enhance the natural circulation capacity. The height of the riser is about 6 m. Even in case of interruption of natural circulation in the primary circuit due to a LOCA the residual heat of the core can be transmitted by steam condensed at the uncovered tube surface of the primary heat exchanger.

2.3. NATURAL CIRCULATION SYSTEMS TO COPE WITH DESIGN BASIS ACCIDENTS

To cope with Design Basis Accidents (DBAs) means are provided to ensure the fulfilment of the basic safety functions, such as reactivity control (reactor trip) and fuel cooling. The systems based on natural phenomena are implemented in many new designs to fulfil these

safety functions, and natural circulation systems play an important role. Different approaches used in new reactor concepts can be summarised as follows.

As to the reactivity control, traditional gravity-driven (in PWR and PHWR) or gas-pressure driven (in BWR) control rods is the main system to ensure reactor scram in currently operating reactors and in the advanced concepts. Although very good reliability records exist for scram excitation, some new reactor concepts have implemented additional passive means to enhance the reactivity control function. For the WWER-1000/V-392 design, a special rapid boronated water supply system has been designed as a diverse system to the gravity-driven control rod insertion system. The concentrated boron solution is supplied to the reactor due to the pressure difference between discharge and suction of the main coolant pump (pump head) where the boron solution tank is joined. The operability of the system has been confirmed by extensive experimental investigation using a scaled model. A similar rapid emergency boration system is also implemented in the Sizewell PWR for diverse reactor shutdown. It consists of four tanks of boron solution (3 m^3 of 7000 ppm concentration of boron in each tank), connected to each cold leg. The inertia of the main coolant pumps is sufficient for the system to fulfil its function. All CANDU plants built in the last 20 years and new ones have a rapid gadolinium nitrate injection system that can shut the reactor down as quickly as the shutoff rod system. This injection system uses high-pressure helium to inject a gadolinium solution into the low-pressure moderator. Instrumentation separate from the shutoff rod system and other safety systems but with equal capability to the shutoff rod system is used to open quick-acting, fail-open valves between the helium gas and the gadolinium solution. As applied to the passive reactivity control, one should note the problem of the deboration possibility in the naturally circulated primary coolant. In some cases, this problem may lead to the consideration of specific reactivity initiated accidents difficult for quantitative analysis.

The safety function "fuel cooling during transients and accidents" is ensured by provision of sufficient coolant inventory, by coolant injection, by sufficient heat transfer, by circulation of the coolant, and by provision of an ultimate heat sink. Depending on the type of transient or accident, a subset of these functions or all of them may be required. Various passive systems/components are proposed for future reactor concepts to fulfil these functions. It is a feature of many new concepts that the water for replenishment of primary coolant inventory is entirely stored inside the containment. This ensures protection against external events and reduces the risk of loss of coolant accidents with containment bypass. Additional features implemented in some new designs to improve the replenishment of primary coolant inventory function include:

(a) Pressurizer relief via the relief tank to the water storage tank;
(b) Removal of heat from the primary circuit to the water storage tank via heat exchangers located in the water storage tank;
(c) Water storage tank combined with the containment sump;
(d) Water storage tank located at higher elevation than the reactor core for gravity-driven injection;
(e) Storage of a portion of water at high elevation under the full primary pressure for coolant injection at high pressure.

Most of the new concepts incorporate a combination of different passive and active means to ensure the function "coolant injection". Passive injection systems at high primary pressure are new in comparison to systems in operating reactors. AP-600 is an example of a design where this function is provided by core make-up tanks (CMT). Pneumatic isolation valves in the injection lines open automatically if one of the initiation setpoints (e.g. low primary pressure,

low pressurizer level) is reached. These valves are fail-safe since they will open even if A.C. power fails. As long as the reactor coolant system (RCS) is still filled with liquid, cold water from the CMT flows to the RCS by natural recirculation. After the coolant starts to boil, steam enters the CMT, the natural recirculation is terminated and injection to the RCS continues due to gravity . To assure continued injection by medium and low-pressure injection systems before the CMTs are empty, stepwise depressurization of the RCS is initiated if the liquid level in the CMT falls below defined setpoints.

Passive accumulator injection at medium primary pressure is applied in current pressurized water reactors as well as in advanced concepts. Improvements of efficiency have been suggested for the future reactors on the basis of experience, such as optimised initial pressure, water/gas ratio, and flow resistance in the injection line. Also, the absence of isolation valves in the injection lines is being considered in some new designs to increase the system reliability. The tendency in some advanced designs in comparison with the existing plants is to widen the primary pressure range for passive injection and to make it more controllable. The Westinghouse AP-600, the Russian WWER V-392 and V-407, the Mitsubishi APWR and the Indian AHWR designs could be mentioned as examples of this tendency. In particular, the Mitsubishi APWR design makes use of an advanced accumulator system to ensure the safety functions of core cooling. It has the function of both the accumulator tank and the low-pressure injection pump of conventional plants. So the low-pressure injection pumps are eliminated and the safety injection system configuration is simplified.

Passive low-pressure injection is foreseen in some new concepts to replace or to back up the traditional pump injection being used for the operating plants. To ensure passive injection, the traditional water storage tank can be installed at higher level than the reactor core or special low-pressure injection tanks at high elevation can be provided. Since the water is at containment atmosphere, injection by gravity can only take place after complete de-pressurization of the reactor coolant system. This is accomplished e.g. by the last step of the de-pressurization sequence in the AP-600 design or by the special de-pressurisation system in the WWER-640/V-407 design; this system starts passively when the primary pressure decreases below 6 bar.

The function "provision of sufficient heat transfer" in the advanced concepts is ensured in the same fashion as in currently operated reactors. This function is assured as long as sufficient water is supplied to the fuel rods. Sufficient water in the core is provided by the systems ensuring injection of the coolant as described above. Heat transport in reactor designs using mainly passive means is ensured during accidents by natural circulation between the core as heat source and heat sink (e.g. steam generators as in the Russian WWER-1000/V-392 design or heat exchangers in the water storage tank as in AP-600 design); the natural circulation may exist in single phase, two phase and boiler-condenser modes. Some advanced designs make use of relatively new natural circulation paths, e.g. natural circulation after LOCA between sump and core via the sump screen and broken pipe in AP-600 or between the core, the flooded pool around the reactor and the spent fuel pool via the depressurization pipes and further connection pipes in WWER-640/V-407 design. The Indian AHWR uses natural circulation driven core heat removal during normal operation and hot shut down, making the core heat removal capability immune to the station black-out event.

The function "ultimate heat sink" for accident conditions in the advanced concepts is mainly ensured either by the water stored in tanks (located inside or outside the containment) or by heat transfer directly to the surrounding atmosphere (via special heat exchanger or via

containment shell). In the first case, the heat sink may be limited in time, and human actions are required to restore it. For this type of the ultimate heat sink, the passive containment cooling water storage tank in the AP-600, which is needed especially for accidents in the design extension area, or the water tanks for passive containment cooling and for passive decay heat removal in WWER-640 /V-407 and AHWR designs are examples. An example of the unlimited heat sink is the use of air heat exchangers in WWER-1000/V-392 design located outside the containment. Another aspect of heat sinks that is sometimes made passive is the feed water to the boilers. In evolutionary CANDU designs, for example, there is gravity feed from an elevated tank into the boilers. High capacity valves can be opened in the steam system to depressurize the boilers and allow gravity flow for makeup.

The approaches described above result in the specific design decisions implemented in new reactor concepts, and some examples of these decisions are given below.

AC-600/1000 (China): The AC-600/1000 designs rely totally on passive safety systems to accomplish safety functions. The high natural circulation cooling capability due to the small flow resistance of the reactor coolant loops is very useful for reactor decay heat removal during accidents. The emergency residual heat removal system is used to remove decay heat from the reactor core following the event of station black out, main steam line break or loss of feed water. The steam generator secondary side, one emergency feed water tank and one emergency air cooler establish a natural circulation circuit. Air coolers are located in a chimney. The containment cooling system consists of the containment cooling water storage tank located at the top of the containment, and cooling sprayers. The system is used to remove decay heat from the inside to the outside of the containment during LOCA or main steam line break located inside the containment. First, the water in the tank on the top of the containment will be sprayed onto the surface of the steel shell of the containment by gravity, cooling the shell and resulting in reducing containment pressure and temperature. The tank capacity can meet the requirements of 72 hours for steel shell cooling after LOCA. After the tank empties, natural circulation flow of air through the annulus between the steel shell and the concert shell can remove the heat continuously.

WWER-640/V-407 (Russia): The Steam generator passive heat removal system is designed to remove the decay heat in the case of non-LOCA events and to support the emergency core cooling in the case of LOCA. The reactor coolant system and passive heat removal equipment layout provide heat removal from the core following reactor shutdown via the steam generator to the water tanks located outside the containment and further to the atmosphere by natural circulation. The water inventory in this tank is sufficient for the long-term heat removal (at least 24 hours) and can be replenished from an external source. The containment passive heat removal system of WWER-640 /V-407 reactor removes heat from the containment in the case of a LOCA. The steam from the containment atmosphere condenses on the internal steel wall of the double-containment being cooled from outside surface by the water stored in the tank. The system operates due to natural circulation and is capable of removing decay heat for 24-hour period following reactor trip.

WWER-1000/V-392 (Russia): This reactor incorporates an important passive system to remove core decay heat in case of station blackout (so called SPOT). The SPOT system consists of four groups of closed natural circulation circuits. In the ribbed tubular air-cooled heat exchanger (four heat exchangers for each circuit), steam extracted from the steam generator condenses, and the condensate flows by gravity to the steam generator boiler water volume. Under normal plant operation, the SPOT system is under standby. In the case of plant

blackout, the SPOT state changes to the operating condition. Natural circulation in the SPOT system is provided by the corresponding layout of the steam generator, heat exchanger and draught air duct.

SWR (Germany): The Siemens AG [now Framatome ANP] has been developing a 1000 MW(e) boiling water reactor, the SWR 1000. One of the main characteristics of this reactor is the replacing of the active safety systems in part with passive safety systems. In many of these passive systems, natural circulation is the essential mechanism. The emergency condenser system consists of four heat exchanger subsystems. It provides passive heat removal from the reactor pressure vessel to a large water inventory stored inside the containment. These condensers commence functioning on the basis of the drop in the RPV water level. If the water level inside the RPV drops, the primary steam enters the tube bundles, condenses and is returned by gravity to the reactor vessel. During the condensation process, the water in the condenser is heated and would start to boil, the resulting steam is discharged from the condenser to the atmosphere. In the event of failure of the active residual heat removal system, four containment-cooling condensers are designed to remove residual heat from the containment to the dryer separator storage pool located above the containment. They use natural circulation both on the primary and on the secondary sides.

AP-600 (USA): The AP-600 is a 600 MW(e), advanced nuclear power reactor developed by Westinghouse. The AP-600 uses passive safety systems to improve the safety, reliability and protect investment. These systems rely on natural forces such as gravity, compressed gas and natural circulation to make the system work. The passive core cooling system is designed to provide adequate core cooling for the design basis accidents. The system consists of two passive residual heat removal systems (PRHR) heat exchangers, two core makeup tanks (CMT), two accumulators, one in-containment refuelling water storage tank (IRWST), and two reactor coolant system (RCS) depressurization spargers. Among others, the system is designed to perform the emergency core decay heat removal, provide core decay heat removal during transients, accidents, or whenever the normal heat removal paths are unavailable. The emergency core decay heat removal system primarily consists of two heat exchangers located in the IRWST. Only one heat exchanger is required for decay heat removal. The PRHR heat exchangers are connected to the RCS through a common inlet line from one of the hot legs. The outlet line is connected to the associated steam generator cold leg plenum, reactor coolant pump suction. The two heat exchangers are elevated above the reactor coolant loops to induce natural circulation flow through the heat exchangers when the reactor coolant pumps are not available. The passive containment cooling system cools the containment following an accident such that the design pressure is not exceeded and the pressure is rapidly reduced. The steel containment provides the heat transfer area that removes heat from inside containment and rejects it to the atmosphere. Heat is removed from the containment vessel by continuous natural circulation flow of air. During an accident, the air-cooling is supplemented by evaporation of water. The water drains by gravity from a tank located at the top of the containment building onto the outer surface of the steel containment. The water tank is sized for 72 hours of operation, after which the tank is expected to be refilled.

CANDU (Canada): The exiting CANDU reactors as well as the proposed new designs rely to varying degrees on heat removal processes driven by natural circulation. Passive heat sinks based on NC, are utilized in current CANDU reactors, which are able to mitigate the accident progression for more than 24 hours. The passive heat sink consists of the heavy water moderator, which is contained within a low-pressure vessel, called a calandria. The calandria vessel is in turn contained in a calandria vault filled with light water, which provides a second

passive emergency heat sink. An elevated reserve water storage tank inside the containment has been included into advanced evolutionary CANDU designs. This tank provides the emergency make up water to the moderator and permits passive heat removal by thermo-siphoning from the shield tank. The amount of water is sufficient for more than 40 hours of passive decay heat removal.

A conceptual CANDU design employs a passive moderator heat rejection system. The idea is to allow the heavy water in the calandria to achieve a temperature near the boiling point and to allow this water to flash to steam as it rises in a pipe from the calandria to an elevated heat exchanger. Sub-cooled heavy water would then be returned to the calandria. The differences in density between the two-phase flow in the riser and the liquid in the down comer would provide the buoyancy force to drive the flow. An integrated passive design for heat rejection through containment was investigated by AECL. The system uses an annular jacket as an intermediate heat sink coupled to in — containment heat sources and a finned outer containment wall. The system employs a natural circulation loop to transfers the heat to the water jacket. Also heat from the water jacket is conducted through the steel wall to air following upward by natural convection.

2.4. NATURAL CIRCULATION SYSTEMS FOR SEVERE ACCIDENT MITIGATION

When considering natural circulation systems for severe accident mitigation, one should note that the implementation of the natural circulation systems intended to cope with DBAs can essentially reduce the probability of severe accidents.Furthermore, many systems designed to cope with DBAs can be also used for severe accident mitigation purposes. The level of knowledge of natural circulation phenomena under severe accident conditions (i.e. with a degraded core, reactor pressure vessel and other plant equipment) is much lower than the level of knowledge for conditions where the plant damage is within the design limits. Keeping in mind the above considerations, in new reactor concepts the priority in the implementation of the natural circulation systems is given to the systems intended to prevent severe accidents. As for the mitigation systems, their implementation is mainly aimed to ensure that the integrity of the containment is maintained, because it is the last barrier against the release of radioactivity to the environment.

Safety systems for the mitigation of severe accident are designed to meet level 4 of the defence in depth strategy against significant releases of radioactivity to the environment. From this point of view, the main goals of severe accident mitigation are as follows:

(a)   Prevention of H_2-detonation,
(b)   Energy removal from the containment,
(c)   Corium retention inside the RPV by in-vessel and/or ex-vessel cooling, or
(d)   Corium retention inside the containment by spreading and cooling of the molten core.

According to the above goals, systems for severe accident mitigation can be classified by function: H_2-control, heat removal and corium/debris retention. Below the passive systems for severe accident mitigation in new designs are discussed in the context of their use of natural circulation as a design principle.

2.4.1. Hydrogen distribution and control

During severe accident sequences hydrogen is produced, and together with steam it is released into the containment. For some accident sequences in BWRs this flow is injected into a water pool; in this case most fission products are contained in the water pool. If the steam/hydrogen flow is released into a dry containment the hydrogen is distributed in the containment and its distribution is influenced by hot and cold structures, condensation, sedimentation and the heat input by fission product decay. The knowledge about the hydrogen distribution is important for the assessment of whether hydrogen accumulates somewhere reaching concentrations with the potential for detonation processes.

Hydrogen detonation can be avoided either by pre-inertisation (as for all BWR containments), by post-inertisation or dilution or by reducing the amount of hydrogen using igniters or catalytic recombiners. It is evident that the mixing of different gas flows as well as the heat addition by recombiners and igniters create complex three-dimensional velocity and concentration fields in the containment volume; the effectiveness of recombiners and igniters are influenced by these fields.

2.4.2. Heat removal from containment

In many new concepts, the containment consists of an inner steel shell for providing leak tightness and an outer reinforced concrete shell for protection against external hazards. It should be noted that compared to the concrete wall the steel shell is more sensitive to the fast or local thermal loads which can be produced by direct containment heating or fission product deposition phenomena. For this containment configuration, the passive containment cooling system (PCCS) utilises the steel shell as a heat transfer surface. In case of an accident the inner containment shell will heat-up and drive an air flow, that enters the gap between inner and outer containment shell through windows at a lower position and leaves for the environment through filtered air outlet at the top. The air-flow will cool the steel shell by natural convection. Steam produced inside the containment due to accident conditions will be condensed on the inner surface of the steel shell and the condensate will collect in the containment sump.

In some PWRs (e.g. AP600, EP1000, AC600/1000), between the inner steel shell of the containment and the outer reinforced concrete shell an air baffle forms an annular wind duct. The PCCS utilises the steel shell as a heat transfer surface. In case of an accident the containment heats up and drives an upward air-flow in the gap between the steel shell and the air baffle [5]. Water from a water storage tank is sprayed onto the top of the steel shell. It flows down the outer surface as a water film counter-current to the air, intensifying heat removal by evaporation. Steam will be condensed on the inner surface of the steel shell with the condensate being collected in the containment sump. The capacity of the water storage tank is sufficient for 72 hours [6]. In the very unlikely case that the operator would not be able to replenish the water in the water tank when it empties after 72 h, the natural convection of air will be sufficient to prevent containment failure although the design pressure will be slightly exceeded [4]. A similar PCCS concept without the seismic issue of an elevated tank utilises an external ground level water storage tank with an insulated floating lid on the water level. The top of this tank is connected to an internal vessel with a low boiling point fluid. If the containment heats up this fluid starts to boil and pressurises the external tank by pushing the floating lid. Therefore the coolant is sprayed onto the top of the containment [7]. Another concept uses the lower part of the annulus between the steel and concrete shell as a water

pool. Air enters the gap trough windows above the water level and leaves it at the top. When the steel shell heats up, the temperature of water will increase up to boiling. The heat will be removed by single-phase convection of water and air or by evaporation, depending on the containment conditions [7].

In Russian WWER-640/V-407 concept [8], at the outer surface of the containment steel shell, rectangular pockets are arranged in rows and columns. The pockets of each column are inter-connected by vertical lines. A NC flow of cooling water from an external pool near the roof will be established. Steam is condensed at the cooled parts of the inner surface of the steel shell. The condensate is collected in the sump to allow for post accident recirculation.

A passive containment cooler (PCC) which is used in some designs primarily for severe accident prevention purposes will also mitigate severe accident consequences as it is foreseen in the design of the ESBWR, and some advanced PWR and CANDU designs. The PCC is a condenser immersed in a special PCC pool above the containment, using the design principles of an isolation condenser. It consists of a tube bundle connecting inlet (top) and outlet (bottom) collectors. The steam-gas mixture from the containment enters the inlet collector of the PCC and will be condensed inside the tubes. The condensate drains towards the RPV and the wet well [9].

In a PCC system for an advanced heavy water reactor design the condensate is collected in a water storage tank for gravity driven injection, and non-condensables are vented to a suppression pool [10]. A PCC proposed for application in a PWR (e.g. the CP-1300) utilises an external pool in a high elevation as a heat sink. The steam-H_2 mixture passes H_2-ignitors before entering the heat exchanger. The condensate is collected in the IRWST and/or used for passive containment spray [7].

In some designs (e.g. some BWRs and PWRs with double concrete containment) a building condenser (BC) is used for passive containment cooling. A BC consists of an internal (inside containment) heat exchanger (HX) in combination with an external (outside containment) pool containing the cooling water. The HX is composed of a number of finned condenser tubes between an inlet- and an outlet collector. It is placed at an upper position inside the containment. The HX tubes are slightly inclined. Thus the outlet is somewhat higher than the inlet. The collectors are connected with the external pool (penetrations). The outlet line ends at a higher elevation in the pool than the inlet line. Cooling water will flow by natural circulation from the pool through the BC back to the pool. The condensate drops down from the outer surface of the HX to a core flooding pool (BWR) or to the containment sump (PWR). A skirt is used in PWR design to separate the condensate from non-condensable gases. As a kind of BC, the modular PCCS [11] can be considered for PWRs with double concrete containment. Modular PCCS uses an internal HX with a skirt (similar to BC) connected with a pool in the gap between the containment shells. Before the cooling water enters the pool it passes through an external HX where heat is transferred to an air-flow. The air-flow will enter the gap through outer concrete shell windows, pass the HX, move over the water surface in the pool and leave the building through a chimney. Condensation of steam and separation of non-condensables functions as in a BC system.

Passive containment cooling can also be ensured by internal plate condensers (PCs) that are fitted to the containment wall and connected with an external heat sink. One example for a PC utilises cooling elements made from ductile cast iron, containing fins at the side facing the containment atmosphere. These fins can absorb loads from fragments impact without any

effects on the cooling system. The cooling water flows through steel pipes in bores along the fins. Natural circulation is established by an external draught cooling tower. PCs were found to be a valuable passive energy sink particularly under convective heat transfer conditions, i.e. beyond its design conditions [12].

Containment spray systems are widely used in current reactor designs as well as in future concepts to reduce the concentration of fission products (e.g. for iodine precipitation and aerosol wash out). Containment spray systems also contribute to containment pressure and temperature reduction. Although containment spray systems in most cases utilise pumps (active), at the secondary side of the cooler natural circulation driven systems can be used. Nevertheless, there are completely passive concepts with a spray water supply from elevated [7] or pressurised [4] tanks, that can contain special chemicals e.g. for iodine precipitation. Another passive concept uses the condensate of a PCC system to feed the spray [7]. An alternative passive system to drive a spray mass flow uses an ejector-condenser (E-C) system [13]. Its principle is based on the dynamic form of natural convection utilising inertia forces instead of gravity for fluid circulation. Steam speeds up to a high velocity in a Laval nozzle. Then it mixes in a mixing chamber with cold water that takes off its mass, heat and kinetic energy. The resulting two-phase mixture gets a supersonic flow, the kinetic energy of which turns into potential form in a diffuser. Thus the outlet pressure can exceed essentially the inlet steam and water pressure. In containment spray application water is taken from the sump, cooled by an external cooler (e.g. draught cooling tower) and fed by the E-C to the spray nozzles. The driving steam for the E-C is taken from a heat exchanger that evaporates part of the supplied water mass flow (bypass) by the heat of the containment atmosphere [14]. For start of the system an external start-up tank is necessary.

2.4.3. In-vessel corium retention

In most innovative reactor designs long-term retention of a totally molten core inside the RPV is foreseen by ex-vessel cooling, provided by flooding the reactor cavity from the outside [16]. In several concepts (e.g. AP600, WWER-640) the emergency water pool is used for this purpose. The emergency pool is a containment sump that covers the RPV and the lower part of the RCS. After depletion of the emergency water sources the level in the pool exceeds the elevation of the main coolant lines, thus allowing for a post accident recirculation through the vessel in a natural circulation mode.

In the SWR-1000 the reactor cavity is flooded from the core flooding pool when the water inventory of the RPV drops to 40% [15]. The water enters the space between the vessel wall and insulation through gaps at the control rod drive penetrations and heats up to the saturation state at the vessel wall. The steam leaves this gap through windows in the insulation and will be condensed at the BC. The condensate will refill the core flooding pool closing the NC loop. Retention of the core melt within the RPV means that there can be no steam explosion in the containment or corium/concrete reaction [17]. In some designs the reactor cavity is flooded via special gravity driven systems. Other concepts utilises accumulators with gas under pressure. Passive reactor cavity flooding for core retention by ex-vessel cooling is also adopted in integral reactor design (e.g. ABV-6 [18]).

In-vessel core retention systems (IVCRS) based on in-vessel cooling of the molten core materials can prevent the RPV from failure by melt-through utilising in-vessel flooding of the molten core materials [19]. Direct contact between corium and steel must be avoided and a cooling capability must be provided. TMI-2 experience showed, that a small gap between the

corium (crust) and the vessel can be sufficient for corium cooling by evaporation of water. An IVCRS for in-vessel cooling can consist of a structure artificially providing such gap (in-vessel core catcher), in combination with a special gravity driven corium flooding system. As an example for an in-vessel core catcher a steel shell with some distance from the inner surface of the lower plenum is proposed. For heat removal a mass flow rate in the order of 10 kg/s is sufficient. Alternatively, IVCRS are proposed using sacrificial material having a large heat capacity inside the lower plenum.

2.4.4. Ex-vessel corium cooling

When the integrity of the RPV is lost by core melt-through the corium has to be collected in a core catcher inside the reactor cavity where it must be cooled for the long term to prevent basemat melt-through. A typical example of this concept is the EPR design [20] where the core catcher is based on a large spreading area with provisions to avoid corium/concrete reaction and to achieve long term cooling of the molten core materials. One of the main features of this spreading concept is that, after the failure of the RPV, no immediate discharge of the corium onto the spreading area should occur. One reason for this delay is to collect the corium. The reactor cavity has to be designed to withstand the thermal and mechanical loads from the RPV failure. Therefore it has to be dry to prevent a steam explosion. Thus it should contain sufficient sacrificial material to decrease the temperature of the corium and ensure its spreadability at lower temperatures. The sacrificial material shall oxidize the remaining Zr without release of non-condensable gases (or at least with very limited amount) and bind non-volatile fission products. This delayed corium discharge will be achieved in a passive way by melt-through of a gate between the reactor cavity and the spreading area. After spreading, the corium is cooled from below by special cooling elements (similar to that used as plate condensers described above) embedded in concrete. This basemat cooling is achieved first by passive and later on by active measures. During the grace period (within 12 h after beginning of the severe accident) the spread corium is flooded from the top due to the melting of special plug-in fuses in the connection lines to the IRWST. The water evaporates at the corium surface and the condensate flows back to the IRWST. By spraying from the dome, fission products in the containment atmosphere are partly washed out.

An optional cooling concept for the corium in a spreading area utilises a spreading compartment separated by a concrete structure in a lower (spreading area) and an upper cavity [21]. Both cavities are connected by vertical channels (a riser and a downcomer). This system is flooded with the water level approximately in the middle between top and bottom of the upper cavity. Condensers at the top of the upper cavity an heat exchangers submerged in the water at the bottom of the upper cavity and in the downcomer drive a single phase NC flow for corium cooling. The cooling water flow is driven by pumps.

2.5. NEEDS FOR ANALYTICAL AND EXPERIMENTAL WORK

Today there is a consensus that the current system thermal-hydraulic computer codes are not sufficiently validated for some conditions and for some phenomena relevant to natural circulation (low pressure, low driving heads, effect of non-condensables, boron transport at low velocities, etc.). It is important to have assurance that the natural circulation systems are effective during all sequences in which they are required to function, and to define the needs for computer codes capable of taking into account all the important phenomena. Extensive work is needed to develop such codes and high quality experimental data are necessary to

validate them. Therefore, separate effect and integral tests may be required both for additional validation of existing and/or development of new computer codes. However the targets for the computer codes accuracy should be clearly defined before asking for or designing new experiments to be sure that the financial resources required for the experiments are spent effectively.

In many cases, sufficient operating experience for the natural circulation systems/components under real plant conditions does not exist. Therefore, additional research and development works including large-scale tests for the direct substantiation of the operability of a new system may be needed individually for each advanced water cooled reactor concept. In particular, even the evolutionary plant designs may require confirmatory testing of some components and systems prior to commercial deployment.

Many experiments have been performed up to now with natural circulation systems/components used in new reactor concepts, and many of them have displayed a number of phenomena that are not adequately predicted by the existing computer codes. For example, it was found that gas stratification in the containment can significantly affect the efficiency of building condenser when the cooled H_2-layer at the top displaces the steam. In advanced BWRs (e.g. the SWR-1000), vent pipes are therefore used connecting a position above the building condenser with the wet well. If heat transfer in the building condenser deteriorates because of steam shortage, the pressure in the containment increases and forces self-controlled venting of H_2/steam mixture to the wet well [15].

The functional reliability of a natural circulation system depends essentially upon the way the natural physical phenomena operate in a particular system and the long-term effect of the environment on the system performance. It requires the identification and quantification of the uncertainties in the interaction between the phenomena, the immediate surroundings and the natural circulation system itself. In this respect, collection of existing and generation of new experimental data would provide information on influences on the functional reliability of the natural circulation systems.

Keeping in mind the above considerations, extensive analytical and experimental works are still needed as applied to new passive systems/components. The contents of these works and the relevant capabilities are discussed in Sections 3 and 4 of this report. The sharing of the relevant results obtained earlier and coordination of the further works on the international level would increase the value of their results and optimize the required manpower and financial resources.

3. NATURAL CIRCULATION MODELLING

3.1. INTRODUCTION

The prediction of nuclear reactor thermal-hydraulic behaviour under operational and accidental conditions can potentially be made by

(a) The analysis of the thermal-hydraulic behaviour in smaller scale facilities and extrapolation to real plants, or
(b) The application of computer codes simulating component or system behaviour to plant situations.

The development of nuclear reactor designs has shown a change from small scale experiments in the early days of nuclear reactor development to the application of qualified versions of large computer codes nowadays supported by operational data from real plants. It is generally understood that the assessment under high accidental loads, e.g. in case of loss-of-coolant accidents or even for core melt sequences can only be based on code calculations. Thus the confidence in the code predictions is highly important. It has to be recognized that the requirements on the quality of new experimental data and of code calculations have increased during recent years; this implies the use of actual geometries, materials and thermal-hydraulic boundary conditions- if possible- as well as validation, documentation and uncertainty analysis.

3.2. MODELLING OF IN-VESSEL PHENOMENA

3.2.1. Single phase flow

In Section 2 several nuclear reactor designs as well as natural circulation applications have been described. The single phase natural circulation flow is driven by a gravity head induced by coolant density differences; the mass flow is established according to the balance between driving head and flow resistance losses. Because the (one component) density is a function of the temperature there is a functional interaction between heat exchange and natural circulation flow.

In general, the determination of the main parameters, e.g. average velocities, pressure drops, heat transfer and 1-D temperature fields for flow inside pipes or around structures, is based on established engineering practise. These parameters can be calculated with industrial codes as well as with thermal hydraulic codes used for nuclear reactor system behaviour.

Some uncertainties exist if two natural circulation flows with different densities caused by different temperatures are mixed. Then diffusion processes, turbulences and other mixing processes become important. Specific experiments would be capable to reduce the uncertainties; in some cases related experiments are necessary for a design.

If 2-D or 3-D flow fields can establish, the use of capable codes isnecessary; the codes listed in Section 3.2.2.2 can be used for calculations of this type.

Mixing processes and 3-D natural convection flow is important for deboration accidents for PWRs. For BWRs similar complicated flow fields exist for sequences with boron injection. For these processes experiments with detailed instrumentation are underway; the data can be used also for code validation.

The capability to calculate single phase natural convection flows with high confidence does allow the optimisation of systems and components, e.g. a decrease in flow resistances and an appropriate arrangement of heat sources and heat sinks.

3.2.2. Two-phase thermal-hydraulics and heat transfer

In general, thermal hydraulic modelling of nuclear reactor systems is based on the one-dimensional approach. Thermal hydraulic modelling of the steady state, transient and stability behaviour of two-phase natural circulation systems is no exception to this general approach. System codes have reached a highly developed modelling status and a wide acceptance. They

can reproduce accurately enough most of the existing safety related steady state and transient experiments, so far as the dominant physical mechanisms are known, as adequate models are included in the codes, and so far as the dominant phenomena are also understood by the code users. Thus, these codes are an excellent tool to analyse in a parametric way the dynamics and interrelation of a larger number of components in complex systems with different physics involved. However, the use of multi-dimensional modelling of two-phase natural convection in large vessels (including the calandria vessel of pressure tube type heavy water reactors), sumps or plenums of nuclear reactors is essential as the flow in these cases are multi-dimensional in nature.

Some of the most commonly adopted thermal hydraulic models applicable for the 1-D and multi-dimensional analyses are briefly described below:

3.2.2.1.   *Models for 1-D thermalhydraulic analysis*

(a) Homogeneous equilibrium model:

This is the simplest model for analysing the thermal hydraulic phenomena in a two-phase system. This considers one conservation equation each for the mass, energy and momentum of the mixture. Hence, it assumes complete thermal and mechanical equilibrium between the phases. This model is also referred to as Equal Velocity and Equal Temperature (EVET) model. Here, the mixture is considered to behave as a single fluid. An equation of state takes into account the variation of fluid properties. To take into account the differences in velocity between the phases, empirical slip models are used. The success of the model depends on the accuracy of the empirical relationships used in the code for the wall friction and wall heat transfer. Use of computer codes based on the homogeneous equilibrium model for accident and safety analysis of nuclear reactor systems is perhaps becoming a thing of the past. However, in the earlier design stages, codes based on this model are still extensively used. Further, most analyses to generate the stability behaviour (basically codes used to generate stability maps) of natural circulation systems are based on the homogeneous equilibrium model.

(b) Partial non-equilibrium models:

These models consider either the thermodynamic or mechanical non-equilibrium between the phases. The number of conservation equations in this case are either four or five. One of the most popular models which considers the mechanical non-equilibrium is the drift flux model. If thermal non-equilibrium between the phases is considered, constitutive laws for interfacial area and evaporation/condensation at the interface must be included. In this case, the number of conservation equations is five, and if thermodynamic equilibrium is assumed the number of equations can be four. Well-assessed models for drift velocity and distribution parameter depending on the flow regimes are required for this model in addition to the heat transfer and pressure drop relationships. The main advantage of the drift flux model is that it simplifies the numerical computation of the momentum equation in comparison to the multi-fluid models. Computer codes based on the four or five equation models are still used for safety and accident analyses in many countries. These models are also found to be useful in the analysis of the stability behaviour of BWRs belonging to both forced and natural circulation type.

(c) Two-fluid models:

The two-fluid models take into account the thermodynamic and mechanical non-equilibrium between the liquid and vapour phases. In this case, the mass, energy and momentum balance equations are written separately for both the phases. The six conservation equations in the two-fluid model represent the propagation of phasic void, velocity, enthalpy and pressure disturbances. For closure, the conservation equations require constitutive equations for the interfacial and wall transfer terms. The most difficult task is the modelling of these constitutive relationships. In spite of several years of research, the interfacial constitutive laws are not yet well established. A classical approach is to define them based on flow regime maps used for identifying the flow patterns (bubbly, slug, churn, annular, etc.). The interfacial transfer relationships (mass, momentum and energy) can be calculated based on the flow pattern dependent relationships, which are selected by suitable flow pattern transition criteria. Most of the large system codes used for safety and accident analysis, for example RELAP5, CATHARE, ATHLET, etc. adopt the one-dimensional two-fluid model. The two-fluid model is not yet commonly used for the stability analysis of nuclear reactor systems.

3.2.2.2.   *Modelling of multi-dimensional thermalhydraulics*

The increasing need for more accuracy of the codes and more detailed descriptions of new cooling concepts leads to a tendency to use at least for local detailed analyses more and more 3D and time-dependent computational fluid dynamic (CFD) codes. There are several motivations for using CFD codes in the nuclear field: Some problems can only be treated in 2D or 3D, like the flow-regime determination, thermal stratification, phase separation, and phase distributions in large pools. CFD codes are required if dynamical 2D or 3D phenomena have to be investigated, like the oscillations of velocities, pressures, temperatures, or phase distributions. The relevance of such investigations may come e.g. from ensuring safe heat transfer from all sub-assemblies under natural convection, from the thermal striping induced thermal fatigue, or flow instabilities due to geysering or sloshing, and from the phase and boron distribution dynamics coupled to neutronics.

Finally CFD codes have to be used for scaling up detailed results from model experiments to full-scale reactor conditions. They are also more and more used even for designing experiments and their instrumentation arrangement. They can also reliably be used to study in a more qualitative manner the relevance of certain phenomena in flow and heat transfer problems, so far as the governing physics is included in the equations or in the numerical modelling. Thus, they are also used to determine the dominant physical phenomena of nuclear flow problems, so that finally a reliable efficient numerical model configuration (input) can be formulated for a system code.

Most CFD codes for two-phase or multi-phase multi-component flows are based on the multi-field approach, assuming that all fluids and phases are defined everywhere in the flow field; this means, the fluids are interpenetrating. The spatial distributions of the different fluids or phases are determined by their relative local volume fractions. As a consequence of this method, one has not only a tremendous increase of the number of equations to be solved, but there are also no explicit phase boundaries existing. This kind of modelling is the basis for the typical working tools available. As such flows are physically and topologically complex, such codes give a valuable support to understand in more detail the macroscopic physical phenomena occurring in multi-phase flows.

The physical models in such codes, e.g. to model interfacial phenomena, are rather simple. Therefore, a quantitative use of such CFD codes for two-phase flows is currently limited to mainly homogeneous flows. Modelling improvements are related to bubble or particle diameters which have to be specified. New developments are going to include multi-group concepts of bubble diameter classes or to develop interfacial area concentration equation models which allow up to now for simple flow regimes to calculate the dynamics of the surface of the interface, which is an important parameter in determining momentum, heat, and mass transfer between the phases. This could also help to improve the modelling of bubble coalescence and fragmentation. For other flow regimes than bubbly or droplet flows, the modelling of interfacial phenomena needs serious improvements.

In going from 1D discretisation to 2D or 3D, one has to use turbulence models when turbulent flows have to be investigated. Some of the two- or multi-phase codes have turbulence models for two-phase flows, but our current knowledge and experimental data base on turbulence is very weak: we have only a few turbulence data for the liquid phase in bubbly flow. This basis is not sufficient to adapt, calibrate, and validate these models. Therefore, none of the existing models can reproduce all those data. For other flow regimes, data as well as models are missing; problematic flow regimes will be bubbly, churn, slug, and droplet flows. The turbulence in non-adiabatic flows is characterized by a rapid change of bubble diameters which will influence the turbulence characteristics. Another related problem occurs in the missing wall functions and in the boundary conditions for the interface phenomena at free surfaces. Thus, the turbulence modelling in two-phase flows can only be accepted as a first step. The models can be used strictly only in an interpolative manner, this means in a parameter range, in which extensive validation was done before. R&D is necessary to improve the models and to extend them for all flow regimes, so that more reliable prediction capabilities can be achieved.

Despite these model deficiencies such codes were rather successful, because many multi-phase problems are governed by large-scale interfacial phenomena. Therefore, most development in the past was based on developing adequate numerical methods to solve the set of equations of multi-field models. The challenge here comes from the weak compressibility of the fluids or phases engaged and from the strong density variations from liquids to gases across interfaces. Therefore, the development of more efficient and more robust solution schemes and solvers is always a target for further improvements.

For such cases, in which separated phases have to be considered, special numerical tools were developed to keep the interface sharp, like interface capturing, interface tracking, or some approximate numerical methods like surface sharpening. In case of dispersed flows special highly accurate numerical schemes would be required to avoid or at least minimize numerical diffusion, but most codes use standard lower order schemes; thus one still has to live with more or less strong numerical diffusion.

In the past, most codes for nuclear applications with multi-phase flows were developed mainly in the large national research centres or in the industry, like AFDM (LANL/FZK), ATHLET (GRS), CATHARE (CEA), COBRA-TF (Pacific NW Lab.), ESTET-ASTRID (EDF), IVA (Siemens), MATTINA (FZK), MC-3D (CEA), RELAP5-3D (INEEL,DOE), ERHRAC (NPIC), TRAC (SNL,USNRC)… They have the advantage that the required nuclear specific modelling is included, and the models and numerics were selected according to the special requirements of nuclear applications. Now, powerful, and comfortable commercial CFD codes are becoming available, which are increasingly suitable for nuclear applications, like CFX-4,

COMET, FIDAP, FLOW-3D, FLUENT, PHOENICS, and others. There are major differences between the principal modelling capabilities available in the commercial codes. None of those has all the modelling required for certain flow phenomena in innovative reactor systems; thus it has to be decided from case to case which code should be used. This brings some concerns regarding the certification effort when one is progressing towards a licensing procedure of a reactor.

With increasing requirements on accuracy and details of codes, also requirements regarding the accuracy and details to be provided by experiments are growing. Whereas for design purposes and for system code improvement and validation mainly realistic large scale experiments are of interest, for the development and validation of CFD codes for two-phase flows one needs primarily single effect experiments with very detailed instrumentation, preferably providing not only local data, but also field data, like PIV and tomography. Topics should be the interfacial phenomena and turbulence near bubbles with rapid diameter change, near free surfaces, and near walls with boiling, the bubble formation, coalescence and fragmentation, data on the interfacial area, and the turbulence in the continuous phases; similar investigations are also needed for all other flow regimes, and the flow regime transitions. Nevertheless, some large scale more complex experiments with a detailed instrumentation are also required to validate the correct interrelation between the different models engaged in the CFD codes.

3.2.2.3. Modelling of heat transfer in two-phase flow

In two-phase flow, local convective heat transfer coefficients are evaluated from the channel local thermal hydraulic conditions and the heater rod surface temperature. In theory all the main two-phase flow patterns such as bubble flow, slug flow, churn flow and annular flow are likely to exhibit different heat transfer characteristics. It is generally recognized that more accurate prediction of flow boiling can be obtained by adopting a flow pattern specific method for each individual flow regime. However, practically all of the existing correlations correlate flow boiling data using a single equation covering all the different flow patterns. General boiling curve is used to define the wall heat transfer regimes (convective, pool boiling, flow boiling, film boiling, etc.) and the related convective heat transfer coefficient. In addition, distinction must be made for condensation and evaporation. Further, well-established models for the critical heat flux (CHF) are required for the calculation of pre-CHF and post-CHF wall heat transfer.

3.2.2.4. Modelling of neutron kinetics

Normally, the equations for neutron kinetics are obtained from the general space and time dependent multi-group diffusion equations for a finite reactor of non-uniform properties. The 3-D neutron kinetic calculations are often made with fast and thermal energy groups and six groups of delayed neutrons. To reduce the sophistication, a modified one group diffusion equation can be considered for fast calculations. In this, only the dynamics of the thermal energy group is simulated in detail.

For simplicity of calculations, most of the large system codes consider the point kinetics model assuming the overall buckling to be almost constant during the transient. The parameters used in these equations such as delayed neutron fraction, prompt neutron life time, delayed neutron precursor concentration, etc. are defined taking into account some phenomena formally neglected during the derivation of the point kinetics equation. An improvement to the

point kinetics model is reflected in the one-dimensional kinetics equation that is also adopted in BWR calculations. In this, the radial buckling is assumed not to change during the transients. In point kinetics, reactivity coefficients for the void and Doppler effect are provided as inputs for the whole core. However, 1D and 3D neutron kinetics models facilitate direct evaluation of these feed back effects.

3.2.2.5. *Modelling of two-phase natural circulation instabilities*

From the modelling point of view, two types of instabilities are important. These are the static and dynamic instability. Static instability can be fully described by the steady state governing equations. Examples of this type of instability are Ledinegg (flow excursion), flow pattern transition instability, flashing instability, etc. For the dynamic instability, the feedback effects are important and hence it requires the solution of the time dependent conservation equations of mass, momentum and energy. Typical example is the density wave oscillations observed in two-phase systems. Often, thermalhydraulic systems exhibit compound instability that is usually a combination of two mechanisms. Here, the instability may begin with one of the known mechanism for static instability that may trigger some secondary mechanisms resulting in an oscillatory behaviour. Typical examples are parallel channel instability and coupled neutronic-thermalhydraulic instability of BWRs.

In generally, a two-phase natural circulation system can be designed to avoid all the different types of instability discussed above. This is done by carrying out a stability analysis, which is usually phenomena-specific and therefore cannot be described in detail in a brief note as the present one. However, the objectives of most stability analyses can be listed as:

(a) To generate stability maps which delineate the stable and unstable zones of operation;
(b) To specify adequate stability margin for design purposes; and
(c) To predict the nature of the unstable oscillatory behaviour of flow, power and temperature (in time domain) if the system passes through an unstable operating zone during power/pressure raising.

Most static instability analyses are carried out with the prime objective of generating a stability map. For the dynamic analysis, however, all the three objectives become important. Both the linear and nonlinear methods are used for the analysis of this type of instability. Mathematically, the dynamic behaviour of any system can be considered to be linear for small perturbations around the steady state operating condition. An analytical solution is sought for the perturbed equations to obtain the characteristic equation for the stability of the system. The characteristic equation is solved numerically to generate the stability map (locus of all neutrally stable points) of the system. The computer codes based on the linear stability method (e.g. RAMONA, NUFREQ, etc.) are very useful to predict the stability maps without consuming much computer time. However, it is beyond its capability to predict the non-linear effects that come into play after the neutral threshold (to achieve the third objective). Hence, direct numerical solution of the non-linear governing equations is carried out using finite difference methods. An additional objective of the non-linear computer codes is to provide an understanding of the basic physical mechanisms involved in BWR behaviour beyond neutral stability. In principle, system codes like RELAP5, ATHLET, CATHARE, etc. can be used for this purpose, although this is not the current practice (generally). If the system codes are used, this will require the use of qualified fine nodalisation as those used for the normal transient analysis (normally a coarse nodalisation) may not even predict the existence of instability (as

the numerical solution technique adopted in these codes are very robust which introduce numerical damping through artificial/numerical diffusion).

For simulating coupled neutronic-thermalhydraulic instability, usually a point kinetics model is used in addition to a fuel heat transfer model (which basically solves the conduction equation in the fuel, fuel-clad gap and clad to obtain the feedback effects of fuel). Point kinetics equations are first order ordinary differential equations that can be easily integrated by using a conventional numerical technique. However, the problem is the introduction of feedback constants in them, which are spatially averaged over the whole core. So uncertainty is therefore introduced at this level in addition to the inaccuracy in neglecting the changes in core power distribution. Similarly, the way in which the neutronics and the thermal hydraulics interact during the calculation has an important effect on the capability to simulate multi-dimensional core dynamics. Grouping of core channels in thermal hydraulic regions having similar geometric and operating parameters can have strong influence on the out-of-phase mode oscillations.

3.2.2.6. *Influence of non-condensable gasses*

Condensation is defined as the removal of heat from a system in such a manner that vapour is converted into liquid. This may happen when vapour is cooled sufficiently below the saturation temperature to induce the nucleation of vapour. This mode of heat transfer is often used in engineering because of possible high heat transfer coefficients. However, condensation heat transfer is degraded when non-condensable gases present in the condensing vapour. The presence of even a small amount of non-condensable gas in the condensing vapour has a profound influence on the resistance to heat transfer in the region of the liquid-vapour interface. The non-condensable gas is carried with the vapour towards the interface where it accumulates. The partial pressure of gas at the interface increases above that in the bulk of the mixture, producing a driving force for gas diffusion away from the surface. This motion is exactly counterbalanced by the motion of the gas-gas mixture towards the surface. Since the total pressure remains constant the partial pressure of gas at the interface is lower than that in the bulk mixture providing the driving force for gas diffusion towards the interface [1].

In-tube condensation of steam-air mixture is important for the passive thermal safety features of new advanced designs and therefore is subjected to experimental investigations at several research institutes. In addition to the studies of the University of California, Berkeley [2] and Massachusetts Institute of Technology [3], some detailed information and previous results of the experimental research being carried out at Middle East Technical University, Mechanical Engineering Department [4].

When the pure steam experiments are considered as the reference for comparison, a first indicator of the effect of air is a remarkable decrease in centreline and inner wall temperatures. Comparisons show that difference between saturation temperature, corresponding to the pure gas case, and measured centreline temperatures varies between 10 K and 50 K, depending on inlet air mass fraction. In other words, the temperature difference increases considerably as air mass fraction increases. It is found that there is a drastic decrease in the performance of the heat exchanger as the inlet air mass fraction increases. The inhibiting effect of air on condensation manifests itself as reduction in heat transfer coefficient. However, the inhibiting effect of air diminishes as system pressure and gas flow rate increase. The heat transfer coefficient can be based on either the measured centreline

temperatures (T_c) or on the predicted one (T_s). The heat transfer coefficient considerably decreases when T_s is used since T_s is always greater than T_c. The ratio of the heat transfer coefficients computed from these two methods shows that increase in air mass fraction leads to larger deviation from the measured one calculated by T_c [4].

In the new advanced passive boiling water reactor design (SBWR and ESBWR), the main component of the passive containment cooling system (PCCS) is the isolation condenser (IC). The function of the IC is to provide the ultimate heat sink for the removal of the reactor coolant system sensible heat and core decay heat. In performing this function, the IC must have the capability to remove sufficient energy from the reactor containment to prevent it from exceeding its design pressure shortly following design basis events and to significantly reduce containment pressure in the longer run.

After a loss of coolant accident, the steam/air mixture from the reactor containment may flow to the IC which will then reject decay heat to a pool of water [5]. Similar advanced design features are also envisaged for AP-600. The researchers are focusing their attention on the AP-600's passive safety core cooling systems, whose major elements are a steel reactor containment shell surrounded by a concrete shield building, natural air conditioning between the containment and the shield building, and large volumes of gravity-fed water stored in tanks above the reactor itself. The passive systems performs the principle safety functions such as primary coolant inventory control, reactivity control and residual heat removal, but they rely on natural forces like condensation, evaporation and gravity rather than the mechanical equipment that is standard in traditional active designs.

3.3.   MODELLING OF EX-VESSEL PHENOMENA

The reactor system is enclosed in a leak-tight containment to protect the public from release of radioactive products; this implies the prevention of leakages from the containment atmosphere into the environment.

Containments of commercial reactors have a volume from several thousand to a maximum of 80000 m³; some small containments are equipped with a pressure-suppression-system (ice boxes or a water pool). Containments are somewhat compartmentalized.

3.3.1.   Design basis accidents (DBAs)

Transients without a loss-of-coolant are part of the DBAs. With the exception of containments with a pressure suppression system no major interaction with the containment atmosphere exist. Steam injected into the water pool of the suppression system is condensed in the pool and creates thus some circulation in the pool. There is experimental and operational evidence that the mixing in the pool is good; therefore, no major analytical efforts are undertaken to model this mixing.

Depending on the break size steam is injected into the containment atmosphere during loss of coolant accidents (LOCA) creating, in the short–term, injection driven flows and a pressure increase. Later condensation of steam on steel and concrete structures occurs. In the long term energy is removed through heat exchangers or to the outside of the containment pressure boundary if this boundary is designed as a steel shell. Some small amounts of hydrogen may be produced during a LOCA, due to the fuel cladding/steam reaction; recombiners in the

containment will reduce a local accumulation as well as the total amount of hydrogen. During all these processes convection flows exist; usually the velocities are low.

Related computer codes have been developed since about 20 years. They are usually of lumped parameter type and can be assessed as being fully developed, in general. Well-known codes are CONTAIN (SANDIA) and COCOSYS (GRS).

3.3.2.   Severe accidents

After the accidents in TMI-2 and Chernobyl, the study of phenomena, reactor system, and containment behaviour for sequences with core melts became a major research area. Compared to phenomena under DBA conditions, the phenomena that are present during accident sequences with core melt are very complex and, evidently, much less understood. The main phenomena influencing containment behaviour are

— the release, mixing and burning of hydrogen,
— the release of volatile fission products and its decrease due to condensation and sedimentation processes,
— the transport of solid or liquid fuel (melt) into the containment and its interaction with concrete and steel structures and with the atmosphere or water.

While loads on the containment wall or structures resulting from DBAs stay within design limits and are well below loads threatening the containment integrity, this is not the case for loads resulting from severe accidents. For these the containment integrity may be threatened or even lost.

A useful overview about severe accidents can be taken from [6]:

— Although severe accidents do not belong to design basis accidents, the knowledge about the loads resulting from these sequences are needed for probabilistic safety assessments and also for the design of advanced LWRs which might take core melt sequences into account in the design process;
— The modelling of phenomena related to severe accidents should be as realistic as possible to avoid unbalanced designs or unrealistic predictions of loads on the containment resulting in unrealistic predictions of doses outside the plant;
— The modelling of phenomena related to severe accidents can only be done with relatively large uncertainty bands due to the limited experimental basis but also due to the uncertainty in predicting reliably the accident progression;
— For the calculation of phenomena and system behaviour the major lumped parameter codes as CONTAIN, MELCOR and COCOSYS in addition to many codes for special purposes(e.g. melt/concrete interaction) are used. For the assessments which need a very detailed simulation of geometrical structures (e.g. hydrogen accumulation, deflagration to detonation-transition and burns) CFD-codes are used with increasing frequency. Nevertheless, validation and model improvements are still needed.

3.4.   MODELLING OF SYSTEM BEHAVIOUR

Various NC systems are relevant within the nuclear technology. As already mentioned in the present report, various computational tools have been applied to the prediction of NC features of those systems. The complexity level of the concerned tools largely varies depending upon

the simulated system and the objectives of the simulation. Simple analytical models solving approximate equations resembling the fundamental principles of the physics making reference to systems assumed in steady state conditions up to sophisticate codes including numerical solutions of partial differential equations in the three-dimensional space and in transient conditions can be distinguished.

In the following discussion, attention is focused on the application of thermal-hydraulic system codes. Under this category codes like APROS, ATHLET, CATHARE, RELAP5 and TRAC are included, all based upon the solution of a main system of six partial differential equations. Two main fields, one per each of the two phases liquid and steam are considered and coupling is available with the solution of the conduction heat transfer equations within solids interfaced with the fluid phases. A one-dimensional solution for the characteristics of the fluid is achieved in the direction of the fluid motion in time dependent conditions. It should be emphasized that more sophisticate models are also available including three-dimensional solutions and multi-field approaches in two and multiphase fluids. However the present qualification level of those sophisticated computational tools is questionable as well as their actual need in the design or in the safety applications.

The mentioned codes have been applied to the simulation of data measured in experimental facilities of different dimensions and complexity as well to the prediction of the NC performance of existing nuclear power plants and of advanced reactor concepts. The discussion is limited hereafter to the main findings from the applications of the system codes to the simulation of NC in Integral Test Facilities (ITF) that are simulators of PWR, BWR and WWER-440. Mention is made of the scaling problem and of the uncertainty expected in the predictions of NC in NPP.

3.4.1. NC simulation in PWR and WWER-440 ITF

NC experiments have been conducted in all ITF for characterizing the loop features and for constituting databases suitable for code assessment. NC experiments have been conducted in the Lobi, Pkl, Bethsy Pmk and Pactel facilities, the first three simulators of PWR and the last two simulators of WWER-440. In relation to all the ITF, NC experiments with decreasing mass inventories of the primary coolant system have been carried out. The electrical power supplied to the core simulator corresponded to the decay power and ranged between 1.5% and 5%, roughly of the nominal core power. In these situations the NC scenario can be characterized by a diagram showing the core power as a function of the primary system mass inventory.

The applications of system codes have been of help for interpreting the experimental scenarios, for optimizing the features of the nodalizations and for characterizing the code capabilities. A list of significant achievements is given below together with references where details of the analyses can be found.

a) The codes have been used to distinguish five main NC flow patterns depending upon the value of the mass inventory of the primary loop (see also Ref. [7]):

— Single phase NC with no void in the primary system excluding the pressurizer and the upper head;
— Stable co-current two-phase NC with mass flow rate increasing when decreasing primary system fluid inventory;

— Unstable two-phase NC and occurrence of siphon condensation;
— Stable reflux condensation with liquid flowing counter-current to steam in the hot legs: flow-rate is sufficient to remove core power till loop mass inventory achieves values as low as 30-40% of the nominal values;
— Natural circulation with part of core rods in dry-out condition not favorable from the current technological and safety point of view.

b) The code has been used for characterizing the oscillations (third dashed item in the list above), showing the different role of the counter-current flow limitation (CCFL) at the entrance of the U-tubes, the siphon effect and the steam condensation both in the rising part of the U-tubes. The flow reversal and the different behaviour of parallel groups of U-tubes could also be observed by the help of the code, Ref. [8].

c) Different codes used by different European organizations have been applied to the comparative analysis of the A2-77 experiment carried out in Lobi facility. Capabilities of the codes were characterized as well as the influence upon the results that should be expected owing to the code-user effect, Ref. [9]. Deficiencies were observed in the predictions of pressure drops at low value of the Reynolds number.

d) The application to the study of NC in WWER-440 showed the code capability in predicting the flow stagnation and the consequent rise in system pressure caused by the loop sealing present in the hot leg of this reactor type, Ref. [10]. Clearing of loop seal occurs before dangerous situation for the system are reached and is also predicted by the code.

e) The code has been used to determine the maximum core power at which the PWR systems or PWR simulators can be operated in NC keeping sub-cooled the core. The limit was found close to 10% of the core nominal power, Ref. [11]. Higher limits were found fixing different thresholds for the system operation.

f) The code has been successfully used in predicting NC phenomena measured in systems that are relevant to the AP-600, including NC across the PRHR (pressurized residual heat removal), and the CMT (core make-up tank) systems, Refs [12] and [13].

3.4.2.   NC simulation in BWR ITF and NPP

NC experiments have also been performed in ITF that simulate the BWR system performance. Relevant NC data have also been recorded from the operation of BWR NPP and used for benchmarking system code performance. The flow map for the operation of BWR systems shows the core power as a function of the core flow rate. A parabola like curve in the considered plane is derived from experiments and confirmed from code applications. A steep power increase up to about 50% of nominal core power can be observed from the mentioned diagram when core flow rate achieves roughly 30% of the its nominal value (i.e. value at 100% core power). This implies that the BWR systems can operate at 50% power in NC. However, in these conditions the system is prone to instabilities, identified in the literature as density wave oscillations (DWO). A wide literature exists related to the DWO that can be considered as a NC phenomenon. A state-of-the-art report on this topic has been recently issued by OECD/CSNI, Ref. [14].

Lesson learned from the application of system codes to BWR related NC experimental situations are summarized in the following, again including references where details for the analyses can be found.

(a)   The curve core power versus core flow rate in NC conditions predictable by system codes is close to the experimental values in relevant ITF, Ref. [15]. The code is also capable of predicting the same curve related to the BWR operation. The capability in predicting the NC flow map in BWR is not affected by the scaling of the system.

(b)   The code has been successfully used in predicting the NC measured between core and a heat exchanger installed in a pool outside the main vessel in a configuration that is typical for the SBWR equipped with the IC (isolation condenser), Ref. [16].

(c)   The code has capability to predict DWO occurring recorded during the NC in typical BWR conditions, Ref. [17]. However, the prediction is largely affected by the user choices.

3.4.3.   Final remarks

The system codes have been widely applied to the prediction of NC in situations relevant to PWR and BWR conditions. The scaling problem has been addressed by demonstrating that the accuracy of the prediction is not affected by the geometric dimensions of the involved systems. No major deficiencies have been detected. It can be concluded that codes are suitable in predicting NC phenomena in conditions relevant to the present generation reactors. An exception is constituted by the predictive capability of DWO. In this case the user may substantially affect the predictive capabilities.

The above conclusions can be extended to a number of systems that are part of the design of advanced reactors like the PRHR and the CMT in the case of the AP-600 and the IC in the case of the SBWR, in relation to which a suitable experimental database exists. However, in this last case, more rigorous procedures may be established where:

—   Precision requirements are established (e.g. core flow rate in NC must be predicted with an error of 3%);
—   Measurements are shown to comply with the fixed error-threshold;
—   Accuracy of the predictions, adopting well established input decks, is shown to lie within established error bands.
—   Needs for experiments and for development of new models are derived from deficiencies found from the above process.

3.5.   SYSTEM CODES DESCRIPTION

It has been shown before that a number of plant situations can only be simulated with computer codes.

The computer code development started together with the development of nuclear reactor systems. With increasing computer capabilities, a sound experimental basis and the set-up of validation matrices the computer code development for system codes has now practically reached its final stage. As examples, short descriptions for ATHLET, RELAP 5 and CATHARE are given below.

There is growing interest in CFD computer codes that are capable of modelling 2-D and 3-D fields, and which have the potential to simulate complex geometries. However, more developments and validation is necessary. The FLUENT code will be described below as an example of a CFD code.

3.5.1. ATHLET 1.2 A computer code

The thermal-hydraulic computer code ATHLET is an advanced best-estimate one-dimensional two-phase system code. ATHLET has been developed by the Gesellschaft fur Anlagen und Reaktorsicherheit (GRS), Germany, for the analysis design basis and beyond design basis accidents (without core degradation) in light water reactors. The ATHLET structure is highly modular, and allows an easy implementation of different physical models. The code is composed of several basic modules for the calculation of different phenomena involved in the operation of light-water reactors:

— thermo-fluid dynamics,
— heat transfer and heat conduction,
— neutron kinetics,
— general control simulation module,
— specific modules as valve, pump, steam generator, pressurizer, leak and break, accumulator, quench front, feel, charge, boron concentration, non-condensable gases.

ATHLET provides a modular network approach for the representation of a thermal-hydraulic system. A given system configuration is simulated by a net of basic fluid dynamic elements, called objects. Their geometry and connections are done in an input deck. There are several object types, each of them applying for a certain fluid dynamic model.

ATHLET offers the possibility of choosing between different models for the simulation of fluid dynamics.In the current released code version, the basic fluid-dynamic option is a five-equation model, with separate conservation equations for liquid and vapour mass and energy, and a mixture momentum equation, accounting for thermal and mechanical non-equilibrium, and including a mixture level tracking capability.

As an option, there is a possibility to use a six-equation model, with completely separated conservation equations for liquid and vapour mass, energy and momentum, taking into account also non-condensable.

The spatial discretization is performed on the basis finite-volume approach. It means, the mass and energy equations are solved within control volumes, and the momentum equations are solved over flow paths — or junctions — connecting the centres of control volumes. The solution variables are the pressure, vapour temperature, liquid temperature and mass quality within a control volume, as well as the mass flow rate at a junction.

Two types of control volumes are available. Within the so-called 'ordinary' control volume a homogenous mass and energy distribution is assumed. Within the 'non-homogenous' control volume a mixture level is modelled. Above the mixture level steam water droplets, below the mixture level liquid with bubbles may exist. The combination of ordinary and non-homogenous control volumes provides the option to simulate the motion of mixture level through a vertical component.

A full-range drift-flux model is available for the calculation of the relative velocity between phases for the five-equation model. The model comprises all flow patterns from homogeneous to separated flow occurring in vertical and horizontal two-phase flow. It also takes into account counter-current flow limitations in different geometry.

Moreover, this fluid-dynamic option allows for the simulation of non-condensable gases, on the basis of the ideal gas formulation.

Another fluid-dynamic option in ATHLET consists of a four-equation model, with balance equations for liquid mass, vapour mass, mixture energy and mixture momentum. It is based on a lumped-parameter approach. The solution variables are the pressure, mass quality and enthalpy of the dominant phase within a control volume, and the mass flow rates at the junctions. The entire range of fluid conditions, from sub-cooled liquid to superheated vapour, including thermodynamic non-equilibrium is taken into account, assuming the non-dominant phase to be at saturation. The option has also a mixture level tracking capability.

For pipe-objects, on the basis of either a 5-equation or a 4-equation model, there is also the possibility to use method of integrated mass and momentum balances an option for fast-running calculations. With the application of the method, the solution variables are now the object pressure, the mass flows at pipe inlet and outlet, and the local qualities and enthalpies (4-equation model) or temperatures (5-equation model). The local pressure and mass flow rates are obtained from algebraic equations as a function of solution variables.

Furthermore, an additional mass conservation equation can be included for the description of boron transport within a coolant system.

3.5.2. The RELAP5/MOD3.2 computer code

The LWR transient analysis code, RELAP5, was developed at the Idaho National Engineering Laboratory (INEL) for the U.S. Nuclear Regulatory Commission (NRC). Code uses include analyses required to support rulemaking, licensing audit calculations, evaluation of accident mitigation strategies, evaluation of operator guidelines, and experiment planning analysis. RELAP5 has also been used as the basis for a nuclear plant analyser. Specific applications have included simulations of transients in LWR systems such as loss of coolant, anticipated transients without scram (ATWS), and operational transients such as loss of feedwater, loss of offsite power, station blackout, and turbine trip. RELAP5 is a highly generic code that, in addition to calculating the behaviour of a reactor coolant system during a transient, can be used for simulation of a wide variety of hydraulic and thermal transients in both nuclear and non-nuclear systems involving mixtures of steam, water, non-condensable, and solute.

The MOD3 version of RELAP5 has been developed jointly by the NRC and a consortium consisting of several countries and domestic organizations that were members of the International Code Assessment and Applications Program (ICAP) and its successor organization, the Code Applications and Maintenance Program (CAMP). Credit also needs to be given to various Department of Energy activities, including the INEL laboratory-directed discretionary funding program. The mission of the RELAP5/MOD3 development program was to develop a code version suitable for the analysis of all transients and postulated accidents in LWR systems, including both large- and small-break loss-of-coolant accidents (LOCAs) as well as the full range of operational transients.

The RELAP5/MOD3 code is based on a non-homogeneous and non-equilibrium model for the two-phase system that is solved by a fast, partially implicit numerical scheme to permit economical calculation of system transients. The objective of the RELAP5 development effort from the outset was to produce a code that included important first-order effects necessary for accurate prediction of system transients but that was sufficiently simple and cost effective so that parametric or sensitivity studies were possible.

The code includes many generic component models from which general systems can be simulated. The component models include pumps, valves, pipes, heat releasing or absorbing structures, reactor point kinetics, electric heaters, jet pumps, turbines, separators, accumulators, and control system components. In addition, special process models are included for effects such as form loss, flow at an abrupt area change, branching, choked flow, boron tracking, and non-condensable gas transport.

The system mathematical models are coupled by an efficient code structure. The code includes extensive input checking capability to help the user discover input errors and inconsistencies. Also included are free-format input, restart, renodalization, and variable output edit features. These user conveniences were developed in the recognition that generally the major cost associated with the use of a system transient code is in the engineering labour and time involved in accumulating system data and developing system models, while the computer cost associated with generation of the final result is usually small.

Main characteristics of the code are as follows:

—   One-dimensional system thermal hydraulic code (enabling also pseudo two- or three-dimensional modelling);
—   Basic two-phase model with 6 balance equations (mass, momentum and energy equation for each phase) with additional capability to model boron in liquid phase and non-condensable gases in vapour phase;
—   Set of closure correlations and models (best-estimate) connected to the basic model by help of system of flow regimes and set of heat transfer modes;
—   Point kinetic model;
—   Other physical models (dynamic model of fuel-clad gap, radiation heat transfer, metal-water reaction, etc.);
—   Special models for NPP components (pumps, various types of valves, separators, turbine, accumulator, pressurizer, etc.);
—   Extensive system of trips and control components for modelling of NPP safety and control system;
—   Very flexible character of the code itself and of the input data.

3.5.3.   CATHARE2 V1.5 REVISION 6 computer code

CATHARE is a system code developed by CEA, IPSN, EDF and FRAMATOME for PWR safety analysis. It can model light water reactors or test facilities using several available modules. Two-phase flows are described using a two-fluid six-equation model and the presence of non-condensable gases can be taken into account by one to four additive transport equations. The code allows a three-dimensional modelling of the pressure vessel. Successive sets of closure laws or "revisions " are developed in an iterative methodology of improvement. The Revision 6 of the closure laws is implemented in the Version V1.5. It includes models,

for the reflooding, the film condensation in presence of non-condensable gases, the interfacial friction in the core, the flashing.

CATHARE has a modular structure. Several modules can be assembled to represent the primary and secondary circuits of any PWR or of any analytical test or system test facility. They are 0-D, 1-D, 3-D modules available. All modules can be connected to walls, or heat exchangers with a 1-D conduction calculation. Many sub-modules are available to calculate the neutronics, the fuel thermomechanics, pump characteristics, accumulators, sources, sinks, etc.

All modules use the 2-fluid model to describe steam-water flows and four non-condensable gases may be transported. The thermal and mechanical non-equilibrium are described. All kinds of two-phase flow patterns are modelled: co-current and counter-current flows are modelled with prediction of the counter-current flow limitation. Heat transfer with wall structures and with fuel rods are calculated taking into account all heat transfer processes (natural and forced convection with liquid, with gas, sub-cooled and saturated nucleate boiling, critical heat flux, film boiling, film condensation). The interfacial heat and mass transfers describe not only the vaporization due to superheated steam and the direct condensation due to sub-cooled liquid, but also the steam condensation or liquid flashing due to meta-stable sub-cooled steam or superheated liquid.

The range of parameters is rather large: pressure from 0.1 to 16 MPa, liquid temperature from 20°C to 1800°C, fluid velocities up to supersonic conditions, duct hydraulic diameters from 0.01 to 0.75 m.

An important experimental program was carried out as a support for the development and validation of the code.

3.5.4. FLUENT computer code

FLUENT code has been developed by Fluent Inc.(USA). The FLUENT code is a state-of-the-art computer code for modelling incompressible and compressible fluid flow and heat transfer in complex geometries. FLUENT provides complete mesh flexibility, solving flows problems with unstructured meshes that can be generated about complex geometries with relative ease. Supported mesh types include 2D triangular/quadrilateral, 3D tetra-hedral/hexahedral/pyramid/wedge, and mixed (hybrid) meshes. FLUENT also allows to refine the grid structure, depending on the flow solution. This solution-adaptive grid capability is particularly useful for accurately predicting flow fields in regions with large gradients, such as free shear layers and boundary layers. In comparison to solutions on structured or block-structured grids, this feature significantly reduces the time required to generate a "good" grid. Solution-adaptive refinement makes it easier to perform grid refinement studies and reduces the computational effort required to achieve a desired level of accuracy; since mesh refinement is limited to those regions where greater mesh resolution is needed.

The FLUENT has the following modelling capabilities:

— Flows in 2D or 3D geometries using unstructured solution-adaptive triangular/tetrahedral, quadrilateral/hexahedral, or mixed (hybrid) grids that include prisms (wedges) or pyramids: (Both conformal and hanging-node meshes are acceptable.);
— Incompressible or compressible flows;
— Steady-state or transient analysis;

- Inviscid, laminar, and turbulent flows;
- Newtonian or non-Newtonian flow;
- Convective heat transfer, including natural or forced convection;
- Coupled conduction/convective heat transfer;
- Radiation heat transfer;
- Inertial (stationary) or non-inertial (rotating) reference frame models;
- Lagrangian trajectory calculations for a dispersed phase of particles/droplets/bubbles, including
  - coupling with the continuous phase flow through porous media
  - one-dimensional fan/heat-exchanger performance-models
  - two-phase flows, including cavitation
  - free-surface flows with complex surface shapes.

3.5.5. ERHRAC and PCCAC-2D,3D computer codes

The ERHRAC computer code is a special computer code developed by Nuclear Power Institute of China (NPIC).

ERHRAC can be used to analyze and calculate the following natural circulation flow characteristics of ERHR system for AC600/1000 PWR:

- The steady state and transient thermal hydraulic behaviour of primary coolant loop, secondary side cycle of SG and air cycle;
- Start-up mode research of triggering natural circulation flow, specially for secondary side cycle of SG;
- The conditions for establishing natural circulation flow and residual heat removal ability.

Emergency residual heat removal (ERHR) system of China advanced AC600/1000 PWR NPP China consists of a tandem three-loop system including primary loop, secondary side cycle of SG and air cycle. After accident such as station black out, the decay heat of reactor core can be removed to atmosphere by natural circulation flow through the mentioned three cycles.

PCCAC-2D, 3D are special two and three dimension computer codes developed by NPIC.

The containment of AC600/1000 is a two-shell structure. Between inner steel shell and outer reinforced cylindrical concrete shell, there is a baffle to form an annular wind channel. In the top of containment, there is a large water storage tank that can meet the requirement of 72 hours water spraying on the steel shell after LOCA.

PCCAC-2D, 3D can be used to predict the pressure and temperature of mixing gas in the containment after the accident of primary pipe rupture or main steam line rupture. The heat removal characteristics from inside containment to atmosphere through the water film on the out surface of steel shell and natural circulation flow of air can be also simulated and calculated by PCCAC-2D or PCCAC-3D.

ERHRAC and PCCAC computer codes will be verified and improved through use of experiments done in NPIC facilities.

4. EXPERIMENTAL INVESTIGATION OF NATURAL CIRCULATION SYSTEMS

4.1. INTRODUCTION

Although a large amount of thermal hydraulic data exist from the beginning of nuclear reactor development there is still some need for additional experimental data. This is on one hand due to the focus on an area not well studied in the past — in this case natural circulation in nuclear reactor application - and on the other hand due to additional and more detailed requirements from modern CFD code developments. Because of the high costs for good experimental data it should be evident that new experiments should only be performed if existing data do not meet the requirements with respect to quality and degree of detail. If new data are required the very best instrumentation should be used, and, if necessary, new instrumentation should be developed. International cooperation is encouraged.

4.2. CURRENT STATUS OF THE EXPERIMENTAL WORK

Natural circulation phenomena have been investigatedto a large extent. There are a large number of experiments and facilities. As an example the experiments performed with APEX (US), SPES (Italy) and ROSA/LSTF facilities have given data of the same design (AP-600) with different scaling. Instead of studying the operational performance of the whole concept, the core make-up tank (CMT) behaviour was investigated with PACTEL facility. PANTHERS, PANDA and NOKO represent facilities which simulate different systems of the same design.

As an example of coordination between different facilities with different scaling and code work is the NACUSP research project. One of the main research items that have been identified for natural-circulation flow is the stability of two-phase natural-circulation flow. The former studies have been usually financed by national sources. Within the Euratom 5th framework programme, the NACUSP project is dealing with this research item. The goal of NACUSP is to improve the economics of operating and future plants through improved operational flexibility, enhanced availability, and increased confidence level on the safety margins regarding the stability issues in boiling water reactors (BWRs). The experimental part of this project focuses on natural-circulation loops being of specific value for the ESBWR.
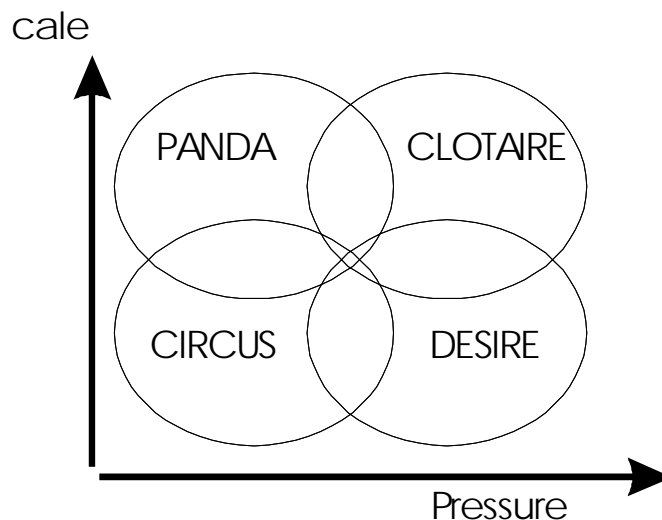

FIG. 1. Overview of experimental facilities.

Experiments will be performed in 4 experimental facilities, which complement each other, ranging from small scale to large scale, and from low-pressure, low-power operating conditions, to nominal and high-power operating conditions. Figure 1 gives an overview of the facilities used.

The DESIRE (at Delft University of Technology) and CLOTAIRE (at Commissariat l'Energie Atomique) facilities will be used to study the natural circulation and stability characteristics at nominal pressures. This is important in view of the study of coupled neutronic/thermohydraulic stability, which is an issue for large BWRs. A good understanding and validation effort of the thermal hydraulic stability is essential as a basis for other work performed within NACUSP on reactor stability and in preparation for future work on regional reactor stability. Because of its flexibility the DESIRE facility will mainly be used to perform parametric studies [1], whereas the CLOTAIRE facility will be used to study the effects of upscaling. The CLOTAIRE facility was originally built to study PWR steam generators [2].

At low pressures the CIRCUS (at Delft University of Technology) and the PANDA (at Paul Scherrer Institute) facilities will be used to study the natural circulation and stability characteristics. It is known that at low-pressure, low-power operating conditions (e.g. start-up) natural circulation flow is susceptible to gravity-driven instabilities. Because of the high sensitivity of the flow to perturbations, these conditions are very challenging for computer codes to predict. CIRCUS will be used for parametric studies [1], whereas specific tests will be performed in the large-scale PANDA test facility. PANDA has already been used to study passive decay heat removal in the ESBWR [3].

The experimental work described above will be performed in close collaboration with computational work using a selection of computer codes. Table I gives an overview of the NACUSP partners and the computer codes used for analyzing the experimental data of the facilities.

TABLE I. NACUSP PARTNERS AND COMPUTER CODES TO ANALYZE TEST-FACILITY DATA.

Partner	Computer codes for facility data
NRG Netherlands	CFX
CEA France	FLICA
DUT Netherlands	MONA
ETH Switzerland	
Forsmark Sweden	
FZR Germany	ATHLET
IBERDROLA Spain	
PSI Switzerland	TRAC-BF1, RELAP5, CFX
UPV Spain	

4.3. EXAMPLES OF NC EXPERIMENTS

This section gives some examples of the NC problems being considered in new reactor concepts and relevant experimental works both performed earlier and to be performed in future.

4.3.1. CAPCN test facility

A high-pressure natural convection loop (CAPCN) was constructed and operated to produce data in order to verify the thermal hydraulic tools used to design the CAREM integral LWR design, mainly the dynamical response. This is accomplished by the validation of the calculation procedures and codes for the rig working in states that are very close to the operating states of CAREM reactor. CAPCN resembles CAREM in the primary loop and steam generators, while the secondary loop is designed just to produce adequate boundary conditions for the heat exchanger. Water enters the heated section from the lower plenum. The nuclear core is simulated by electric heaters. The heated water flows up through the riser to the upper plenum where a liquid-vapor interphase exists. The water exits this plenum through an outer volume in contact with the steam generator. The steam generator has two coils, once through, secondary inside. The sub-cooled water flows down through a downcomer or cold leg to the lower plenum. Natural circulation flow may be regulated by a valve in the cold leg and a bypass to the bottom of the riser. This rig was constructed according to ASME for the following primary parameters: 150 bar and 340°C. The primary loop may operate in saturated or sub-cooled regimes, with a heating power up to 300kW and different hydraulic resistance. The circuit configuration allows the study of stationary states similar to CAREM conditions of pressure, specific flow and enthalpy. Height was kept in a 1:1 scale.

Many experiments were performed in order to investigate the thermal-hydraulic response of the system in conditions similar to CAREM operational states. The influence of different parameters like vapor dome volume, hydraulic resistance and dome nitrogen pressure was studied. Perturbations in the thermal power, heat removal and pressure relief were applied. The dynamic responses at low pressure and temperatures, and with control feedback loops were also studied. It was observed that around the operating point self-pressurized natural circulation was very stable, even with important deviation on the relevant parameters.

The data obtained is being used to test numerical procedures and codes. A sensitive analysis was performed and most sensitive parameters were identified. A representative group of transients were selected, in order to check computer models. Simulation models are in current development against a reference transient, without adjustment. When this contrast is clear, models will be compared against the representative group of transients. The information on specific models should be incorporated into CAREM modelling.

4.3.2. Driving forces of NC in the containment

In many passive safety systems natural circulation is an essential part of the system. The main aim is to use density differences in a pool or in a closed loop to transfer thermal energy from a source to a heat sink without using other energies than gravitational energy. This process can take place with or without phase changes.

Passive systems with phase changes can develop considerable driving forces. The pressure differences often are in the range from 1 kPa–100 kPa. Examples are the passive containment

cooling system, developed by General Electric, or the Emergency Condenser, developed by Siemens.

Passive systems without phase changes have much smaller driving forces with pressure differences in the range from 1 Pa to 1000 Pa. An example is the building condenser, developed by Siemens. The natural circulation with single-phase flow is valid both on the primary and on the secondary side, as long as the temperature differences are small. But small driving pressures are not equivalent with ïneffective". For example: heating up water from 5°C to 10°C gives a density difference of 0.3% kg/m^3 (or 0.03%).

If the pool height is 5 m, then the maximum driving pressure is about 15 Pa. This corresponds to a vertical flow velocity of 0.17 m/s. Suggesting that the rising plume has a diameter of 2 m, the mass flow is about 500 kg/s and the thermal flux is about 10.5 MW.

In other passive systems natural circulation with pressure differences in the range <<1 Pa can determine whether a component can reach the right operating conditions or not. Assuming that radiolytic gas is accumulated from the original concentration 10^{-5} by a factor 100 in a "bull eye" of a conventional RPV level measurement, then the density difference is about 0.03 kg/m³. In a "bull eye" with a gas space of 5 cm height the driving pressure results to 0.015 Pa. Nevertheless in a "bull eye" that was properly formed this small pressure difference was sufficient to initiate a counter-current flow (a special form of natural circulation) of the enriched gas mixture against the fresh steam inside the connecting pipe. So in this "bull eye" no accumulation of radiolytic gas above the ignition concentration was possible. In another "bull eye", which was not properly designed, the opposite was true.

So the effectiveness of systems with natural circulation is not primarily a question of high driving forces but of the proper design. Normally a simple calculation is sufficient for the designer to calculate the driving forces in a balance with flow resistances. It is not necessary to know each detail of the flow fields like degree of turbulence, exact velocity profiles in different regions of the circuit or the exact form and flow velocity of a raising plume in a pool. Rough calculations normally are sufficient to decide whether a system using natural circulation is properly designed or not.

Fundamental research seems to be necessary in all cases where components normally are tested with pure steam instead with nuclear steam, which always has a small content of radiolytic gas. To avoid handling pure hydrogen and pure oxygen in a laboratory it could be possible to generate "radiolytic gas" by an electorolytical apparatus continuously and in small quantities. Such experiments can be very instructive about the accumulation of the radiolytic gas, about the natural circulation effects in components with stagnating steam atmosphere and about the possibilities to get a passive transport of the enriched steam back to the RPV or to another line with intensive steam flow.

The opposite of natural circulation is stratification. In most cases where stratification takes place, it is neglected both by the designer and by the computer code. Experiments in the PANDA facility showed that stratification could become the essential effect in containment's atmosphere. So a deeper knowledge about the counterparts "natural circulation" and "stratification" seem to be unavoidable to do the right calculations with mixed or with separated media in a containment or in a pool.

4.3.3. Experiments for Indian AHWR

The proposed Indian AHWR is a vertical pressure tube type, heavy water moderated, boiling light water cooled reactor employing two-phase natural circulation as the normal mode of coolant circulation. It also relies on natural circulation for heat removal during shutdown and accident scenarios such as LOCA. Both the passive shutdown heat removal system and the passive containment cooling system employ condensers, which reject heat to large pools of water. To test the adequacy of the natural circulation systems employed and to validate the performance of the various computer codes developed several experimental facilities have been proposed. Some of them are already in operation and others are in various stages of implementation. A brief description of the various test facilities is given in the following to subsections.

The integral test loop is being set up to simulate the primary system thermal hydraulic behavior of AHWR during normal operating and accident conditions. The facility has been designed based on a 3-level approach. Primary system scaling is based on the power-to-volume scaling philosophy (level-1). Important local phenomena, which can potentially influence the integral system behavior (e.g. CHF, flow pattern transition, etc.), have been simulated (level-2). Boundary flows (accumulator injection, break flow, etc.) of energy and mass, which can significantly modify the integral system behavior have also been simulated (level-3). It is a full elevation and full pressure facility simulating the AHWR with a volume scale ratio of 400. The facility incorporates all the essential components of AHWR with velocity simulated to 1:1 scale. It can be used to generate experimental data on the steady state and stability behavior of AHWR. It also incorporates safety systems such as the shutdown heat removal system and emergency core-cooling system, which includes an advanced accumulator and the gravity driven cooling system (GDCS).

The high-pressure natural circulation loop is a simple rectangular loop, having similar geometry as one of the parallel channels of AHWR. It is a full pressure test facility set up to investigate the steady state and stability behaviour of natural circulation. The facility is already in operation. Experiments conducted in this facility include steady state two-phase natural circulation and stability of two-phase natural circulation. The parametric influences investigated include the effect of pressure, power and inlet sub-cooling. The facility has provisions to investigate the geometry effects such as loop height, pipe diameter, inlet and exit orificing. The facility is designed to operate up to 115 kg/cm^2 pressure, at 315°C.

An experimental facility to study the flow pattern transition instability under 2-phase natural circulation conditions has been designed. The design pressure corresponds to 125 bar. It is proposed to carry out experiments on flow pattern transition instability with four different diameter tubes. This will also facilitate investigation of the effect of scaling on two-phase natural circulation. The facility has been set up and commissioned with instruments. To investigate the flow pattern transition, visualization of the flow patterns is possible using neutron radiography. This technique will also facilitate the measurement of the cross-sectional average void fraction and its profile, which will also be compared with similar measurements, obtained by conductance probes.

4.3.4. Experiment for AC600/1000 in China

When a station blackout accident occurs, the decay heat of AC600/1000 reactor core can be removed to the atmosphere as the ultimate heat sink through natural circulation flows established by the primary coolant loop, the secondary side cycle of SG and air cycle

respectively. Nuclear Power Institute of China (NPIC) has built a passive emergency residual heat removal (ERHR) experiment facility in order to research the natural circulation flow characteristics for AC600/1000 ERHR system and to verify the computer code ERHRAC. The facility parameters are as the following:

Heating power:	80–400 kW
Design pressure in the secondary side of SG:	8.6 MPa
Elevation difference between air cooler and SG:	7.2 m
Equivalent diameter of chimney:	0.7 m
Height of chimney:	12 m

The core make-up water tanks are used in the design of AC600/1000 so as to eliminate the high-pressure safety injection pumps and increase reliability of the safety system. The function characteristics and coolant flow transient of core make-up water tank, accumulator and automatic depressurization system can be tested using NPIC core make-up water tank experiment facility to simulate a small LOCA. The facility parameters are as the following:

Design pressure:	17.2 Mpa
Design temperature:	310°C
Core make-up tank volume:	1 m^3
Accumulator volume:	1 m^3
RPV volume:	0.76 m^3
Pressurizer volume:	0.7 m^3
Break sizes:	0.5,1,2,5,10 mm

4.4. CONCLUSIONS

Several conclusions can be drawn from the survey of experimental data and the identification of needs; they are listed below:

a) The development and validation of CFD codes increased the requirements on the quality and details of experimental data. This has, e.g. led to a new instrumentation like tomography of two-phase flows to get knowledge about the spatial distribution of different fluids or phase. In addition, local turbulences on a micro scale should be modelled. New challenges result for the quality of experimental results from the required knowledge of detailed interfacial phenomena. The required knowledge as listed above should be available for steady state phenomena and transient flows.

b) For sequences with phase changes, especially for the condensation process, the influence of non-condensable gases on interfacial interactions, heat transfer and friction losses has to be investigated in more detail as compared with existing knowledge and with ongoing research.

c) For reactors using the natural circulation mode for core cooling, the neutronic-thermal hydraulic interactions are of vital importance because these might lead to core and flow instabilities. Instabilities with large amplitudes may influence stable operation.

d) A validation of models in computer codes should be based on different experiments in different facilities — if possible. Nevertheless the necessity to have well-based scaling laws to extrapolate from smaller scales to real plant sizes is of high importance. In addition, data from plant transients performed intentionally or unintentionally should be used more often for code validation.

e) There is a large amount of data from Separate-Effect tests and Integral tests selected systematically by CSNI for the purpose of code validation; see [Validation Matrices] for

the requirements on the selected data and the matrices. Nevertheless, some special tests focusing on NC-relevant phenomena and system behavior should be incorporated into these matrices. In addition, it should be evaluated whether further tests are needed to increase the confidence in the experimental database.

5. CONCLUSIONS AND RECOMMENDATIONS OF THE TECHNICAL COMMITTEE MEETING

A Technical Committee Meeting on Natural Circulation Data and Methods for Innovative Nuclear Power Plant Design was held at in Vienna in July 2000.

The meeting presentations and discussions were directed toward three related aspects of natural circulation phenomena:

(a) Design considerations for development and deployment of innovative concepts using natural circulation phenomena;
(b) Computer codes and incorporated models for analysis of natural circulation phenomena;
(c) Experimental facilities and data for support of concept design and analysis.

Within the area of computer codes and models, two classes of models were discussed:

(a) Systems codes — Established systems codes are used to model complete plant systems, including instrumentation and control. These are typically one dimensional (1D) models with multi-dimensional phenomena addressed within component models where necessary;
(b) Multi-dimensional generic flow models — Two types of models were discussed:
— Computational fluid dynamic (CFD) models
— Large eddy simulation (LES) models.

Following the meeting presentations, a general discussion of the subject was held among participants, resulting in the following conclusions and recommendations.

5.1. DESIGN CONSIDERATIONS

(a) Natural circulation systems are now implemented or being considered in many future reactor designs. Natural circulation is applied both to ensure the sufficient coolant flow in the core (reactors based on primary coolant natural circulation during normal operation) and to fulfill or support the fundamental safety functions. It should be noted that reactors based on natural circulation during normal operation, e.g. the Dodewaard Reactor in the Netherlands and VK-50 in Russia operated for an extended period of time;
(b) There is a consensus that natural circulation systems can provide more reliable means for a number of safety functions (e.g. decay heat removal from the core, heat removal from the containment atmosphere) and can be cost effective as these systems are less vulnerable to failures and therefore, the number of parallel trains in one system can be reduced. Different designs use natural circulation in different ways. Common design concepts and their respective needs relevant to natural circulation should be identified;
(c) If natural circulation is used as an operational principle of design (full power to be removed from the core by natural circulation) the most important task seems to be preventing the core from two phase natural circulation instabilities induced by neutronic feedback;

(d)   If natural circulation is used as a working principle for safety systems, 1D codes can cope with the phenomena of natural circulation in many cases with some limitations and some uncertainties. The main drawbacks of natural circulation systems include the lower driving forces and less possibility to alter the course of an accident if something unexpected happens. Due to low driving forces, the operation of the natural circulation systems may be adversely affected by small variations in thermal-hydraulic conditions. The lower driving forces might also lead to quite large equipment where the role of 3D phenomena is essentially increased;

(e)   In cases where multi-dimensional phenomena are present, the safety relevance and need for a 3D approach should be investigated first. An example is the effect of thermal stratification on the building condenser, observed in PANDA;

(f)   The effect of non-condensable gases on condensation has been known for many years, and design features to address the problem (e.g. steam jet air ejectors for steam turbine cycles) are provided. In order to cope with this problem in future natural circulation systems, special design features should be considered for condensers.

5.2. COMPUTER CODES AND INCORPORATED MODELS

(a)   System codes have reached a highly developed modelling status and a large acceptance. They can reproduce accurately enough most existing safety related experiments, so far as the dominant physical mechanisms are known and understood;

(b)   System thermal-hydraulic codes have been successfully applied for normal operation and accident conditions in the licensing of existing natural circulation BWRs. However, there is a consensus that current system thermal-hydraulic codes typically being used for safety analyses are not sufficiently validated to address all of the relevant conditions and phenomena of natural circulation based innovative designs (low pressure, low driving heads, increased effect of non-condensable gases, effect of buoyancy at low velocities, etc);

(c)   Different codes are used for design and to study the different phenomena. The capabilities of the different codes to represent each case should be evaluated. More robustness is needed in the codes with regard to effectively addressing natural circulation phenomena;

(d)   Consideration should be given to improvements in the code validation matrix with regard to natural circulation phenomena;

(e)   Limitations exist whenever natural circulation phenomena are predominantly of a higher dimensional nature. 1D codes can be improved in this case by introducing special, component-related models that do not change the 1D structure (like reported for the core makeup tank modelling in APROS) or by introducing more-dimensional components (e.g. 2D downcomer). For development of more optimised designs, enhanced confidence in safety analyses, etc. There is a need for more accuracy of the codes and more detailed descriptions of new cooling concepts. This leads to a tendency to use, at least for local detailed analyses, 3D and time-dependent CFD codes. CFD codes are used even for designing experiments and their instrumentation arrangement. They can also be reliably used to study in a more qualitative manner the relevance of certain phenomena in flow and heat transfer problems, so far as the governing physics is included in the equations or models. Work is needed to improve CFD codes by appropriate modelling and related experiments, e.g. for the phenomena of non-condensable gases and instabilities as related to natural circulation;

(f)   For more quantitative use in natural convection, especially with time dependent flow, improvements of the turbulence models are needed. Sometimes, LES is a necessary

alternative. With two-phase flows, a quantitative use of CFD is currently limited to mainly homogeneous flows; for other flow regimes, the modelling of interfacial phenomena needs improvements. The turbulence modelling in two-phase flows can only be accepted as a first step. New correlations and models for two-phase flow should be developed, especially, in the turbulent flow regime. R&D is necessary to improve the models and to extend them for all flow regimes;

(g) Interfacial phenomena are still open to investigation. The interfacial heat transfer, interfacial mass transfer, and interfacial shear stress should be modelled and incorporated into the thermo-hydraulic codes;

(h) Theoretical and semi-theoretical studies could be considered international co-operative activities. This co-operation will provide better understanding of nuclear power technology and probably will reduce public reaction against nuclear technology.

5.3. EXPERIMENTAL FACILITIES AND DATA

(a) Increasing needs for accuracy and detail of codes result in corresponding needs regarding the details to be provided by experiments. For the development and validation of CFD codes one needs primarily single effect experiments with very detailed instrumentation. Instrumentation should be developed to provide improved local and field data for CFD codes. For design purposes and for system code improvement and validation, relatively realistic large-scale experiments are of interest. Thus some large scale more complex experiments with detailed instrumentation are likely to be needed to validate the correct interrelation between the different models used in the CFD codes;

(b) In some cases, uncertainties exist because of a lack of data for friction loss modelling and condensation (more general: phase interaction) particularly at low pressure. Perhaps dynamic flow charts can be useful here;

(c) Further experiments are likely to be needed for code validation related to the effects of non-condensable gases;

(d) As natural circulation systems used in different advanced designs are widely different in operating conditions and geometry, work on the scaling of natural circulation phenomena demands attention. Effective scaling laws will enable inter-comparison of data generated by various facilities.

5.4. GENERAL

(a) The consideration of advanced designs is especially important to the future of the nuclear power industry. Advanced reactors in general have the following goals:
— Satisfying stringent safety requirements (e.g. by use of a combination of both active and passive safety systems),
— Improving the economics of power generation

(b) TCM participants concluded that additional analytical and experimental work is highly recommended both for the development of new, and the validation of current, computer codes. Basic research in natural circulation phenomena could help to improve codes and design capabilities. In addition, large-scale tests of natural circulation systems could provide direct substantiation of their functioning under the real plant conditions;

(c) The papers presented to this TCM show that a large scope of analytical and experimental investigations has been performed and are being planned in Member States in relation to natural circulation systems and equipment.

REFERENCES

Section 1

[1]   INTERNATIONAL ATOMIC ENERGY AGENCY, Progress in Design, Research and Development, and Testing of Safety Systems for Advanced Water Cooled Reactors, IAEA-TECDOC-872, Vienna, 1996.

[2]   INTERNATIONAL ATOMIC ENERGY AGENCY, Technical Feasibility and Reliability of Passive Safety Systems for Nuclear Power Plants, IAEA-TECDOC-920, Vienna, 1996.

[3]   INTERNATIONAL ATOMIC ENERGY AGENCY, Status of Advanced Light Water Cooled Reactor Designs 1966, IAEA-TECDOC-968, Vienna, 1997.

[4]   INTERNATIONAL ATOMIC ENERGY AGENCY, Integral Design Concepts of Advanced Water Cooled Reactors, IAEA-TECDOC-977, Vienna, 1997.

[5]   INTERNATIONAL ATOMIC ENERGY AGENCY, Advances in Heavy Water Reactor Technology, IAEA-TECDOC-984, Vienna, 1997.

[6]   INTERNATIONAL ATOMIC ENERGY AGENCY, Technologies for Improving the Availability and Reliability of Current and Future Water Cooled Nuclear Power Plants, IAEA-TECDOC-1054, Vienna, 1998.

[7]   INTERNATIONAL ATOMIC ENERGY AGENCY, Evolutionary Water Cooled Reactors: Strategic Issues, Technologies and Economic Viability, IAEA-TECDOC-1117, Vienna, 1999.

[8]   INTERNATIONAL ATOMIC ENERGY AGENCY, Experimental Tests and Qualification of Analytic Methods to Address Thermohydraulic Phenomena in Advanced Water Cooled Reactors, IAEA-TECDOC-1149, Vienna, 2000.

[9]   US NUCLEAR REGULATORY COMMISSION, Compendium of ECCS Research for Realistic LOCA Analysis, NUREG 1230, USNRC, Washington (DC), 1988.

[10]   OECD NUCLEAR ENERGY AGENCY, M.J. Lewis, R. Pochard, F. D'Auria, H. Karwat, K. Wolfert, G. Yadigaroglu, H.L.O. Holmstrom, Eds, Thermohydraulics of Emergency Core Cooling in Light Water Reactors – A State of The Art Report, OECD/CSNI Rep. No. 161, Paris, 1989.

[11]   OECD NUCLEAR ENERGY AGENCY, N. Aksan, D. Bessette, et al., Eds, CSNI Code Validation Matrix of Thermalhydraulic Codes for LWR LOCA and Transients, OECD/CSNI Rep. No. 132, Paris, 1987.

[12]   OECD NUCLEAR ENERGY AGENCY, A. Annunziato, H. Glaeser, J. N. Lillington, P. Marsili, C. Renault, A. Sjoberg, Eds, CSNI Code Validation Matrix of Thermalhydraulic Codes for LWR LOCA and Transients, OECD/CSNI Rep. No. 132, Rev. 1, Paris, 1996.

[13]   OECD NUCLEAR ENERGY AGENCY, N. Aksan, F. D'Auria, H. Glaeser, R. Pochard, C. Richards, A. Sjoberg, Eds, A Separate Effects Test Matrix for Thermal-Hydraulic Code Validation: Phenomena Characterization and Selection of Facilities and Tests" – Vols. I and II, OECD/CSNI Rep. OCDE/GD (94) 82, Paris, 1993.

[14]   US NUCLEAR REGULATORY COMMISSION, D'Auria F., Galassi G.M., Relevant Results Obtained from the Analysis of LOBI/MOD2 Natural Circulation Experiment A2-77A"EU-supported activity, USNRC NUREG/IA-0084, Washington, DC, 1992.

[15]   EUROTHERM Seminar no. 16, "Natural Circulation in Industrial Applications", Pisa (I), Oct. 11-12 1990.

[16]   EUROTHERM Seminar no. 63, "Single and Two-Phase Natural Circulation", Genova (I), Sept. 6-8 1999.

Section 2

[1]   INTERNATIONAL ATOMIC ENERGY AGENCY, The Safety of Nuclear Power: Strategy for the Future (Proc. Int. Conf. Vienna, 1991, IAEA, Vienna (1992).

[2]   INTERNATIONAL ATOMIC ENERGY AGENCY, Status of Advanced Water Cooled Reactor Designs 1996, IAEA-TECDOC-968,Vienna, 1997.

[3]   INTERNATIONAL ATOMIC ENERGY AGENCY, Evolutionary Water Cooled Reactors: Strategic Issues, Technologies and Economic Viability, IAEA-TECDOC-1117, Vienna, 1999.

[4]   TOWER, S.N., et al., Passive and simplified system features for the advanced Westinghouse 600 MWe PWR, Nucl. Eng. Des. **109** (1988) 147–154.

[5]   NOVIELLO, L., "Key developments of the EP1000 design", Evolutionary Water Cooled Reactors: Strategic Issues, Technologies and Economic Viability, IAEA-TECDOC-1117, Vienna, 1999.

[6]   ZSHANG, S., "Experiment research and calculation method of natural circulation flow for AC600/1000", Natural Circulation Data and Methods for Innovative Reactor Design (proc. Mtg Vienna, 2000).

[7]   LEE, S.W., et al., Assessment of passive containment cooling concepts for advanced pressurized water reactors, Ann. Nucl. Energy **24** 6 (1997) 467–475.

[8]   AFROV, V.G., et al., "Metodiceskie Ocobennosti Obosnovania Passivnych Sistem Bezopasnosti AES WWER-640", Russian-German Seminar on Experiments in Large Scale Facilities, St.Petersburg, Russian Federation, 1997.

[9]   HART, J., et al., "TEPSS — Technology enhancement for passive safety systems", FISA-99 — EU Research in Reactor Safety, Luxembourg, 1999.

[10]   SAHA, D., et al., "An experimental study on the behaviour of a passive containment cooling system using a small scale model", Progress in Design, Research and Development and Testing of Safety Systems for Advanced Water Cooled Reactors, IAEA-TECDOC-872, Vienna, 1996.

[11]   BRUSA, L., et al., "Innovative containment cooling system for double concrete containment (INCON)", FISA-99 — EU Research in Reactor Safety, Luxembourg, 1999.

[12]   HICKEN, E.F., et al., "European BWR R&D cluster of innovative passive safety systems", FISA-99 — EU Research in Reactor Safety, Luxembourg, 1999.

[13]   SOPLENKOV, K.I., et al., "Design and testing of passive heat removal system with ejector-condenser", Progress in Design, Research and Development and Testing of Safety Systems for Advanced Water Cooled Reactors, IAEA-TECDOC-872, Vienna, 1996.

[14]   NARABAYASHI, T., et al., "Thermohydraulics study of steam injector for next generation reactor", Proc. Int. Conf. on New Trends in Nuclear System Thermohydraulics, Pisa, 1994, vol. 1, 653–661.

[15]   MESETH, J., "Natural circulation and stratification in the various passive safety systems of the SWR 1000", Proc. Mtg. on Natural Circulation Data and Methods for Innovative Reactor Design, IAEA, Vienna, 2000.

[16]   THEOFANOUS, T.G., "In-vessel retention as a severe accident management strategy", Proc. NEA/CSNI workshop on In-vessel Core Debris Retention and Coolability, Garching, 1998, NEA/CSNI R(98), 1853–74.

[17]   BRETTSCHUH, W., "SWR 1000: The new boiling water reactor power plant concept", Evolutionary Water Cooled Reactors: Strategic Issues, Technologies and Economic Viability, IAEA-TECDOC-1117, Vienna, 1999.

[18]   BARANAEV, Y.D., et al., "Emergency heat removal in the integral water cooled ABV-6 reactor for the Volnolom floating nuclear power plant", Integral Design Concepts of Advanced Water Cooled Reactors, IAEA-TECDOC-977, Vienna, 1997.

[19]   RICHARD, P., et al., "In-vessel core retention strategy (IVCRS)", FISA 99 — EU Research in Reactor Safety, Luxembourg, 1999.

[20]   LEVERENZ, R., "Design description of the European pressurised water reactor", Evolutionary Water Cooled Reactors: Strategic Issues, Technologies and Economic Viability, IAEA-TECDOC-1117, Vienna, 1999.

[21]   GRÖTZBACH, L.N., et al., "Numerical analysis of experiments modelling LWR sump cooling by natural convection", Proc. Mtg. on Natural Circulation Data and Methods for Innovative Reactor Design, IAEA, Vienna, 2000.

[22]   DELMASTRO, D.F., "Thermal-Hydraulic Aspect of CAREM Reactor", Proc. Mtg. on Natural Circulation Data and Methods for Innovative Reactor Design, IAEA, Vienna, 2000

[23]   Integral Design Concepts of Advanced Water Cooled Reactors, IAEA-TECDOC-977, Vienna, 1997.

Section 3

[1]   BERGLES, A.E., Two-phase Flow and Heat Transfer in the Power and Process Industries, McGraw Hill, New York, 1981.

[2]   KUHN, S.Z., SCHROCK, V.E., PETERSON, P.F., Final Report On U.C. Berkeley Single Tube Condensation Studies, Dept. of Nuclear Eng., UCB-NE-4201, 1994.

[3]   SIDDIQUE, M., GOLAY, M.W., KAZIMI, M.S., The Effect of Noncondensable Gases on Steam Condensation under Forced Convection Conditions, Dept. of Nuclear Eng., MIT, MIT-ANP-TR-010, 1992.

[4]   TANRIKUT, A., YESIN, O., "Experimental research on in-tube condensation in the presence of air", Experimental Tests and Qualification of Analytical Methods to Address Thermohydraulic Phenomena in Advanced Water Cooled Reactors, IAEA-TECDOC-1149, 1998.

[5]   FALUOMI, V., "Evaluation of the condensation phenomenon in presence of non-condensable gases for PCCS related geometry", Experimental Tests and Qualification of Analytical Methods to Address Thermohydraulic Phenomena in Advanced Water Cooled Reactors, IAEA-TECDOC-1149, 1998.

[6]   Analysis of Severe Accidents in Light Water Reactors Euro-Course-97, Madrid, 1997, European Commission DG XII.

[7]   D'AURIA, F., GALASSI, G.M., VIGNI, P., CALASTRI, A., Scaling of natural circulation in PWR systems, J. Nuclear Engineering & Design **132** 2 (1992) 187–206.

[8]   D'AURIA F., GALASSI G.M., Characterisation of instabilities during two-phase natural circulation in PWR typical conditions, J. Experimental Thermal and Fluid Science **3** 90 (1990).

[9]   D'AURIA, F., GALASSI, G.M., "Relevant results obtained from the analysis of LOBI/MOD2 natural circulation experiment A2-77A", EU-supported activity, USNRC NUREG/IA-0084, Washington, DC (1992).

[10]   AMBROSINI, W., BELSITO, S., D'AURIA, F., FROGHERI, M., OECD/CSNI ISP 33: Post-test Analysis of the PACTEL Natural Circulation Experiment Performed by CATHARE 2 v1.3E Code, University of Pisa Report, DCMN - NT 208(93), Pisa (I), May 1993 — OECD CSNI Final Workshop on ISP 33 — Lappeenranta (SF), 1993.

[11] D'AURIA, F., FROGHERI, M., MONASTEROLO, U., "Removable power by natural circulation in PWR systems", ASME-JSME Int. Conf. on Nuclear Engineering (ICONE-5), Nice, 1997 (ICONE5-2431).

[12] D'AURIA, F., GALASSI, G.M., ORIOLO, F., FIORINO, E., FRUTTUOSO, G., "Evaluation of Relap5/mod3.1 application to Spes-2 experiments", Proc. Int. Mtg on Advanced Reactor Safety (ARS '97), Orlando, 1997.

[13] TUUNANEN, J., VIHAVAINEN, J., D'AURIA, F., KIMBER, G., Assessment of Passive Safety Injection Systems of ALWRs, VTT Research Notes, Espoo, 1999.

[14] AMBROSINI, W., ANEGAWA, T., BLOMSTRAND, J., DE BETOU, J., LANGENBUCH, S., LEFVERT, T., VALTONEN, K., State of the Art Report on Boiling Water Reactor Stability (SOAR ON BWRS) (D'AURIA, F., ed.), OECD-CSNI Rep. OECD/GD (97) 13, Paris, 1997.

[15] AMBROSINI, W., D'AURIA, F., GALASSI, G.M., MAZZINI, M., The research program on the instability of boiling channels to be carried out by the PIPER-ONE apparatus, J. Energia Nucleare **10** 3 (1993).

[16] BOVALINI, R., D'AURIA, F., GALASSI, G.M., MAZZINI, M., "Post-test analysis of PIPER- ONE PO-IC-2 experiment by Relap5/mod3 codes", Progress in Design, Research and Development, and Testing of Safety Systems for Advanced Water Cooled Reactors, IAEA-TECDOC-872, Vienna, 1996.

[17] D'AURIA, F., FROGHERI, M., GALASSI, G.M., "Participation to OECD/NEA BWR Benchmark with Relap5/mod2 code", Proc. Int. Conf. Nuclear Option in Countries with Small and Medium Electricity Grid, Opatjia, 1996.

Section 4

[1] DE KRUIJF, W.J.M., VAN DER HAGEN, T.H.J.J., ZBORAY, R., MANERA, A., MUDDE, R.F., "CIRCUS and DESIRE; Experimental Facilities for Research on Natural-Circulation Cooled Boiling Water Reactors", this publication.

[2] BOUCHTER, J.C., CAMPAN, J.L., GUIRAND, J.M., SERMET, E., "Steam Generator Experiment for 3-D Computer Code Qualification — CLOTAIRE International Program", proc. NURETH-4, Karlsruhe, Germany (1989).

[3] HUGGENBERGER, M., et al., "ESBWR related passive decay heat removal tests in PANDA", (proc. ICONE-7, Tokyo), ICONE-7322 (1999).

BIBLIOGRAPHY

DELMASTRO, D., CONVERTI, J., CLAUSSE, A., The influence of gravity on the stability of boiling flows', Nucl. Engineering and Design **127** 1 (1991) 129–139.

DELMASTRO, D., CLAUSSE, A., Experimental phase trajectories in boiling flow oscillations', Int. J. Experimental Heat Transfer, Fluid Mechanics and Thermodynamics **9** 1 (1994) 47–52.

JUANICÓ, L.E., Identificación de Cuencas Dinámicas en Flujos en Ebullición, Doctoral Thesis, Instituto Balseiro, 1998 (in Spanish).

Annex

PAPERS PRESENTED AT THE
TECHNICAL COMMITTEE MEETING

Part 1

DESIGN CONSIDERATIONS

Natural convection and natural circulation flow and limits in advanced reactor concepts

R.B. Duffey

Atomic Energy of Canada Ltd, Canada

Abstract. Existing reactor designs and new concepts rely to varying degrees on heat removal processes driven by natural convection as a potentially important design feature or ultimate heat removal mechanism. This is independent of whether the nuclear core is cooled by water, gas or liquid metal, since in many shut down or emergency conditions forced cooling is assumed or predicted to be lost. However, using natural convection to advantage is possible, since it can provide significant cost-savings by the elimination of pumps and ancillary equipment and also can result in simplified and hence higher reliability safety systems. It is highly desirable to build on the inherent or existing heat removal processes than to graft design or add them on afterwards. The limits to the heat removal are set by the natural circulation flow and heat removal capability, so these need to be predicted with accuracy. The capability limit is determined by well-known physically linked parameters, including the flow rates, driving heads, heat sinks, fluid thermal expansion, and flow thermal and hydraulic stability. In natural convection plants, there are opportunities for the limits to be set by the absolute power output available from naturally convective flow, and the onset of instability in that flow. We are interested in the ultimate or maximum power output both in order to minimize power generation costs, and to determine how far the natural circulation designs can be developed. This paper reviews some of the fundamental equations and analytical solutions for natural convection flows, and examines their application to determine the limits of heat removal as a means of establishing simple criteria and fundamental design limits. This type of physical analysis can be used to investigate the flow and stability limits for a thermally expandable fluid, which encompasses the extremes of both low and supercritical pressure applications. To illustrate the approach, simple analytical expressions are derived for the ultimate or maximum heat removal. We can then relate the maximum thermal hydraulic limits to hypothetical reactor power output. The relationship between some of the various enhanced design features is then clear when seeking the ultimate or maximum safe power output at least cost. Hypothetical natural circulation designs are discussed as a basis.

1. INTRODUCTION

Existing reactor designs and new concepts rely to varying degrees on heat removal processes driven by natural convection as a potentially important design feature or ultimate heat removal mechanism. This is independent of whether the nuclear core is cooled by water, gas or liquid metal, since in many shut down or emergency conditions forced cooling is assumed or predicted to be lost. However, using natural convection to advantage is possible, since it can provide significant cost-savings by the elimination of pumps and ancillary equipment and also can result in simplified and hence higher reliability safety systems. It is highly desirable to build on the inherent or existing heat removal processes than to graft design or add them on afterwards. The limits to the heat removal are set by the natural circulation flow and heat removal capability, so these need to be predicted with accuracy. The capability limit is determined by well-known physically linked parameters, including the flow rates, driving heads, heat sinks, fluid thermal expansion, and flow thermal and hydraulic stability

In natural convection plants, there are opportunities for the limits to be set by the absolute power output available from naturally convective flow, and the onset of instability in that flow. We are interested in the ultimate or maximum power output in order to both minimize power generation costs (both capital and operating), and to decide or determine how far the natural circulation designs can be developed. We call this a hypothetical design, to indicate the conceptual nature of the analysis.

Different designs have differing heat removal characteristics. For example, single-phase gas and liquid metal systems rely on single-phase natural convection, whereas water -cooled designs can utilize boiling two-phase flow. The use of flashing-driven, natural-circulation systems are being considered in advanced boiling designs, and also the use of high pressure super critical water. This important development concept for innovative designs increases the thermal efficiency by using a higher coolant temperature. The large variations in fluid properties, primarily density and enthalpy, near the critical point also introduce the potential for flow instabilities similar to those in a boiling system.

Using natural convection to advantage is possible, since it can provide significant cost-savings by the elimination of pumps and ancillary equipment and also can result in simplified and hence higher reliability safety systems. It is highly desirable to build on the inherent or existing heat removal processes than to graft design or add them on afterwards. The limits to the heat removal are set by the natural circulation flow and heat removal capability, so these need to be predicted with accuracy. The capability limit is determined by well-known physically linked parameters, including the flow rates, driving heads, heat sinks, fluid thermal expansion, and flow thermal and hydraulic stability

To illustrate the approach, simple analytical expressions are derived to illustrate the ultimate or maximum heat removal. We can then relate the maximum thermal hydraulic limits to hypothetical reactor power output and cost. The relationship between some of the various enhanced design features is then clear when seeking the ultimate or maximum safe power output at least cost. Hypothetical natural circulation design are discussed as a basis.

2.   GENERAL THEORY OF NATURAL CIRCULATION FLOW RATE

In designing heat removal systems, we often rely on both single and two-phase natural circulation. The fluid heats and expands, and may boil and the two-phase flow generates an increased pressure drop. The inlet flow is derived from a pump, or a downcomer with a hydrostatic head, so that when there are many channels in parallel, as in a reactor, heat exchanger or condenser, the boundary condition is a constant pressure drop.

We can derive a formulation for the natural circulation flow, which includes the subcooled length and the effect of flow on the loss coefficients; is consistent with homogeneous stability analysis, and extends previous work. This result can then be coupled with the instability treatment to determine the *natural-circulation limit on instability*.

Consider any natural-circulation system as a loop or U-tube, where the driving force for the flow is due to the gravitational head difference between the water in the downcomer and that in the boiling channel and riser. In the steady state, which is sufficient for our discussion, this head difference is balanced by the pressure losses incurred by the flow and venting of the boiling two-phase flow, so in a natural circulation loop, the pressure drop boundary condition is zero around the loop. Thus, the net gravitational hydrostatic head is exactly balanced by the friction and form losses in the single and two-phase flow. Consider a uniformly heated channel of equivalent hydraulic diameter, D, with a subcooled inlet flow rate, G. To a good approximation, we take the flow as steady and incompressible. The momentum equation in the vertically inclined channel is expressed in the usual way in Equation (1).

$$\frac{\partial G}{\partial t} + \frac{\partial (G^2/p)}{\partial z} = -\frac{\partial p}{\partial z} - \left(\frac{f}{2D} + k\right)(G^2/p) + pg\cos\theta \tag{1}$$

By integrating the momentum (Equation (1)) around the loop, we have the sum of the pressure drop components (Rohatgi and Duffey, 1994),

$$\frac{fG^2}{2D}\left\{\frac{Z_\lambda}{\rho_\ell} + \frac{L - Z_\lambda}{\overline{\rho_m}}\right\} + \frac{G^2}{2}\left\{\frac{k_i}{\rho_\ell} + \frac{k_e}{\rho_{me}}\right\} +$$
$$g\left\{z_d\rho_\ell + (z_s - z_d)\rho_g - Z_\lambda\rho_\ell - (L - Z_\lambda)\overline{\rho_m} - (z - L_s)\rho_{me}\right\} = 0 \tag{2}$$

Here we have where, by definition, the subcooled length, Z_λ, is for $X_{in} < 0$,

$$Z_\lambda = -\frac{h_{fg}X_{in}AGL}{Q} \tag{3}$$

and, G, ρ_{me}, k_i, k_e, X_{in}, X_e and X_a are mass flux, mean mixture density in the boiling section, mixture density at the exit, inlet and exit loss coefficients, inlet and exit qualities, and mean quality of the boiling region, respectively.

We have defined mean channel and exit densities given by,

$$1/P_m = v_g + X_a v_g$$
$$1/P_{me} = v_g + X_e v_g$$
$$1/P_{me} = v_g + X_a v_g$$

Equation (2) is now cast in phase-change and subcooling number form (Rohatgi and Duffey, 1994). The resulting expression is, after much algebra and neglecting the small terms with the vapor to liquid density ratio:

$$N_p^2(1 + \overline{k_e}) + N_p\left[(1 - N_s)(2 + \overline{k_e}) + \overline{k_i} + \left(\frac{N_f}{N_{fr}}\right)\left(1 - \frac{2}{L^*}\right)\right] + N_s^2 + \frac{N_f N_s}{N_{fr}} = 0 \tag{4}$$

where,

$$\text{Froude Number} \quad N_f = \frac{gL\rho_\ell^2}{G^2} \tag{4.1}$$

$$\text{Subcooling Number} \quad N_s = \frac{\Delta h_i \rho_\ell}{h_{fg}\rho_g} \tag{4.2}$$

$$\text{Friction Number} \quad N_{fr} = \frac{fL}{2D} \tag{4.3}$$

Phase Change (Zuber) Number $\quad N_p = \dfrac{Q_o \rho_l}{A G h_{fg} \rho_g}$

(4.4)

and

Downcomer Number

$$L^* = L / Z_D.$$

(4.5)

Equation (4) is quadratic in N_p and N_s and the roots provide the possible set of solutions for all liquid single and boiling two-phase flow. We can easily obtain the power required for given flow rate and core inlet subcooling from Equation (4), and vice versa. The Froude number will vary with the flow direction; the downcomer dimension, L^*, is a design parameter; with the non-dimensional length being the ratio of the channel to downcomer heights L^*, and typical values can be taken for the loss coefficients.

The natural circulation map describes the two allowed power and flow relationships for a given heated channel length to downcomer head ratio, L^*, for given loss coefficients and Froude number. The two solutions correspond to single (liquid only) and two-phase flow for the same downcomer number at a given subcooling. The solutions of interest in a boiling loop are in the two-phase region. The intersection at zero subcooling number, for a large exit loss, is given very nearly by,

$N_{p\ (Ns=0)} = (2N_f /k_e N_{fr} L^*) - 1$

(5)

It is clear that the dependency between N_p and N_s is nearly linear for a given set of loss coefficients and downcomer height, L^*. Thus, the power to flow ratio is uniquely defined, and the curves describe the allowed flow states for a particular set of design values for the loss coefficients and relative downcomer height, L^*. It is evident the flow can be bistable about the saturated line.

Since the flow is effectively bistable (double valued) for a given set of conditions, theoretically one can have single or two phase flow for the same pressure drop, an effect that is often observed during flow reversals and instabilities too. The effect of the relative driving head is shown by the following figure, where for a given set of loss coefficients the solutions to Equation (4) is shown for variations in L^*, the relative heated length to downcomer height.

Now variations in downcomer height also can correspond to variations in total loop fluid inventory. The effect of changing total loop inventory on flowrate is determined by the shifts in the void in the boiling regions. So initially decreasing the inventory leads to an increasing flowrate, as the driving head increases since there is more boiling on the "hot" side (the riser or heated section). Eventually as the void increases, the flow reaches a maximum and then decreases as the driving head falls in the "cold leg" or downcomer.

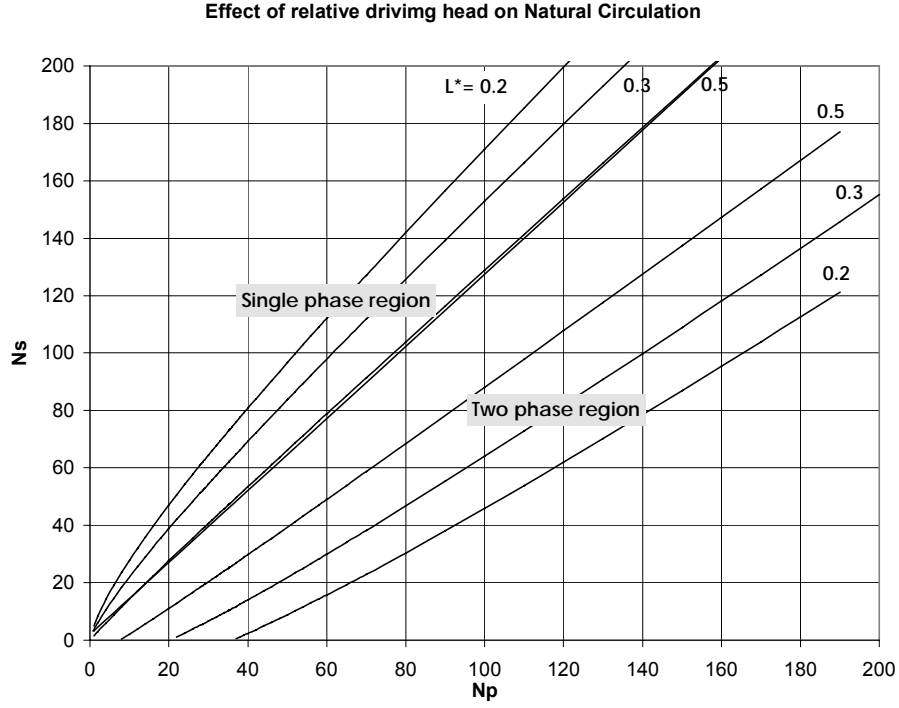**Effect of relative drivimg head on Natural Circulation**

FIG. 1. Solutions to the natural circulation flow equation for varying downcomer driving heads

Physically, the argument can be shown in more detail, and to illustrate the effects, Equation (2) can be solved assuming steady flow, taking a separator elevation equal to the downcomer height, and mean densities taken for the two-phase regions in the hot (riser, *R*) and cold (downcomer, *D*) regions. Lumping the loss terms together into an "effective" loss coefficient (Duffey and Sursock, 1987) it is possible to derive simple equations that describe the general behavior of the flow (and agree with the trends in the data). Thus, the loop flowrate is approximately given by:

$$W = \frac{\hat{W}}{\phi}\sqrt{\left(\frac{1-I}{V_R} + \psi \frac{W_1^2}{\hat{W}^2}\right)} \tag{6}$$

where,

$$\hat{W} = \rho_1 A \sqrt{\frac{2gL}{k_1}}$$

is the maximum possible flow if it were all liquid, and Φ is a two-phase friction multiplier, and I is the fractional liquid inventory in the loop, W_1 the single-phase flowrate, V_R is a measure of the hot side fractional volume to the total system volume, and Ψ is a simple interpolation function for a smooth flow transition. Since it is evident that the two-phase mass flow goes as $(1-I)^{1/2}$, we could maximize the flow in a design by adjusting the values of the losses, relative volumes and heated lengths.

It is well known that a two-phase natural circulation flow can exhibit instabilities over certain regimes (Gulshani et al, 1995) so we now examine that phenomenon and give some relevant analytical results.

3.   GENERAL STATIC INSTABILITY THEORY AND THE ONSET OF CHF

We have derived two results, which enable both the stability and natural circulation characteristics to be evaluated analytically and with the minimum of computation.

The requirement for *both* dynamic and static instabilities is that the increase in the two-phase pressure drop should be either equal to or greater than the decrease in the single-phase pressure drop as the inlet flow decreases. The relevant limit is actually the static (non-linear) instability boundary, which may lead to CHF, has been called the "zeroth mode" of dynamic instability. Thus, in dynamic dispersion-type analysis, it corresponds to the time-independent, zero-frequency (or infinite wave number), real wave number case which, corresponds precisely to the homogeneous equilibrium limit for the flow. In non-linear (called "excursive instability"), the channels could switch from one flow rate to another while maintaining the same total pressure drop. When non-linearly unstable, the channel flow fluctuates, or reverses, and dryout can ensue .

The static limit is the non-linear limit of conditionally instability, where departure from nucleate boiling or critical heat flux will occur at low and high qualities, respectively. There are sufficient data in the literature which show that instability in multiple channels precedes the limit of classic *single* channel (mass-flow controlled) dryout (Mathison, 1967); (D'Arcy, 1967). This differs from the result for the zero frequency condition, which can only be written as a cubic in, (N_s / N_p), and does not give a critical subcooling number. The condition of static instability in parallel channels is the Ledinegg condition (Saha et al, 1976); (Duffey and Hughes, 1991),

$$\frac{\partial \Delta P}{\partial G} = 0 \tag{7}$$

This condition, when applied to Equation (1) and with the vapor to liquid density ratio being small, leads to the following *characteristic Equation* (8), which is derivable after many pages of straightforward but extensive algebra:

$$N_p^2 N_{fr}\left(1+\overline{k_e}\right) + 2 N_p N_{fr}\left[(1-N_s)(2 + \overline{k_e}) + \overline{k_i}\right] + 3 N_{fr} N_s^2 + 2 N_f(2 + N_s) = 0 \tag{8}$$

where N_f, N_s, N_{fr}, and N_p are again the Froude, Subcooling, Friction and Phase Change numbers, respectively. In addition, the k-parameters are loss coefficients normalized with the Friction Number. (The last term in brackets is corrected for a typographical error in the earlier paper (Rohatgi and Duffey, 1994) which omitted the number 2.)

It is important to note that arising naturally from the analysis, the instability region is bounded by the two roots of Equation (8), where the pressure drop versus flow rate is a minimum, maximum or point of inflection. The region of instability for a parallel channel system as bounded by these roots, which correspond to low (subcooled boiling) and high (saturated boiling) vapor qualities. This result has been rederived and confirmed by (Babelli et al, 1995), who retained the vapor to liquid density ratio, and the convective acceleration term, to derive

a "corrected result" more complex than Equation (8). The overall effect of the corrections is generally small. The two roots of the quadratic have been termed the *first and second analytic instability lines* by (Babelli et al, 1995), corresponding to the low and high quality flow states respectively.

The conditions for existence of positive real solution in Equation (8) which is quadratic in N_p and N_s, are as follows:

$$N_s \geq 1 + \frac{\overline{k_i}}{\left(\overline{k_e} + 2\right)} \tag{9}$$

and

$$N_s^2\left(\overline{k_e}^2 + \overline{k_e} + 1\right) - N_s\left[4\overline{k_i} + 2\overline{k_e}\,\overline{k_i} + (1 + \overline{k_e})\left(\frac{2N_f}{N_{fr}}\right)\right] + \overline{k_i}^2 \geq 0 \tag{10}$$

The above equation is also quadratic in N_s and provides a lower bound for the static instability. For large values of N_p and N_s, the asymptotic form of Equation (8), has the limits, for small,

$$\frac{N_p}{N_5} = 1 \, or \, \frac{N_p}{N_5} = 3 \tag{11}$$

or

$$\frac{N_p}{N_s} = 0 \, or \, \frac{N_p}{N_s} = 2 \tag{12}$$

4.   DATA DEFINE REGIONS OF STABILITY AND CHF

The regions of instability and natural circulation are defined by the roots of Equations (3) and (8), using typical values for the loss coefficients. The parametric dependencies come by plotting maps in the convenient non-dimensional space of N_p and N_s. Equation (10) provides the lower limit for inlet subcooling such that the flow will be stable for subcooling below this limit. Flows with the subcooling number greater than the critical subcooling number are potentially unstable, and the region of instability can then be characterized from the roots of Equation (8).

As is well known, the inlet loss coefficient has a stabilizing effect while the exit loss coefficient is destabilizing. As the inlet loss coefficient is increased, the unstable region moves to a higher subcooling number and is smaller; whereas as the exit loss coefficient is increased, the unstable region moves to a lower subcooling number and becomes larger.

The influence of the number of channels, n, is, where the loss coefficients for the parallel channels and components are reduced by a factor of (k/n^2), but the channels are often connected to a common separator, chimney and/or riser at the exit with $k_e = 3$. Therefore, the unstable region is increased, and extends to lower values of the subcooling and phase change

numbers. Thus, in this example, the parallel channels are seen to be more unstable than a single channel, with the exit loss being more significant.

The parallel channel phenomenon is even more complex if the channels are not identical and have different cross-section areas, hydraulic diameters, flow resistance, power and flow (Popov et al, 2000). With channels with different geometry, losses and flow conditions operating in parallel, then the flow can have out-of-phase oscillations and flow diversion, and each channel has its own unstable boundary. If the power is gradually increased in a parallel channel system, keeping the inlet flow and subcooling fixed, the channels first go into subcooled and then saturated nucleate boiling. As power is further increased, the flow in the channels may oscillate as a result of a churn and slug flow regime (especially at low mass flow rates), and flow diversion from one channel to the other may occur.

A similar behaviour is expected when the flow is gradually reduced and the power maintained constant. The flow diversion from one channel into another may lead to local dryout. Therefore, as a first approximation, the metastable minimum and maximum point in the characteristic curve indicate the onset of flow diversion and dryout, respectively. It has indeed been observed that CHF could occur in the negative slope region between the minimum and maximum of the pressure drop vs. flow characteristic curve.

The results indicate that as the Froude number decreases, the flow becomes unstable, where zero Froude number is for horizontal flows, and negative Froude number is for downflow. On the other hand, the critical subcooling number decreases with the increase in the exit loss coefficient, implying that the stable region is smaller. Both these results have been also confirmed for density-wave instabilities.

Stability maps for vertical up, horizontal and down flows are shown in Np vs Ns space, in Figure 2, where the line for zero exit quality demarcates the region such that flows to the left are generally stable. The central ellipsoidal unstable region is bounded by curves that are the loci of two extrema of the pressure drop flow-rate curve. The first characteristic boundary of the unstable region close to the zero-quality line is the precursor of static instability, and represents the transition from the single-phase region to the two-phase region. The second characteristic boundary represents the transition from two-phase region to very-high-void region. One interesting result is that the unstable regions are asymptotic to a value of $N_p/N_s \sim 3$, which is consistent with the asymptotic maximum power limits given by Equation (11). The line near $N_p/N_s \sim 1$ also marks the onset of geysering instability in a closed vertical channel.

5. COMPARISONS TO STABILITY AND CHF DATA

To compare to the prediction of the first and second roots (instability lines) at low and high quality there are many data in the literature. We must know, or be able to estimate or calculate the loss coefficients and use only data where the channel pressure drop is constant, relevant to the reactor situation.

Definitions for the experimental onset of instability are not universal, and were often reported as the onset of density wave oscillations, not static instability, obtained by usually raising the power until some unstable or oscillating flow was observed. Data review yielded over 300 data points, extracted from 30 years of the literature, covering a range of pressures from 0.1 to 19 MPa,(i.e. nearly 1-190 bars), for tubes, rod bundles and parallel channels. In Figure 3, the data and theory are shown, with the density wave data cluster at the lower subcoolings and powers.
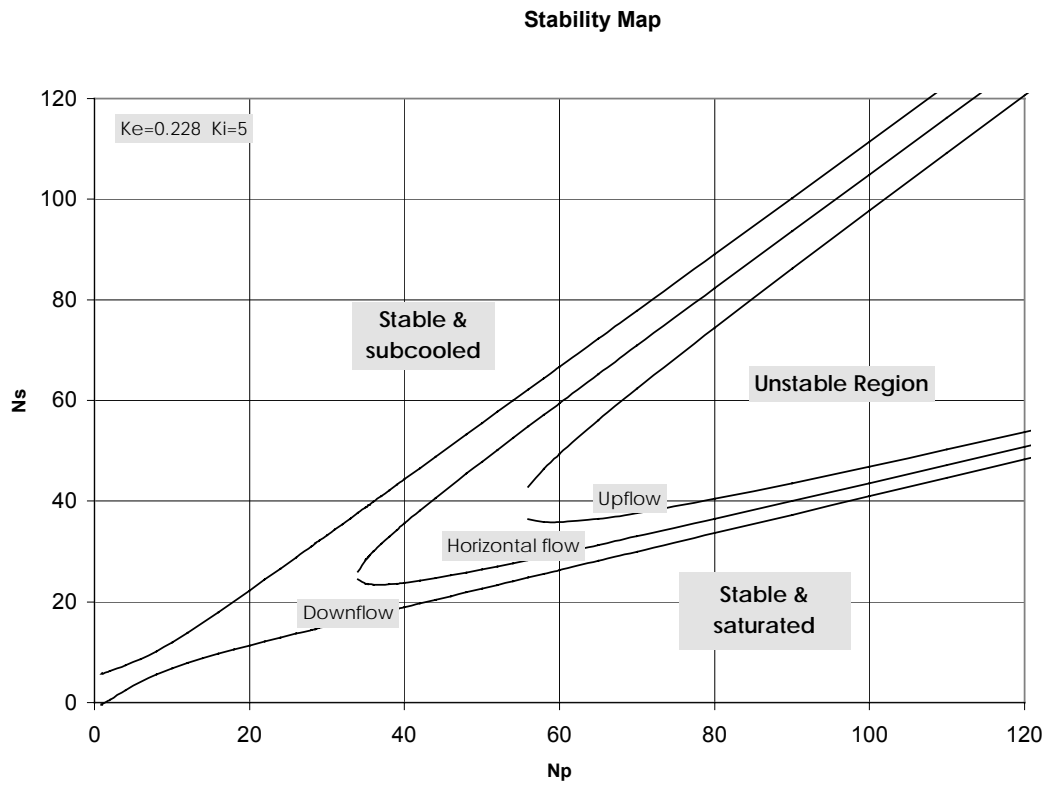
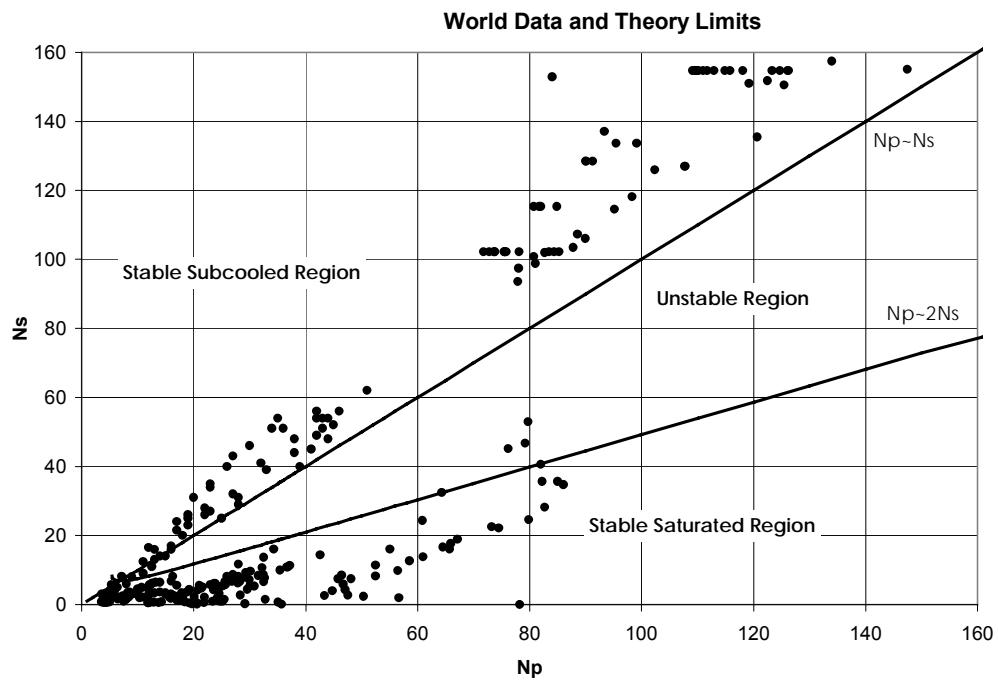*FIG. 2. Typical stability maps for different flow directions.*

FIG. 3. Comparison of data and stability theory showing stability and CHF boundaries.

In non-dimensional N_p versus N_s space, *the data clearly map out a central unstable (uninhabited) region*. The best fit through the lower limit of the saturated data is given by a line of slope ($N_p /N_s) = 3$), which is the asymptotic limit of Equation (8).

From this form of plot we see that stability is possible when operating in the high N_p and lower N_s region, and the first and second unstable lines are given by,

$$N_p /N_s = N*　\hspace{8cm}(13)$$

For the second characteristic line at high quality, we have *N* is O(3)*, from both theory and experiment: for the first characteristic line in the low quality subcooled region, stability is possible when *N* is 0(1)*.

Now, in a natural circulation loop with n channels, we define the region of instability as given by the intersection of the unstable region from the instability with the natural circulation flow. We find that we can maintain stable natural-circulation flow below the critical subcooling number. However, for larger subcooling, the natural-circulation line is in an unstable region and therefore, flow will be unstable. Basically, the downcomer level should be maintained high enough to have imposed pressure higher than the high-void-region extreme of the pressure drop-flow curve.

The intersection of the natural circulation flow with the unstable region for larger downcomer heights *(L* ~ 0.3)* is at a value of N_p/N_s of about *2*, which implies the maximum stable power level for the system is close to the theoretical and experimental stability limit. For lower downcomer heights, *L* ~ 0.5*, the intersection is closer to the minimum value of the unstable region. Thus, we also have the analytical result which determines the instability boundary and the onset of CHF in a natural circulation system.

6.   NATURAL CIRCULATION POWER LIMITS IN ADVANCED DESIGNS

It is important to note that stability limits in natural circulation systems arise before (and as a prelude to) CHF or DNB. Indeed, conventional forced flow CHF and DNB correlations cannot be applied to natural circulation and parallel channel systems if either the loss coefficients are unknown or not reported, or the appropriate constant pressure drop was not maintained or achieved in the tests. Throttling the inlet flow to set a flow boundary condition artificially stabilizes the channel. In actual plants, it is well known that the plant maintains a constant pressure drop, by having multiple parallel channels and/or a controlled downcomer hydrostatic head.

Designs of pressurized systems limit the heat removal to that determined when there is no bulk boiling. The flow is always subcooled, and the heat exchange is by single-phase (liquid) flow in the heat exchanger. Heat removal in normal and accident conditions can be set by the convective heat removal by natural circulation.

We would like to establish the maximum or ultimate heat removal in a natural circulation design where there is a known elevation difference between the heat source (core) and sink (HX). The maximum power limit is when the heat generated is completely removed by the heat exchanger loop, and the HX outlet temperature is close or equal to the secondary side (boiling) temperature. The turbine stop valve (design) pressure of course sets the secondary

side temperature. Thus, there is a relation between the core maximum (saturation or subcooled) temperature, and hence the power, and the secondary pressure.

For the purposes of the maximum design output evaluation, we define the maximum core outlet temperature as the saturation temperature at the primary pressure. Thus the ultimate limit is taken as bulk boiling at the core exit and not conventional DNB. We consider the two-phase (boiling) limit later and use results available from the literature (Duffey and Sursock, 1987); (Duffey and Rohatgi, 1996).

The overall loop flow W, in a natural-circulation system with a thermally expandable fluid, utilizing the Boussinesq approximation, $\Delta\rho = \rho\beta\Delta T$, for the expansion coefficient, β, is given by the well-known result

$$W_{1\Phi} = \left\{ \frac{2A^2\beta\rho_\ell^2 g\Delta ZQ}{c_P K} \right\}^{1/3} \tag{14}$$

Here A is the flow area, K the loop loss coefficient, ΔZ the effective available driving head between the heat source and sink, Q the power, g acceleration due to gravity, ρ_ℓ the liquid density and c_p the heat capacity.

Since the two-phase flow rate $W_{2\Phi}$ in the loop is given very nearly by:

$$W_{2\Phi} \approx \left\{ \frac{2A^2 g\Delta Z\rho_\ell^2 Q}{h_{fg}\theta^2 K} \right\}^{1/3} \tag{15}$$

or

$$W_{2\Phi} \approx W_{1\Phi} \left\{ \frac{c_P}{\theta^2 h_{fg}\beta} \right\}^{1/3} \tag{16}$$

where $\theta^2 = \rho_\ell/(\rho_\ell - \rho_g)$ and h_{fg} is the latent heat and $C_p/h_{fg}\beta$ is a dimensionless evaporation number.

Thus we expect to find that most major loop and system parameters have a relatively weak (one-third power) influence on the flowrate.

6.1. The single phase case

For the *single-phase case,* the natural circulation flowrate is found by integration of the loop momentum equation and coupling this to the energy equation. Thus, the primary temperature increase is given by the standard result,

$$\Delta T = \left(\frac{k_1}{2g\beta\Delta Z} \right)^{1/3} \left(\frac{Q}{\rho_1 c_1} \right)^{2/3} \tag{17}$$

where the fluid thermal expansion drives the convective flow around the loop. Also, from the heat balance across the HX, we have a second relation for the power, taking the primary to secondary temperature difference as close to that due to conduction across the tube wall only, with a correction coefficient for any surface, plugging, corrosion, and thermal resistance effects. To maximize the heat removal we assume the HX to not be limiting in capacity, and hence may take the core outlet temperature as saturated boiling, and the inlet temperature as close to the HX secondary temperature.

From the two expressions for the power, there is the following result for the maximum heat removal in a natural convection loop with onset of bulk boiling at the core exit is the limit,

$$\hat{Q} \propto \left(\frac{k_1}{2g\rho_1^2 c_1^2 \beta \Delta Z} \right) \tag{18}$$

The trends are somewhat counter intuitive for several reasons. The maximum heat removal is very sensitive to the HX design, relies on maximizing the primary to secondary temperature drop, and hence minimizing the core to HX elevation difference, and also maximizing the loop flow resistance.

6.2.   The two-phase case

The other common design is when there is *two-phase boiling flow* with direct steam to the turbine. When steam is fed directly to the turbine, again there is a direct relation of the maximum power output to the secondary (turbine stop valve) pressure. The maximum heat removal is due to the circulation of two-phase mixture when the downcomer is liquid and the core is two-phase and heat removal is then totally evaporative

The maximum power output in a natural circulation boiling system without a HX is *not* derived on the basis when the natural circulation driving head is equal to the two-phase losses. Instead, as we have noted above, the ultimate or maximum power output is set by the onset of flow instability and hence subsequent CHF.

The form of the natural circulation line has been found above to be $N_p/N_s \sim$ *constant* for a given downcomer head to core height ratio, L^*. The limiting maximum power solutions for the unstable case are, from Equation (12) and (13) and the data comparisons in Figure 3,

$N_p/N_s \sim 3$ (19)

with a residual dependency on the loss coefficients. When there is a natural circulation loop, then the intersection of the stability region with the natural circulation flow is very nearly, for typical design values, when,

$N_p/N_s \sim 2$ (20)

By comparing a wide range of parallel or multichannel instability data at high pressure (5MPa) on a N_p versus N_s plot, the data do indeed group around a line given by $N^* = 3 + 10/N_s$ (Rohatgi and Duffey, 1994).

Now the maximum two-phase flow in the whole natural circulation loop at intermediate inventories, is given by Equation 15:

$$W_{2\Phi} \approx \left\{ \frac{2A^2 g \Delta Z \rho_l^2 Q}{h_{fg} \theta^2 K} \right\}^{1/3}$$

Combining the equations for the maximum flowrate at the instability limiting case, we find the hypothetical maximum core power at this maximum flowrate to be:

$$\hat{Q} = \left(\frac{g \Delta Z A^2 \rho_l^3 c_l^3 \Delta T_i^3}{k_l \rho_g h_{fg}} \right)^{1/2} \left(N^* \right)^{3/2} \tag{21}$$

This result clearly shows to optimize the design power output, the minimum loss coefficients, and the maximum elevation (driving) head and flow area should be obtained.

The maximum unstable channel power is less than that ultimately obtainable from the boiling flow in a channel which is given by:

$$\hat{Q} \sim h_{fg} \left(\frac{2A^2 p_e p_g g Z_D}{K} \right)^{1/2}$$

which is typically of order *10MW(t)*. It is therefore important to compare the various limits to see which may be the design constraint.

6.3. The supercritical case

For the supercritical fluid case, near and above the critical point at an absolute temperature, *T*, there is no distinguishable phase-change, but we still have a thermally expandable near-perfect gaseous fluid, with $\beta \approx 1/T$. Thus, to first order only, we have the supercritical flow rate W_{SC}

given by

$$W_{SC} \approx W_{1\Phi} \left\{ \frac{1}{T\beta} \right\}^{1/3} = W_{1\Phi gas} \tag{22}$$

However, the thermal expansion coefficient is, in fact, non-linear with temperature changes near the critical point, as are many other properties, and the Boussinesq approximation is no longer a good approximation. The virial coefficients accommodate this deviation from perfect gas behaviour, but the properties are extremely non-linear near the critical point.

Therefore, for the higher-pressure case we may adopt a numerical analysis, based on iterative integration around the loop of the momentum equation (since mass is also conserved) for varying loop power inputs, using the thermophysical properties of the supercritical fluid as a function of actual thermodynamic state. Thus the general flow variation with major loop parameters (elevations, losses etc.) follows Equation (4) but with a non-linear expansion coefficient.

Taking the necessary boundary condition for parallel channels of constant pressure drop, differentiating the integral form of the mixture momentum equation, we may solve for the critical mass velocity, $<G>$, when the flow is unstable. The case and result for a heated supercritical flow is quite complex and requires numerical evaluation. For the adiabatic supercritical flow case, the analysis greatly simplifies. After making some algebraic manipulations, the criterion results in an unstable mass velocity given by:

$$< G > \propto C \frac{\mu}{D_e},$$

where μ is the kinematic viscosity, D_e the equivalent diameter, and C the constant of proportionality for the Reynolds number dependency of the friction factor. Thus, the dependency of the friction losses and the viscosity variation are quite important.

To investigate the feasibility of natural convection cooling for the primary circuit of a supercritical water-cooled reactor called, a simple steady-state, natural-circulation program was written, including the full physical variations of the thermophysical properties of supercritical water. With the initial and boundary conditions to the core, the operating pressure and temperature, the circuit resistance coefficients and the elevation difference between the core and the heat exchanger were specified. With an initially assumed flow the analysis iterated around the loop on flow to calculate the steady-state density and enthalpies in the circuit. To understand the parametric trends, many thousands of these calculations were done for different input conditions. The trends are shown in Figure 4 which confirms the expected that for a given inlet temperature the outlet temperature increases with increasing channel power, with decreasing elevation difference between core and heat exchanger, and with increasing circuit loss coefficient.
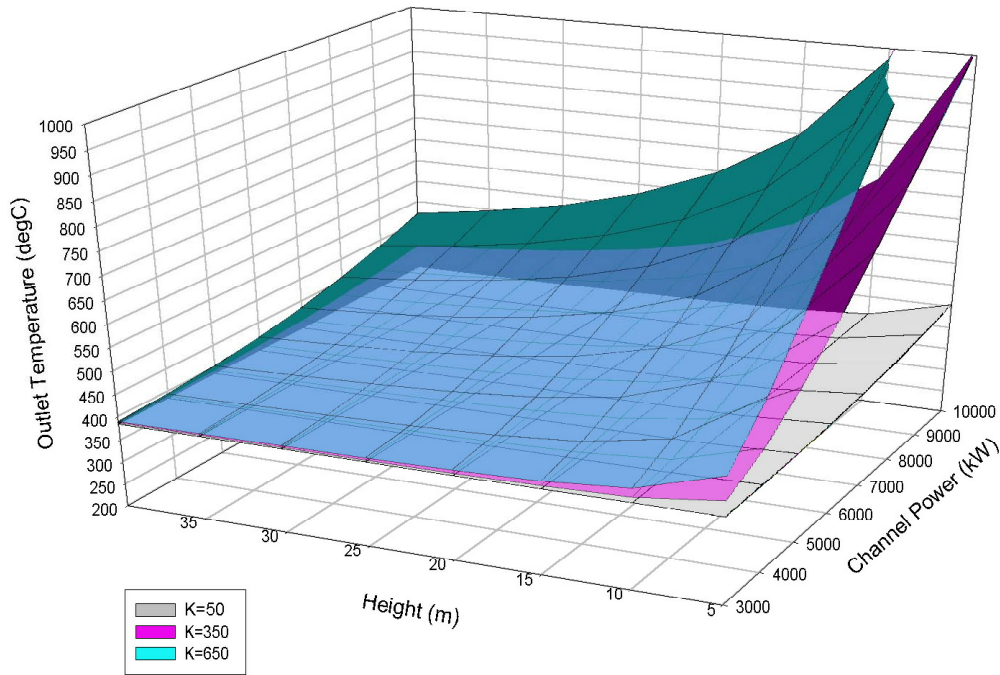
FIG. 4. Typical natural circulation map for SCW flow.

The effect of the large density and enthalpy changes around the critical temperature can be seen when the inlet temperature is a parameter. Below about 370°C, the outlet temperature/channel power surface is relatively flat (except for high loss coefficient combined with high power), whereas as soon as the inlet temperature exceeds 380°C the outlet temperature rises sharply regardless of the channel power and loss factors. If the fluid enters the core below the critical temperature, it is at relatively high density and low enthalpy, and exits above the critical temperature at low density and high enthalpy. The large density difference gives a large natural-convection driving force: the large enthalpy change allows a high channel power with relatively low flow and pressure drop.

To utilize the maximum design flexibility of elevation and loss coefficients within a maximum outlet temperature limit with a high-powered channel, it is necessary to keep the inlet temperature below the critical temperature and the outlet above the critical temperature. If the inlet temperature is allowed to rise above the critical temperature, the much-reduced density and enthalpy changes result in a very much higher outlet temperature.

7. CONCLUSIONS

Explicit equations have been reviewed and stated for the region of static instability for single and parallel channels, as well as for the flow in natural-circulation. The equilibrium results have two roots or solutions, at low and high quality. It was shown that the down flow is more unstable than the up flow. We have stated the expression of critical subcooling number that is the lowest subcooling number for which the flow could be unstable. We have calculated the regions of stability for single and multiple channels with a range of loss coefficients.

Comparisons to a wide range of existing stability data points in tubes, channels and rod bundles show naturally grouping along the low and high quality limits. Analytically and empirically the maximum (second) unstable line has a value of $N_p/N_s) = 3$; and in highly subcooled flows the minimum (first) unstable line has a value of $N_p/N_s) = 0.7$. The region of static instability effectively corresponds to the onset of CHF or DNB in all parallel channel systems with a constant pressure-drop boundary condition.

The analysis enables the power limits for natural circulation in advanced designs to be determined, where the maximum heat removal is set by the stability, CHF or DNB limit. Working and actual illustrations of these limits are given, for single, two-phase and supercritical flows.

NOMENCLATURE

A Flow area

D Hydraulic diameter

f Friction factor

g Acceleration due to gravity

G Mass Flux

h_{fg} Heat of vaporization

k Loss coefficient

K_2 Loss coefficient in the loop

L Heated length

L* Heated length to downcomer height

N_f Froude number

N_{fr} Friction number

N_p Phase change(Zuber) number

N_s Subcooling number

P Pressure

Q Channel power

$\underset{\sim}{\overset{M}{Q}}$ Maximum power

W Mass flow rate

$\hat{W}$ Maximum flow rate

X Quality

Z Vertical elevation

Z_D Downcomer liquid level

Z_s Two phase level in separator

Z_λ Nonboiling (subcooled) length

γ Density ratio,

ρ Density

ν Specific volume

Subscript:
a average
e exit
g vapor
i inlet
l liquid
m mixture

REFERENCES

BABELLI, I., NAIR, S., and ISHII, M., 1995, *"Study of Flow Instabilities in Two-Phase Mixture Flowing Downward in a vertical Annular Channel"*, ASME/AIChE/ANS National Heat Transfer Conference, Portland, Oregon.

D'ARCY, D.F., 1967, *"An Experimental Investigation of Boiling Channel Flow Instability"*, Proceedings Symposium on Two-Phase Flow Dynamics, EUR 4288e, Vol. II, pp. 1173-1223.

DUFFEY, R.B., HUGHES, E.D., 1991, *"Static Flow Instability Onset in Tubes, Channels, Annuli and Rod Bundles*, International J. Heat and Mass Transfer, Vol. 34, No.10, pp. 2483-2496.

DUFFEY, R.B., and SURSOCK, J.P., 1987, *"Natural Circulation Phenomena Relevant to Small Breaks and Transients"*, Nuclear Engineering and Design, 102, pp. 115-128.

DUFFEY, R.B., and ROHATGI, U.S., 1996, *Physical Interpretation of Geysering Phenomena and Periodic Boiling Instability at Low Flows.,* Fourth International Conference on Nuclear Engineering, ICONE 4, ASME/JSME, New Orleans.

GULSHANI, P., and HUYNH, H.M., 1995, *"MMOSS-1: A CANDU Multiple-channel Thermosyphoning Flow Stability Model - Identical Channel Case"*, 16th Annual Conference of Canadian Nuclear Society, Saskatoon, Saskatchewan, June 4-7.

MATHISON, R.P., 1967, *"Out of Pile Instability in the Loop Skalvan"*, Proc. Symp. On Two Phase Flow Dynamics, EUR 4288e, Eindhoven, CEC. Vol. II, pp.1999.

POPOV, N.K., ROHATGI, U.S., RUMMENS, H.E.C., and DUFFEY, R.B., 2000, *"Two-phase Flow Stability in Low Pressure Parallel Vertical Heated Annuli"*, Proc. ASME/JSME/SFEN International Conference on Nuclear Engineering, ICONE 8, Baltimore, Maryland, USA, April 2-6, Paper #8568.

ROHATGI, U.S., and DUFFEY, R.B., 1994, *"Natural Circulation and Stability Limits in Advanced Plants: The Galilean Law"*, Proc. International Conference on New Trends in Nuclear System Thermal Hydraulics, Pisa, Italy, May, Vol.1, pp. 177-185.

SAHA, P., ISHII, M., and ZUBER, N.,1976, *"An Experimental Investigation of the Thermally Induced Flow Oscillations in Two-phase Systems"*, Trans. Am. Soc. Mech. Eng., J. Heat Transfer, Nov., pp. 616-622.

Thermal–hydraulic aspects of CAREM reactor

D.F. Delmastro

Centro Atómico Bariloche,
San Carlos de Bariloche, Argentina

Abstract. CAREM is an innovative reactor with an integrated self-pressurized primary system, developed by Argentina. The primary system coolant circulation is of natural circulation type and several passive safety systems are included. The thermal-hydraulic behavior of CAREM reactor was study using generic numerical codes. Several transients and accidental situations were analyzed. A High Pressure Natural Convection Loop was constructed and operated to produce data in order to verify the thermal hydraulic tools used to design CAREM reactor, mainly its dynamical response. This is accomplished by the validation of the calculation procedures and codes for the rig working in states that are very close to the operating states of CAREM reactor. Several dynamical experiments were performed and new ones are planned. The data obtained is being used to test our numerical procedures and codes. In this paper an overview of the thermal-hydraulic aspects of CAREM reactor is presented. The analytical dynamical studies and experimental facility, studies and results are briefly presented.

1.   INTRODUCTION

The CAREM nuclear power plant design is based on a light water integrated reactor. The whole high-energy primary system, core, steam generators, primary coolant and steam dome, is contained inside a single pressure vessel.

The flow rate in the reactor primary systems is achieved by natural circulation. Figure 1 shows a diagram of the natural circulation of the coolant in the primary system. Water enters the core from the lower plenum. After been heated the coolant exits the core and flows up through the riser to the upper dome. In the upper part, water leaves the riser through lateral windows to the external region. Then it flows down through modular steam generators, decreasing it enthalpy. Finally, the coolant exits the steam generators and flows down through the down-comer to the lower plenum, closing the circuit. The driving forces obtained by the differences in the density along the circuit are balanced by the friction and form losses, producing the adequate flow rate in the core in order to have the sufficient thermal margin to critical phenomena. Reactor coolant natural convection is produced by the location of the steam generators above the core. Coolant acts also as moderator.

Self-pressurisation of the primary system in the steam dome is the result of the liquid-vapour equilibrium. The large volume of the integral pressuriser also contributes to the damping of eventual pressure perturbations. Due to self-pressurisation, bulk temperature at core outlet corresponds to saturation temperature at primary pressure. Heaters and sprinkles typical of conventional PWR's are thus eliminated.

2.   NUMERICAL STUDIES

The thermal hydraulic behavior of the CAREM reactor was study using generic numerical codes. Several transients and accidental situations were analyzed.

The dynamic analysis of the plant during operational transients and accidents has been performed mainly with RETRAN-02 code [1].

As an example, Figures 2 and 3 show the power and pressures evolution for a 5% decrease in the reference value during 150 seconds. In this case a classical controller was used.
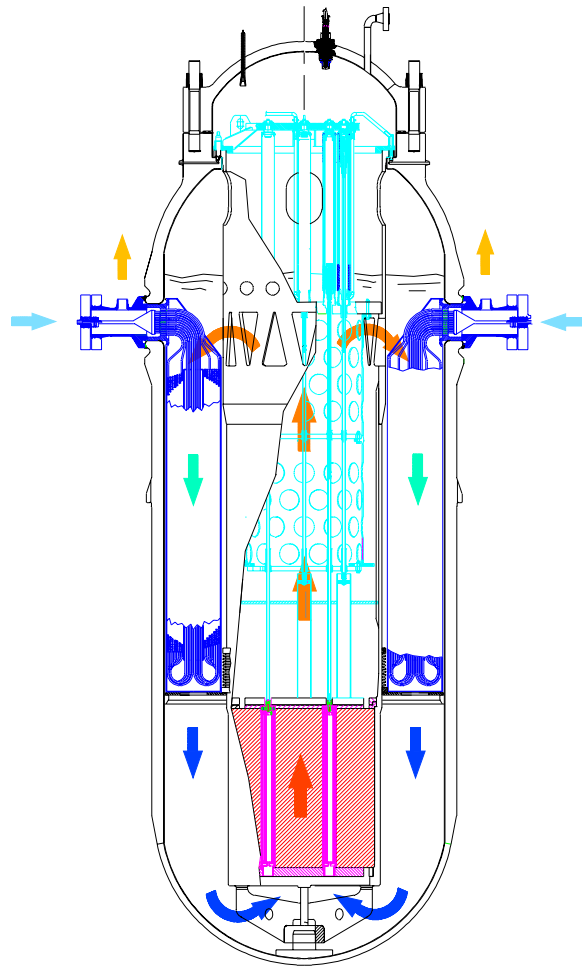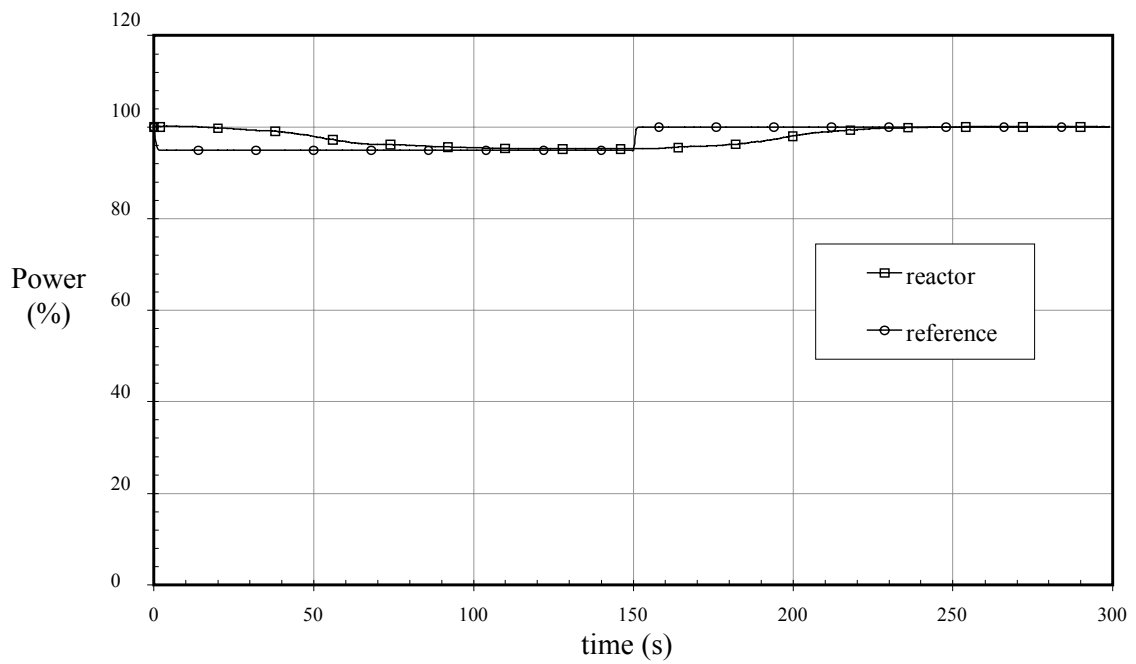
FIG. 1. Primary system cool ant natural circulation.

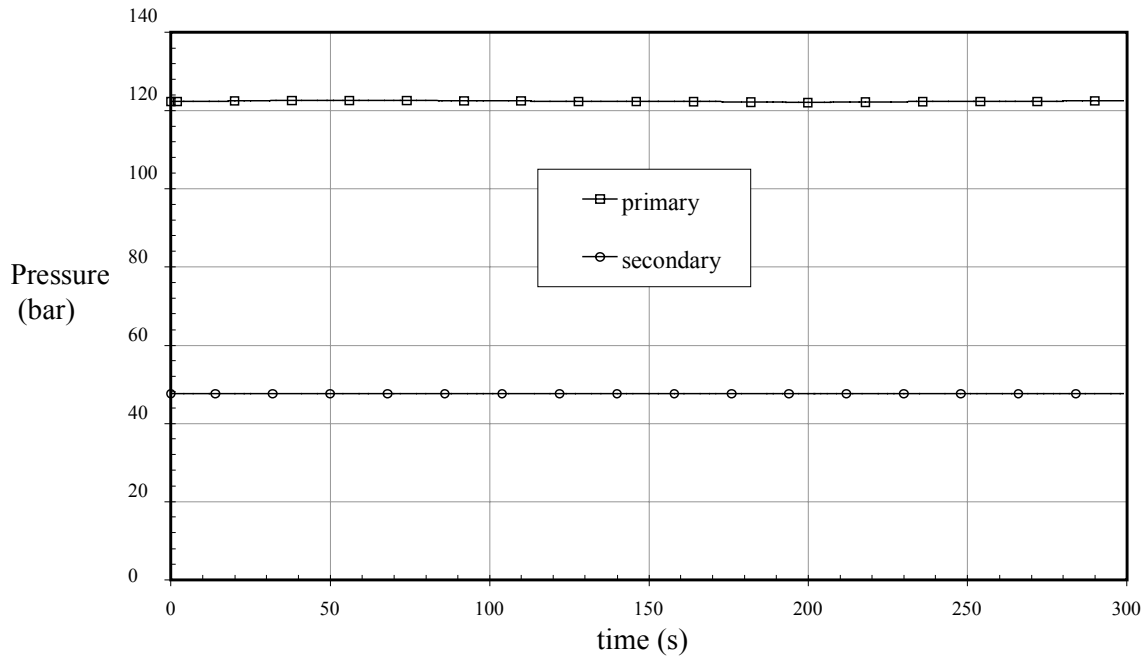*FIG. 2. Power evolution during a temporary decrease of the power reference value.*

FIG. 3. Pressures evolution during a temporary decrease of the power reference value.

3. EXPERIMENTAL STUDIES

A High Pressure Natural Convection Loop (CAPCN) was constructed and operated to produce data in order to verify the thermal hydraulic tools used to design CAREM reactor, mainly its dynamical response. This is accomplished by the validation of the calculation procedures and codes for the rig working in states that are very close to the operating states of CAREM reactor.

3.1. High pressure natural convection loop

CAPCN resembles CAREM in the primary loop and steam generators, while the secondary loop is designed just to produce adequate boundary conditions for the heat exchanger. Water enters the heated section from the lower plenum. The nuclear core is reproduced by electric heaters. The heated water flows up through the riser to the upper plenum where a vapor interphase exists. The water exits this plenum through an outer volume in contact with the steam generator. The steam generator has two coils, once through, secondary inside. The subcooled water flows down through a downcomer or cold leg to the lower plenum. Natural circulation flow may be regulated by a valve in the cold leg and a by pass to the bottom of the riser.

The secondary loop pressures and cold leg temperatures are controlled through feedback loops operating valves. The pump allows the regulation of the flow. The condenser is an air cooled type with flow control.

Both loops allow automatic control and can be pressurized by nitrogen injection.

This rig was constructed according to ASME for the following primary parameters: 150 bar and 340°C. The primary loop may operate in saturated or subcooled regimes, with a heating

power up to 300kW and different hydraulic resistance. The circuit configuration allows the study of stationary states similar to CAREM conditions of pressure, specific flow and enthalpy. Height was kept in a 1:1 scale.

Figure 4 shows a simplified diagram of the facility. A CAPCN general view is presented in Figure 5.
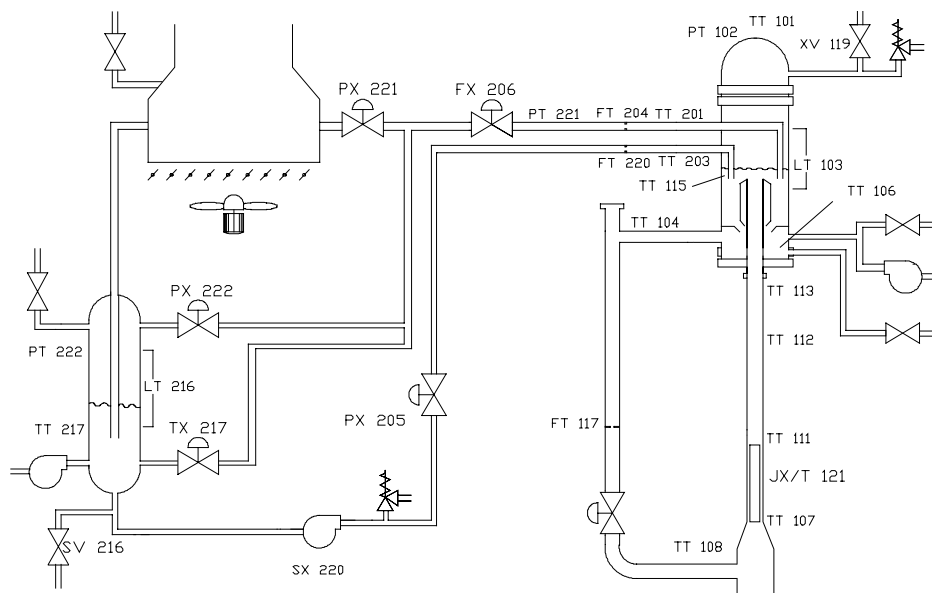
FIG. 4. CAPCN simplified process and instrumentation diagram.
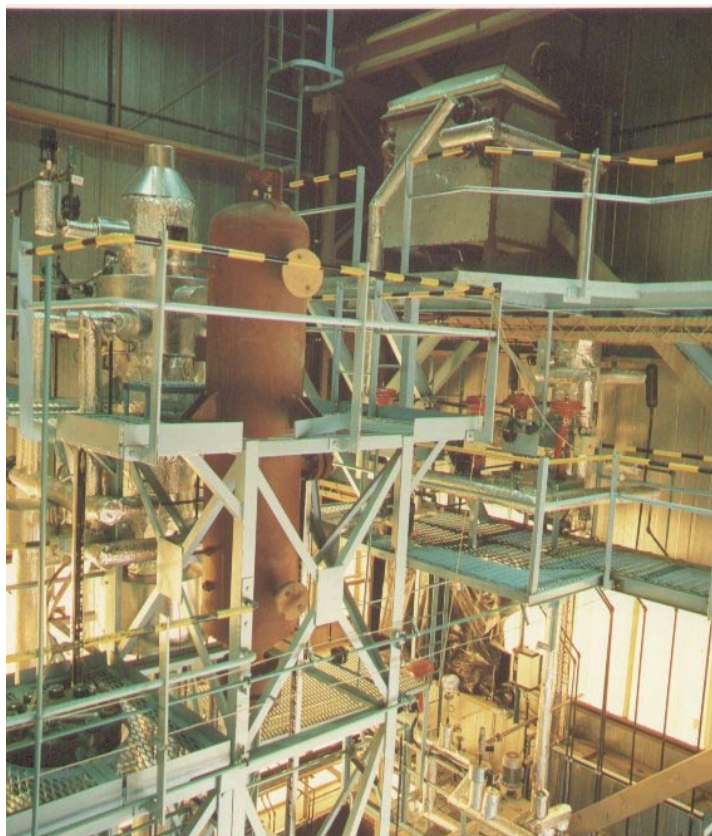
FIG. 5. CAPCN general view.

3.2. Experimental results

Many experiments were performed in order to investigate the thermal-hydraulic response of the system in conditions similar to CAREM operational states. The influence of different parameters like vapor dome volume, hydraulic resistance and dome nitrogen pressure was studied. Perturbations in the thermal power, heat removal and pressure relief were applied [2].

As an example Figures 6 to 8 show the power, pressure and mass flow rate evolution during a heating power increase perturbation. As it can be seen a 5% power increase during 150 seconds produce pressure and mass flow rates increases of 2% and 3%. It was also observed that during this transient the temperature changes were very small.

The dynamic responses at low pressure and temperatures, and with control feedback loops were also studied.

It was observed that around the operating point self–pressurized natural circulation was very stable, even with important deviation on the relevant parameters.
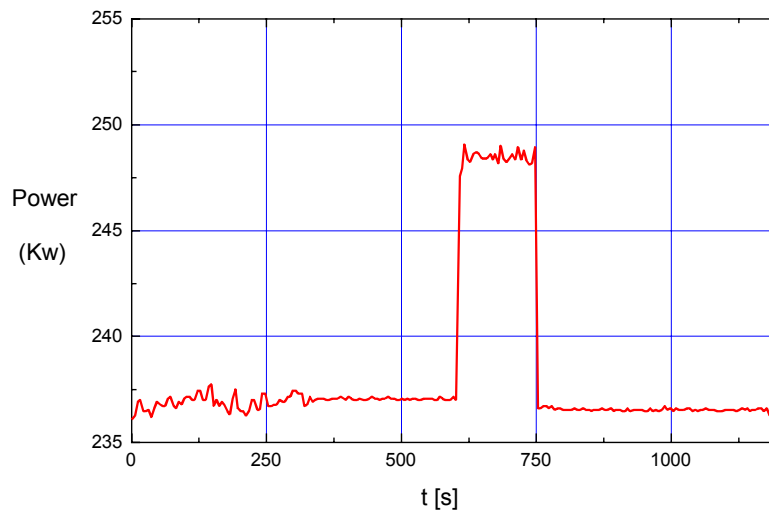
FIG. 6. Heating power increase perturbation.
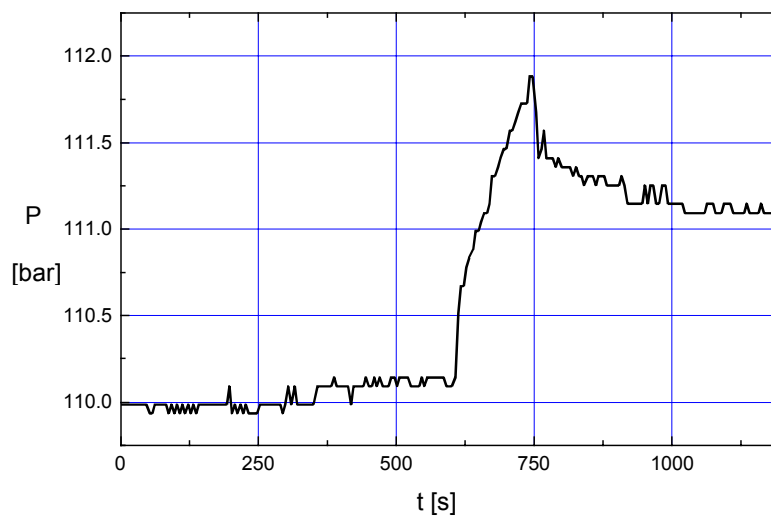
FIG. 7. Pressure evolution during a heating power increase perturbation.
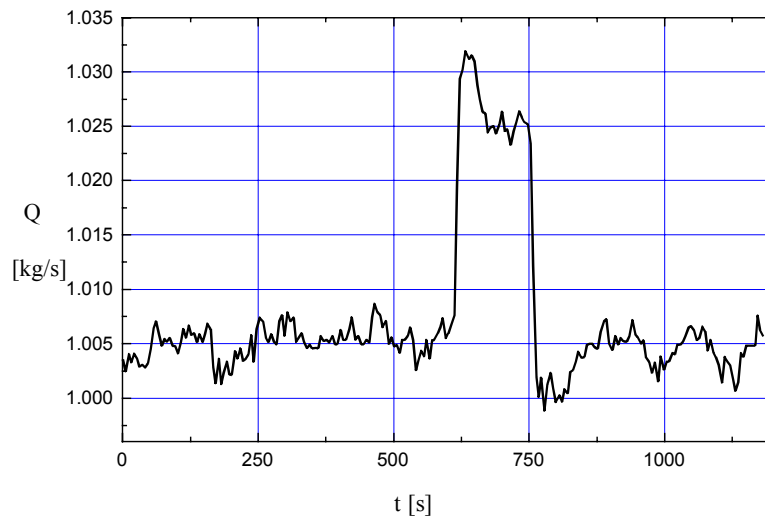
FIG. 8. Mass flow rate during a heating power increase perturbation.

3.3. Results processing and computer models validation

Every transient was graphically display as a verification procedure, in order to identify anomalies that could lead to reproduce a test. The deviations in transients were numerically processed and presented as trend graphs. A sensitive analysis was performed and most sensitive parameters were identified.

A representative group of transients were selected, in order to check computer models.

Simulation models are in current development against a reference transient, without adjustment. When this contrast is clear, models will be compared against the representative group of transients. The information on specific models should be fed in CAREM modeling.

New dynamical experiments are planned, but the final selection will be based on the results of the contrast of the computer models against the representative group of transients.

4. CONCLUSIONS

An overview of the thermal hydraulic aspects of CAREM reactor was presented. The analytical dynamical studies and experimental facility, studies and results were briefly presented.

It was observed that around the operating point self–pressurized natural circulation was very stable, even with important deviation on the relevant parameters.

REFERENCES

[1] RETRAN-02 - A Program for transient Thermal-Hydraulic Analysis of Complex Fluid Flow Systems (1987).
[2] MASRIERA, N.; "Ensayos en el CAPCN del período Mayo – Julio de 1998", 0758-8700-3TAIN-011-1O (1998).

Natural circulation and stratification in the various passive safety systems of the SWR 1000

J. Meseth

Siemens AG, Unternehmensbereich KWU, Germany

Abstract. In some of the passive safety systems of Siemens' SWR 1000 boiling water reactor (i.e. the emergency condensers and containment cooling condensers), natural circulation is the main effect on both the primary and secondary sides by which optimum system efficiency is achieved. Other passive safety systems of the SWR 1000 require natural circulation on the secondary side only (condensation of steam discharged by the safety and relief valves; cooling of the RPV by flooding from the outside in case of core melt), while still other systems require stratification to be effective (i.e. the passive pressure pulse transmitters and steam-driven scram tanks). Complex natural circulation and stratification can take place simultaneously if fluids with different densities are enclosed in a single volume (in a core melt accident, for example, the nitrogen, steam and hydrogen in the containment). Related problems and the solutions thereto planned for the SWR 1000 are reported from the designer's viewpoint.

1. INTRODUCTION

In recent years the Power Generation Group (KWU) of Siemens AG, in conjunction with German electric utilities and with the support of European partners, has been developing the SWR 1000, a medium-capacity boiling water reactor (BWR) with an electrical generating capacity of approximately 1000 MW (Figure 1 presents the conceptual arrangement of the containment). This reactor is evolutionary in its design for normal plant operation. The main difference to the existing Siemens BWR design is the increased water inventory in the reactor pressure vessel (RPV) which allows full depressurization without high-pressure coolant makeup. As a result, no high-pressure flooding system is required for the RPV.

However, this evolutionary development has been supplemented by an innovative approach which involves replacing the active safety systems in part with passive features. If all essential safety functions can be fulfilled by an active system and additionally by a diverse passive system, the probability of loss of both systems due to failure is much lower than with only an active system. The core damage frequency over the plant operational period is thus some 5E-9 per annum. As the passive safety systems are able to become effective without actuation from outside sources, operating personnel are in principle not necessary in order to return the plant to a safe condition. Human error can be more or less ruled out, as operating personnel need not actively intervene after an accident for a period of several days.

The passive safety systems utilize basic laws of physics such as gravity, for example, enabling these systems to function without electrical power supply or actuation by instrumentation and control (I&C) systems. In many of these passive systems and devices, natural circulation is essential under accident conditions, while stratification is essential while in the standby mode (i.e. under normal plant operating conditions). Other passive systems function on the basis of both natural circulation and stratification, while still others require neither natural circulation nor stratification to be effective.

Natural circulation is very effective if phase transitions take place as in an RPV with natural circulation. Here, evaporation occurs in the core which is located at a quite low elevation within the plant design. However, the opposite is also possible, i.e. condensation in an apparatus located at a quite high elevation in the design.
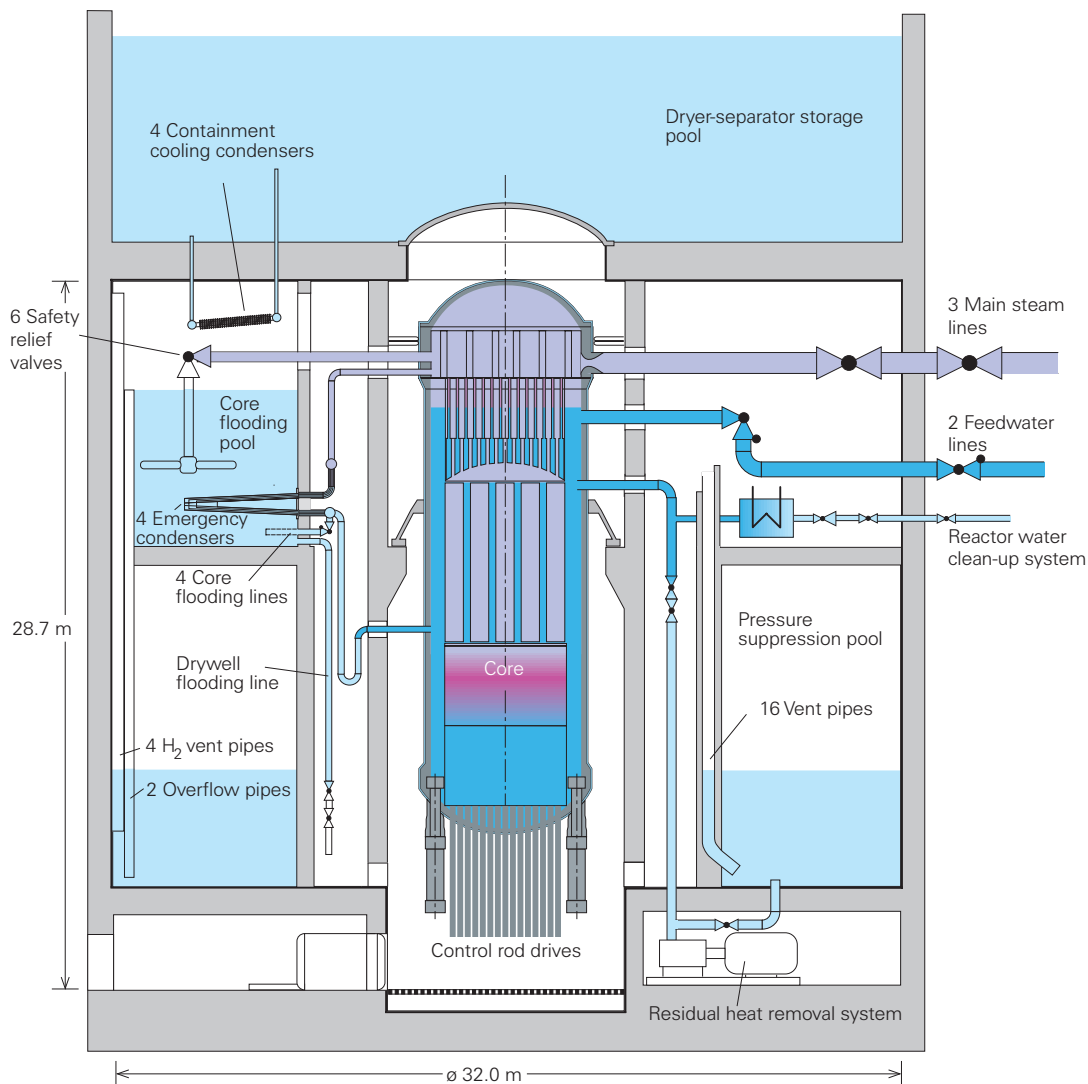
FIG. 1. Conceptual arrangement of the SWR 1000 containment with passive safety systems.

The driving pressures of these passive safety systems are comparably high, i.e. several kPa per meter of elevational difference. It is only in single-phase flows that driving pressures remain low, at only several Pa per meter of elevational difference. If a choice has to be made between single-phase flow and phase-transition flow, the latter is the preferable condition.

In the following, the main passive systems and devices of the SWR 1000 are described with respect to the various conditions in which natural circulation or stratification can take place.

2. EMERGENCY CONDENSERS

The emergency condenser system consists of four separate heat-exchanger subsystems, each having a nominal heat transfer capacity of 55 MW at about 71 bar reactor pressure. The emergency condensers are connected to the RPV without isolating elements, and thus actually form part of the RPV. Each emergency condenser consists of a steam line leading from the RPV nozzle to a heat exchanger tube bundle. This tube bundle is located inside the core flooding pool at a low elevational position. The outlet on the heat exchanger primary side is the reflooding line with integrated anti-circulation loop.
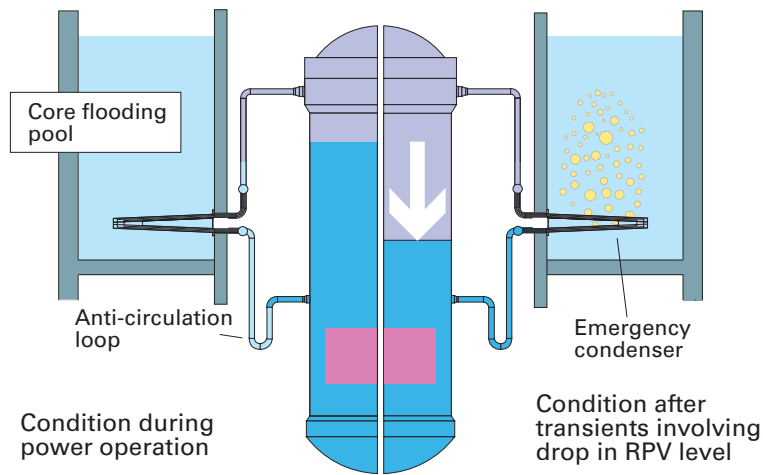
FIG. 2. Conceptual arrangement of emergency condenser
(at normal and reduced RPV water levels).

The working principle of the emergency condenser design is illustrated in Figure 2. Given the normal water level inside the RPV there prevails a stratified condition inside the emergency condenser. The upper part of the steam line is filled with steam while the lower part is filled with water. The water remains cold (except for a small layer below the RPV water level), as the anti-circulation loop prevents hot water from the RPV from entering the reflooding line from below. No convection occurs and thus thermal losses are negligible as long as the water level in the RPV remains normal. The water level in the steam line of the emergency condenser is several meters lower because the density of the water inside the RPV is lower than that of the water in the emergency condenser.

This stratified condition changes to natural circulation if the water level inside the RPV drops by more than 0.7 m. Consequentially, when the water level in the emergency condenser then drops by more than 0.5 m, steam enters the heat exchanger bundle. The steam then condenses inside the heat exchanger tubes and the resultant condensate flows via the reflooding line back into the RPV. If the water level inside the RPV is lower than the inlet nozzle of the reflooding line, the maximum driving pressure differential will be reached at a pressure of about 0.5 bar. This pressure differential is used to overcome the flow resistances in the steam line, heat exchanger tube bundle and reflooding line. The emergency condenser continues to function as long as the water level inside the RPV remains lower than 0.7 m below the normal RPV water level. This has been experimentally tested and verified under the direction of Prof. E.F. Hicken on the emergency condenser test facility at Germany's Jülich Research Center.

On the secondary side, natural circulation also occurs once the emergency condenser begins to work. At low heat transfer rates there is single-phase flow, while at higher rates two-phase flow occurs due to water evaporation. Normally, the water inventory of the flooding pool below the heat exchanger bundle could not be used as a heat sink due to stratification. To overcome this problem, the heat exchanger is enclosed in a chimney. Water enters the chimney at the bottom of the pool and exits at the top several meters above the heat exchanger bundle.

3.   SAFETY-RELIEF VALVE SYSTEM

This system is commonly used in most existing BWR plants. However, the system used in the SWR 1000 features some differences to previous standard designs:

- Three of the six valves work on the pressurization principle and the other three on the depressurization principle, so a common mode failure is not possible due to diversity;

- The quenchers are located in the flooding pool (instead of the condensation pool) at a comparably high elevational position (about 2.5 m below the water level);

- The main valves are activated passively for automatic depressurization by means of diaphragm pilot valves, which in turn are activated by passive pressure pulse transmitters.

On the primary side a forced-flow condition prevails as long as the RPV pressure is more than 0.25 bar higher than the pressure in the drywell. In the pool there would normally be a forced-flow condition near the quenchers and natural circulation at distances greater than 1 m away from the quenchers. With an arrangement such as that in existing BWR plants, only the pool water above the quenchers (or only about 40% of the water inventory) could be used as a heat sink due to the stratification of the warm water above the cold. In the SWR 1000, the quenchers have been modified to prevent this limitation. The quenchers are mounted to the wall of the flooding pool and the more than 2000 quencher holes are directed solely towards the center of the pool. This gives a maximum pulse of about 50 kN for each quencher directed into the pool. These enormous forces lead to forced convection in the pool and to a complete mixture of the water inventory. Restrictions due to natural convection are thus eliminated entirely.

4.   CONTAINMENT COOLING CONDENSERS

In the event of failure of the active residual heat removal systems, four containment cooling condensers (CCC) are designed to remove residual heat from the containment to the dryer-separator storage pool located above the containment. The CCCs are actuated by rising temperatures in the containment. They use natural circulation both on the primary and on the secondary sides. The nominal heat transfer capacity of each condenser is 4 MW based on a containment pressure of 3 bar (absolute) and a cooling water temperature of 100°C. In a hypothetical core melt accident the thermal capacity could be 2 or 3 times higher, depending on the higher containment pressure and temperature. The containment cooling condenser has been experimentally tested at nearly original scale at the PANDA facility of the Paul Scherrer Institute in Switzerland.

The working principle of the CCC is shown in Figure 3. It comprises a simple heat exchanger mounted about 1 m above the water level of the core flooding pool. If the temperature in the drywell atmosphere increases over that in the dryer-separator storage pool, the water inside the heat exchanger tubes heats up. It flows to the outlet line due to the slope of the exchanger tubes. The outlet line ends at a higher elevational level than the inlet line, so the lifting forces are increased for the whole system. Depending on the heat transfer rate and cooling water temperature, secondary-side flow can be either single-phase, intermittent or two-phase.

Depending on the type of loss-of-coolant accident (LOCA) and on the time after onset of accident conditions, the medium on the heat exchanger primary side is either nitrogen, a

nitrogen-steam mixture or pure steam. In the hypothetical case of a core melt accident, a hydrogen-steam mixture would also be possible. Given nitrogen, steam and mixtures thereof, primary flow is downwards because the densities of pure gases and a nitrogen-steam mixture increase with decreasing temperature. This results in the expected downward flow. Condensed steam drops into the core flooding pool. However, the opposite is true for a hydrogen-steam mixture, as the density of this mixture decreases with decreasing temperature, resulting in an upward flow through the heat exchanger tube bundle. This does not pose any problem for the SWR 1000 because both directions of flow on the primary side are equivalent.
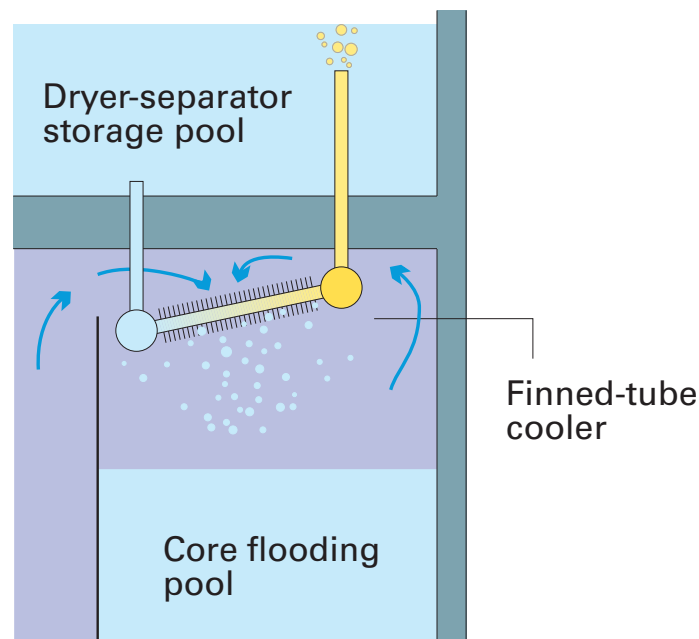
FIG. 3. Conceptual arrangement of a containment cooling condenser.

Nevertheless, problems will arise if more hydrogen is generated than can be accommodated in the containment above the CCCs. The atmosphere in the containment is stratified with a high hydrogen content above the CCCs and a high steam content below. With increasing hydrogen mass the boundary between both stratified regions would drop lower and lower. After a certain time the CCCs would become ineffective because they would be surrounded by cooled hydrogen. To prevent this condition from occurring Siemens designed a hydrogen overflow line. The upper end of this line is located at a higher elevation than the CCCs and its lower end is higher than the lower end of the vent pipes. When the heat transfer capacity of a CCC deteriorates, the pressure in the containment increases until the hydrogen overflow pipe is empty of water (but the vent pipes still contain some water). This produces a forced-flow condition of cooled hydrogen-steam mixture from the drywell to the wetwell. The steam condenses in the wetwell pool and the hydrogen rises into the wetwell pool atmosphere. The hydrogen mass flow is self-controlled. The boundary of the stratified regions stabilizes at a position at which as much steam is condensed as is being generated.

In the case of a hypothetical core melt accident, there first occurs normal natural circulation in the drywell. Later, there is natural circulation with opposed flow directions on the primary side and with stratification between the cold hydrogen above and hot steam below. In the final phases there is a self-induced forced-flow of hydrogen from the drywell to the wetwell. To

simulate all these effects by way of computer code modeling would pose a considerable challenge. The experimental tests performed at the PANDA test facility were much easier, and demonstrated that the entire system is effective and stable, and the pressure differential of several kPa between the drywell and wetwell was generated without any problems.

5.   PASSIVE PRESSURE PULSE TRANSDUCERS

Passive pressure pulse transducers (PPPT) are small heat exchangers with the primary and secondary sides enclosed in a small housing (see FIG. 4). In this design, the primary side is outside the heat exchanger tubes and the secondary side inside. The primary side is connected to the RPV without isolating elements, and thus forms part of the RPV. The pressure on the secondary side during standby condition is more or less atmospheric. The PPPTs were tested at the emergency condenser test facility at Jülich in five different design variants.
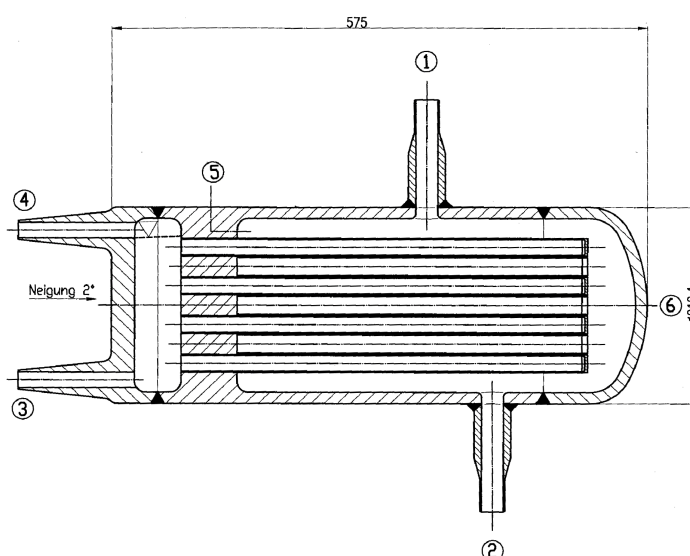
FIG. 4. Drawing of a passive pressure pulse transducer.

The PPPTs function similarly to the emergency condensers: as long as the RPV water level is higher than the reference level, there is stratification on the primary and secondary sides and negligible heat loss. When the RPV water level drops below the reference level, the water level in the PPPTs drops accordingly until steam comes in contact with the heat exchanger tubes. In principle there is natural circulation on both the primary and secondary sides. The water inside the tubes is heated up by the steam and the condensed steam returns to the RPV. When the water inside the tubes evaporates, the pressure on the secondary side increases and would reach primary-side pressure after a longer period of time. A switching device is actuated once the secondary side reaches a pressure of 6 bar (gage) in order to obtain a shorter actuation time period.

Pressure differentials of several Pa on the primary side lead to pressure increases of several bar on the secondary side. This is a good example showing that passive devices are not necessarily connected by small driving or acting forces.

On the secondary side, forced or natural circulation should be prevented in order to obtain short actuation times. Otherwise the main secondary-side water inventory must be heated until a level of 6 bar (gage) is reached. In the last of the five design variants tested, nearly stratified conditions were achieved on the secondary side and the actuation time was only about 5 s.

6.   PASSIVE CORE FLOODING SYSTEM

The four subsystems making up the passive core flooding systems connect the four core flooding pools with the headers of the four emergency condensers. These subsystems each consist of a connecting line and an integrated check valve. Normally the check valve should open when the RPV pressure drops below the pressure at the bottom of the flooding pool, and the water should flow from the flooding pool to the RPV by gravitational force alone. Under such conditions, however, only small forces are available to open the check valve. To eliminate this problem, a spring integrated into the check valve opens the valve at an RPV pressure some 2.5 bar higher than in the case of normal check valves.

When this low RPV pressure is reached, the RPV water level is lower than the inlet nozzle of the reflooding line. This means that the emergency condenser headers are filled with steam. When the spring-loaded check valve opens, steam flows from the header to the core flooding pool and is condensed there by means of a device similar to a quencher. At this point in the process the check valves serve the same function as supplementary relief valves and the pressure drop in the RPV accelerates after the check valves open. This steam blowing phase is the only phase in which natural circulation is used. The warm water of the core flooding pool flows to the water surface and the quencher is always surrounded by cold water.

Once the RPV pressure reaches the same value as that at the bottom of the core flooding pool, flow direction in the core flooding line reverses, and the water flows by gravitational force from the core flooding pool into the RPV irrespective of whether natural convection or stratification prevails in the pool or in the RPV.

The passive core flooding system was also tested at the emergency condenser test facility at Jülich. Experimental results were in a good agreement with the related theoretical analyses.

7.   STEAM DRIVEN SCRAM TANKS

Figure 5 shows the basic design of the SWR 1000 scram systems. The control rods can be inserted into the core in about 70 s by electric drives, or rapid control rod insertion can be implemented within 3 s by means of the hydraulic scram system. In addition there is a boron system which pumps a pentaborate solution into the RPV over a period of some 30 minutes.

The SWR 1000 has four scram tanks operating at a pressure of about 140 bar. In the existing Siemens BWR design this high pressure is generated by nitrogen. The first of the two valves downstream of the tanks is normally in the closed position while the second valve is open. To actuate a scram, the first valve is opened in a very short time and the water is routed from the tanks to the piston drives of the control rods. Several seconds after scram initiation the second valve must be closed. Otherwise the entire water inventory of the tank would be discharged into the RPV, and after that the nitrogen would follow.

It is not allowable for large quantities of nitrogen to ingress the RPV of the SWR 1000, as the emergency condensers would become ineffective given a certain content of non-condensable gases. Therefore, steam serves as the high-pressure medium inside the scram tanks, generated by electrical heating of the upper part of the water inventory such that the upper part of the scram tank is filled with saturated steam and saturated water. Due to the stable stratification no convection occurs inside the tank, and the main inventory of the tank remains cold.

In the event of a scram, the first valve is opened. The cold water flows from the tank to the piston drives of the control rods and the pressure inside the tank decreases. But with decreasing pressure, new steam is generated out of the saturated water inventory such that the pressure reduction is comparably small. Normally the second valve closes after several seconds, as otherwise hot water and steam could ingress the scram system which would generate thermal stresses in the piping which is not designed for strong temperature gradients.
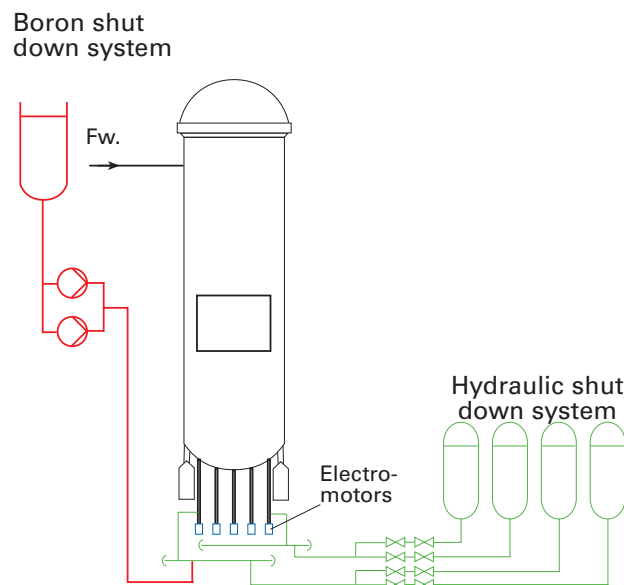
FIG. 5. Conceptual arrangement of the SWR 1000 scram systems.

To avoid thermal stressing in the event that the second valve fails to close, a skirt is integrated into the scram tank. The thermally stratified water behind the skirt remains at its given elevational level after the water level inside the skirt drops due to the outflow of cold water. After a certain time the driving steam comes in contact with the cold parts of the skirt and condenses (see Fig. 6). Thus, the pressure inside the scram tank is reduced by condensation of steam. When the pressures in the RPV and in the scram tank are the same, flow within the scram system ceases despite the fact that both valves are still open.

This scram tank design was experimentally tested at a VVT laboratory in Finland. Results demonstrated that this principle of pressure reduction is effective. Prior to scram initiation, strongly stratified conditions prevailed both inside and behind the skirt. Subsequent to scram, natural circulation developed both behind and inside the skirt. Again, the small pressure differentials of several Pa in the natural circulation circuits resulted in pressure reductions in the scram tanks of some 60 bar and more.
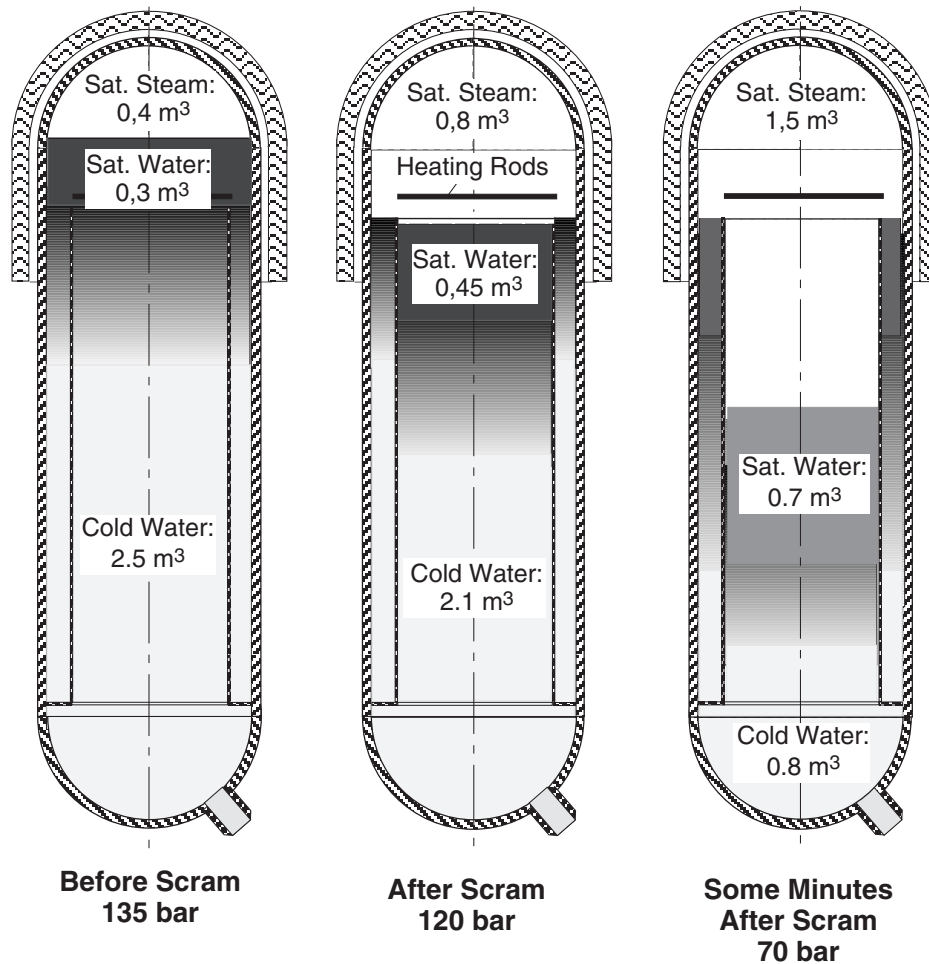
FIG. 6. Pressure reduction in the scram tank by steam condensation with falling water level.

8. FLOODING OF THE RPV FROM OUTSIDE IN A CORE MELT ACCIDENT

When the water inventory of the RPV decreases from about 400 Mg to 160 Mg, the drywell around the RPV is flooded from the core flooding pool when two valves in the flooding line are opened either actively or passively (see Fig. 7). The main aim of flooding the RPV from outside is to achieve long-term retention of even a totally molten core inside an intact RPV. Experiments are in preparation which will show that cooling of the RPV is possible with thermal flux densities far below film boiling despite the numerous nozzles at the RPV bottom.

The water flows downward, driven by gravitational force alone, and fills the space around the RPV within about 30 minutes. At first the water is subcooled, but it heats up due to the hot RPV until evaporation begins. The generated steam flows through openings in the insulation of the RPV to the containment cooling condensers. The condensate again flows downward into the core flooding pool and back to the space round the RPV.

In this case, natural circulation is very effective due to both steam generation at a low elevation and condensation at a high elevation in the same circuit. Because no water is lost in this natural circulation circuit, the passive transport of decay heat takes place as long as the CCCs are filled with water on the secondary side.
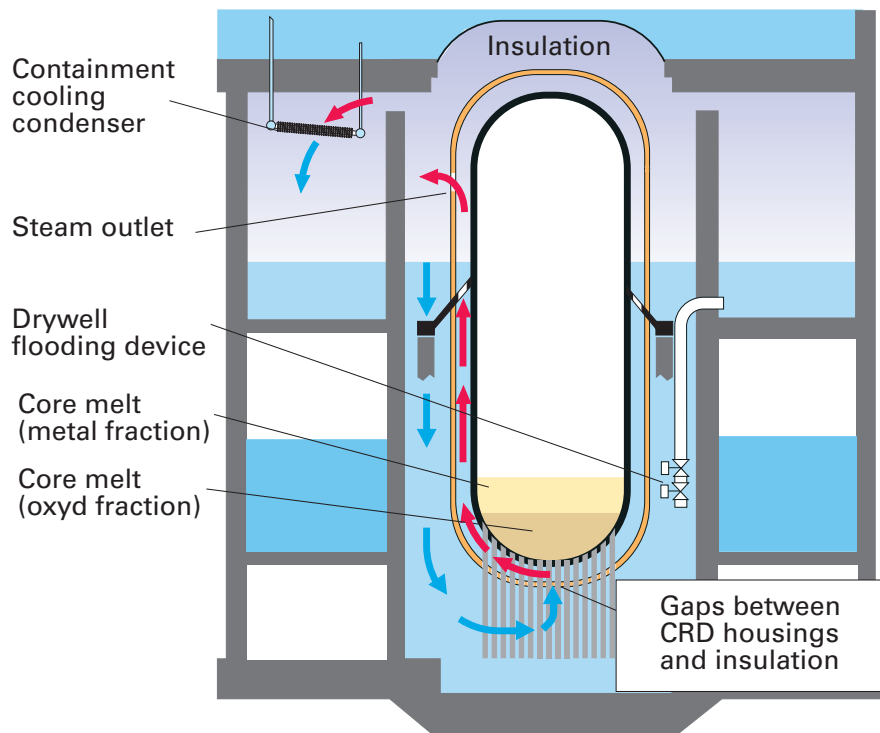
FIG. 7. Conceptual drawing of flooding of RPV from outside during a core melt accident.

9. SUMMARY

It was demonstrated that the change from stratified conditions to natural circulation (and vice versa) is essential for many passive safety systems of the SWR 1000. It would be useful if these flow phenomena could be studied by means of computer code analyses. But in many cases, suitable computer codes are not yet available and development of such codes to serve as a basis for actual decision-making would be too time-intensive.

Designers of new nuclear power plant concepts normally cannot wait until suitable computer codes are ready in order to find solutions to problems. Basic decisions are often made using only a calculator and sound engineering judgement. At the moment it is still easier for the designer to prove its preliminary decisions by way of experimental testing rather than calculational analyses. One can only hope that such computer tools will be available prior to entering the plant design licensing period and that computed results are in good agreement with the results of experimental testing.

Development and validation of natural circulation based systems for new WWER designs

Y.A. Kurakov
Minatom RF, Moscow, Russian Federation

Y.G. Dragunov, A.K. Podshibiakin, N.S. Fil,
S.A. Logvinov, Y.K. Sitnik
OKB Gidropress, Podolsk, Russian Federation

V.M. Berkovich, G.S. Taranov
Atomenergoproject, Moscow, Russian Federation

Abstract. Elaboration and introduction of NPP designs with improved technical and economic parameters are defined as an important element of the National Program of nuclear power development approved by the Russian Federation Government in 1998. This Program considers the designs of WWER-1000/V-392 and WWER-640/V-407 power units as the priority projects of the new generation NPPs with increased safety. A number of passive systems based on natural circulation phenomena are used in V-392 and V-407 designs to prevent or mitigate severe accidents. Design basis, configuration and effect of some naturally driven systems of V-392 design sited at Novovoronezh are mainly reflected in the present paper. One of the most important mean for severe accident prevention in V-392 design is so called SPOT - passive heat removal system designed to remove core decay heat in case of station blackout (including failure of all diesel generators). This system extracts the steam from the steam generator, condenses it and returns water to steam generator by natural circulation. The SPOT heat exchangers are cooled by atmospheric air coming by natural circulation through a special direct action control gates which operate passively as well. Extensive experimental investigation of the different aspects of this system operation has been carried out to validate its functioning under real plant conditions. In particular, full-scale section of air heat exchanger-condenser has been tested with natural circulation steam, condensate and air paths modeled. The environment air temperature and steam pressure condensing were varied in the wide range, and the relevant experimental results are being discussed in this paper. The effect of wind velocity and direction to the containment is also checked by the experiments.

1.   INTRODUCTION

The Program of Russian Federation nuclear power development for 1998-2005 years and for the period till 2010 (approved by Russian Federation Government Resolution No. 815 dated July 21, 1998) has defined that the elaboration and implementation of new generation NPP designs with enhanced safety is the necessary factor of nuclear power extension in Russia. The new generation NPP projects shall meet up-to-date national and international requirements and envisage: (1) the probability of limiting release and serious core damage at beyond-design accidents less than 10^{-7} and 10^{-5} per reactor-year, respectively; (2) reduction of urgent evacuation area to 300-500 meters and emergency planning area to protect the population in case of beyond-design accidents to 700-3000 meters.

The safety of new NPP is provided by consistently implementing the defense-in-depth principle, based on the application of a system of barriers in the way of ionizing radiation and radioactive substance release into the environment, and also by realizing the engineering and organizational activities to protect these barriers. The National Program of nuclear power development considers the design of 1000 MW power unit with WWER-1000/V-392 reactor to be the priority project of new generation plants. This unit is so designed that radiation effect on the population and the environment is considerably below the allowable values established

by the up-to-date regulatory documentation. The permit of Russian Federal Nuclear and Radiation Safety Authority (Gosatomnadzor) was granted to construct the power units with V-407 reactor plant on the Sosnovy Bor and Kola sites and two units with V-392 reactor plant on the Novovoronezh site.

Extensive application of passive safety means, using natural physical processes, along with the traditional active systems is a specific feature of both these designs. The IAEA Conference on "The Safety of Nuclear Power: Strategies for the Future" [1] has noted that the use of passive safety features is a desirable method of achieving simplification and increasing the reliability of the performance of essential safety functions, and should be used wherever appropriate. However, the application of passive means is connected with some problems, which have to be solved by each plant designer. The passive systems have their own advantages and drawbacks in comparison with the active systems both in the area of plant safety and economics. Therefore a reasonable balance of active systems and new passive means is adopted in V-392 design to improve safety and public acceptability of nuclear energy.

One important problem related to the implementation of the passive means is that, in the most cases, sufficient operating experience of the passive systems/components under real plant conditions does not exist. Besides, the existing computer codes for transient and accident analysis are not sufficiently validated for the conditions and phenomena which are relevant to the passive system functioning (low pressure, low driving pressure and temperature heads, increased effect of non-condensable, boron transport at low velocities, and the like). As a result, the time- and money-consuming research and development works may be needed individually for each reactor concept to validate the operability of the passive safety means proposed in the design. Therefore, the extensive experimental investigations and tests have been already performed and are being planned to substantiate the design of the safety features proposed for new units with WWER-1000/V-392 and WWER-640/V-407 reactor plants.

2. PASSIVE SYSTEMS IN NEW WWER DESIGNS

Safety features desired in future plants have been summarized by INSAG-5 in "The Safety of Nuclear Power" [2]. It notes that the Basic Safety Principles of INSAG-3 [3] remain valid and should become mandatory, and the extension of INSAG-3 principles gives further opportunities for improvement of safety on which new plant designs should begin to draw. These opportunities include several design approaches such as avoiding complexity, reducing dependence on early operator actions, among others, and include specifically giving considerations in the design process to passive safety features. Such functions as the containment heat removal, hydrogen management, core debris cool down and prevention of the containment floor melt-through are probably among the most appropriate areas for passive systems usage. Both novel and more or less proven passive means are proposed in many new water-cooled reactor designs [4] to fulfill these and other functions.

Some future reactor designs have only added a few passive components to the traditional systems, some others make wide use of the passive systems and components. New WWER concepts V-392 and V-407 are of this last category since a number of relatively innovative passive safety means are implemented in these designs to ensure or to back up the fundamental safety functions: reactivity control, fuel cooling and confinement of radioactivity.

2.1. Reactivity control

Traditional gravity-driven control rods are the main system to ensure reactor scram both in currently operating and new WWERs. For existing pressurized water reactors, this system is not sufficient to bring the reactor to a cold shutdown state; therefore the control rod system of existing WWERs is supported by pumped emergency supply of the borated water to the primary circuit. New WWER designs V-407 and V-392 have an increased number of gravity-driven scram rods to maintain shutdown margin even in the absence of boron supply during the reactor cooling down.

Although very good reliability records exist for scram excitation, some failures of the gravity-driven control rod insertion have been recognized. The failures occurred for the different reasons; in particular, the cases of insertion speed reduction and incomplete insertion due to fuel assembly deformation have been reported during last ten years (see for example [5]). Besides, some failure modes may be considered which could prevent all the control rods to insert, and it was the basis for designers to analyze Anticipated Transient Without Scram events.

Keeping that in mind, for WWER-1000/V-392 a special quick boron supply system has been designed as a diverse system to the gravity-driven scram system. A concentrated boron solution tank is connected to the suction and discharge pipes of each main coolant pump. The valves in the connecting pipes will automatically open if there is a demand for reactor trip but the reactor power after some time is higher than its value after scram should be. The concentrated boron solution is supplied to the reactor due to pressure difference between discharge and suction of the main coolant pump (pump head). Inventory and concentration of the boron solution is selected to ensure compliance with safety criteria in the design events accompanied by control rod system failure to trip the reactor. Even in case of loss of power, the pump head during coastdown is sufficient to push all the boron solution from the tank (i.e. for this case the boron supply function is ensured passively). The operability of the quick boron supply system has been confirmed by extensive experimental investigation using a scaled model.

2.2. Fuel cooling

The safety function "fuel cooling during transients and accidents" is ensured by provision of sufficient coolant inventory, by coolant injection, sufficient heat transfer, by circulation of the coolant, and by provision of an ultimate heat sink. Depending on the type of transient/accident, a subset of these function or all of them may be required. Various passive systems and components are proposed for WWER-1000/V-392 and WWER-640/V-407 reactor concepts to fulfill these functions.

For WWER-640/V-407 reactor, steam generator passive heat removal system (SG-PHRS) which does not require the electricity supply is designed to remove the decay heat in case of non-LOCA events and to support the emergency core cooling function in case of LOCAs. Reactor coolant system and passive heat removal equipment layouts provide heat removal from the core following reactor shutdown via steam generator to the tanks of chemically demineralized water outside the containment and further to the atmosphere by natural circulation as it is shown in Figure 1. Reactor power that can be removed from the core by coolant natural circulation is about 10% of the nominal value, which guarantees a reliable

residual heat removal. Thus, in case of non-LOCAs the decay heat is removed by coolant natural circulation to steam generator boiler water. The steam generated comes into the passive heat removal system where steam is condensed on the internal surface of the tubes that are cooled on the outside surface by the water stored in the demineralized water tank outside the containment. The water inventory in this tank is sufficient for the long-term heat removal (at least 24 hours) and can be replenished if necessary from an external source.
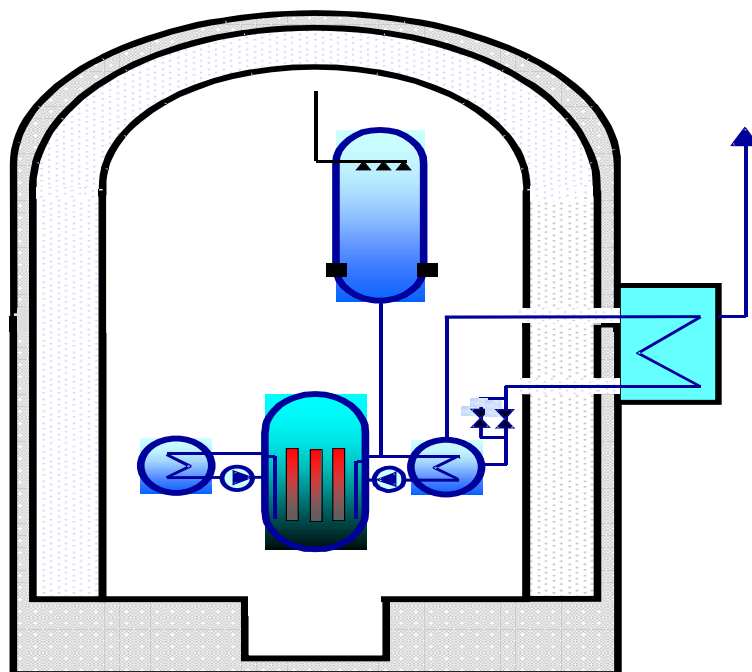
FIG. 1. V-407. Passive heat removal for non-LOCAs

Containment passive heat removal system (C-PHRS) of V-407 reactor removes heat from the containment in case of a LOCA and is designed to fulfill the following functions: (1) emergency isolation of service lines penetrating the containment and not pertaining to systems intended to cope with the accident; (2) condensation of the steam from the containment atmosphere; (3) retention of radioactive products released into the containment; (4) fixing of the iodine released into the containment atmosphere. The steam from the containment atmosphere condenses on the internal steel wall of the double-containment being cooled from the outside surface by the water stored in the tank. So, the system operates due to natural circulation of the containment atmosphere and water storage tank. The design basis of this system is to condense the amount of steam equivalent to decay heat release during 24 hours after reactor trip without the water storage tank replenishment.

The emergency core cooling system of V-407 reactor comprises three automatically initiated subsystems: (1) hydroaccumulators with nitrogen under pressure, which are the traditional ECCS accumulators being used at operating WWER-1000 reactors, (2) elevated hydrotanks open to the containment, and (3) equipment for deliberate emergency depressurization of the primary circuit. All these subsystems are based on the principle of passive operation providing for long-term residual heat removal in case of a loss-of-coolant accident accompanied by the plant blackout (i.e. AC power supply is not needed for ECCS operation). In the first stage of the accident, primary pressure is decreased due to loss of coolant and operation of the passive heat removal system. The further cooling down and pressure decrease are realized via steam

generator PHRS and containment PHRS. When the pressure difference between primary circuit and containment has decreased to 0.6 MPa, the passive valves of the emergency depressurization system open connecting reactor inlet and outlet with the fuel pond space. When the reactor and containment pressure difference has decreased below 0.3 MPa, the ECCS hydrotanks begin to flood the reactor. This sequence results in creating of so called emergency pool where the reactor coolant system is submerged to and in connection of this emergency pool with the spent fuel pond. The natural circulation along the flow path shown in Figure 2 (reactor inlet plenum - core - reactor outlet plenum - "hot" depressurization pipe - fuel pond - "cold" depressurization pipe - reactor inlet plenum) provides the long-term heat removal from the core in case of a LOCA combined with loss of all electric power. The water in the emergency pool and spent fuel pool reaches the saturation point in about 10 hours. The steam generated will condense on the internal surface of the steel inner containment wall, and condensate flows back into the emergency pool. This configuration ensures also the heat removal from reactor vessel bottom to keep the corium inside the reactor in case of postulated core melt event.
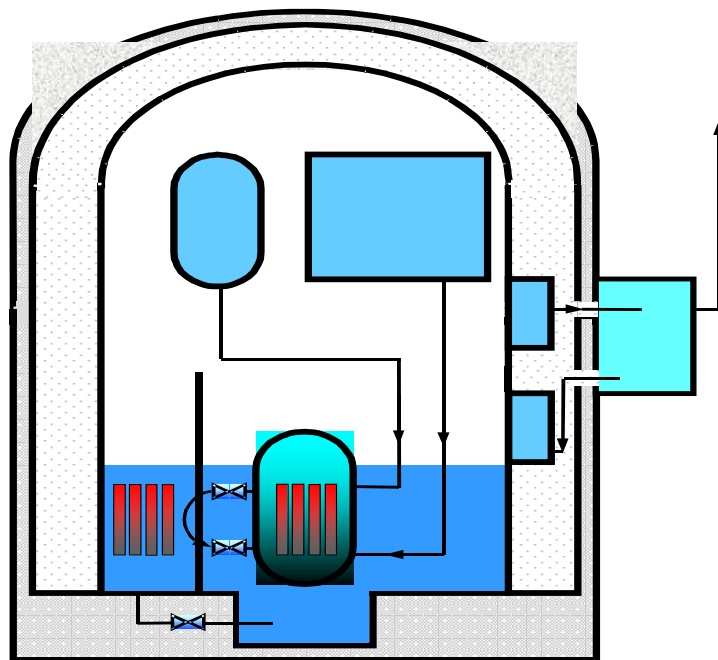
FIG. 2. V-407. Passive heat removal for LOCAs

The passive residual heat removal system (PHRS) is included in the V-392 design to remove heat from the reactor plant. The design basis of this system is that in case of station blackout, including loss of emergency power supply, the removal of residual heat should be provided without damage of the fuel and of the reactor coolant system boundary for a long time period. The PHRS consist of four independent trains; each of them is connected to the respective loop of the reactor plant via the secondary side of the steam generator. Each train has pipes for steam and condensate, valves and modular air-cooled heat exchanger installed outside of the containment as it is shown in Figure 3. The steam that is generated in the steam generator due to the heat released in the core condenses in the air-cooled heat exchanger, and condensate is returned back to the steam generator. The motion of the cooling media (steam, condensate and air) takes place in natural circulation.
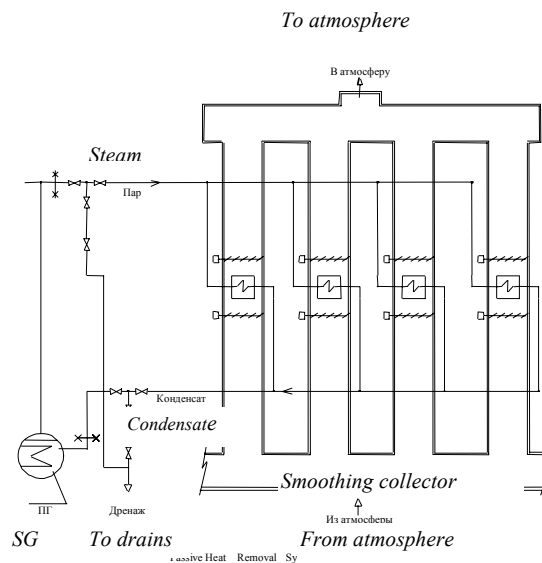
To atmosphere

В атмосферу

Steam

Пар

Конденсат

Condensate

Smoothing collector

Из атмосферы

ПГ   Дренаж

SG   *To drains*   *From atmosphere*

Passive Heat Removal Sy

FIG. 3. V-392. Passive heat removal system

The passive system for reactor flooding during LOCA in V-392 design comprises two groups of hydroaccumulators as it is shown in Figure 4. First group (so called first stage accumulators) consists of four traditional ECCS accumulators being used at operating WWER-1000 reactors; these accumulators are pressurized by nitrogen to 6 MPa and connected in pairs to the upper and lower plenums through special nozzles in the reactor pressure vessel. Second stage accumulators are 8 tanks connected to the reactor coolant system through the check valves and special spring-type valves. These valves are kept closed by the primary pressure; when the primary pressure drops below 1,5 MPa, the spring open the valve. Such a connection configuration and valve design ensures continuity of hydrostatic head irrespective of the primary pressure change during an accident. Installation of hydraulic profiling of the outlet route ensures a step-wise limitation of the water flow rate from the tank when the water level in the tank is decreasing. The water inventory in the second stage accumulators (about 1000 t) ensures the core cooling for 24 hours during a LOCA even if all active ECCS mechanisms are inoperable. Joint operation of the second stage accumulators and SPOT gives a possibility to increase the period indicated.

2.3.   Confinement of radioactivity

This safety function is ensured by protecting and maintaining the integrity of the potential radioactivity release barriers (fuel, reactor system boundary and containment). These barriers are passive components as themselves; in addition, several passive means are proposed in V-407 and V-392 concepts for the protection of these barriers (some of them are reflected above). As the containment is the last and most important barrier, both these designs imply substantial improvement of the containment protection against different loads related to

design basis and severe accidents, and various passive systems are important part of this protection in V-407 and V-392 designs. This design decision is derived from the assumption that the active systems are more vulnerable to failures under conditions inside the containment during an accident.

In V-407 design, containment over-pressurization is avoided by passive containment cooling system (C-PHRS) as described above. To limit considerably the release of fission products beyond the containment, a permanent under-pressure is maintained in the inter-containment gap of the V-392 design. This safety function, one of the most important, is fulfilled by two systems: (1) an exhaust ventilation system equipped with a filtering plant with suction from the inter-containment gap and outlet into the stack; (2) a passive system of suction from the inter-containment gap. The first system is intended to control removal of steam-gas mixture from the inter-containment gap under accidents with total loss of power. The system is capable to remove at least 240 kg per hour that is equivalent to the inner containment leaks of 1.5% containment volume per 24 hours. The second system consists of lines connecting the inter-containment gap with the PHRS exhaust ducts, which are always in the hot state. This solution enables permanent removal and purification of inner containment leaks irrespective of the electricity supply and operator actions. According to estimations, the under-pressure is maintained at any point of the inter-containment gap with inner containment leaks up to 2.8% of containment volume per day (the design basis for the containment is 0.3%). The technical solution described above in combination with the systems for the containment pressure decrease (traditional spray system and new passive heat removal system) allows to give up the filtered venting system designed for V-392 in spite of this system follows the current requirements that filtered venting should not increase the risk of loosing the containment function and filtered venting is not required in the short term of a core melt accident.

Special systems and components are implemented in both new WWER designs to prevent hydrogen burning or explosion. For example, in V-392 design the hydrogen suppression system comprises passive catalytic hydrogen igniters based on an efficient high porosity cellular material. Each of 50 elements of this system is capable to oxidize about 30 grams of hydrogen per hour at its volumetric concentration 4%. This system prevents the explosive concentration of hydrogen even if 100% of the core Zr will be oxidized during an accident.
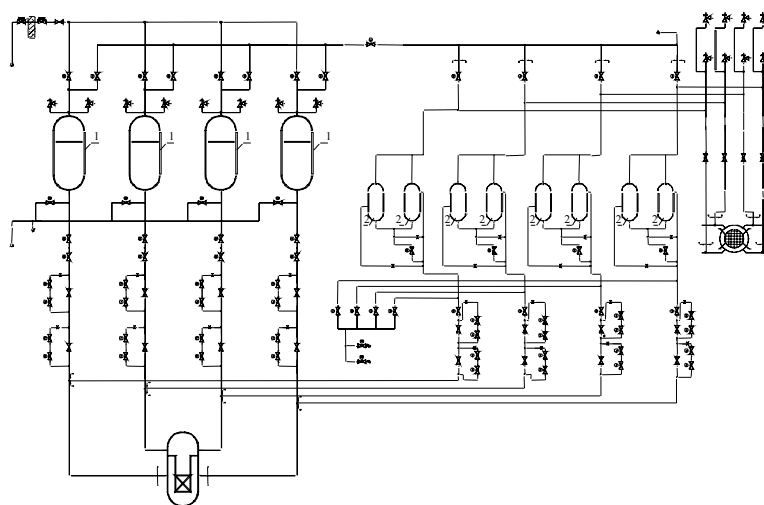

FIG. 4. V-392. Passive core flooding system

3.   RESIDUAL HEAT REMOVAL SYSTEM FOR NVAES-2

Functional and structural diversity of WWER-1000/V-392 safety systems provide deep protection against common-course failures, and application of passive systems and active systems actuation without personnel interference yield deep protection against human errors. These engineering solutions used in NVAES-2 design enable the attainment of increased safety level, compared to the existing WWER-1000 plants.

For existing plants where the most of safety functions are ensured by active systems, the electric power supply is an important precondition for the successful operation of the safety systems. In spite of the very reliable emergency power supply from diesel-generators, loss of offsite power remains to be very essential contributor to the estimated core melt frequency from the internal initiating events (for example, more than 80% for unit 4 of Balakovo NPP [6]). For NVAES-2 with V-392 reactor plant, this figure is reduced to about 30% at absolute value 7.91×10^{-9}. As a whole, total core melt frequency for NVAES-2 is about three orders of magnitude less than for Balakovo-4 which is the latest WWER-1000/V-320 unit commissioned in Russia.

Passive residual heat removal system from the core via steam generators to the atmosphere as the ultimate heat sink (so called SPOT) plays an important role in the core melt frequency reduction mentioned above. The design basis for this system is that in case of station blackout during the most unfavorable atmosphere conditions the heat removal capacity with account for the failure of one channel shall amount to not less than 2% of the reactor rated power. The heat removal at the initial stage of the accident is performed due to partial water evaporation from the secondary side via steam generator relief valves to the atmosphere.

The SPOT system consists of four groups (corresponding to the number of reactor coolant system loops) of closed natural circulation circuits. In the ribbed tubular air-cooled heat exchanger (four heat exchangers for each of these circuits), steam extracted from the steam generator condenses, and the condensate flows by gravity to the steam generator boiler water volume. Under normal reactor plant operation, the SPOT system is under standby when all the SPOT circuits are in the warmed-up state. In case of plant blackout, the SPOT state changes from the standby to the operating condition. In addition to its main purpose (core decay heat removal in case of complete loss of a.c. power), the SPOT system can maintain the hot standby parameters of the reactor plant; for this purpose the SPOT has a special controller. The system is thermally insulated, so the heat losses in standby conditions are less than 0.1% of reactor rated power. Natural circulation in the SPOT system is provided by the corresponding layout of the steam generator, heat exchanger and draught air duct.

The steam circuit pipeline runs from fresh steam line to collector which distributes the steam by smaller tubes to four heat exchanger. The condensate from each heat exchanger is supplied by tubes to the collecting receiver and then by pipeline to the steam generator. Two isolation valves are installed at heat exchanging module inlet and outlet to isolate it in case of damage or maintenance. Small diameter pipelines with valves installed on them are provided for removal of air from heat exchanger when filling them with water during hydrotest and for periodical removal of non-condensables under standby conditions. Cooling air is taken from the atmosphere outside the reactor building. Air goes through the protective net and enters the annular corridor located around the reactor building and then to the heat exchanging modules. The air takes the heat from the steam and goes to the draught air ducts, which have the common outlet collector-deflector. Inlet and outlet gates and controller are installed on the airside of each heat-exchanging module. The gates open to switch on the heat exchanging

module to operation. The controller can be used to change the airflow rate to ensure additional SPOT system functions (for example, to maintain the reactor plant in the hot standby conditions).

Under standby conditions, the I&C system ensures for each heat exchanging module the measurements of the air inlet and outlet temperature, outlet air humidity, water level and temperature in the condensate lines. Information on the air humidity is especially important to detect a leak in due time. For this aim, humidity measurement is installed close to the upper part of the air space of the heat exchanger. Under accident conditions, power supply to the instrumentation is ensured by the sources of category 1. Under these conditions the number of measured parameters is reduced to condensate and air temperature and air humidity at the heat exchanger outlet.

4.   EXPERIMENTAL INVESTIGATION OF SPOT SYSTEM

The SPOT is 16 air cooled heat exchangers-condensers (four ones for each steam generator), located outside around containment. The heat exchanger is canned in the box connected with exhaust stack above to ensure the air circulation. The design basis of the SPOT is the removal of 60 MW heat at the maximum design temperature of the external air (plus 50°C) taking into account failure of one train, so the power of one heat exchanger is 5MW. The air flowrate is controlled by partial opening of the air gates to ensure that the power of the heat exchanger should not be excessive in the minimum design temperature of external air (minus 40°C). Under standby conditions the air gates are closed, but the heat exchangers are in the hot state due to air leakage through air gates and heat transfer through the building constructions. These thermal losses are estimated in the design by value less than 0,1% of reactor rated power. The levers with load open the gates under de-energization of the electromagnets keeping the air gates in the closed position, and the air natural circulation through heat exchangers begins.

To confirm the design solutions mentioned above and the system characteristics, the extensive experimental investigations have been performed in OKB Gidropress. The investigations were carried out at the external air temperature from minus 19°C to plus 30°C and the pressure in the steam-condensate circuit from 0,5 MPa to 6,4 MPa. The start-up of the system from hot standby condition is performed, the heat losses are determined at the closed air gates, the system power against external air temperature and steam pressure is determined, the heat removal control is checked by the partial opening of the air gates. The investigations have given the convincing substantiation that the SPOT design functions are performed for WWER-1000/V-392 in the real conditions.

The test rig constructed in OKB Gidropress in 1991, includes the full scale heat exchanger of the SPOT system with representation of air and steam-condensate circuits as shown in Figure 5. The heat exchanger consists of about 200 flat spirals having small slope in relation to horizontal. The tube bank about 2 m high and total surface more than 300 m^2 has two inlet and two outlet collectors. On the sections with cross-sectional air flow, the tubes have ribs for intensification of the heat transfer to the air.

The tube bank is canned in heat-transfer box of square cross-section, which forms the heat exchanger air flow circuit. The lower and upper part of this box are connected with horizontal boxes for air inlet and outlet accordingly. The box upper outlet is connected to exhaust stack. The air gates are installed before of the heat exchanger and after one in pairs in one plane, each of these overlaps half of the cross-section of the circuit. The gate is the flat plate rotated

about one's own axis. The lever with load which is retained by the electromagnet, when the gate is closed, is attached to the axis. The horizontal inlet box, the box of the heat-transfer bank, the horizontal outlet box and exhaust stack together create the circuit for air natural circulation. In this circuit (see Figure 6) the elevations of its components (including the height from inlet box axis up to top of the exhaust stack) and cross sections of all air circuit elements per one real heat exchanger are represented in the full scale. Whole air circuit, starting from the heat exchanger, has been covered by thermal insulation and sheathed by aluminium sheets to create adequate conditions concerning to the heat losses of the real SPOT system.

During the tests, the parameters necessary both for the confirmation of the SPOT design operation and for the development and validation of calculation models for the whole system and its separate elements have been measured. The set of the measured parameters includes:

- flow rate, pressure and temperature of the superheated steam,
- feedwater flow rate,
- flow rate and temperature of the condensate,
- flow rate, pressure and temperature of the saturated steam supplied to the heat exchanger,
- pressure and temperature of the atmospheric air,
- pressure difference along the heat exchanger in the steam-condensate circuit,
- air temperature in the air circuit elements,
- temperature of the heat-transfer tube surface,
- temperature of the thermal insulation.

These measurements have been shown in the control room of the test rig and the registration of the parameters have been realized by the data acquisition system IMPACT 3590 with subsequent treatment by a personal computer.
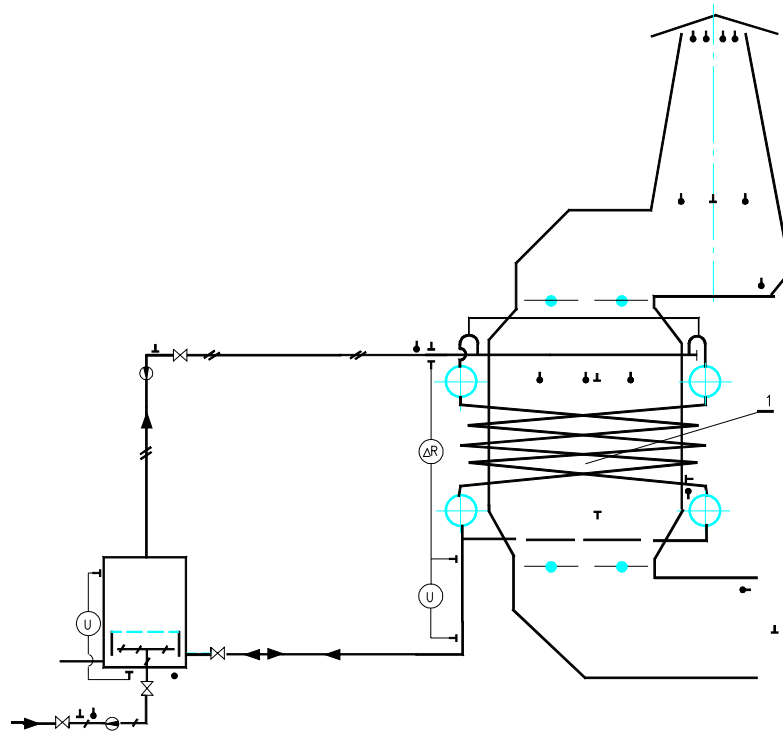
FIG. 5. Test rig flow diagram.
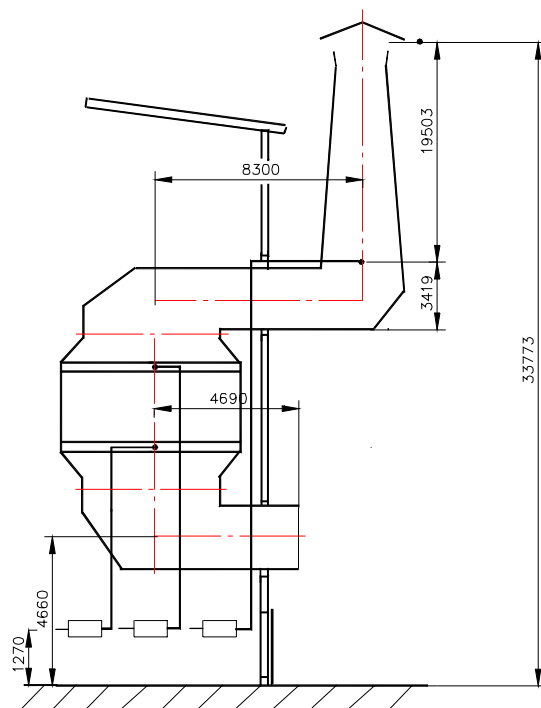
FIG. 6. Air circuit.
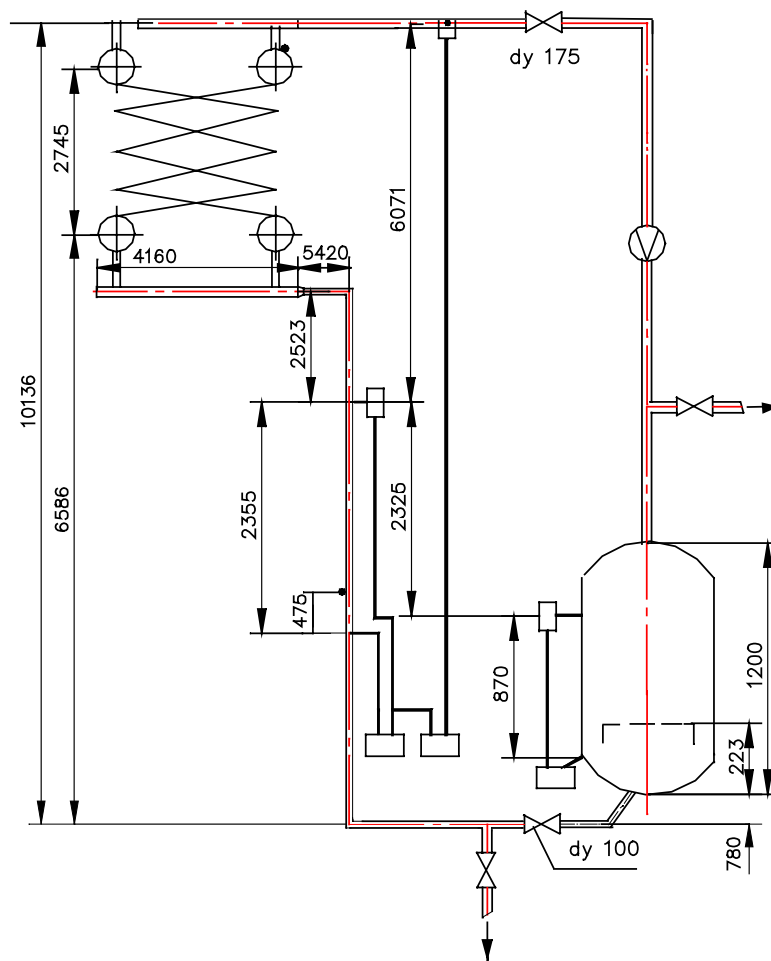
FIG. 7. Steam-condensate circuit.

The investigations to define the heat losses in hot standby condition with the closed air gates have been performed from 07.04.92 to 16.02.93 (totally 30 experiments). In experiments, the steam pressure before the heat exchanger accounted from 0,6 MPa to 6,39 MPa, the steam temperature before the heat exchanger accounted from 159°C-280°C and external air temperature accounted from minus 8°C to plus 18°C. It was found that the direct recalculation of the test results to define the system heat losses results in a larger losses than it is anticipated by the SPOT design (less than 0,1% of the reactor rated power). It was also determined that temperature of the external surface of the heat exchanger thermal insulation exceeds significantly the design value 45°C. The reasons of these differences for the test rig have been found and the recommendations have been developed for the design modification of the SPOT system thermal insulation for WWER-1000/V-392.

To define the dependence of the thermal power removed by the heat exchanger against the external air temperature and steam pressure, the tests have been performed under stationary conditions in the range of external air temperature from –19°C to +30°C and steam pressure at the heat exchanger inlet from 0,54 MPa to 6,39 MPa. During the period from 27.03.92 to 15.02.93, thirty experiments have been performed under positive external air temperature and ten experiments under negative one; the air gates were open partially in eleven experiments to evaluate possibility of the SPOT power control. It was determined that the heat exchanger removes from 5 MW to 7.4 MW at the pressure 6,3 MPa and the external air temperature from plus 30°C to minus 19°C. It was confirmed that the heat exchanger design geometrical characteristics ensure necessary power of the heat exchanger at the maximum design temperature 50°C and fully open air gates. For evaluation of the removed power control by means of partial closing of the lower air gates, two series of the experiments have been performed at the external air temperature plus 18-19°C and minus 11-16°C and steam pressure 6,3 MPa. The gates have been deviated on 10, 20 and 30 degrees in relation to horizontal. It was determined that the design configuration of the air gates ensures the power control of the heat exchanger under turn angles 0-40 degrees, after that the regulating capacity is lost. For example, the heat exchanger power at the turn angle of the gates 10 degrees is approximately 2,5 times less than under fully open gates, and at the angle 30 degrees the power is only approximately 15% less than the power at fully open gates.

To investigate the influence of the non-condesable gas on the heat exchanger operation, two experiments have been performed with supply of the different nitrogen quantity to the steam generator model. The gas quantity in these experiments was approximately 5,5 and 1,3 times more than quantity which corresponds to the real conditions of the reactor plant operation. A number of effects related to the nitrogen supply have been noted. In particular, the condensate temperature is reduced concerning saturation temperature due to decreasing of the partial steam pressure. The nitrogen is distributed on the collectors unequally, according to their location concerning steam pipeline. Discharge of a part of nitrogen with condensate flow was observed. The experiments have been performed with putting the heat exchanger into operation at the fresh steam supply and at the different quantity of nitrogen injected. It was determined that in all cases the heat exchanger power is stabilized in 40-50 seconds, and the value of the stationary power does not depend on quantity of the nitrogen injected and is only determined by the external air temperature. The tests performed have shown that the nitrogen is discharged gradually with the condensate. So, at the injection of the nitrogen quantity, which exceeds possible injection in real conditions about 5,5 times, the nitrogen has practically discharged completely from the heat exchanger in 10 minutes after the air gates opening.

94

The investigation of the stability of the SPOT heat exchangers parallel operation for the different loops has been performed on TDU-1 facility in one of the institutes of the Science Academy of Belorussia. The experiments have been performed on the two-loop three-circuit test rig by 1 MW power. The steam generator and the SPOT air heat exchanger-condenser were modelled in each loop. It has allowed to model operation of two train of the SPOT in parallel at the different loading of the heat exchangers. The experiments have been performed at the air temperature from plus 5°C to plus 31°C and at the steam pressure from 0,6 MPa to 5,4 MPa. The experiments have demonstrated steady operation of the heat exchangers, the variations of the condensate and heat transfer tubes temperatures were not noted. In the same institute the experiments have been performed on the SPOT-2 facility, which models the circulation circuit WWER-1000 and the SPOT circuit in scale 1:5500 in relation to the power and ensures the hydraulic similarity and real difference of the equipment elevations. These experiments have confirmed the possibility of the long-time passive heat removal in case of the main circulation pipeline rupture and station blackout.

The containment model have been developed and constructed in scale 1:80 for the experimental investigation of the possible influence of the wind on the SPOT effectiveness. The investigations have been performed for the wind speed from 0 to 90 m/s (from the calm atmosphere to hurricane) at the wind direction from 0 to 360 degrees in relation to the reactor building axes. These experiments have shown the absence of the circulation reversal in the exhaust air stacks and have confirmed the design solution correctness, at which the SPOT trains are connected by the common inlet collector and the common outlet collector with the deflectors.

5.   CONCLUSION

Broad objectives for advanced nuclear power plants have been documented [7] by the International Atomic Energy Agency. With regard to the safety enhancements, this document states that the plant design should seek to take the maximum, feasible advantage of inherent safety features, and efforts should be made to utilize passive safety systems to the extent that they can be shown as reliable and cost effective as active systems for the same function. Following these recommendations, a reasonable balance of active and passive systems based on the weighing of their advantages and disadvantages with regard to the designated functions, overall plant safety, and construction and operation costs has been found in WWER-1000/V-392 and WWER-640/V-407 designs.

A number of the relatively innovative passive safety means are used in new Russian plant designs with V-392 and V-407 reactors to fulfil the fundamental safety functions, such as reactivity control, fuel cooling and radioactivity confinement. Their implementation allowed to significantly increase the power plant safety in terms of the expected severe core damage and excessive radioactivity release frequencies. For example, the estimated core melt frequency of WWER-1000/V-392 is three orders of magnitude less than for the operating power units with WWER-1000/V-320 reactor.

As the sufficient operational experience for some passive systems and components is absent, the extensive experimental investigation and tests have been carried out or planned to prove the functioning of these systems under plant conditions. In particular, the experiments are already performed for residual heat removal system (SPOT), quick boron supply system, the system to keep the rarefied atmosphere in the containment wall's gap, emergency core cooling system, and some others.

The experimental investigations and tests performed have confirmed the design functioning of the passive safety means proposed and allowed to optimize their general configuration and initiating signals. These investigations have also created the necessary experimental data base for the modeling of the passive safety means by the system thermohydraulic codes. Further investigations are being planned for additional verification of the passive safety systems and for the optimization of their design.

REFERENCES

[1]   INTERNATIONAL ATOMIC ENERGY AGENCY, "The Safety of Nuclear Power: Strategy for the Future", Proceedings of an International Conference organized by the IAEA, Vienna, September 1991 (IAEA, Vienna, 1992).

[2]   INTERNATIONAL NUCLEAR SAFETY ADVISORY GROUP, "The Safety of Nuclear Power", Safety Series No. 75-INSAG-5 (IAEA, Vienna, 1992).

[3]   INTERNATIONAL NUCLEAR SAFETY ADVISORY GROUP, "Basic Safety Principles for Nuclear Power Plants", Safety Series No. 75-INSAG-3 (IAEA, Vienna, 1988).

[4]   INTERNATIONAL ATOMIC ENERGY AGENCY, "Status of water-cooled reactor designs 1996", IAEA-TECDOC-968 (IAEA, Vienna, 1997).

[5]   M.A.GUERRERO, et al., Experience with incomplete RCCA insertion, Nuclear Europe Worldscan, Vol. XX, No. 5-6, May-June, 2000.

[6]   AFROV, A., BERKOVICH, V., GENERALOV, V., DRAGUNOV, Y., KRUSHELNITSKY, V., Design of NPP of new generation being constructed at the Novovoronezh NPP site, in IAEA-TECDOC-1117, pp590-615 (IAEA, Vienna, 1999).

[7]   INTERNATIONAL ATOMIC ENERGY AGENCY, "Objectives for the development of advanced nuclear power plants", IAEA-TECDOC-682 (IAEA, Vienna, 1993).

Natural circulation limits achievable in a PWR

F. D'Auria
University of Pisa, Italy

M. Frogheri
University of Genoa, Italy

Abstract

The present paper deals with the Natural Circulation (NC) phenomenon in Pressurized Water nuclear Reactors (PWR). In the first part, data gathered from relevant experiments in PWR simulators are considered. These allowed the establishment of a flow map that has been used for evaluating the NC performance of various reactor concepts. In the second part, a theoretical study has been completed to assess the power removal capability by NC from the core of a PWR having the current geometric configuration. Taking as reference a PWR equipped with U-tubes steam generators, two-phase conditions occur in the core at power levels less than 20% nominal power. Therefore, for core power larger than this value the reactor cannot be classified any more as a PWR. The study shows that from a thermohydraulic point of view, the core can operate at power levels close to the current nominal value without experiencing thermal crisis. Limited consideration has been given to the neutronic design of the core.

1.   INTRODUCTION

Natural Circulation (NC) is an important mechanism in several industrial systems and the knowledge of its behaviour is of interest to nuclear reactor design, operation and safety. In the nuclear technology, this is especially true for new reactor concepts that largely exploit the gravity forces for the heat removal capability. Natural circulation in a PWR occurs due to the presence of the heat source (core) and the heat sink constituted by the steam generators. In a gravity environment, with core located at a lower elevation than steam generators, those driving forces generate a flowrate suitable for removing nuclear fission decay power. At present, the NC core power removal capability is only exploited for accident situations, basically to demonstrate the inherent safety features of the plants.

The evaluation of the NC Performance (NCP) in experimental facilities simulating the integral system behaviour of a PWR has been the object of previous activities, e.g. Refs. [1], [2] and [3]. The NC scenarios occurring at different values of the primary system mass inventories were considered. Data have been gathered and analyzed coming from the PWR simulators Semiscale, Spes, Lobi, Bethsy, Pkl and Lstf. The thermohydraulic design of all the considered facilities has been achieved by adopting the same set of scaling laws that can be synthesized as follows: power-to-volume-scaling, full-height, time-preserving. Reference is made to both single phase and two-phase natural circulation. In order to evaluate the NCP of the mentioned facilities, significant information comes from the analysis of the trend of the core inlet mass flowrate and the primary loop mass inventory. The flowrate and the residual masses have been normalised taking into account of the volume of each facility and of the power level (typically n times 1% of the nominal core power, where n ranges between 1 and 5) utilized in the selected experiment. Four main flow patterns were characterized depending upon the value of the mass inventory of the primary loop (see also Ref. [4]):
a) single phase NC with no void in the primary system excluding the pressuriser and the upper head;
b) stable co-current two-phase NC with mass flowrate increasing when decreasing primary system fluid inventory;

c) unstable two-phase NC and occurrence of siphon condensation (Ref. [5]);
d) stable reflux condensation with liquid flowing countercurrent to steam in the hot legs: flowrate is sufficient to remove core power till loop mass inventory achieves values as low as 30-40% of the nominal values.

A Natural Circulation Flow Map (NCFM) has been obtained from the envelope of experimental data: this constituted a significant result of the research. The NCFM has been used for evaluating the NCP of the Pactel and the RD-14M facilities, simulators of the WWER-440 and of the CANDU reactors, respectively. The application of thermalhydraulic system codes allowed the extension of the use of the map to the study of NCP in operating reactors and in reactors under design. Westinghouse PWR (equipped with U-Tubes Steam Generators, UTSG), Babcock & Wilcox PWR (equipped with Once Through Steam Generators, OTSG), WWER-1000 (equipped with Horizontal Tubes Steam Generators, HTSG), EPR (designed by a Siemens-Framatome Consortium, equipped with UTSG), AP-600 (passive type reactor designed by Westinghouse and equipped with UTSG) and EP-1000 (a passive type reactor under design by Westinghouse equipped with UTSG) have been considered. Significant results are discussed in the first part of the paper, also providing judgements in relation to the NCP of the considered systems.

The second part of the paper deals with the use of the NCFM for the analysis of the NCP of an existing UTSG PWR outside the design and the operating limits: in those conditions the system may not be classified any more as a PWR. In order to analyze the new system performance, a qualified thermalhydraulic system computer code and a qualified nodalisation (as far as possible) are adopted, e.g. Refs. [6] and [7]. The NCFM is used as a reference to confirm the qualification level of the numerical tools and to give an idea of the distance between the considered thermohydraulic configuration and the values of the relevant NC parameters that are consistent with the current design limits. Therefore, the main purposes of the paper can be synthesized as:

- to characterize the NC as a system phenomenon in PWR;
- to give an overview of the NCFM based upon experimental data and of its application;
- to show the possibility for PWR in the current geometrical layout to operate in NC at 100% core power.

The achieved results can be useful in the framework of the design of advanced Nuclear Power Plants.

2. THE NATURAL CIRCULATION FLOW REGIMES

The study of NC is of primary interest in the nuclear technology. In the case of PWR, primary circuit layout is designed to optimize the NC performance. Following accidents originated by recirculation pumps trip or even small break Loss of Coolant Accidents, NC may constitute the main mechanism to transfer energy from the core to the steam generators, therefore keeping the NPP in a safe condition. In addition, the 'quasi-steady' thermalhydraulic configuration of the reactor loops makes easier the assessment of system code capabilities used for simulating the evolution of generic transient. Owing to the above reasons, all Integral Test Facilities (ITF) built so far that simulate PWR have been used to characterize the NC. A wide experimental database has been gathered and is available.

In the present context, only data measured in ITF designed following the criteria 'time-preserving', 'power-to-volume-scaling' and 'elevation-scaling-factor-equal-to-unity' are taken into account. The main features of these facilities are summarized in Table I. Additional details can be found in Refs. [8] and [9]. The actual Kv, last row of Table I, gives the ratio between the volume of the reference reactor for the largest ITF (i.e. Lstf) and the volume of the considered facility. An idea of the relative dimensions of the loops and, therefore, of the electrical core power can be derived. NC experiments have been performed in all these facilities with core power close to the decay power value typical of NPP, as documented in Ref. [1].

The NC experiments of interest, around ten, have been conducted with primary loop in single-phase and two-phase conditions:

- at constant pressure of the primary system, close to the saturation pressure of the hot leg in nominal conditions;

- with core power in the range 1%-5% of nominal value as already mentioned;

- with the SGs at nominal conditions of level and pressure;

- having available feedwater flowrate and temperature suitable for removing core power;

- by stepwise draining of primary coolant achieving a quasi steady-state at the end of each draining step.

The NC flow patterns or regimes a) to d) defined in Section 1. have been identified. Based on the results of computer codes calculations and of experiments performed in the PWR simulators (see Table I), the NC regimes are characterized in Fig. 1, taken from Ref. [9]. The mass flowrate at core inlet is given as a function of the primary system mass inventory. Other than the flow regimes, the transition zones and the occurrence of dryout situation at mass inventory roughly below the 40% of the nominal value, can be noted. The dryout occurs owing to the sharp decrease in the heat transfer coefficient in the core when void fraction and mass velocities reach a lower boundary. The wideness of the transition zones comes from uncertainties of the database, generally originated by lack of quality assurance, as well as from differences in some boundary and initial conditions. More details related to each flow regime are given below.

TABLE I. RELEVANT HARDWARE CHARACTERISTICS OF THE PWR SIMULATORS CONSIDERED FOR NATURAL CIRCULATION

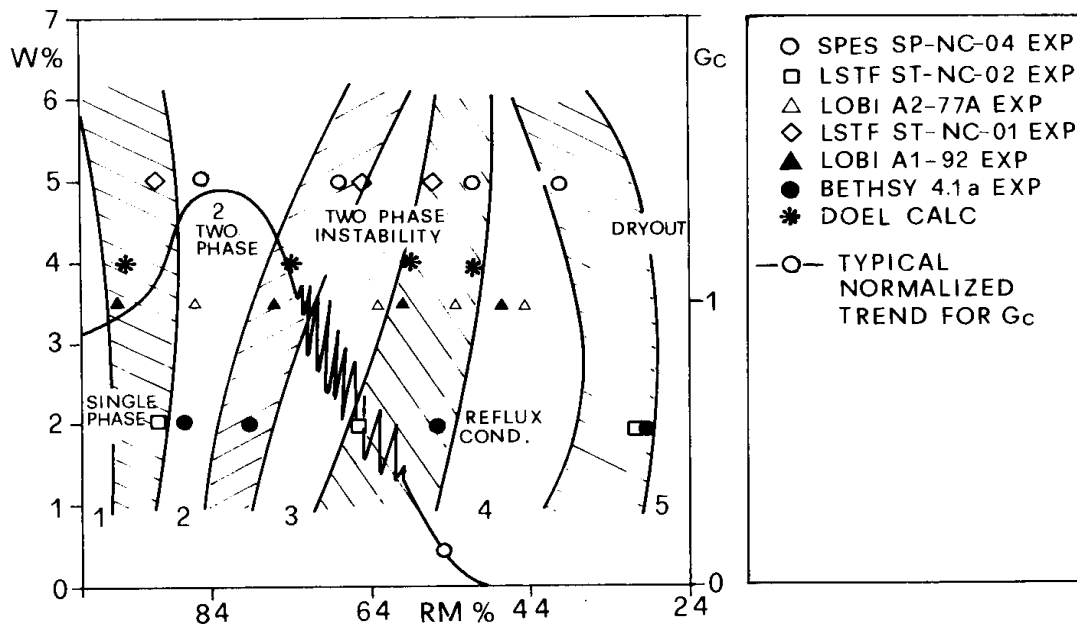| Item	1 Semiscale Mod2A	2 Lobi Mod2	3 Spes	4 PKL-III	5 Bethsy	6 Lstf
Reference reactor and power (MW)	W-PWR 3411	KWU-PWR 3900	W-PWR 2775	KWU-PWR 3900	FRA-PWR 2775	W-PWR 3423
No of fuel rods simulators	25	64	97	340	428	1064
No of U-tubes per SG	2/6	8/24	13/13/13	30/30/60	34/34/34	141/141
Internal diameter of U-tubes (mm)	19.7	19.6	15.4	10.0	19.7	19.6
Actual Kv	1/1957	1/589	1/611	1/159	1/132	1/48

FIG. 1. Characterization of natural circulation flow regimes based on experimental data
and system codes calculations

Single-Phase NC (SPNC)

SPNC regime implies no void occurrence in the upper plenum of the system. Therefore,
coolant at the core outlet shall be subcooled up to nearly saturated. Core flowrate derives from
the balance between driving and resistant forces. Driving forces are the result of fluid density
differences occurring between [descending side of U-Tubes & vessel downcomer] and [core
& ascending side of U-Tubes]. Resistant forces are due to irreversible friction pressure drops
along the entire loop. Resulting fluid velocities are sufficient for removing core power in
(subcooled) nucleate boiling or forced convection heat transfer regimes: no film boiling
condition is experienced in the core. It may be noted that the secondary side of SG is also a
natural circulation system working in two-phase conditions. SPNC may occur at any primary
system pressure, consistently with SG pressure. However, typical primary system pressures
range between 8 and 16 MPa with secondary pressure close to the nominal operating
condition. It is expected from the NPP design that SPNC, provided the availability of SG
cooling, is capable to remove the nuclear heat decay from the core. Experimental database,
including NPP tests, confirms this capability.

Stable Two-Phase NC (TPNC)

TPNC regime occurs as a consequence of coolant loss from the primary system. Owing to
this, both driving and resistant forces increase when decreasing mass inventory of primary
system. Assigned the typical geometrical layout of PWR, the former effect, i.e. increase of
driving forces, is prevalent at small decreases of mass inventories. The opposite occurs for
larger decreases of mass inventories. The net result is a 'peak' in core mass flowrate versus
primary system inventory (when primary mass flowrate decreases), as can be observed in Fig.
1. Forced convection, subcooled and saturated heat transfer regimes occur in the core.
Condensation occurs inside the U-Tubes of SG. The average core void fraction is typically

100

less than 30%, whereas at the outlet values around 50% can be reached without occurrence of thermal crisis in the considered pressure range.

Siphon Condensation NC (SCNC)

The decreasing of NC driving forces, the small temperature difference across U-Tubes of steam generators, and the occurrence of the CounterCurrent Flow Limiting Phenomenon (CCFL) at the entrance of U-tubes are at the origin of wide system oscillations of core inlet flowrate, e.g. Ref. [10]. The phenomenon has been investigated in Refs. [5] and [11], based on a natural circulation experiment performed in Lobi facility, Ref. [12]. Evidence of the phenomenon has been found also in other facilities. At mass inventories of the primary system around 70% of the nominal value, the efficiency of the condensation heat transfer across U-Tubes causes the release of almost all core thermal power in the ascending side of U-Tubes. Liquid level builds up and is prevented to drain down by the steam-liquid mixture velocity at the tube entrance, i.e. the CCFL condition occurs. Therefore, liquid level rises in the U-Tubes till reaching the top. During this period, typical duration of the order of 10 s, flowrate at core inlet is close to zero and core boil-off occurs. Once the liquid level reaches the upper bend of U-Tubes, the siphon effect occurs and causes the emptying of the ascending side of U-Tubes and the re-establishment of core inlet flowrate. A new cycle starts. The phenomenon is made more complex by the interaction of the several thousands of U-Tubes that constitute a SG tube bundle. Different groups of tubes may stay at a different stage of the oscillation at the same time, also causing flow reversal in the tube bundle. Suitable core cooling still can be achieved in these conditions.

Reflux Condensation (RCNC)

At 'low' mass inventories of primary coolant and/or at low core power, steam velocities in the upper part of the system including hot legs and steam generator entrance are low. Weak interactions occur at the steam-liquid interface that are not enough to cause CCFL. In these conditions, the liquid that is condensed or entrained in the ascending side of the U-Tubes may flow back to the hot leg and to the core. Stratified countercurrent steam and liquid flow simultaneously in the hot legs. Mass flowrate at core inlet is close to zero, although a 'minor' natural circulation path may establish between core and downcomer inside the vessel. However, upward two-phase mixture and downward liquid flows occur at the core outlet. Core thermal power can be removed by boil-off in the saturated nucleate boiling heat transfer regime.

Dryout occurrence

The terms 'dryout occurrence' appear in the right part of Fig. 1, when primary system mass inventory is roughly lower than 40% of the nominal value. Dryout is caused by the combination of low flow and high void fraction. As a consequence, film boiling heat transfer regime is experienced with low coefficient for heat transfer. Rod surface temperature increases in various zones of the core and the overall process of thermal power transfer from fuel rods to the fluid may become unstable. The system operation in these conditions is not acceptable from a technological point of view. It may be noted that the temperature excursion is strongly affected by primary system pressure and thermal power levels: the linear rod power plays a role in these conditions. At primary system pressure around 15 MPa (nominal operation for PWR), 'post-dryout' surface temperature jumps may be as low as a few tens of Kelvin, tolerable for the mechanical resistance of the rod-clad material.

3.   THE NATURAL CIRCULATION FLOW MAP

The similitude of the geometry and of the operational parameters of the PWR simulators (or Integral Test Facilities, ITF) allowed a direct comparison between results of NC experiments. The database that was gathered from ten experiments performed in the six ITF listed in Table I has been used to establish a Natural Circulation Flow Map, Refs. [2] and [3]. In all the considered ITF, the NC regimes discussed in the previous chapter are experienced. The linear power of fuel rod simulators, the fraction of nominal core power and the primary system pressure mainly differentiate the considered experiments. In relation to pressure, PKL experiments have been performed at a pressure value roughly one half the value adopted in the other facilities. The identified differences and the ranges of design and of other operational parameters (e.g. pipe diameter, system volume, number of steam generators, heat losses to the environment, not explicitly discussed here), produce an envelope for any expected NC situation in a typical PWR. The envelope for NC system behaviour is assumed applicable when decay heat removal conditions are established.

Measured values of core inlet flowrate (G, Kg/s), core power (P, MW), primary system fluid mass inventory (RM, Kg) and net volume of the primary system (V = const., m3), have been used for setting up the NCFM. The diagram G/P versus RM/V has been preferred for the NCFM over other possible choices including non-dimensional quantities.The experimental database from ITF (six ITF, ten experiments) and the envelope of curves are given in Figs 2 and 3, respectively. The envelope in Fig. 3 is assumed to constitute the NCFM of PWR at decay core power.

3.1.   Use of the NCFM

Seven commercial NPP systems and three ITF, not used for setting up the database presented in Fig. 2, are considered for demonstrating the use of the NCFM, Ref. [3]. Main characteristics of the NPP and of the ITF can be drawn from Tables 2 and 3, respectively.
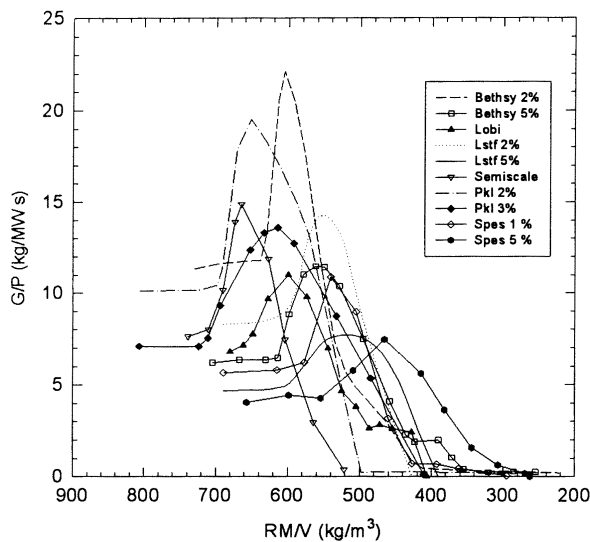
FIG. 2. Natural Circulation system behaviour measured in ten experiments performed in six PWR simulators.
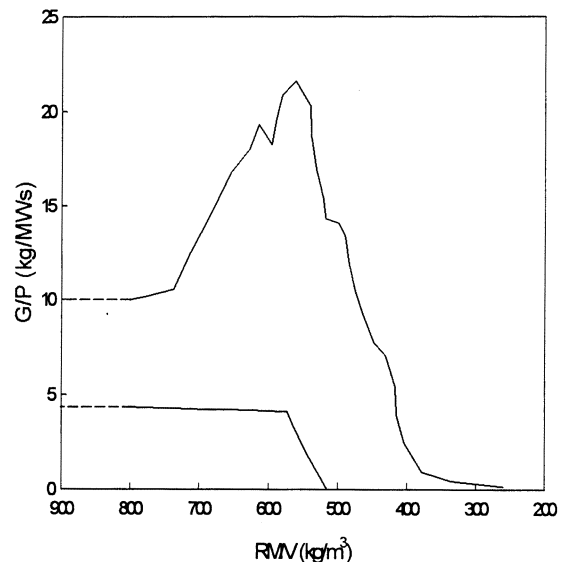
FIG. 3. Natural circulation flow map achieved from the envelope of measured curves in PWR simulator.

TABLE II. RELEVANT CHARACTERISTICS OF NPP CONSIDERED FOR THE APPLICATION OF THE NCFM

	1 PWR	2 PWR	3 PWR	4 WWER-1000	5 EPR	6 AP-600	7 EP-1000
Nominal Power (MW)	1877	870	2733	3000	4250	1972	2958
Primary System volume (m3)	167	150	330	359	459	211	339
SG type	U-Tubes	U-Tubes	Once-Through	Horizontal	U-Tubes	U-Tubes	U-Tubes
No. of loops	2	4	2	4	4	2	3
No. of pumps	2	4	4	4	4	4	6
Nominal mass inventory (Mg)	108	108	224	240	307	145	227
Nominal Core Flow (Kg/s)	9037	3150	17138	15281	20713	8264	14507
Pressurizer and SG pressure (MPa)	15.6 6.	14.0 3.1	15.0 6.4	15.7 6.3	15.5 7.2	15.5 5.5	15.8 6.4

TABLE III. RELEVANT CHARACTERISTICS OF ITF CONSIDERED FOR THE APPLICATION OF THE NCFM

	Pactel (original)	Pactel (with CMT) °	RD14M
Reference reactor and power (MW)	WWER-440 1375	WWER-440 1375	CANDU 1800
No. of rods	144	144	70
No. of SG	3	3	2
SG type	Horizontal	Horizontal	U-Tubes
Actual Kv +	1/433	1/462	1/378

° CMT = Core Make-up Tank.
+ Definition introduced for database in Table I.

Reactors 1 to 4 (Table II) have been built and are in operation. Reactors 5 to 7 are in a more or less advanced design stage. The geometric layout of primary systems for reactors 1, 2, 5, 6 and 7 is similar to the geometric layout of ITF originating the database for the NCFM. However, differences are present in the relative elevations between core and SG. Reactors 3 and 4 are equipped with OTSG and HTSG, respectively. So the geometric layout of the primary system is different from the geometric layout of ITF originating the database for NCFM.

Pactel and RD14M (Table III) are experimental simulators of WWER-440 and CANDU NPP, respectively. Their geometric layout is different from those of a PWR. In the case of WWER-440, six loops equipped with HTSG are connected to the vessel, though only three are simulated in Pactel. Horizontal core configuration characterizes the CANDU design, that otherwise is equipped with UTSG.

A comparison has been made between measured (case of ITF) and calculated (case of NPP) system behaviours during NC and the data that characterize the NCFM. To this aim, code calculations assuming stepwise draining of primary system fluid mass inventory have been performed (case of NPP) and relevant NC experimental data are utilized (case of ITF).

In the case of NPP, the qualification level of the adopted code and nodalisation affects the calculated NCP. Furthermore, in the case of new generation 'passive' safety reactors 6 and 7, the emergency loops connected with the primary system are assumed to come into operation once the coolant draining process is initiated.

Calculated or measured transient scenarios reflect the NC flow regimes identified in Fig. 1, Ref. [3]. The RCNC regime is not achieved in the systems equipped with HTSG and OTSG and is not evident from the RD14M database. The SCNC regime is also not evident in all the calculations or available experimental databases. Mostly SPNC is calculated in the NPP 6 and 7.

Significant results are shown in Figs 4 to 6. The following observations apply:

- NCP of UTSG equipped PWR and of WWER-1000 is qualitatively similar (Fig. 4). Therefore the last generation of HTSG WWER shows a reasonable NCP. The good performance of the PWR-2 can be noted (low power NPP equipped with four UTSG).
- The OTSG equipped PWR show an 'early' NC flowrate decrease and an early stop of NC due to void formation in the 'candy-cane' and the rising part of the hot leg (Fig. 4).
- NC flowrate in AP-600, as expected, is not affected by draining because of liquid mass supplied by the 'passive' emergency cooling loops (Fig. 5). This behaviour does not show up in the case of EP-1000 presumably due to lack of qualification of the adopted code model.
- The WWER-440 simulator (Pactel) exhibits a decrease of the NC flowrate at relatively high mass inventories of the primary loop. The presence of the hot leg loop seal is at the origin of a partial flow stagnation (Fig. 6). Removal of the hot leg loop seal is effective in improving NCP as shown by the calculated WWER-1000 transient. The consideration of a passive system also improves the NCP of the Pactel.
- The CANDU simulator exhibits two different behaviours depending upon the considered experiment (Fig. 6). This shows the need of a deeper investigation before drawing conclusions. It may be noted that larger driving forces characterize CANDU systems for NC compared with PWR systems, owing to the larger distance of heat source and sink. However, larger pressure drops are also expected owing to the longer core and to the presence of small equivalent diameter pipes at core inlet and outlet.

Any attempt to judge the results, i.e. the NCP of involved NPP and ITF, should consider the quality of the used databases (DB). The result of a two step evaluation can be found in Table IV. The second column considers the demonstration of the quality of the starting DB. If 'N' appears in the second column, the evaluation in the third column is not meaningful. The third column considers the quality demonstration of the used DB, e.g. the nodalisation in the cases of code use and, finally, the NCP judgement (more details are provided in Ref. [3]).

The 'NS' mark for PWR-3 is due to the poor NCP also at high values of the RM inventory caused by the long vertical hot leg. Quality of data is assumed to be suitable. The 'N' in the case of EP-1000 (third column) is related to the available nodalisation. The dash (-) in the case of RD14M comes from the contradictory DB available at the moment.
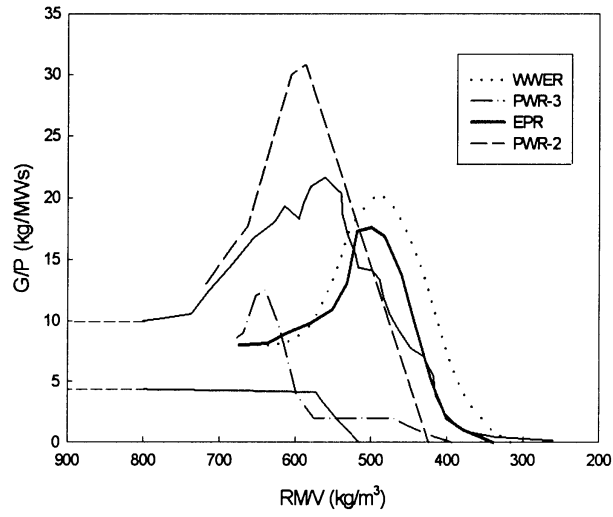
FIG. 4. Evaluation of the NCP for PWR-2, PWR-3, WWER-1000 and EPR by using the NCFM.
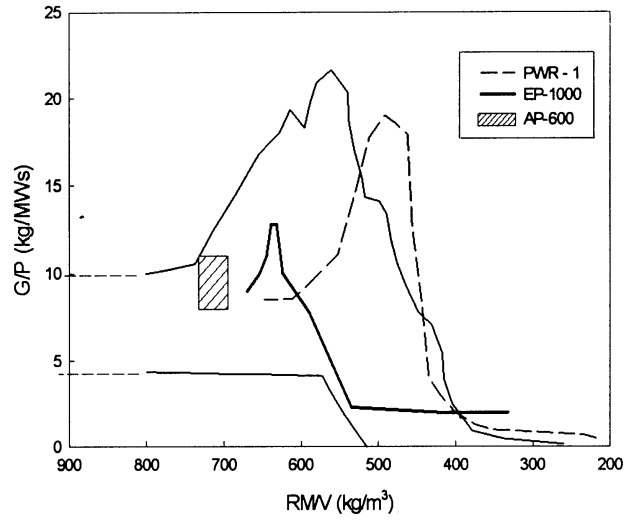

FIG. 5. Evaluation of the NCP for PWR-1, EP-1000 and AP-600 by using the NCFM.
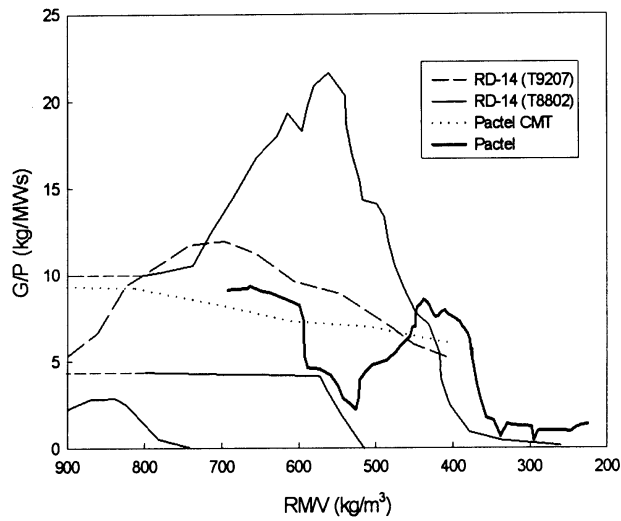

FIG. 6. Evaluation of the NCP for Pactel and RD14M simulators by using the NCFM.

TABLE IV. SUMMARY OF NCP EVALUATION FOR THE CONSIDERED NPP AND ITF

NPP or ITF	QUALITY OF STARTING DB	QUALITY OF DB &NCP EVALUATION
PWR-1	Y	Y & S
PWR-2	N	Y & S
PWR-3	Y	Y & NS
WWER-1000	Y	Y & S
EPR	N	Y & S
AP-600	Y	Y & S
EP-1000	N	N & -
Pactel	Y	- & S
Pactel with CMT	Y	- & S
RD14M	N.A.	-

Y   Confirmed.   N   Not Confirmed.
N.A.   Not Available.   -   Not applicable.
S   Suitable (for NCP).   NS   Not Suitable.

4.   CORE POWER REMOVAL CAPABILITY BY NATURAL CIRCULATION

The generic objective of the activity is to achieve an estimation of the maximum thermal power removable by NC in PWR systems. As already mentioned, no care is given to the thermohydraulics-neutronics interaction and, therefore to the actual possibility of generating the considered fission power. The analysis is carried out into two parts the former related to ITF, to give more realism to the calculated results, the latter related to a PWR. In all cases, the primary system pressure and the SG conditions (pressure, level and feedwater temperature) are kept constant at the nominal values if not differently specified. The main circulation pumps are at zero speed and the locked rotor hydraulic resistance of the impeller is taken into account. The core power and the feedwater flowrate levels are consistently modified.

4.1.   Results related to experimental facilities

Results are related to experimental facilities 2, 3, 5 and 6 listed in Table I and are summarized in Table V, ref. [13]. Calculations related to PWR-1 of Table II are also discussed in Ref. [13]. These are not considered hereafter owing to a large 'mass error' that characterizes the achieved results as documented in the same Ref. [13]. Qualified nodalisations of the ITF, suitable for the Relap5/mod 2 code, were used. The qualification came from the simulation of the NC tests performed in the considered ITF, e.g. ref. [12], and from the demonstration that calculated results adequately reproduce the available experimental values.

TABLE V. REMOVABLE POWER BY NATURAL CIRCULATION IN ITF

ITF	Core power when void achieves 0.1 at the upper core level (°)	Core power when dryout occurs (°)	Void at the upper core level when dryout occurs	Primary system mass inventory at dryout (°)	G/P at dryout (Kg/MWs)	RM/V at dryout (Kg/m3)
Bethsy	15	70	0.8	69	1.12	475
Lobi	20	70	0.7	80	1.23	570
Lstf	10	30	0.9	62	1.87	480
Spes	15	50	0.6	75	1.29	528

(°) % of the nominal operational value.

The main results of the study can be summarized as follows, ref. [13]:

- A uniform increase of NC flowrate with core power is calculated, until core power achieves values around 40% of the nominal value. Further increases of core power do not cause proportional increases in core flow.

- Oscillatory flows are calculated for core power larger than 40% in Bethsy and Lobi.

- The primary mass inventory decrease occurs via the pressurizer relief valve that is assumed to open and to close in order to keep constant the system pressure.

- PWR cores, in the actual configuration can operate in NC conditions with power up to about 15% the nominal value.

- The largest facilities are designed to operate at low core power (ITF design finalized to the simulation of small break LOCA). This may explain the small value, in terms of % core power, at which dryout occurs.

- Neglecting the Lstf case, up to 70% core power can be removed by NC before experiencing dryout. This can be assumed as the thermalhydraulic limit for system (not any more PWR) operation in NC.

4.2. Results related to a UTSG PWR

A NC study was conducted utilizing a nodalisation for the PWR-1 in Table II, suitable for the Relap5/mod3.2.2, Ref. [14]. 'Quasi' steady-state thermalhydraulic NPP conditions are obtained at the end of transient calculations. The aim is to derive mutual relationships between significant NC parameters and to search for realistic boundary conditions allowing the maximum core power in NC. Use is also made of the NCFM derived above. Relevant results are given in Figs 7 and 8 and in Table VI.
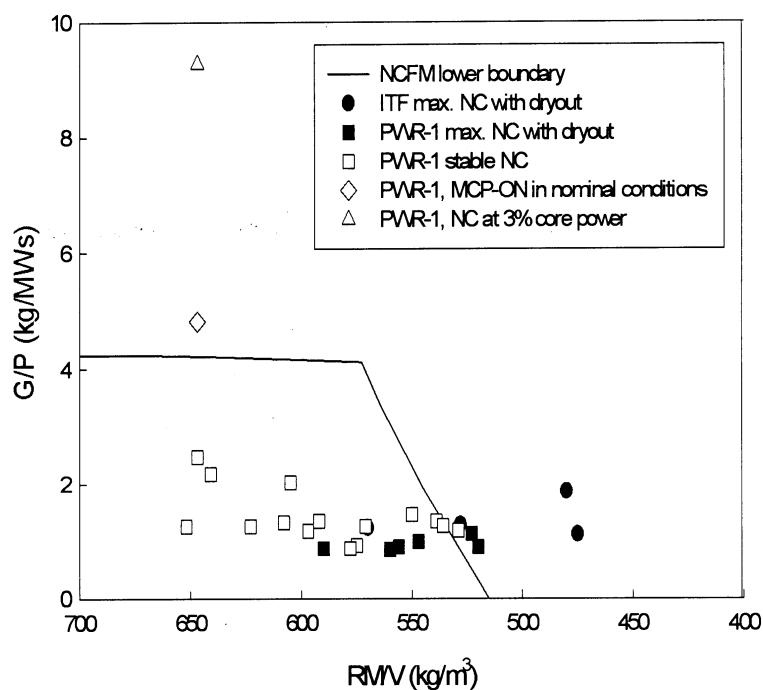
FIG. 7. Study of NC in PWR-1: 'quasi' steady NC conditions relevant for calculating the maximum removable thermal power in the NPP and in the ITF.
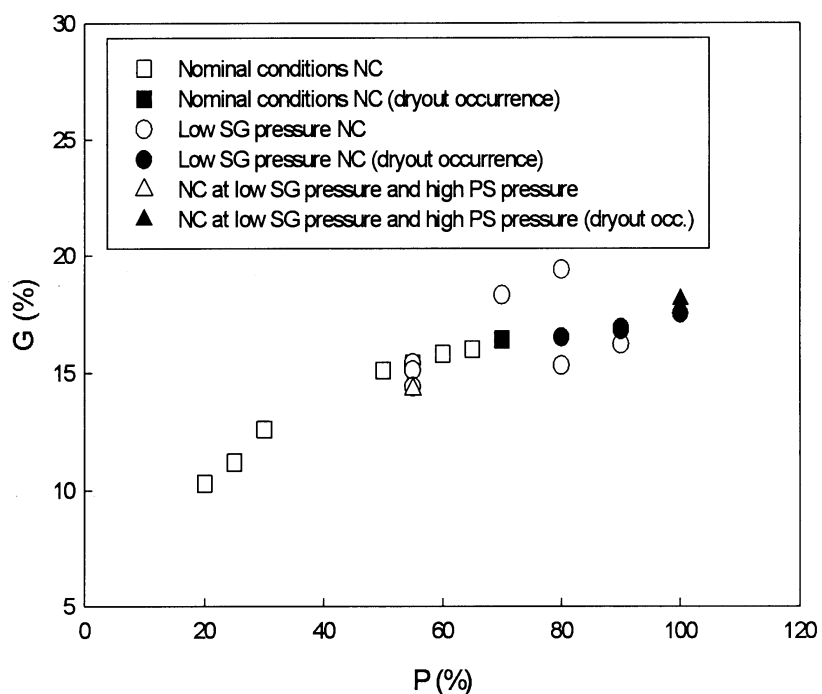
FIG. 8. Study of NC in PWR-1: core flowrate versus core power at different pressure and temperature related boundary conditions.

TABLE VI. REMOVABLE POWER BY NATURAL CIRCULATION IN PWR-1

No.	ID.	P MW/%	G (Kg/s)/%	SG PRE MPa	RM KgE5/%	PS PRE MPa	UP T/Tsat K	UP Void -	G/P Kg/sMW	RM/V Kg/m³
1#	KK01	1876/100	9037/100	6.1	1.08/100	15.6	598/618	0.	4.82	647
2^	KK01	56/3.0	520/5.8	8.1*	1.08/100	13.6	577/608	0.	9.28	647
3	KK01	376/20	930/10.3	6.0*	1.08/100	15.4	615/617	0.	2.47	647
4	KN03	469/25	1016/11.2	6.0*	1.07/99.1	16.2	620/620	0.10	2.17	641
5	KN04	563/30	1140/12.6	6.0*	1.01/94.0	16.2	620/620	0.21	2.02	605
6	KN05	938/50	1370/15.1	6.0*	0.92/85.0	16.2	620/620	0.47	1.46	550
7	KN07	1032/55	1396/15.4	6.0*	0.90/83.3	16.2	620/620	0.48	1.35	539
8	KN08	1126/60	1428/15.8	6.0*	0.89/82.9	16.2	620/620	0.49	1.27	536
9	KN09	1219/65	1450/16.0	6.0*	0.88/82.0	16.2	620/620	0.51	1.19	529
10§	KN10	1313/70	1490/16.4	6.0*	0.87/80.8	16.2	620/620	0.62	1.13	523
11	KL10	1032/55	1396/15.4	3.5*	0.99/91.4	16.2	620/620	0.44	1.35	592
12	KL10	1313/70	1650/18.3	3.5*	0.95/88.2	16.2	620/620	0.49	1.26	571
13§	KL12	1500/80	1492/16.5	3.5*	0.91/84.6	16.2	620/620	0.60	0.99	547
14§	KL11	1688/90	1523/16.8	3.5*	0.87/80.4	16.2	620/620	0.77	0.90	520
15	LL11	1032/55	1365/15.1	3.5**	1.01/93.9	16.2	620/620	0.31	1.32	608
16§	LL11	1688/90	1525/16.9	3.5**	0.93/86.3	16.2	620/620	0.57	0.90	556
17	LL12	1500/80	1380/15.3	3.5**	0.96/88.8	16.2	620/620	0.49	0.92	575
18	LL13	1032/55	1300/14.4	2.5**	1.04/96.3	16.2	620/620	0.20	1.26	623
19	LL13	1500/80	1750/19.4	2.5**	1.00/92.3	16.2	620/620	0.48	1.17	597
20	LL14	1688/90	1460/16.2	2.5**	0.97/89.4	16.2	620/620	0.50	0.87	578
21§	LL15	1876/100	1587/17.5	2.5**	0.94/86.6	16.2	620/620	0.63	0.85	560
22	HL15	1032/55	1290/14.3	2.5**	1.09/101.	18.5	631/633	0.01	1.25	652
23§	HL15	1876/100	1630/18.1	2.5**	0.97/89.3	18.5	633/633	0.58	0.87	578
24	HL16	1032/55	1295/14.3	2.5+	1.09/101.	18.5	594/633	0.	1.25	652
25§	HL16	1876/100	1630/18.1	2.5+	0.99/91.4	18.5	633/633	0.50	0.87	590

Nomenclature

ID	Calculation identification	§		Dryout occurrence
G	Core flowrate	#		Nominal working conditions for the current system
P	Core Power	^		Reference NC result
PRE	Pressure	*		Feedwater temperature same as in nominal condition
PS	Primary System	**		Feedwater temperature set at 363 K
RM	Mass Inventory in PS	+		Feedwater temperature set at 333 K
T	Fluid Temperature	+		Feedwater flowrate set at 1.3 times the equilibrium value
Tsat	Saturation temperature	UP		Upper Plenum
Void	Void fraction.			

All the reported data relate to conditions where core power equals SG removed power. This is also valid when dryout situations occur and testifies of the small excursion of rod surface temperature. The excursion is actually limited to a few tens of Kelvin and is stable as a function of time. The main comments to the achieved results are:

- SPNC can be obtained up to about 20% core power, thus confirming the results related to ITF in Table V.
- TPNC allows removal of up to about 70% core power assuming nominal system conditions, again confirming the results related to ITF.
- Lowering SG pressure and increasing primary system pressure bring to increases in the NC thermal power removal capabilities. More than 90% core power can be removed in NC with SG pressure as low as 2.5 MPa.
- Dryout occurrences are undesirable. However, temperature excursions of rod surfaces are limited in space and do not affect the 'stable and steady' NC scenario.
- The NCFM obtained from the analysis of experimental NC scenarios at low core power values has been used as reference for high power NC scenarios. The information in Fig. 7, mainly the values of G/P and RM/V when dryout occur, shows that the NCFM (G/P versus RM/V) can be adopted also for high core power values. Dryout occurs with G/P close to unity (Kg/s/MW) or below this threshold. Lower values of G/P at dryout are experienced at higher core power.

4.3. Results related to the UTSG PWR without loop seal

The analysis documented in the previous section has been extended. Loop seal piping and pumps available in the PWR-1 nodalisation have been modified and deleted, respectively. The loop seal, 'U-shaped' cold leg piping connecting SG outlet with the MCP, has been substituted by a 'L-shaped' piping connecting the SG outlet and the horizontal part of the cold leg. New calculations have been performed with results documented in Table VII and in Figs 9 and 10.

Table VII has the same structure as Table VI. However, the columns reporting primary system pressure, upper plenum fluid temperature and upper plenum void fraction in Table VI have been substituted by columns giving the steam line flowrate, the maximum rod surface temperature and the maximum void fraction in the core, respectively. Thermalhydraulic conditions in the core (void fraction and maximum cladding temperature) and at the outlet of the SG (dome temperature and steam line flowrate) can be seen in Figs 9 and 10, respectively.

Starting from the situation depicted by the data in Table VI, a number of strategies can be pursued to design a natural circulation PWR, taking the goal of full core power and allowing for two-phase flow in the core. For instance, system geometry (number of SG U-Tubes, mutual position between RPV and SG, core hydraulic diameter) can be substantially modified, steam generator pressure can be lowered, feedwater temperature can be lowered, primary system pressure can be increased. Strategies requiring (almost) no system geometry changes and minimizing the necessary variation in the values of operational parameters have been followed:

a) The occurrence of dryout, (stable condition with limited temperature excursion) is allowed.

b) The feedwater temperature and the operating pressure of the SG are decreased, thus allowing a loss of thermal efficiency of the plant.

TABLE VII. REMOVABLE POWER BY NATURAL CIRCULATION IN PWR-1 WITHOUT PUMPS AND LOOP SEALS.

No.	ID.	P	G	SG PRE/Tsat	RM	GSL	PCT/Tsat	MCV	G/P	RM/V
		MW/%	(Kg/s)/%	MPa/K	KgE5/%	(Kg/s)/%	K	-	Kg/sMW	Kg/m3
1	KK01	1876/100	9037/100	6.1/550	1.08/100	1030/100	615/618	0.	4.82	647
2	KN08	1126/60	1428/15.8	6.0/549*	0.89/82.9	620/60	627/620	0.69	1.27	536
3^	NC00	1126/60	1880/20.8	6.0/549*	0.92/89.3	620/60	627/620	0.44	1.67	586
4^	ND03	1876/100	1955/21.6	6.0/549*	0.79/76.7	1030/100	791/620	0.83	1.04	500
5^	NI03	1876/100	2083/23	3.5/516**	0.93/90.3	1000/97	630/620	0.60	1.11	591

Nomenclature: See Table VI. In addition,

GSL   Steam line flowrate   §   Dryout occurrence
MCV   Maximum Void Fraction in the core   *   Feedwater temperature same as in nominal condition
PCT   Peak Cladding Temperature   **   Feedwater temperature set at 393 K
                                                      ^   Modified PWR (pump and loop seals removed).
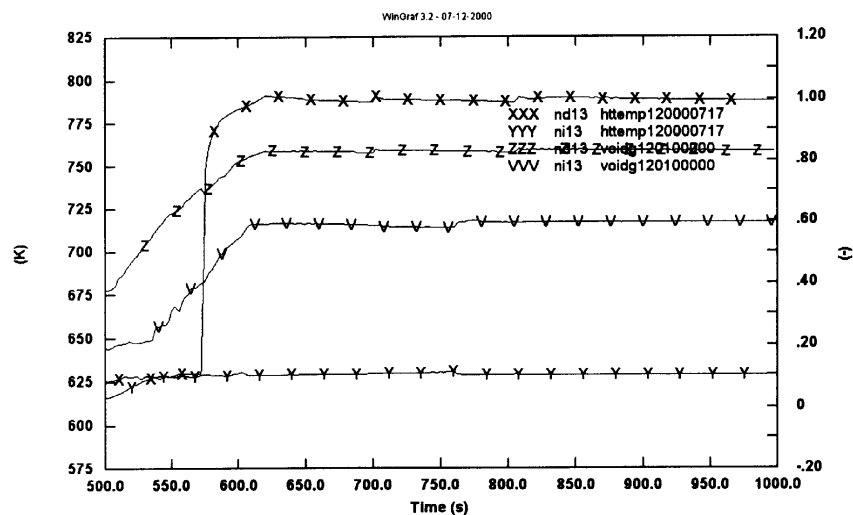
FIG. 9. Proposed NC system: Maximum values of core void fraction and of rod surface temperature calculated at stable operating conditions in code runs ND03 and NI03.
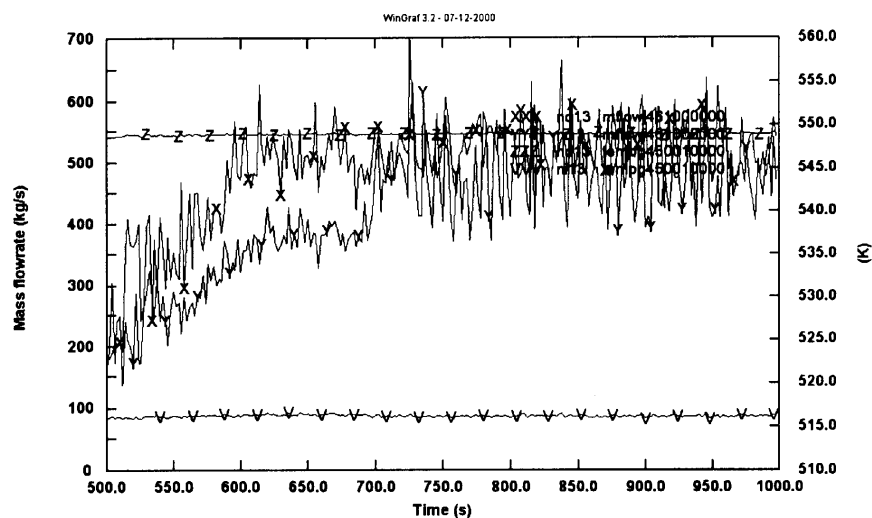
FIG. 10. Proposed NC system: Fluid temperature in SG dome and steam line flowrate calculated at stable operating conditions in code runs ND03 and NI03.

The database supplied by the two calculations identified as ND03 and NI03 in Table VII, constitutes the result of the activity. System configurations considered as input for calculations ND03 and NI03 comply with the strategies at items a) and b) above. In the Table VII, calculations KK01 and KN08 are taken from Table VI in order to set reference values for the considered parameters.

The comparison between results of calculations KN08 and NC00 shows the advantage derived from adopting the 'L-shaped' cold leg at the outlet of the SG instead of the 'U-shaped' cold leg. Core flowrate in NC conditions at 60% core nominal power increases from about 1400 to about 1800 Kg/s showing that pumps at rest conditions introduce a noticeable pressure drop in the loop. Keeping the 'L-shaped' configuration and all operational parameters of run NC00 (or KN08), it has been shown that 85% core power can be removed by NC without the occurrence of dryout. This value can be compared with the 70% limit applicable to the 'U-shaped' cold leg configuration, (run KN10 in Table VI).

The results from calculations ND03 and NI03 (Table VII and Figs 9 and 10) bring to the following remarks:

- The removal capability of 100% core power by NC has been demonstrated starting from a steady state condition for the system fixed at 3% core power with primary loop in subcooled conditions and pressurizer and SG at nominal pressure.
- Film boiling cooling establishes on the surface of fuel rods in a region of the core (calculation ND03). This conditions is characterized by a stable temperature jump (DTsat, difference between local clad temperature and fluid saturation temperature) of about 180 K. Maximum values of void fraction that are calculated for the core are typical for the nominal operation of Boiling Water Reactors.
- Excursion from the nucleate boiling is achieved at two of the ten axial levels of the core region (upper half) that are characterized by a power peak factor close to 1.5. A proper design of core power distribution, i.e. consistent with the moderation features of the new system, could reduce the spatial extension of the film boiling region.
- The decrease of steam temperature at the SG outlet of about 20 K, consequence of the pressure decrease, prevents dryout occurrence on the fuel rod clad surface, calculation NI03. In this case, no attempt has been made to optimize the combination between feedwater temperature and SG pressure keeping the goal of maintaining the core in nucleate boiling.
- The mass inventory for the primary loop stabilizes at about 80% and 93% of the initial value in the two operational configurations calculated by code runs ND03 and NI03, respectively. This includes the fluid in the pressuriser. Stable liquid level in the pressuriser, i.e. buoyant fluid in a dynamic condition, establishes as the result of the procedure considered for power rise. The level value is such to allow the operation of heaters, though they are not called into operation in the present framework.
- The G/P and the RM/V values that characterize the working points in the NCFM for code runs ND03 and NI03 lie in the area of the square symbols of Fig. 7, though the present values are not reported in that figure.

5. CONCLUSIONS

The database gathered in natural circulation tests performed in PWR simulators and the results of system code calculation related to the same experiments constituted the starting point for the present investigation. The experimental database has been utilized to set up a reference natural circulation flow map. This allowed the judgement of the performance, in

natural circulation conditions, of current PWR systems not necessarily of the same type as those used for deriving the map.

It was found that the PWR equipped with Once-Through steam generators have a poor natural circulation performance when primary mass inventory is decreased. Otherwise, reasonable natural circulation performances of Russian designed reactors WWER were characterized. This is mainly true for the WWER-1000. Passive systems in the AP-600 innovative reactor are effective in keeping the primary system under single-phase natural circulation notwithstanding removal of coolant mass.

Power removal by natural circulation strongly depends upon primary and secondary system boundary condition. Two thermohydraulic thresholds have been considered and the neutronic-thermalhydraulic coupling has been neglected. The void formation in the core that prevents a PWR from being 'pressurised' and the technological limit constituted by the critical heat flux are the reference thresholds. When primary and secondary system boundary conditions are kept close to their nominal values, it was found that:

- single phase natural circulation is effective for removing up to around 20% of core nominal power,
- two phase natural circulation, with the primary system in a boiling condition, is effective for removing up to about 70% of core nominal power avoiding the occurrence of the dryout.

A deeper investigation showed that 100% core power can be removed in two-phase natural circulation, provided the steam generator pressure and the feedwater temperature are lowered to values of the order of 3 MPa and 100°C, respectively. An increase of primary pressure also brings to the increase of the power removal capability by natural circulation.

The substitution of the current 'U-shaped' loop seal with a 'L-shaped' pipe and the elimination of the pump component improved the natural circulation performance of the considered system. Two reference sets of natural circulation conditions suitable for additional investigation have been established at 100% reactor core power:

a) film boiling allowed within a limited extension core region;

b) reduced pressure in steam generator.

In the former case, roughly one-tenth of the fuel rod clad surface was calculated with a temperature 180 K larger than the saturation value. Steam conditions at the outlet of the steam generator are the same as in current design PWR. In the latter case, all fuel rod clads are predicted in the nucleate boiling heat transfer regime, though core average void fraction is close to 40%. Better core cooling conditions are obtained at the expenses of lower temperature of the steam and then of lower thermal efficiency for the plant.

Continuation of the study, if interest is shown from the technical community derived from the economic benefit of the proposed solutions, requires the investigation of the following aspects:

- role of the pressurizer;
- design of suitable neutron kinetic parameters for the core region and analysis of the thermalhydraulic-neutronic feedback;
- design of suitable start-up procedure;
- accident analysis.

REFERENCES

[1] D'AURIA, F., GALASSI, G.M., VIGNI, P., CALASTRI, A. "Scaling of Natural Circulation in PWR Systems", J. Nuclear Engineering and Design, vol 132 1991, pp 187-205.

[2] D'AURIA, F., FROGHERI, M., LEONARDI, M. "Natural Circulation Performance in Western type and Eastern type PWR", Simulator Multiconference, San Diego (CA), April 11-13, 1994.

[3] D'AURIA, F., GALASSI, G.M., FROGHERI, M. "Natural Circulation Performance in Nuclear Power Plants", 2nd Conf. of the Croatian Nuclear Society, Dubrovnik (HR), June 17-19, 1998.

[4] KUKITA, Y., TASAKA, K. "Single Phase Natural Circulation in Pressurized Water Reactors under degraded Secondary Cooling Conditions" ASME Winter Meeting 1989.

[5] D'AURIA, F., GALASSI, G.M. "Characterisation of Instabilities during Two-Phase Natural Circulation in PWR typical conditions" J. Experimental Thermal and Fluid Science, Vol. 3, 1990.

[6] D'AURIA, F., FROGHERI, M., MARSILI, P., GIANNOTTI, W. "Standardised Procedure for Thermalhydraulic System Codes Assessment", IAEA Meet. On User Qualification on Accident Analyses for NPP – Vienna (A), Aug. 31-Sept. 4, 1998.

[7] D'AURIA, F., FROGHERI, M., GIANNOTTI, W. "Relap5/mod3.2 post test analysis and accuracy quantification of Spes test SP-SB-04" USNRC NUREG/IA-0155, Washington (US), February 1999.

[8] ANNUNZIATO, A., GLAESER, H., LILLINGTON, J.L., MARSILI, P., RENAULT, C., SJOBERG, A. "CSNI Code Validation Matrix of Thermalhydraulic Codes for LWR LOCA and Transients" OECD/CSNI Report No. 132-Rev. 1, Paris (F), July 1996.

[9] D'AURIA, F., GALASSI, G.M., INGEGNERI, M. "Evaluation of the data base from high power and low power small break LOCA counterpart tests performed in LOBI, SPES, BETHSY and LSTF facilities", University of Pisa Report, DCMN - NT 237(94), Pisa (I), Nov. 1994.

[10] AKSAN, N., D'AURIA, F., GLAESER, H., POCHARD, R., RICHARDS, C., SJOBERG, A. "Separate Effects Test Matrix for Thermal-Hydraulic Codes Validation: Phenomena Characterisation and selection of Facilities and Tests", OECD/CSNI Report OCDE/GD (94) 82, Paris (F), Jan. 1995.

[11] D'AURIA, F. GALASSI, G.M. "Flowrate and Density Oscillations during Two-Phase Natural Circulation in PWR typical Conditions", J. Nuclear Engineering and Design , Vol 122, 1990.

[12] D'AURIA, F., GALASSI, G.M. "Relevant results obtained from the analysis of LOBI/MOD2 natural circulation experiment A2-77" USNRC NUREG/IA-0084, Washington (US), April 1992 (2).

[13] D'AURIA, F., FROGHERI, M., MONASTEROLO, U. "Removable Power by Natural Circulation in PWR Systems" ICONE-5, Nice (F) May 26-30, 1997.

[14] D'AURIA, F., FROGHERI, M. "Use of Natural Circulation Flow Map for assessing PWR performance" Eurotherm Sem. No. 63: Single and Two-Phase Natural Circulation, Genova (I), Sept. 6-8 1999.

Activities of passive cooling applications and simulation of innovative nuclear power plant design

F. Aglar, A. Tanrıkut

Turkish Atomic Energy Authority, Turkey

Abstract. This paper gives a general insight on activities of the Turkish Atomic Energy Authority (TAEA) concerning passive cooling applications and simulation of innovative nuclear power plant design. The condensation mode of heat transfer plays an important role for the passive heat removal application in advanced water-cooled reactor systems. But it is well understood that the presence of noncondesable (NC) gases can greatly inhibit the condensation process due to the build up of NC gas concentration at the liquid/gas interface. The isolation condenser of passive containment cooling system of the simplified boiling water reactors is a typical application area of in-tube condensation in the presence of NC. The test matrix of the experimental investigation undertaken at the METU-CTF test facility (Middle East Technical University, Ankara) covers the range of parameters; P_n (system pressure) : 2-6 bar, Re_v (vapor Reynolds number): 45000-94000, and X_i (air mass fraction): 0-52%. This experimental study is supplemented by a theoretical investigation concerning the effect of mixture flow rate on film turbulence and air mass diffusion concepts. Recently, TAEA participated to an international standard problem (OECD ISP-42) which covers a set of simulation of PANDA test facility (Paul Scherrer Institut-Switzerland) for six different phases including different natural circulation modes. The concept of condensation in the presence of air plays an important role for performance of heat exchangers, designed for passive containment cooling, which in turn affect the natural circulation behaviour in PANDA systems.

1. INTRODUCTION

Nuclear energy is one of the options presently available to cope with energy needs along the forthcoming century. This challenge is requiring a tremendous effort to assure nuclear energy competence in terms of economics and safety with respect to the other potential sources of energy. In the case of water cooled power reactors, new advanced designs have been proposed of either an evolutionary or a passive type, the latter being particularly appealing for using natural forces to carry out safety functions under the most adverse conditions posed by hypothetical accidents. In this regard containment of passive reactors is to be equipped with what has been called Passive Containment Cooling Systems (PCCS).

PCCS's features depend on specific designs. However, most of them share their reliance on steam condensation to mitigate long term pressure rise in containment. New boundary conditions and device geometries prompted renewed to investigate steam condensation to eventually demonstrate PCCS's capability to meet their goals. As a result, experimental and analytical programs were launched worldwide, often on the basis of a fruitful international co-operation [1].

Concepts of passive safety systems with no active components have been investigated for new generation light water reactors [2]. The primary objectives of the passive design features are to simplify the design, which assures the minimised demand on operator, and to improve plant safety. To accomplish these features the operating principles of passive safety systems should be well understood by an experimental validation program. Such validation programs are also important for the assessment of advanced computer codes, which are currently used for design and licensing.

In an application, the proposed advanced passive boiling water reactor design, simplified boiling water reactor (SBWR), utilises as a main component of the passive containment

cooling systems (PCCS) the isolation condenser (IC). The function of the IC is to provide a passive heat exchanger for the removal of the reactor coolant system sensible heat, and core decay heat to a reservoir of water within the containment. In performing this function, the IC must have the capability to remove sufficient energy from the reactor containment in order to prevent the containment from exceeding design pressure shortly following design basis event and to significantly reduce containment pressure in the longer run [3]. However, it is well established that the presence of noncondensable (NC) gases in vapors can greatly inhibit the condensation process. The mass transfer resistance to condensation results from a build-up of NC gas concentration at the liquid/gas interface leading to a decrease in the corresponding vapor partial pressure and thus the interface temperature at which condensation occurs [3]. As a result, reduction in heat transfer rate is unavoidable with respect to the pure condensation case.

A part of the long-term research and development efforts of the Turkish Atomic Energy Authority (TAEA) is planned to concentrate on passive cooling systems. In this paper, a general insight on activities of the TAEA concerning condensation in the presence of air is given. Moreover, TAEA participated to an international standard problem (OECD/NEA ISP-42) which covers a set of simulations of PANDA test facility, which is the scaled model of SBWR for different phases of natural circulation modes. The concept of condensation in the presence of air plays an important role for the performance of heat exchangers, designed for passive containment cooling, which in turn affect the natural circulation behaviour in such innovative systems.

2. EXPERIMENTAL STUDY

The test facility named as Middle East Technical University Condensation Test Facility (METU-CTF) was installed at the Mechanical Engineering Department of METU. The experimental set up consisting of an open steam or steam/gas system and open cooling water system is depicted in the flow diagram of Figure 1 [4].

Steam is generated in a boiler (1.6 m high, 0.45 m ID) by using four immersion type sheathed electrical heaters. Three of these heaters have a nominal power of 10 kW each and the fourth one has a power of 7.5 kW at 380 V. All the heaters can be individually controlled by switching on or off. The boiler tank was designed to withstand an internal pressure of 15 bar, at $T = 20^0 C$, and was tested at this pressure. The maximum operating pressure of the tank is 10 bar. To ensure dry steam at the exit of the boiler, a mechanical separator directly connected to the exit nozzle was installed. The boiler tank was thermally insulated to reduce the environmental heat loss.

Compressed air can be supplied either to the boiler tank or to the steam line via nozzle after the orifice meter on the horizontal part of the pipe, which connects the boiler and the test section.

The pipe connecting the boiler tank and the test section has a length of approximately 2 m and an ID of 38.1 mm. The pipe was connected to the boiler tank via an isolation valve. This isolation valve is used to isolate the boiler until inside pressure of the tank is increased to a predetermined level.

The test section is a heat exchanger of countercurrent type, that is steam or steam/gas mixture flows downward inside the condenser tube and cooling water flows upward inside the jacket pipe.

The condenser tube consists of a 2.15 m long seamless stainless steel tube with 33/39 mm ID/OD. The jacket pipe surrounding the condenser tube is made of sheet iron and has a length of 2.133 m and 81.2/89 mm ID/OD.

A total of 13 holes were drilled with an angle of 30^0 at different elevations along the condenser tube length to fix the thermocouples for inner wall temperature measurements. Similarly, 15 holes were drilled radially at different elevations for installation of the thermocouples to be used for cooling water temperature measurements. The jacket pipe was thermally insulated to reduce environmental heat loss. Ten thermocouples were fixed to a 2 mm diameter Inconel guide wire and installed at the central temperature measurements.

The experimental text matrix has been constituted by pure steam and steam/air mixture runs and the effect of NC gas has been analyzed by comparing the pure steam runs with mixture runs with respect the temperature, heat flux, air mass fraction, and film Reynolds number. The range of the measured parameters; P_n = 2-6 bars, Re_v = 45,000-94,000, and X_i = 0 %-52%.
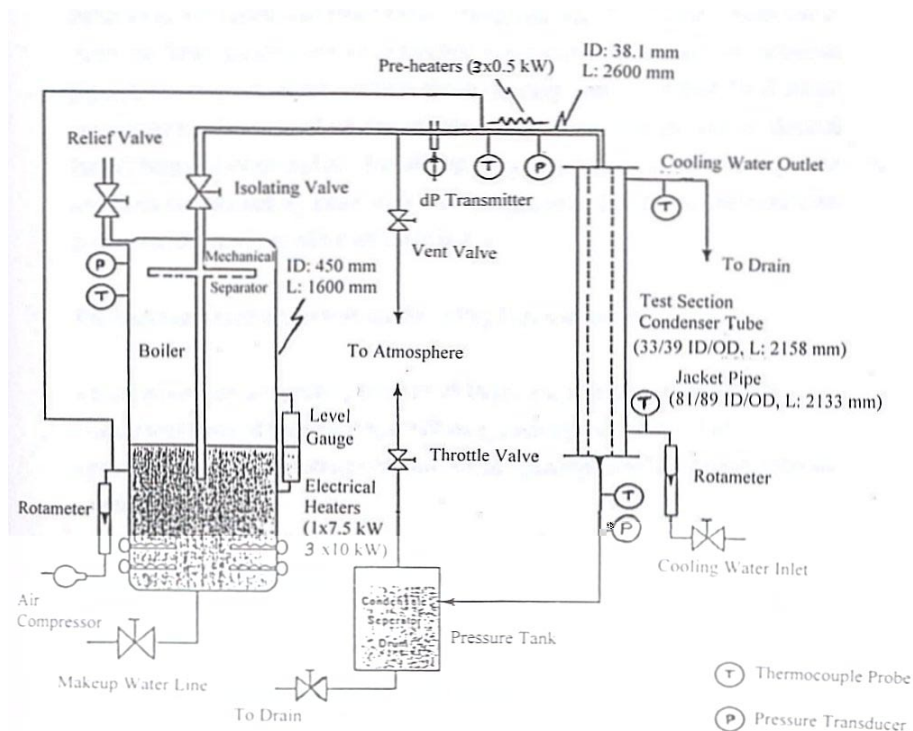
FIG. 1. Schematic view of the METU-CTF [4]

3.   THEORETICAL STUDIES

Although many of the theoretical studies have been performed to investigate the effect of NC gases on steam condensation, in recent years studies have been prosecuted by simple correlations such as the correlation introduced by UCB. In this correlation, the local heat transfer coefficient is expressed in the form of a "degradation factor" defined as the ratio of

the experimental heat transfer coefficient to a reference, pure steam, heat transfer coefficient. The reference heat transfer coefficient is calculated from Nusselt theory. Moreover, the enhancement of heat transfer coefficient due to the shear stress of the gas on liquid film is considered, f_{shear}, and conveyed to the correlation. The other effects enhancing the condensation heat transfer coefficient are also taking into account, f_{others}, and are correlated in terms of liquid side Reynolds number, Re_L. The suppression of the condensation heat transfer coefficient by the accumulation of the NC gas at the interface is clarified and denoted as f_2. In this present study, both the enhancement and the suppression factors given in UCB formulation are modified by considering mixture side Reynolds number and the Sherwood number defining the radial concentration gradient of NC gas respectively.

f Type Correlation Modified by Sherwood Number

$$f = f_1.f_2 \tag{1}$$

where
f is the degradation factor, f_1 is the enhancement factor, and f_2 is the suppression factor.

$$f_1 = f_{shear}.f_{others} \tag{2}$$

$$f_{shear} = \frac{\delta_1}{\delta_2} \qquad \text{where;} \tag{3}$$

δ_1 : Film thickness without interfacial shear stress

δ_2 : Film thickness with interfacial shear stress.

The interfacial shear stress is influenced by both the interface velocity and the mixture side velocity. Moreover, the entrainment from a liquid film is associated with the onset of disturbance waves at the interface and, in general, depends on both the vapor and the liquid flow rates. In fully turbulent flow, above a film Reynolds number of 3000 the condition for the onset of entrainment depend mainly upon the vapor velocity [5]. For this reason, the f_{others} in Equation (2) is correlated as,

$$f_{others} = 1 + C_1.Re_L^{z1} + C_2.Re_M^{z2} \tag{4}$$

The build up of NC gases at the interface and its back diffusion into the core constitute a primary problem. The accumulation of NC gas at the interface is the principle reason for the mass diffusion resistance in radial direction, which causes lower condensation rates. This effect is encompassed into the correlations with the aid of air mass fraction in UCB correlation. However, air mass fraction is not defining the ongoing process, which is originally governed by concentration gradient formed between the interface and the core. Therefore, the Sherwood number is used instead of air mass fraction in the suppression factor, f_2. When the variation of f_2 is investigated with the Sherwood number, the segregation of individual runs from each other is observed and this situation is attributed to inlet pressure which is, therefore, superimposed into the correlation as air mole fraction. Under the light of these arrangements, the suppression factor is formulated as follows.

$$f_2 = 1 - C_3.Shrr^{z3} \tag{5}$$

where

$$Shrr = y_g.Sh \tag{6}$$

y_g: Mole Fraction of air
Sh: Sherwood Number
C_1-C_3 and z_1-z_3 are the constants to be determined.
Results and the comparison of the correlations are given in section 4.2.

4. RESULTS

4.1. Experimental results

The heat flux distribution for experimental runs corresponding to the nominal system pressure, P_n, of 2, 3, and 4 bars, and including pure vapor and different mixture of air and vapor, are presented in Fig. 2, 3, and 4 respectively [4,6].

An increase in system pressure increases local heat flux and this can be attributed to the increase in wall subcooling degree that enhances the thermal driving force for heat transfer. Moreover, higher system pressure associated with the higher inlet temperature leads to a greater number of molecular collisions helping in the diffusive transport of energy. However, in our experimental investigation, the dependency of the wall subcooling degree, either measured (T_c-T_w) or predicted from Gibbs-Dalton Law (T_s-T_w), on system pressure is such that the wall subcooling degree remains nearly the same for the same inlet air mass fraction and for the different system pressure. This implies that the vapor mass flow rate may dominate over system pressure, concerning the effect on local heat flux, for cases with air/vapor mixture (Fig. 5). The situation is rather different in pure vapor runs, that is increase in system pressure has a strong effect on enhancement of predicted, and even measured, wall subcooling degree and hence on increase of local heat flux (Fig. 6).

4.2. Results of correlations

Using UCB condensation data base [7] for both pure and steam/air mixture available, the unknown parameters of the correlations have been estimated by using Marquardt-Levenberg non-linear parameter estimation method [8] which provides quicker convergence than alternative methods. Results of present correlations are given in Table I.

5. TAEA ACTIVITIES ON OECD/NEA ISP-42

TAEA participated to the OECD/NEA International Standard Problem No:42 (ISP-42) which is hosted by the Paul Scherrer Institut (PSI), Switzerland. The ISP-42 test was performed in the PANDA test facility, at the PSI, as a sequence of Phases A through F, representing typical passive safety system operating modes covering certain specific phenomena. The configuration used for ISP-42 was corresponding to the European Simplified Boiling Water Reactor containment and passive decay heat removal system at about 1:40 volumetric and power scale, and full scale for time and thermodynamic state.

$$ \text{** Mean Deviation} = \frac{1}{n} \sum_{1}^{n} \text{abs} \left[\frac{(h_{cal} - h_{exp})100}{h_{exp}} \right] $$
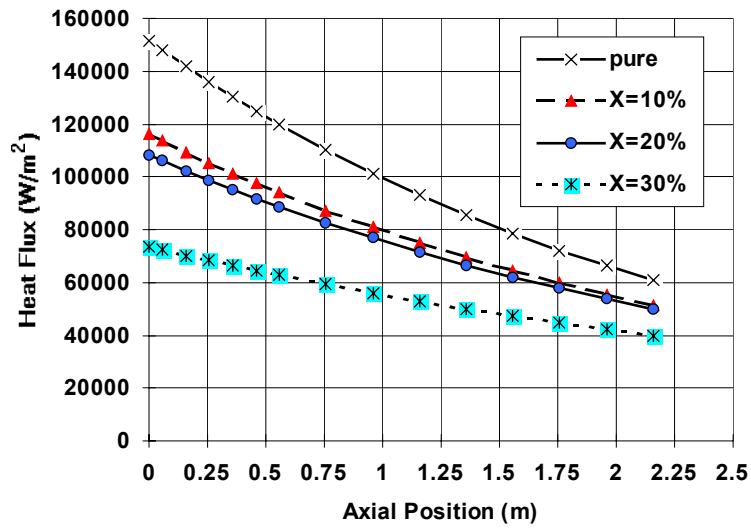
FIG. 2. Heat flux distribution along the condenser tube (P_n=2 bar, Re_v=54000–63000) [6].
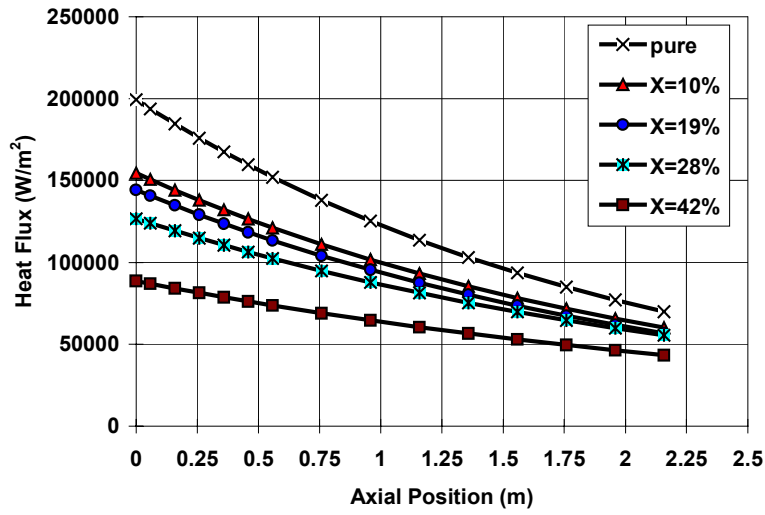
FIG. 3. Heat flux distribution along the condenser tube (P_n=3 bars, Re_v=67000–78000 and Re_v= 54000 for X_i=42%) [4].
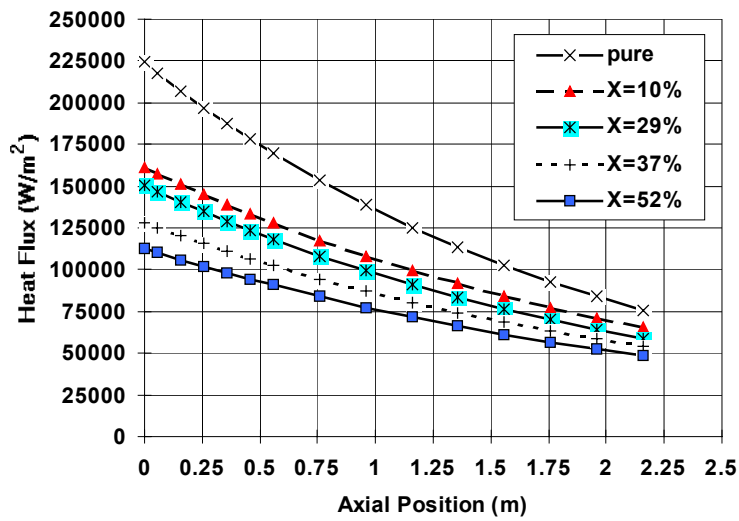
FIG. 4. Heat flux distribution along the condenser tube (P_n=4 bar, Re_v=77000–86000 and Re_v = 45000 for X_i=52 %) [4].
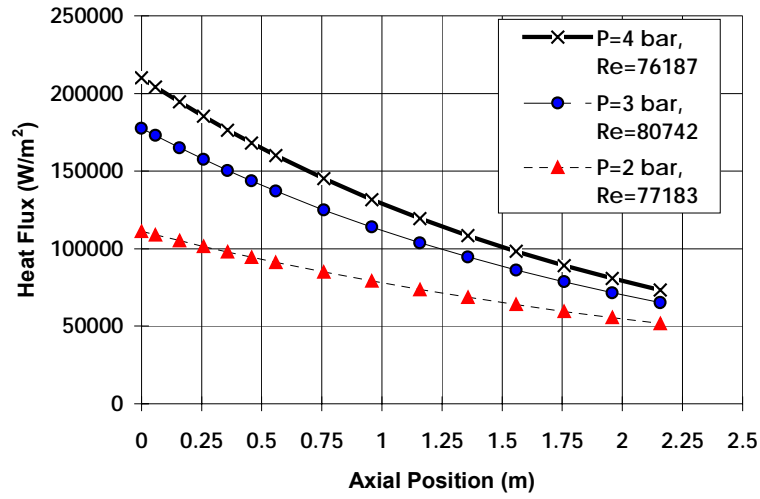
FIG. 5. Effect of system pressure (air/steam mixture; X_i=20 %) [4].
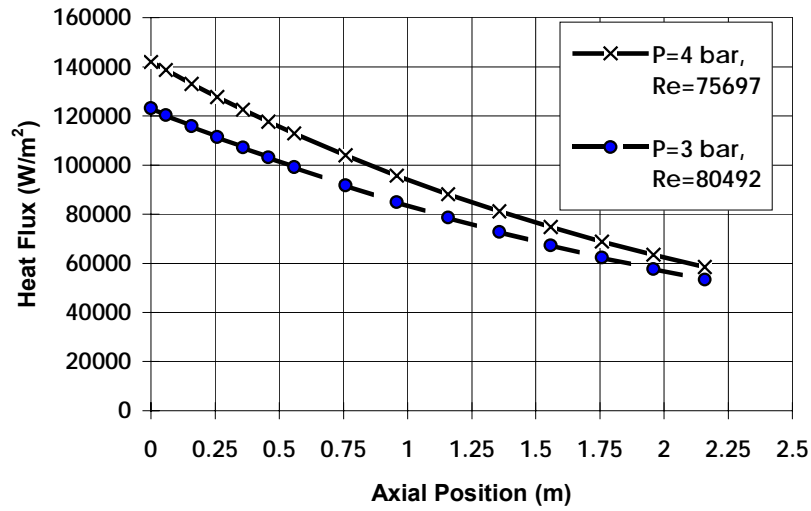
FIG. 6. Effect of system pressure (pure steam) [4].

TABLE I. COMPARISON OF CORRELATIONS

PURE STEAM	Mean Deviation[**], %	
	$f_{exp}>1.4$	$f_{exp}< 1.4$
Present Study	5.26	7.18
UCB	10.57	
STEAM+NC GAS Based on X_g	Mean Deviation, %	
	$X_g<0.1$	$X_g>0.1$
Present Study	10.23	18.39
UCB	12.41	20.58
STEAM+NC GAS Based on Sh Number	Mean Deviation, %		
	Shrr<5	5<Shrr<25	Shrr>25
Present Study	17.22	16.17	9.16

Both the experimental results and prediction of the RELAP5/mod3.2.2 code reveals the fact that the system behaviour during Phase-A is highly affected by the performance of Passive Containment Cooling System (PCCS) heat exchangers. The objective of Phase-A is to investigate the start-up of passive cooling system when steam is injected into a cold vessel (dry-well) filled with air and to observe the resulting gas mixing and associated system behaviour. This simulation demonstrates the importance of both pure steam condensation and steam condensation in the presence of air for natural circulation in the system which in turn governs the realistic system behaviour. The system transient has been developed into two distinct parts: first, system heat-up and pressurization period (~3800 s) due to evaporation in the reactor pressure vessel with constant heat input from the heaters in the core and weak heat removal rate from PCC heat exchangers as the result of high air mass fraction; second, system pressure stabilization period (from 3800 s to the end of analysis) during which PCC heat exchangers become active as the result of venting of air from PCC tubes. The results of RELAP5 predictions for PCC-1 heat exchanger are presented in Figs. 7 and 8 for time 1500 s and 5000 s, respectively. These two distinct times are selected to demonstrate the PCC heat exchanger performance during aforementioned two distinct parts of the transient. In these figures, only the results of 5 tubes (out of 20 tubes) which were lumped to single pipe consisting of 10 control volumes were shown. Two parameters are essential with respect to PCC heat exchanger performance; local heat flux and air mass fraction. As given in Section 4.1, the system pressure is also an important parameter for the rate of condensation. However, the effect of the system pressure is expected to be small in these two figures since the pressure difference is small, i.e. 0.7 bar.

As could be seen in these figures, the local heat flux is affected by the presence of air inside the PCC heat exchanger tubes, as expected. Since the local air mass fraction is about 0.94 (almost pure air) and constant throughout the length of the condenser tubes as predicted at t=1500 s (Fig. 7), the local heat flux values are suppressed to about 0.2 % of the local heat flux values predicted at t=5000 s during which condenser tubes are full of almost pure steam down to 1.3 m (about ¾ of total length). The maximum air mass fraction at the bottom of the condenser tubes is less than 0.3 at 5000 s. It is to be noted that some amount of air is accumulated in bottom part of tubes and lower drum of PCC-1 after 3800 s due to terminated vent flow from PCC lower drum to the wet-well tanks. The accumulation of air at the bottom of tubes shorten the active condensation length to about ¾ of total lenght, as seen in Fig. 8, and this reveals the fact that percent of shortening of active condensation length is also the function of system pressure and differential pressure developed between PCC lower drum and wet-well tanks. In other words, system pressure and differential pressures developed between components in a system operating under natural circulation could highly affect the rate of vent of air from PCC tubes and in turn the effective condensation length.

6. CONCLUSIONS

In this paper, activities of the TAEA concerning condensation in the presence of NC gas were given. In the experimental analysis, it was observed that the overall agreement between the analytical analysis and the experimental data obtained for heat flux or heat transfer coefficients is reasonably good. For example, the heat flux significantly decreases as the inlet air mass fraction increases. Moreover, it could be promulgated that the effect of superheating of inlet stream possesses no considerable effect on the heat flux. Another conclusion emerging from experimental studies is that the local heat flux values for pure steam and mixture runs come closer towards the bottom of the condenser tube.
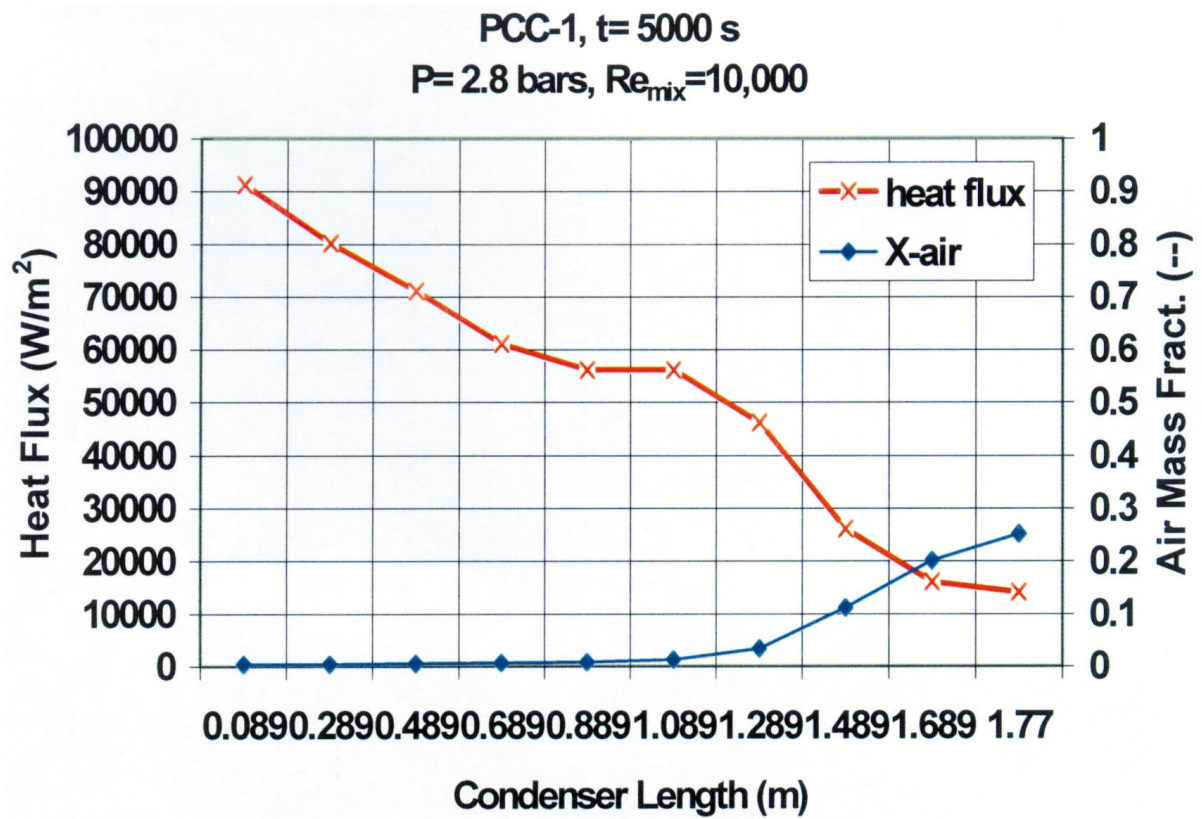
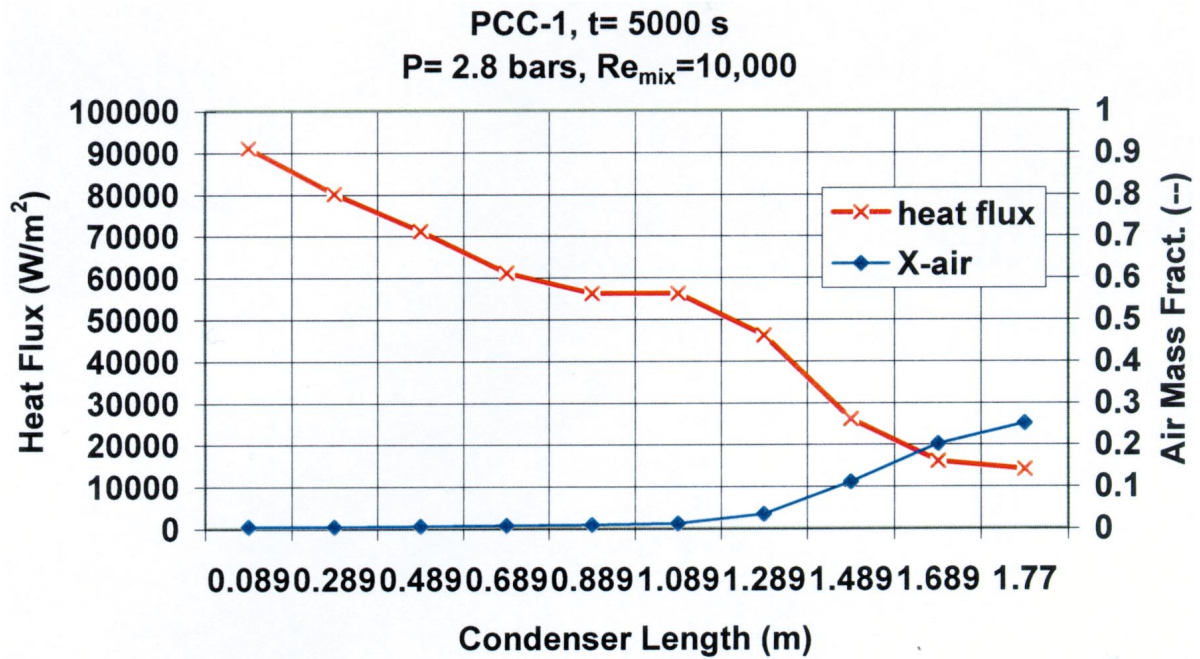*Fig. 7. Local heat flux and air mass fraction distribution along the axis of the PCC-1 for t= 1500 s.*

Fig. 8. Local heat flux and air mass fraction distribution along the axis of the PCC-1 for t= 5000 s.

The correlations obtained from UCB database show that the mixture side Reynolds number is also a strong parameter affecting heat transfer coefficient. However, it should be noted that the given correlations stay behind the real phenomenon occurring inside the tube. Because, neither interfacial waviness nor the suction effect is taken into account. At the same time, these correlations depend on the flow regimes of either phase. If turbulent- turbulent flow regime is in question, these correlations fail. Therefore, the studies have been concentrated on an analytical solution in which a film-wise condensation of a down-flow steam/NC gas mixture in a vertical tube is considered. In this analytical model, the mixture side is treated as turbulent flow. The effect of Prandtl number, interfacial shear stress, interfacial waviness, entrainment and deposition and especially the suction have been covered in our model. The two-fluid formulation constitutes the main routine. The interfacial temperature is estimated using the stagnant film theory. Moreover, for the mixture side, the turbulence model is developed in order to elaborate suction effect, which is one of the primary reasons of the enhancement of the mixture side heat transfer coefficient. Finally, it should be stated that the diffusion layer theory is superimposed into the model to define the closure relations.

The condensation is an important heat transfer mode for natural circulation in innovative systems nuclear reactor systems like the Simplified Boiling Water Reactor design. The realistic prediction of local heat flux in heat exchangers of passive containment cooling system is essential and due to this reason physical models in computer codes for condensation and effect of NC gases on condensation should be assessed. Though very preliminary, ISP-42 study on PANDA reveals us the fact that the realistic prediction of the performance and behaviour of PCC heat exchangers could affect the overall system behaviour and the rate of condensation heat transfer is the function of air mass fraction at the inlet of condenser tubes and effective condensation length.

REFERENCES

[1]   HERRANZ, L.E., et al., "Modelling Containment Passive Safety Systems in Advanced Water Cooled Reactors", IAEA Technical Committee Meeting, Villigen (Switzerland), 14-17 September 1998.

[2]   MURASE, M., KATAOKA, Y., FUJII, T., "Evaporation and Condensation Heat Transfer with Noncondensable Gas Present", Nuclear Engineering and Design, 141, pp. 135-143 (1993).

[3]   SIDDIQUE, M., MICHAEL, W. G., MUJID, S. K., "Theoretical Modeling of Forced Convection Condensation of Steam in a Vertical Tube in the Presence of a Noncondensable Gas", Nuclear Technology, vol. 106, pp. 202-215 (1993).

[4]   TANRIKUT, A., "Tube Condensation in the Presence of Air," Ph.D. Thesis, Mechanical Engineering Department, Middle East Technical University, Ankara (1998).

[5]   COLLIER, J. G., and THOME, J. R., Convective Boiling and Condensation, Oxford Science, London (1994).

[6]   TANRIKUT, A., and YESIN, O., "An Experimental Research on In-tube Condensation in the Presence of Air," 2nd International Symposium on Two-phase Flow and Experimentation, Pisa (Italy), 23-26 May 1999, pp. 367-374.

[7]   KUHN, S. Z., SCHROCK, V. E., PETERSON, P. F., "Final Report on U. C. Berkeley Single Tube Condensation Studies," Dept. of Nuclear Eng., UCB-NE-4201 (1994).

[8]   AĞLAR, F.,"Determination of Heat Transfer Coefficient for Saturated Flow Boiling of Water", M. Sc. Thesis, Mechanical Engineering Department, Middle East Technical University, Ankara (1993).

Experiment research and calculation method of natural circulation flow for AC600/1000

S. Zhang

Nuclear Power Institute of China,
China

Abstract. Passive safety concept is extensively used in the design for next generation advanced PWR nuclear power plant. The decay heat of reactor core can be removed through natural circulation flow of coolant following an accident. This not only increases reliability of engineered safety systems and reduces core melt frequency, but also simplifies systems and increases plant economy. Nuclear Power Institute of China (NPIC) has performed preliminary experiment research and relative theoretical analysis for passive characteristics of advanced PWR nuclear power plant AC600/1000. Three tests about natural circulation flow have finished as the following: residual heat removal through SG secondary side, core makeup tank behavior and wind flow of containment. The above mentioned three mechanism tests have verified natural circulation flow concept of AC600/1000. By the end of this year NPIC will finish other two single tests in order to research the following key technology of the passive safety systems: The natural circulation characteristics of tandem system of SG secondary side loop and air flow loop for emergency residual heat removal system (ERHRS) after station blackout accident; The water flow behavior in primary coolant system contained by core makeup tank, pressurizer, accumulator and reactor pressure vessel after small break accident; Computer code development and verification. Meanwhile, NPIC will cooperate with Karlsruhe Technology Center of Germany to research natural circulation characteristics of air in the annular channel between the steel shell and the concrete shell of containment. NPIC plans to build two large integral test facilities. One of which is used to research natural circulation flow and residual heat removal through primary loop, secondary loop and air flow loop from reactor core to ultimate sink ---atmosphere after station blackout accident. It is also used to research the passive safety injection features for emergency core cooling system. The second integral test facility will be used to research the comprehensive heat removal behavior of passive containment cooling system. The paper will describe the utilization of natural circulation concept in the passive safety systems, experiment research performed by NPIC and computer codes as well for AC600/1000.

1. INTRODUCTION OF PASSIVE SAFETY AND NATURAL CIRCULATION CHARACTERISTICS FOR AC600/1000

1.1. Main design characteristics of AC600/1000

145 fuel assembly and 3658 mm active section core is used in AC600. 177 fuel assembly and 4267mm active section core is used in AC1000. Neutron instrumentation system inserts into core from top of pressure vessel so that there is not any penetration in the bottom head of reactor pressure vessel. Steel water reflector is used to save neutron and to reduce neutron fluency on wall of reactor pressure vessel. Modularization construction, advanced digital instrumentation and control system are considered in AC600/1000 design. Passive safety systems including passive emergency residual heat removal, passive safety injection and passive containment cooling sub-systems are very important for AC600/1000 design.

No any penetration below top of reactor core is useful to reduce core melt frequency. Integral reactor top structure and large size reactor vessel are also used in AC600/1000 design. The inner diameters of reactor pressure vessels are 4000mm for AC600 and 4340 mm for AC1000. Low power density of reactor core, low neutron leakage, 80% stainless steel +20% water reflector and large size reactor pressure vessel are able to assure 60 year life time of plant. Gray rods are used in AC600/1000 to achieve daily load follow. Linear power density of core is 134.2/140W/cm for AC600/1000 respectively, much lower than current PWR nuclear power plant so that AC600/1000 reactor core has larger safety margin.

1.2. Passive safety features of AC600/1000

Natural circulation concept is used in the AC600/1000 passive safety system design. The system is actuated by gravity, natural circulation or pressurized gas. Following accident, AC600/1000 is able to maintain core cooling and containment integrity without operator's intervention. This is an important safety requirement in the AC600/1000 design.

Emergency residual heat removal system (ERHRS) is used to remove decay heat from reactor core following accident. Secondary side of SG, emergency feedwater tank and air cooler establish a natural circulation cycle. Air coolers are located in a chimney. The heat transfer area is about $750m^2$ for each air cooler. Emergency feedwater tank volume is $25m^3$ for each SG cycle.

1	Reactor Pressure Vessel	1/1
2	Steam Generator	1/2
3	Reactor Coolant Pump	2/4
4	Pressurizer	1/1
5	Emergency Make-up Tank	1/2
6	Emergency Air Cooler	1/2
7	Chimney	1/2
8	Pneumatic Isolation Valve	2/4
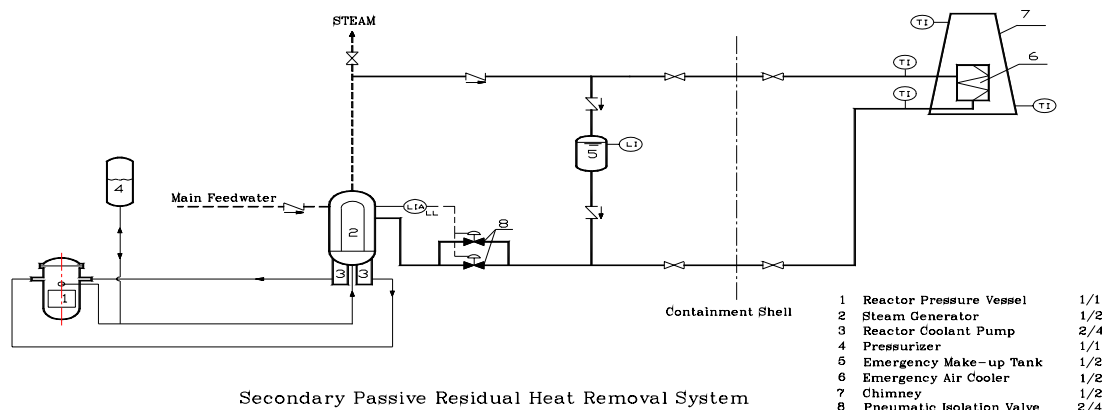
FIG. 1. Secondary passive residual heat removal system.

Passive safety injection system of AC600/1000 (PSIS) is mainly used to mitigate the consequence of LOCA. The core cooling water is provided through use of the following four water sources: core make-up water tank (volume is 2 or 3 x $40m^3$), accumulator (volume is 2 or 3 × $40m^3$), refueling water storage tank and containment sump. Low pressure safety injection subsystem uses two or three active pumps, design flow rate of each which is 142 kg/s.
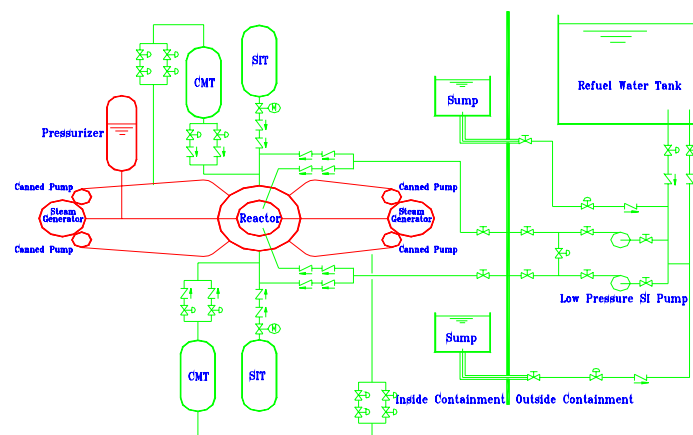
FIG. 2. Passive safety injection system for AC600.
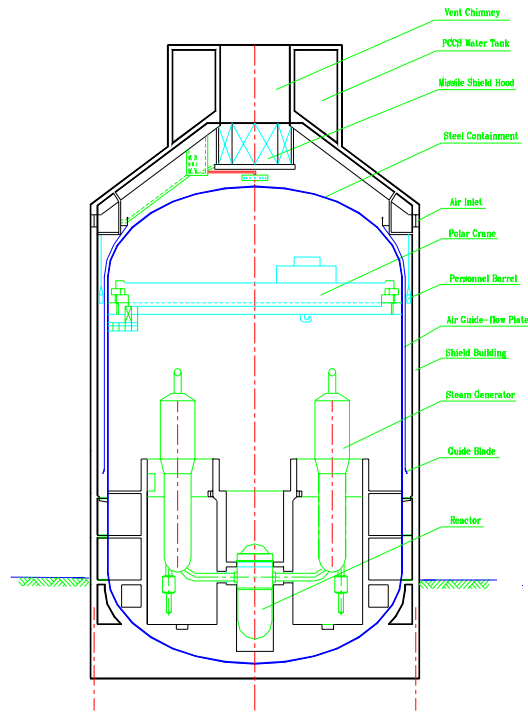
FIG. 3. Passive containment cooling system.

The containment of AC600/1000 is a two-shell structure. Between inner steel shell and outer reinforced cylindrical concrete shell, there is a baffle to form an annular wind duct. Containment top water storage tank capacity can meet the requirement of 72 hours for steel shell cooling after large LOCA. In the top of containment, there is a cooling water distribution to make the heat removal more efficient and quick in the early phase of an accident. For long term cooling, peak pressure of the containment is not larger than 90% of containment design pressure. For severe accident, containment pressure is below failure pressure. Containment spray system is eliminated in the AC600/1000 design.

2.   MAJOR EXPERIMENT RESEARCH RELATED TO SAFETY FOR AC600/1000

2.1.   Experiment Research Plan

Experimental studies about passive safety characteristics for AC600/1000 ar divided the following three steps:

(1)   Mechanism demonstration tests include emergency residual heat removal test through natural circulation flow of SG secondary side, core make-up tank performance test and wind tunnel test for passive containment cooling. Above three mentioned tests finished by the end of 1996.

(2)   Part function demonstration tests include emergency residual heat removal test through natural circulation flow of SG secondary side and atmosphere loop and thermal hydraulic transient behavior test research during small break LOCA for core make-up tank, pressurizer, accumulator and reactor pressure vessel. Above two mentioned tests will be finished by end of this year. Meanwhile, NPIC will cooperate with Karlsruhe Technology Center of Germany to do air natural circulation flow test for AC600/1000 passive containment cooling system.

(3)   Comprehensive function demonstration tests. NPIC plans to construct the following two large test facilities: a. Integral thermal hydraulic test facility. It is a tandem system of primary coolant cycle, secondary side cycle of SG and air flow cycle, which can be used to research station black out accident, small break LOCA and computer code development. b. Integral containment cooling test facility. It is used to simulate and research comprehensive characteristics of passive containment cooling system for AC600/1000.

2.2. Experimental study of secondary-side passive emergency residual heat removal system for AC600/1000

The main purpose of the experimental study is to demonstrate capability of decay heat removal, to determine behavior of the system and components, to find start-up characteristics and procedures and to obtain a database for developing computer codes for AC600/1000 passive emergency residual heat removal system.

The total 166 sets of experimental data are identified. The test results illustrate that short disturbances of wind speed, power and valve opening have no significant impact on natural circulation flow, implying that the system seems to tolerate these disturbances. A correlation of two-phase, natural circulation flow rate is derived from constitutive equations by use of lumped system parameters were obtained. The empirical coefficients m and n were obtained by non-linear regression of 83 test data. Compared with 166 sets of the measured data, the deviation of 98.8% of the data points is within ±15%.

TABLE I. STEADY STATE TEST PARAMETER RANGES

Parameter	Unit	Range
Elevation difference between air cooler and SG/L_{th}	m	11.04, 15.04
Slope angle of air-cooler/θ	rad	0, $\pi/3$
Pressure/P	MPa	4.0~7.6
Heating power/q_c	kW	85~140
Natural circulation flowrate/W	kg/s	0.044~0.075
Wind speed/V	m/s	0.65~2.9

FIG. 4. Schematic diagram of ERHRS test facility.
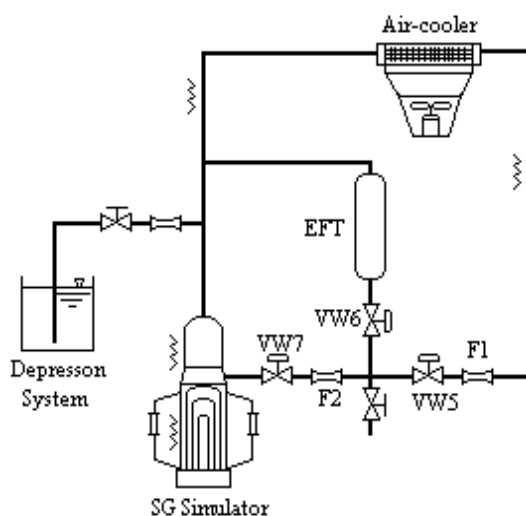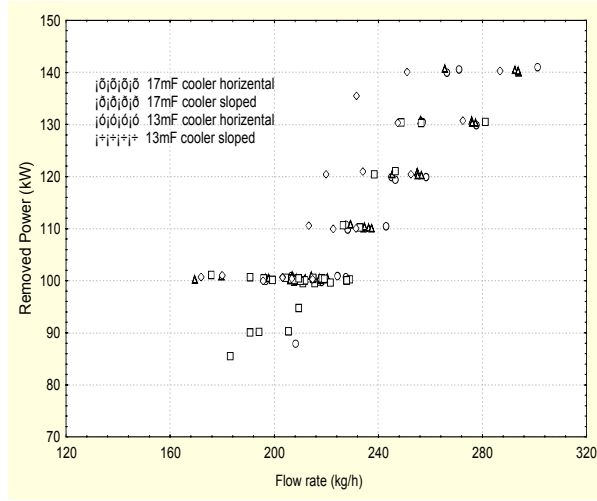
FIG. 5. Plot of removed power vs. NC flow rate.

$$W = m \cdot K_{eff}^{n} \cdot \sqrt[3]{-C/2 + \sqrt{(C/2)^2 + (B/3)^3}} + \sqrt[3]{-C/2 - \sqrt{(C/2)^2 + (B/3)^3}}$$

$$B = (\frac{\beta \rho_{ls} h_{f\alpha}}{C_P} - \Delta\rho) L_{th} g \frac{2 A_e^2 \overline{\rho}}{K_{eff}}$$

$$C = -\frac{\beta \rho_{ls} q_s L_{th} g}{C_P} \frac{2 A_e^2 \overline{\rho}}{K_{eff}}$$

$$K_{eff} = (-0.242\theta + 2.044) \times 10^6 / \mathrm{Re}_m^{0.044}$$

$$\mathrm{Re}_m = \frac{U_m L_{th}}{\nu} = (\frac{D_e L_{th}^2}{A_e^2})(\frac{q_s \Delta\rho}{\rho_{ls} \rho_{gs} h_{fg} \nu})$$

It is noted from transient research that AC600/1000 ERHR system is able to remove decay heat. Three start-up modes are available to trigger natural circulation flow. Computer code ERHRAC simulating natural circulation flow characteristics of ERHRS for AC600/1000 has been developed based on the test data.

2.3. Full pressure core make-up tank test

Passive core make-up water tank is used so as to eliminate high pressure safety injection pumps. Transient characteristic research of core make-up water tank in the case of small LOCA were performed. The break sizes are: 2, 6, 12, 18, 30 mm respectively. Thermal hydraulic behaviors of pressurizer and draining flow rate measurement from core make-up water tank to primary coolant system following small LOCA were researched and carried out in the test. A total of 80 sensors were used to measure temperatures, liquid level and flow rate.

The above figures show the pressure curves of CMT for all 5 break sizes. It is evident that there exists a pressure oscillation phase during pressure drop down, especially for ϕ30mm break size and lasts from 50s to end of draining. In general, the blow down phase is longer, steam condensation in CMT is more. The draining behaviors of CMT are complex and change with break size. The draining mass flow rate increases rapidly at the beginning and has a low oscillation phase before stable draining phase. All break sizes have obviously a high flow rate peak. After about 500s, all flow fluxes are nearly the same.
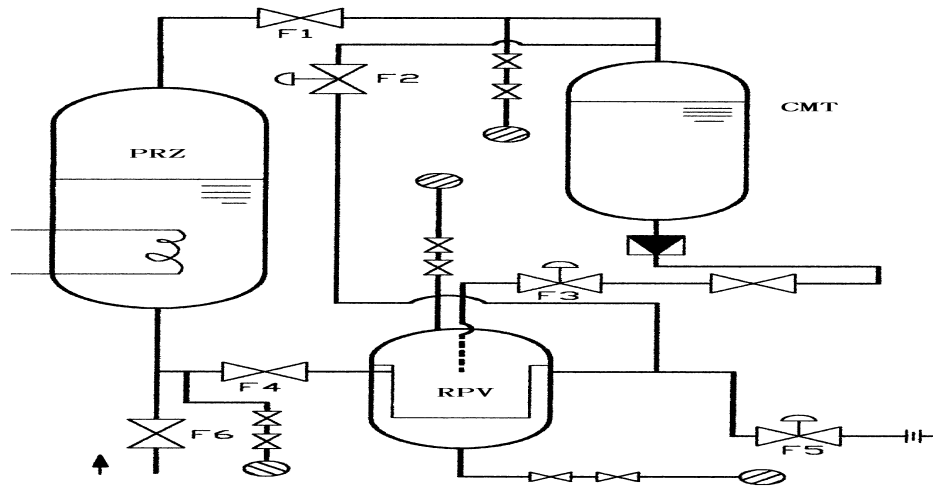
FIG. 6. Schematic diagram of CMT test rig.
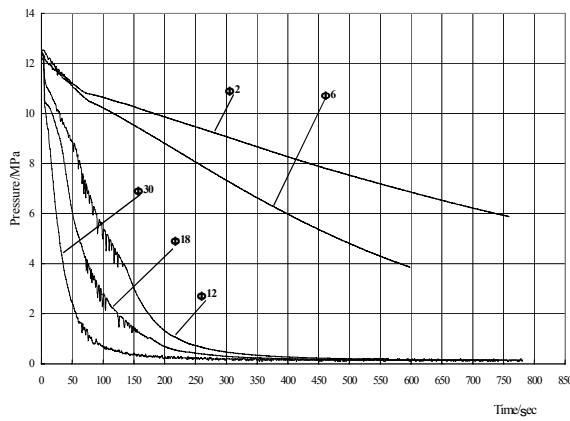
FIG. 7. Pressure variation in CMT.
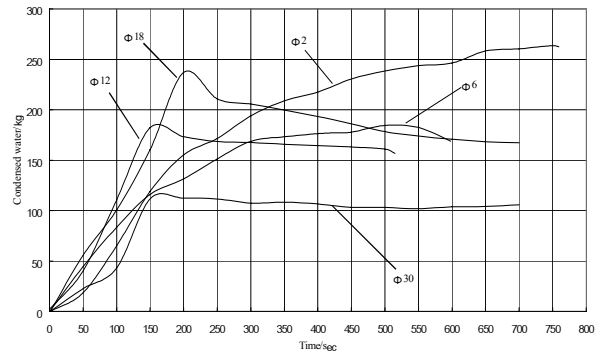
FIG. 8. Condensed steam vs. time in CMT.

TABLE II. TEST INITIAL CONDITIONS

Parameter	Unit	Break size(mm)				
		2	6	12	18	30
Initial water storage	kg	1028	1031	1030	1037	1032
System pressure	MPa	14.81	14.97	14.33	14.16	15.15
Upper temp. of RPV	°C	315	322	324	306	312
Bottom temp of RPV	°C	257	259	257	295	309
Pressure at water injection	MPa	12.39	12.20	12.11	12.11	12.33

2.4. Wind channel test for passive containment cooling system

The wind channel test will research air flow resistance characteristic and effects of air channel shape and air inlet location on natural circulation flow.

The influence of environment wind and surrounding buildings on the natural convection flow had been especially considered. Moreover, the velocity field at the lower turning of air baffle

and the surface wind pressure distribution of containment were needed for design. The main purposes of the test were: a) To verify the feasibility of passive containment cooling system design. Main emphasis was put on the influence of the environmental wind; b) To supply a database for preliminary design and design improvement, especially the experimental data of velocity field in annuli and pressure drop of each section. The velocity field in the low baffle end zone was calculated and tested.

The model tests (1/10 in scale) with different flow deflectors were done to study the way of improvement. Both test and calculated results indicated that there were an enclosed vortex in the stagnant bottom and an obvious separate bubble formed at the rear of the baffle. The flow deflectors could reduce the separate bubble. Another model test was run in 0.2—0.5 m/s water velocity. A larger vortex at the upper stream of flying object protect shielding and a smaller bubble at the down stream of it were proved by both test and calculation.

A pressure distribution test in the surface of containment was done in a low velocity wind tunnel with various wind speeds, air entrances, yaw and pitch angles. The test shows that the pressure is positive in the area of $-35° \leq \theta \leq 35°$. The influence of wind on natural convection of containment was also done with a 1/50 integral model. The test results revealed that natural convection flow rate was enhanced in general by outside wind and horizontal wind ($\alpha = 0$) had the better effect than $\alpha < 0°$ or $\alpha > 0°$. The position of chimney might influence the air flowing around the containment. The distance between containment and chimney should be larger than 4 times of chimney diameter. However, smoke wind tunnel test showed no exhausted hot air was re-circulated under any **d** outside wind conditions.
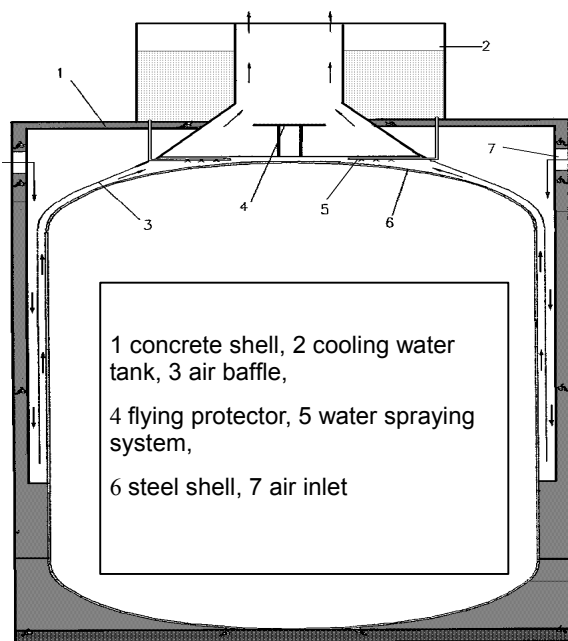
FIG. 9. Diagram of containment structure.
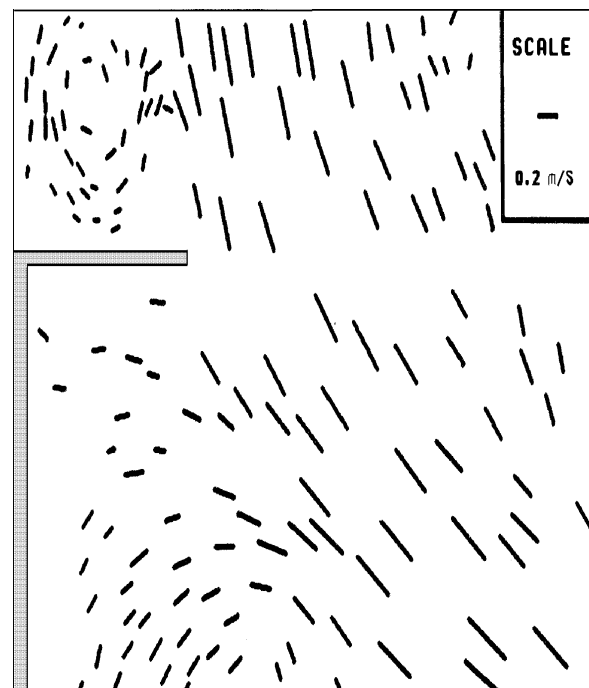
FIG. 10. Flow field near flying protect shielding.

131
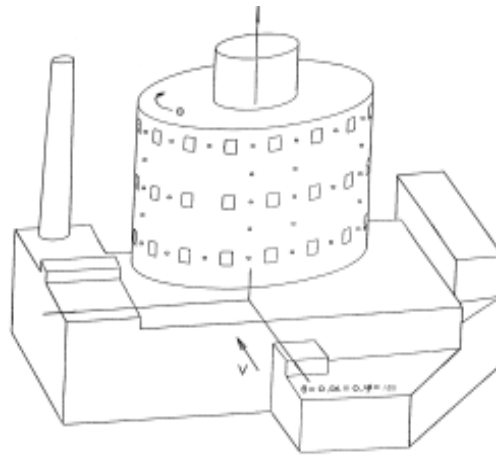
FIG. 11. Tunnel test model.

2.5. Summary

1) The studies of passive ERHR system, CMT injection system and passive containment cooling system prove that the design of all these passive systems are feasible and reliable in principle and can meet basically the required safety functions.

2) Some undesired thermal hydraulic phenomena were found and identified in these studies. For example, the flow vortex in the containment air duct, and "water hammer" of ERHR test may have bad impacts on its safety functions and should be avoided in the next step tests and AC600/1000 design.

3) All data obtained have been already used for design improvement and next R&D program planning.

3. ANALYSIS CODE DEVELOPMENT AND CALCULATION FOR NATURAL CIRCULATION BEHAVIOR OF AC600/1000

3.1. Theoretical analysis and research for AC600/1000 passive containment cooling behavior

PCCAC-2D is a two dimension computer code which has be already used in the design of AC600/1000 passive containment cooling system. PCCAC-3D is a three dimension computer code which will be finished by the end of next September. PCCAC-2D, 3D can be used to predict the pressure and temperature of mixing gas inside the containment following the accident of primary pipe rupture or main steam line rupture. The heat removal characteristics from inside containment to atmosphere through the water film on the out surface of steel shell and natural circulation flow of air can be also simulated and calculated by PCCAC-2D or PCCAC-3D.

It follows from preliminary calculation results that the maximum pressure 0.37 Mpa of mixing gas in the containment will occur in 1123S after double ended rupture accident of cold leg pipe. The maximum temperature 138°C will occur in 14S after the accident.

132
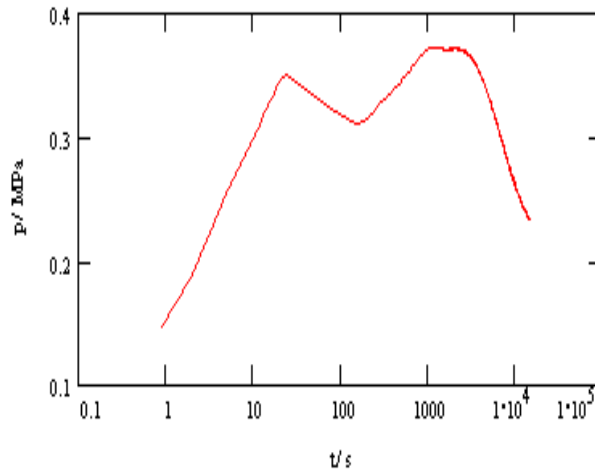
FIG. 12. Maximum pressure in containment
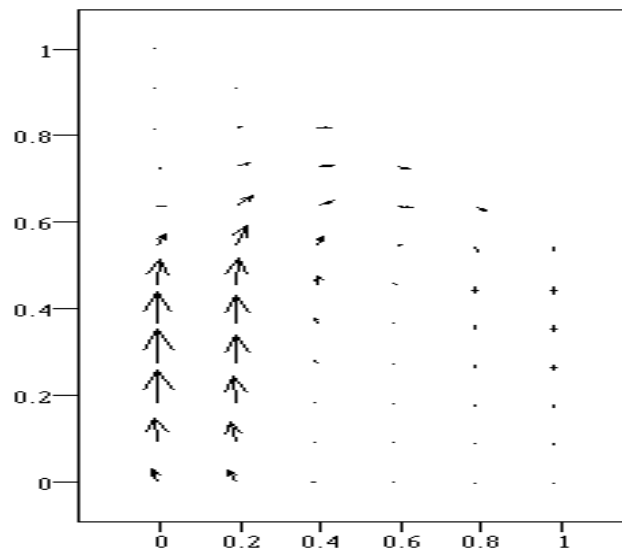
FIG. 13. Flowrate distribution in containment

The maximum pressure 0.34MPa of mixing gas in the containment will occur in 16.8S after double ended rupture accident of hot leg pipe. The maximum temperature 143°C will occur in 6.8S after the accident. The maximum pressure 0.387MPa of mixing gas in the containment will occur in 395.3S after main steam line rupture accident. The maximum temperature 153°C will occur in 3S after the accident.

The flow fields of coolant in the containment indicate that main flow vortex will be established at 0.9S following accident, will be in equilibrium at 5.2S and will be destroyed at 24.8S because of the end of blow down. The temperature fields of coolant in the containment show that high temperature area is in around and above the break and low temperature area is in the bottom near steel shell at the beginning of the accident. Then the temperature fields become uniform after main flow vortex equilibrium. The natural circulation mass flowrate of air in the channel between steel shell and concrete shell of containment varies with time and reaches maximum 168 kg/s at 8000S. After 72 hours, the spray water will be ended and the natural circulation mass flowrate will reach 120 kg/s. It can be noted from the preliminary analysis and calculation that AC600 passive containment cooling system is able to remove decay heat of reactor from inside to outside of containment.
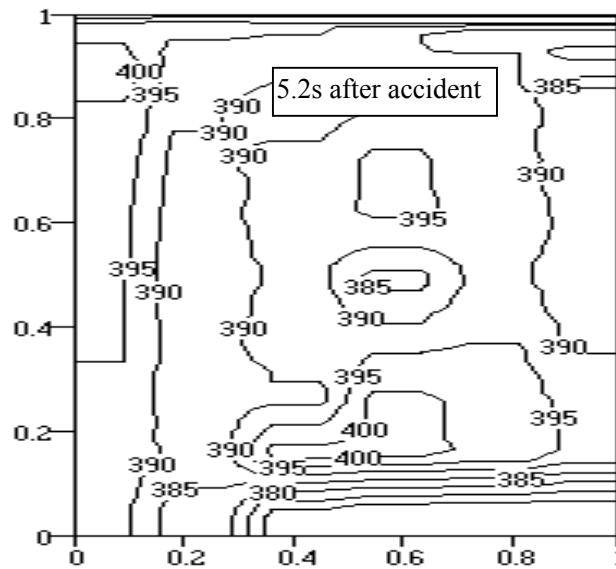
FIG. 14. Temperature(K) distribution in containment.
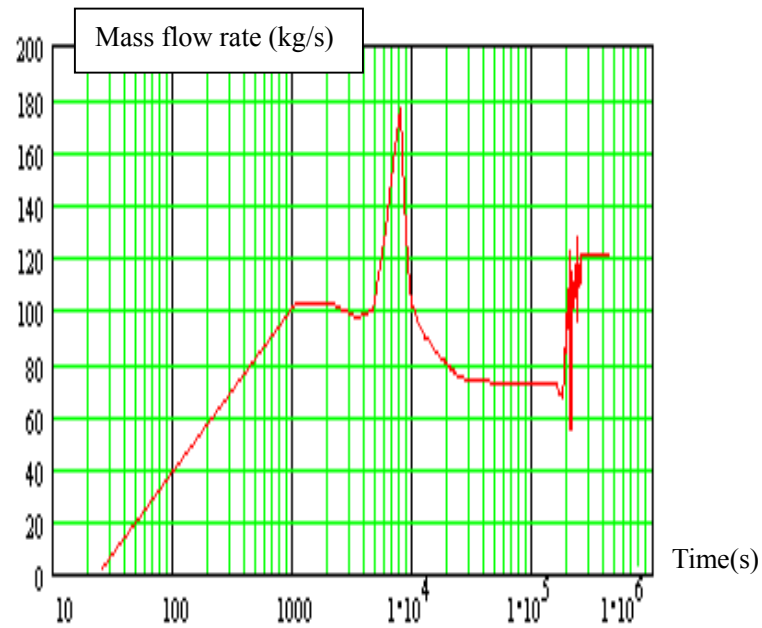
FIG. 15. Natural circulation mass flowrate of air.

3.2. Station blackout accident calculation for AC600/1000

ERHRAC is a special computer code for AC600/1000 design. ERHRAC can be used to calculate the natural circulation flowrates of three cycles (primary coolant cycle, secondary side cycle of SG and air flow cycle).The links connecting those three cycles are the steam generator and air cooler, establishing a tandem system.

In the unlikely event of a station black out accident, the flowrate through reactor core rapidly reduces. The changeover of coolant flow in primary coolant loop from the forced circulation

to the natural circulation is initiated automatically when main pump coast down is ended. In the secondary side loop, from steam generator the steam passes on to an air cooler, in which its heat is transferred to the air and steam is condensed to water. Then condensed water returns back to the steam generator by gravity to establish a natural circulation flow cycle.

Natural circulation flow rate is: 4% rated flowrate for each primary coolant loop and 3% rated flowrate for each secondary side loop of SG respectively. Air flowrate is about 290Kg/s for each air cooler.
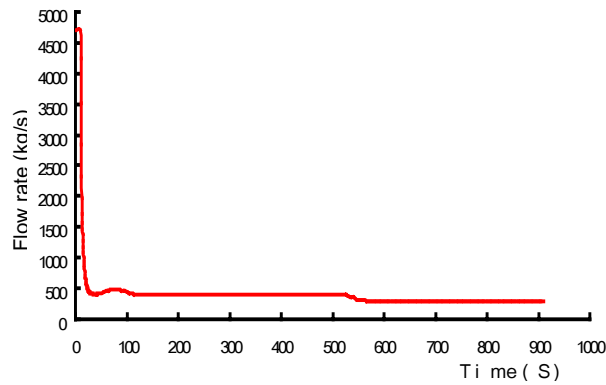
FIG. 16. Primary coolant flowrate per loop.
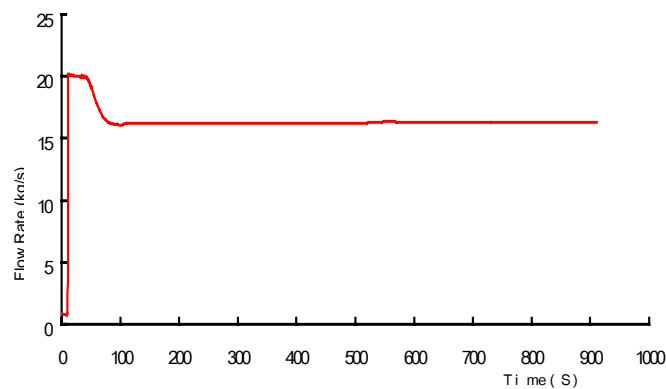
FIG. 17. Natural circulation flowrate for secondary side loop of each SG
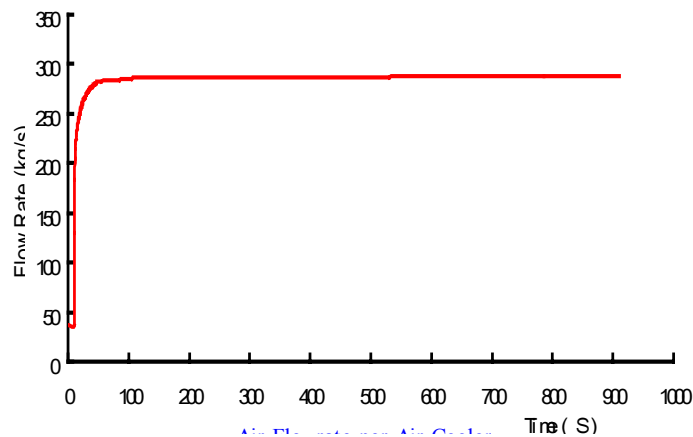
FIG. 18. Air flowrate per air cooler

135
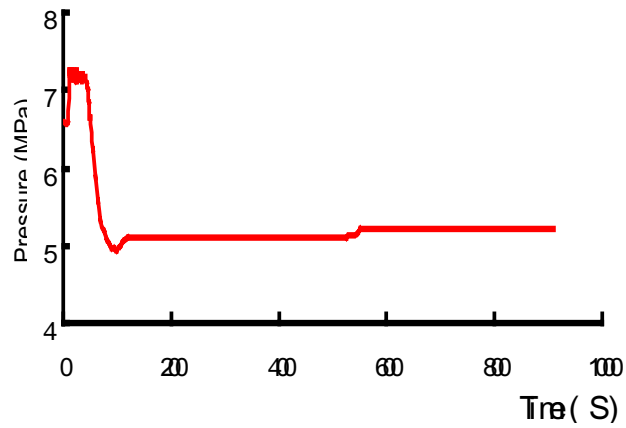
FIG. 19. Steam generator secondary side pressure

4.   CONCLUSION

Compared with current PWR NPP in China, AC600/1000 has the following 4 key advantages:

(1)   The safety and reliability of nuclear power plant can be increased through use of passive safety systems and advanced I&C systems.

(2)   Advanced core design and fuel management are used in AC600/1000 to increase availability factor and operation life time of NPP, to reduce generation cost and to improve economic efficiency.

(3)   System simplification and modularization technology can shorten construction period of NPP and reduce total capital cost.(4) AC600/1000 utilizes proven design technology and verified engineering experiments so that a prototype NPP is not required.

AC600/1000 is much safe, simple and economic NPP. AC-600/1000 will be next generation NPP of China.

Part 2

NATURAL CIRCULATION ANALYTICAL CAPABILITY AND EXPERIMENTAL DATA FOR CODE VALIDATION

Scaling of the steady state and stability behaviour of single and two-phase natural circulation systems

P.K. Vijayan, A.K. Nayak, M.H. Bade,
N. Kumar, D. Saha, R.K. Sinha

Bhabha Atomic Research Centre,
Mumbai, India

Abstract. Scaling methods for both single-phase and two-phase natural circulation systems have been presented. For single-phase systems, simulation of the steady state flow can be achieved by preserving just one nondimensional parameter. For uniform diameter two-phase systems also, it is possible to simulate the steady state behaviour with just one non-dimensional parameter. Simulation of the stability behaviour requires geometric similarity in addition to the similarity of the physical parameters appearing in the governing equations. The scaling laws proposed have been tested with experimental data in case of single-phase natural circulation.

1. INTRODUCTION

Natural circulation is being increasingly employed in many innovative designs of nuclear reactor cooling systems. The basic advantage of natural circulation systems is the enhanced safety due to its passive nature. One of the basic requirements, which arise prior to the incorporation of such systems in nuclear reactors, is the assessment of their performance. Generally, in the nuclear field the assessment is carried out by validated computer codes. Code validation is usually done with data obtained from scaled test facilities. The topic of the present paper is the scaling laws used for constructing such scaled facilities for simulating single and two-phase natural circulation. Such a scaled facility in nuclear parlance is also known as an integral test facility (ITF).

Scaling laws make possible the comparison of the performance of different natural circulation systems and to extrapolate the data from small scale to prototype systems. Scaling laws for nuclear reactor systems are arrived at using the governing conservation equations. Pioneering work in the field of scaling laws for nuclear reactor systems have been carried out by Nahavandi et al. (1979), Zuber (1980) and Heisler (1982). The scaling law proposed by Zuber is also known as the power-to-volume scaling philosophy and is widely used for the construction of scaled test facilities simulating nuclear reactor systems. Power to volume scaling can be applied to both forced and natural circulation systems. However, the power-to-volume scaling philosophy has certain inherent distortions (especially in downsized components), which can suppress certain natural circulation specific phenomena like the instability (Nayak et al. (1998)). Hence it is necessary to examine the scaling laws which are specific to natural circulation. In the present paper, the reported scaling laws for single- and two-phase natural circulation loops are reviewed with respect to their use for predicting the steady state and stability behaviour. Then scaling procedures for single and two-phase systems are presented and tested against the available data on the steady state and stability performance of natural circulation loops. This exercise has shown that the steady state behaviour of single-phase loops can be simulated by a single dimensionless parameter. This is also true for uniform diameter two-phase loops. The simulation of the stability behaviour requires simulation of at least three dimensionless parameters in addition to geometric scaling. For the stability behaviour, scaling of the characteristic equation (obtained by the linear stability analysis method) appears to be the appropriate method for achieving similarity.

2.   REVIEW OF SCALING LAWS

Several scaling laws have already been proposed for the design of scaled loops simulating natural circulation phenomenon. Such scaling laws are available for both single- and two-phase natural circulation loops.

2.1.   Single-phase natural circulation

Zuber (1980), Heisler (1982) and Ishii-Kataoka (1984) provide scaling laws for single-phase natural circulation. All the three scaling laws are derived from the governing differential equations. One of the problems associated with these scaling laws is that the number of similarity groups are too many and they do not provide steady state or stability solutions in terms of the proposed similarity groups. Therefore, testing of these scaling laws with the available experimental data is rather difficult without the use of system codes. This arises due to the fact that more than one scaling parameter is a function of the flow rate, which for a natural circulation loop is not known apriori. To overcome this problem, Vijayan et al. (1992) proposed a scaling procedure by which the steady state flow rate can be obtained as a function of just one similarity group. This procedure has been extended recently to nonuniform diameter loops (Vijayan (1999), see also section 3). They have also obtained the stability solution in terms of the similarity groups.

2.2.   Two-phase natural circulation

For two-phase natural circulation, scaling laws are provided by Ishii-Kataoka (1984) which is widely applied. The PUMA facility simulating the SBWR has been designed based on this philosophy. The power to volume scaling philosophy proposed by Zuber (1980) is also applicable for two-phase systems. The integral test facility being set-up to simulate the Advanced Heavy Water Reactor (AHWR) has been designed based on this philosophy. Prior studies by Nayak et al. (1998) has shown that this philosophy is well-suited for pressure-tube-type reactors where it is possible to use full-size components for most parts of the loop. It requires 1:1 scaling for elevation, pressure, temperature and velocity with the same fluid used in the prototype and the model. Such constraints do not exist for the scaling philosophy proposed by Ishii and Kataoka.

3.   PROPOSED SCALING LAWS FOR SINGLE-PHASE NATURAL CIRCULATION

Consider a simple nonuniform diameter natural circulation loop as shown in Fig. 1 with a horizontal heat source at the bottom and a horizontal heat sink at the top. The heat sink is maintained by providing cooling water to the secondary side of the cooler at a specified inlet temperature of T_s. In this analysis, the secondary side temperature is assumed to remain constant. The heat flux at the heat source is maintained constant. Assuming the loop to be filled with an incompressible fluid of constant properties except density (Boussinesq approximation where density is assumed to vary as $\rho=\rho_r[1-\beta(T-T_r)]$) with negligible heat losses, axial conduction and viscous heating effects, the governing differential equations can be written as

$$\frac{\partial W}{\partial s} = 0 \tag{1}$$

$$\Gamma \frac{dW}{dt} = g\rho_r\beta \oint T dz - \frac{W^2}{2\rho_r} \sum_{i=1}^{N} \left(\frac{fL}{D} + K \right)_i \frac{1}{A_i^2} \tag{2}$$

Where $\Gamma = \Sigma L_i/A_i$. It is also possible to absorb the local pressure loss coefficient, K_i into an equivalent length, Le_i such that $K_i = f_i Le_i/D_i$. With this correction, the momentum equation can be written as:

$$\Gamma \frac{dW}{dt} = g\rho_r\beta \oint T dz - \frac{W^2}{2\rho_r} \sum_{i=1}^{N} \left(\frac{fL_{eff}}{DA^2} \right)_i \tag{3}$$

Similarly, the energy equation for the different sections of the loop is given as:

$$\frac{\partial T}{\partial t} + \frac{W}{\rho_r A_h} \frac{\partial T}{\partial s} = \frac{q_h P_h}{A_h \rho_r Cp} \qquad \text{Heater} \qquad \text{(4a)}$$

$$\frac{\partial T}{\partial t} + \frac{W}{\rho_r A_c} \frac{\partial T}{\partial s} = -\frac{UP_c(T - T_s)}{A_c \rho_r Cp} \qquad \text{Cooler} \qquad \text{(4b)}$$

$$\frac{\partial T}{\partial t} + \frac{W}{\rho_r A_p} \frac{\partial T}{\partial s} = 0 \qquad \text{Pipe} \quad \text{(4c)}$$
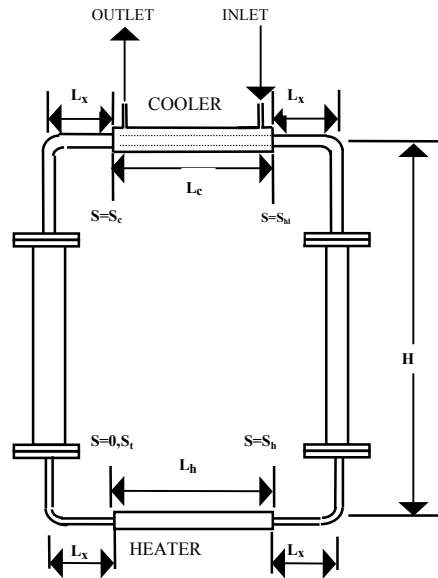
FIG. 1. Schematic of non-uniform diameter natural circulation loop.

The above equations can be non-dimensionalised using the following substitutions.

$$\omega = \frac{W}{W_{ss}}; \; \theta = \frac{T - T_s}{(\Delta T_h)_{ss}}; \; S = \frac{s}{H}; \; Z = \frac{z}{H}; \; \tau = \frac{t}{t_r}; \; a_i = \frac{A_i}{A_r} \text{ and } d_i = \frac{D_i}{D_r} \tag{5}$$

Where t_r, A_r and D_r are respectively the reference values of time, flow rate and hydraulic diameter defined as

$$t_r = \frac{V_t \rho_r}{W_{ss}}; \; A_r = \frac{1}{L_t} \sum_{i=1}^{N} A_i L_i = \frac{V_t}{L_t} \text{ and } D_r = \frac{1}{L_t} \sum_{i=1}^{N} D_i L_i \tag{6}$$

It is easy to see that the reference time is nothing but the loop circulation time. D_r and A_r are respectively the length average hydraulic diameter and flow area of the loop and the total circulation length, $L_t = \Sigma L_i$. In case of negligible local pressure losses, $\Sigma (L_{eff})_i$ becomes equal to the total circulation length, L_t of the loop. The non-dimensional equations can be expressed as:

$$\gamma \frac{d\omega}{d\tau} = \frac{Gr_m}{Re_{ss}^3} \oint \theta dZ - \frac{L_t}{D_r} \frac{\omega^2}{2} \sum_{i=1}^{N} \left(\frac{f l_{eff}}{da^2} \right)_i \tag{7}$$

$$\frac{\partial \theta}{\partial \tau} + \frac{\omega}{a_h} \frac{\partial \theta}{\partial S} = \frac{V_t}{V_h} \qquad\qquad \text{heater} \tag{8a}$$

$$\frac{\partial \theta}{\partial \tau} + \frac{\omega}{a_c} \frac{\partial \theta}{\partial s} = -St \frac{P_c L_t}{A_c} \theta \qquad\qquad \text{cooler} \tag{8b}$$

$$\frac{\partial \theta}{\partial \tau} + \frac{\omega}{a_p} \frac{\partial \theta}{\partial s} = 0 \qquad\qquad \text{pipes} \tag{8c}$$

Where $\gamma = \Sigma S_i / a_i$, $(l_{eff})_i = (L_{eff})_i / L_t$, $Gr_m = D_r^3 \rho_r^2 \beta g \Delta T_r / \mu^2$, and $St = Nu / Re_{ss} Pr$. Assuming fully developed forced flow correlations are valid, the friction factor, f_i can be expressed as

$$f_i = \frac{p}{Re_i^b} = \frac{p \omega^{-b}}{Re_{ss}^b (d/a)_i^b} \tag{9}$$

Where $p = 64$ and $b = 1$ for laminar flow and assuming Blassius correlation to be valid for turbulent flow p and b are respectively 0.316 and 0.25. In a non-uniform diameter loop, it is possible that some pipe sections are in turbulent flow (Re>4000) and some in laminar flow (Re<2000) and still others in transition flow (2000<Re<4000). However, if we assume the entire length of the loop to be under either laminar or turbulent flow conditions, then equation (7) can be expressed as

$$\gamma \frac{d\omega}{d\tau} = \frac{Gr_m}{Re_{ss}^3} \oint \theta dZ - \frac{L_t}{D_r} \frac{p \omega^{2-b}}{2 Re_{ss}^b} \sum_{i=1}^{N} \left(\frac{l_{eff}}{d^{1+b} a^{2-b}} \right)_i = \frac{Gr_m}{Re_{ss}^3} \oint \theta dZ - \frac{p N_G \omega^{2-b}}{2 Re_{ss}^b} \tag{10}$$

Where N_G is a geometric parameter defined as $N_G = \frac{L_t}{D_r} \sum_{i=1}^{N} \left(\frac{l_{eff}}{d^{1+b} a^{2-b}} \right)_i$ \hfill (11)

3.1. Steady state solution

The governing equations for the steady state condition are obtained by dropping the time dependent terms. Also, by definition ω (the non-dimensional flow rate) is unity at steady state. Therefore, the steady state momentum and energy equations can be written as:

$$\frac{Gr_m}{Re_{ss}^3}\oint\theta dZ = \frac{pN_G}{2\,Re_{ss}^b} \tag{12}$$

$$\frac{1}{a_h}\frac{d\theta}{dS} = \frac{V_t}{V_h} \text{ for heater }; \quad \frac{1}{a_c}\frac{d\theta}{dS} = -St\frac{P_cL_t}{A_c}\theta \text{ for cooler and } \frac{1}{a_p}\frac{d\theta}{dS} = 0 \text{ for pipes} \tag{13}$$

The steady state solutions for the temperature of the various segments of the loop can be obtained from Eq. (13) (see Vijayan (1999)). Using these steady state solutions, the integral in equation (12) can be calculated as $\oint\theta\,dZ = 1,$ for the loop shown in Fig. 1. Hence, the steady state flow rate can be expressed as

$$Re_{ss} = \left[\frac{2Gr_m}{pN_G}\right]^{\frac{1}{3-b}} = C\left(\frac{Gr_m}{N_G}\right)^r \tag{14}$$

Where C=(2/p)^r and r = 1/(3-b). Thus, knowing the value of p and b the constants C and r in equation (14) can be estimated. For laminar flow (where p=64, and b=1) equation (14) can be rewritten as

$$Re_{ss} = 0.1768\left[\frac{Gr_m}{N_G}\right]^{0.5} \tag{15}$$

Similarly, assuming Blassius friction factor correlation (p=0.316 and b=0.25) to be valid for turbulent flow we can obtain the following equation

$$Re_{ss} = 1.96\left[\frac{Gr_m}{N_G}\right]^{0.364} \tag{16}$$

In the transition region, one can expect a continuous change in the exponent of equation (14) from 0.5 to 0.364 as well as for the constant from 0.1768 to 1.96. It may be noted that both equations (15) and (16) are the exact solutions of equation (12) assuming the same friction factor correlation to be applicable to the entire loop. For closed loops, often the same friction factor correlation may not be applicable for the entire loop even if the loop is fully laminar or fully turbulent. An example is a fully laminar loop with part of the loop having rectangular cross section and remaining part having circular cross section. Hence, one has to keep in mind the assumptions made in deriving the relationship (14) while applying it.

The relationship expressed by Eq. (14) is derived for a rectangular loop with both the heater and cooler having the horizontal orientation. For other orientations also, it can be easily shown that the same relationship holds good if the loop height in the definition of the Gr_m is replaced with the centre-line elevation difference between the cooler and the heater, Δz (see

Vijayan et al. (2000)). The same is true for other loop geometries like the figure-of-eight loop used in Pressurised Heavy Water Reactors (PHWRs). For the figure-of-eight loop, the heater power used in the Gr_m is the total power of both heaters. The equations are also applicable for identical parallel-channel or parallel-loops systems if the parallel channels/loops are replaced by an equivalent path having the same hydraulic diameter and total flow area.

3.2. Stability behaviour

Equation (14) has shown that simulation of the steady state behaviour is possible by simulating Gr_m/N_G for any natural circulation loop. The transient and stability behaviour, however, are described by equations (8) and (10). Substituting the steady state solution, the transient momentum equation can be rewritten as

$$\gamma \frac{d\omega}{d\tau} = \left(\oint \theta dZ - \omega^{2-b} \right) (p/2)^{\frac{3}{3-b}} / \left(Gr_m^{\frac{b}{3-b}} / N_G^{\frac{3}{3-b}} \right) \tag{17}$$

From equations (17) and (8), it is obvious that the transient and stability behaviours are governed by the physical parameters Gr_m, St and the geometric parameters of N_G, γ, V_t/V_h, $P_c L_t/A_c$ and the area ratio a_i. To reduce the number of independent parameters, it is customary to combine St and $P_c L_t / A_c$ into a single dimensionless parameter called St_m. Similarly, Gr_m and N_G can be combined as $Gr_m^{b/3-b}/N_G^{3/3-b}$ so that the transient and stability behaviour can be expressed as

$$\omega(\tau) = f\left(\frac{Gr_m^{b/(3-b)}}{N_G^{3/(3-b)}}, St_m, \frac{V_t}{V_h}, \gamma \text{ and } a_i \right) \tag{18}$$

Further reduction in the number of independent parameters is possible for special cases. For example, with a uniform diameter loop, $(V_t / V_h) = (L_t / L_h)$, $a_i = 1$ and $N_G = L_t / D$ so that

$$\omega(\tau) = f\left(\frac{Gr_m^{b/(3-b)}}{(L_t / D)^{3/(3-b)}}, St_m, \gamma \text{ and } \frac{L_t}{L_h} \right) \tag{19}$$

In addition to L_t/L_h other length scales also affect the stability behaviour. This can be established by carrying out a linear stability analysis. In this method, the loop flow rate and temperature are perturbed as

$$\omega = \omega_{ss} + \overline{\omega}\varepsilon e^{n\tau} \text{ and } \theta = \theta_{ss} + \overline{\theta}\varepsilon e^{n\tau} \tag{20}$$

Where ε is a small quantity, $\overline{\omega}$ and $\overline{\theta}$ are the amplitudes of the flow and temperature disturbances respectively, and n is the growth rate of the perturbations. Substituting Eq. (20) in equations (10) and (17), and using the continuity of temperature perturbation in various segments as the boundary condition, the characteristic equation for the stability behaviour can be derived. The characteristic equation for a uniform diameter loop with horizontal heat source and sink can be expressed as Y(n)=0 (Vijayan and Austregesilo (1994)), where

144

$$Y(n) = n - \frac{(p/2)^{3/(3-b)}}{(Gr_m)^{b/(3-b)}(D/L_t)^{3/(3-b)}}\{\psi(n, St_m) + 2 - b\} \tag{21}$$

where $\psi(n, St_m) = \frac{L_t}{nH}\{1 - \exp(-nH/L_t)\} \exp(-nS_x H/L_t)\left(\frac{\overline{\theta}_h - \overline{\theta}_c}{\overline{\omega}}\right)$ and

$$\left(\frac{\overline{\theta}_h - \overline{\theta}_c}{\overline{\omega}}\right) = \frac{L_t}{nL_h}\{\exp(-nL_h/L_t) - 1\} + \left(\exp\{-n(S_c - S_t - S_h)H/L_t\} - 1\right)\frac{B + C}{D}$$

$$B = \frac{L_t}{nL_h}\exp(-nS_c H/L_t)\{1 - \exp(nL_h/L_t)\} \; ; \; C = \frac{(\theta_{hl})_{ss} St_m}{n}[1 - \exp\{-nL_c/L_t\}]$$

and $D = \exp\{St_m L_c/L_t\} - \exp(-n)$. Where $S_t = L_t/H$ and $S_x = s_x/H$. S_c, S_t and S_x are the dimensionless distances from the origin (i.e. S=0 in Fig. 1) in anticlockwise direction. It is obvious from equation (21) that, apart from the parameters listed in (19), the ratios of the lengths are also required to be preserved to simulate the stability behaviour.

4.   TWO-PHASE NATURAL CIRCULATION

Two-phase natural circulation is the normal mode of coolant circulation in many advanced designs of BWRs. Typical examples are the simplified boiling water reactor (SBWR) and the advanced heavy water reactor (AHWR). Two-phase natural circulation is also the predicted mode of coolant circulation in most of the current designs of water cooled reactors during small break LOCA. Hence two configurations of loops as shown in Fig 2, one with a heat exchanger and another with a steam-water separator, are of interest to nuclear industry. For the development of the scaling relationships, only uniform diameter loops with adiabatic pipes operating without any inlet subcooling are considered here. The scaling laws for two-phase natural circulation can be obtained from the conservation equations of mass, momentum and energy applicable for homogeneous equilibrium flow.

$$\frac{\partial\rho}{\partial t} + \frac{1}{A}\frac{\partial W}{\partial s} = 0 \tag{22}$$

$$\frac{\partial(\rho h)}{\partial t} + \frac{1}{A}\frac{\partial(Wh)}{\partial s} = \frac{4q}{D} \tag{23a}$$

H   H

$$\frac{\partial(\rho h)}{\partial t} + \frac{1}{A}\frac{\partial(Wh)}{\partial s} = 0 \tag{23b}$$

$$\frac{\partial(\rho h)}{\partial t} + \frac{1}{A}\frac{\partial(Wh)}{\partial s} = -\frac{4U(T_{sat} - T_s)}{D} \tag{23c}$$

$$\frac{1}{A}\frac{\partial W}{\partial t} + \frac{1}{A^2}\frac{\partial(W^2/\rho)}{\partial s} = -\frac{\partial p}{\partial s} - \rho g\sin\theta - \frac{fW^2}{2DA^2\rho} \tag{24}$$
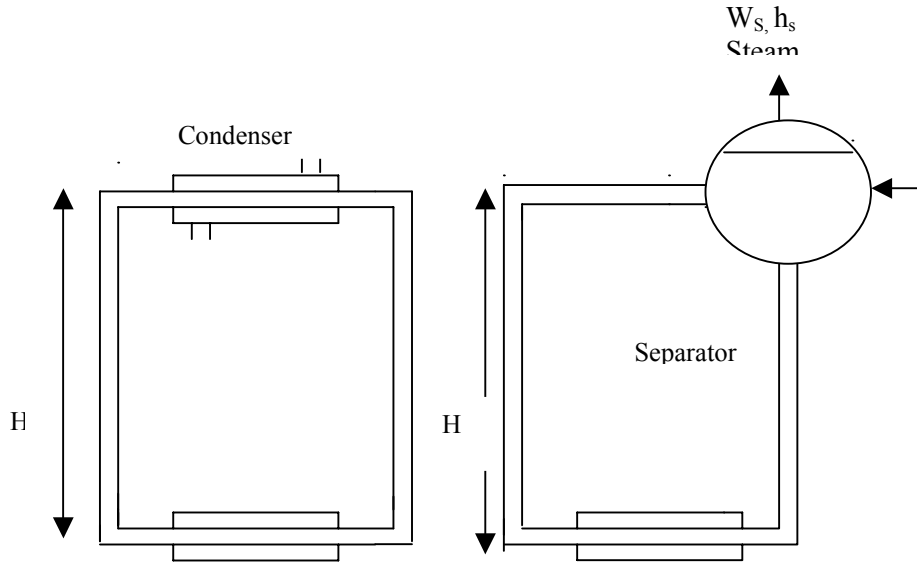
FIG. 2a (left) Uniform diameter two phase loop with condenser.
FIG. 2b (right) Uniform diameter two phase long with separator.

For the loop with the steam separator, instead of Eq. (23c) a point model of mass and energy equations is used, which assumes complete separation and thermal mixing in the separator. The feed water flow rate is assumed to be controlled to match the steam production rate. Integrating the momentum equation over the loop we get,

$$\frac{L_t}{A}\frac{\partial W}{\partial t} + \frac{1}{A^2}\oint \partial \left(W^2/\rho\right) = -g\oint \rho dz - \frac{W^2 f_L}{2DA^2\rho_L}\left[L_{sp} + \left(\overline{\phi}_{LO}^2 L_{tp}\right)_h + \left(\phi_{LO}^2 L_{tp}\right)_p + \left(\overline{\phi}_{LO}^2 L_{tp}\right)_c\right]$$

(25)

These equations are nondimensionalised using the following substitutions

$$\omega = \frac{W}{W_{ss}}; \quad h^* = \frac{h - h_r}{\Delta h_{ss}}; \quad S = \frac{s}{H}; \quad Z = \frac{z}{H}; \quad \rho^* = \frac{\rho - \rho_r}{\Delta \rho_{ss}}; \quad \tau = \frac{t}{t_r}$$

(26)

Where $t_r = V_t\rho_L/W_{ss}$ and $\Delta\rho_{ss}$ (always taken as positive) and Δh_{ss} are respectively the steady state density and enthalpy differences across the heated section. The nondimensional equations obtained are

$$\frac{\partial \rho^*}{\partial \tau} + \frac{L_t\rho_L}{H\Delta\rho_{ss}}\frac{\partial \omega}{\partial S} = 0$$

(27)

$$\left(\rho^* + \frac{\rho_r}{\Delta\rho_{ss}}\right)\frac{\partial h^*}{\partial \tau} + \frac{L_t\rho_L\omega}{H\Delta\rho_{ss}}\frac{\partial h^*}{\partial S} = \frac{\rho_L L_t}{L_h\Delta\rho_{ss}} \qquad \text{heater}$$

(28a)

$$\left(\rho^* + \frac{\rho_r}{\Delta\rho_{ss}}\right)\frac{\partial h^*}{\partial \tau} + \frac{L_t\rho_L\omega}{H\Delta\rho_{ss}}\frac{\partial h^*}{\partial S} = 0 \qquad \text{pipes}$$

(28b)

$$\left(\rho^* + \frac{\rho_r}{\Delta\rho_{ss}}\right)\frac{\partial h^*}{\partial\tau} + \frac{L_t\rho_L\omega}{H\Delta\rho_{ss}}\frac{\partial h^*}{\partial S} = -\frac{St_m^* L_t\rho_L}{D\Delta\rho_{ss}} \quad \text{cooler} \tag{28c}$$

$$\frac{\partial\omega}{\partial\tau} + A^2\rho_L\sum_{i=1}^{N}\left(\frac{\omega^2}{A_i^2(\Delta\rho_{ss}\rho_i^* + \rho_r)}\right)_{in}^{out} = \frac{Gr_m^*}{Re_{ss}^2}\oint\rho^* dZ - \frac{p}{2}\frac{N_G^*\omega^{2-b}}{Re_{ss}^b} \tag{29}$$

Where $Gr_m^* = \dfrac{D^2\rho_L\Delta\rho_{ss}gH}{\mu_L^2}$; $\quad St_m^* = \dfrac{4UD(T_{sat} - T_s)}{Re_{ss}(\Delta h_{ss}\mu_L)}$; $\quad Re_{ss} = \dfrac{DW_{ss}}{A\mu_L}$ and $\qquad$ (30a)

$$N_G^* = \frac{L_t}{D}\left[l_{sp} + (\overline{\phi}_{LO}^2 l_{tp})_h + \left(\overline{\phi}_{LO}^2 l_{tp}\right)_p + (\overline{\phi}_{LO}^2 l_{tp})_c\right] = \frac{L_t}{D}\sum_{i=1}^{N}(\phi_{LO}^2 l)_i \tag{30b}$$

with $(\phi_{LO})^2 = 1$ for single-phase region and $l_i = L_i/L_t$. In writing the above equation, the local pressure losses were considered to be negligible.

4.1. Steady state flow

The steady state governing equations (all temporal derivatives = 0 and $\omega_{ss} = 1$) are

$$\frac{d\omega}{dS} = 0 \tag{31}$$

$$\frac{dh^*}{dS} = \frac{H}{L_h} \text{ for heater;} \quad \frac{dh^*}{dS} = -\frac{St_m^* H}{D} \text{ for cooler and} \quad \frac{dh^*}{dS} = 0 \quad \text{for pipes} \tag{32}$$

$$A^2\rho_L\sum_{i=1}^{N}\left(\frac{1}{A_i^2(\Delta\rho_{ss}\rho_i^* + \rho_r)}\right)_{in}^{out} = \frac{Gr_m^*}{Re_{ss}^2}\oint\rho^* dZ - \frac{pN_G^*}{2Re_{ss}^b} \tag{33}$$

The LHS of the momentum equation becomes zero for the uniform diameter loop shown in Fig. 2a. For non-uniform diameter loops with a tall riser (H in Fig. 2b) its value becomes negligible compared to the friction pressure drop. Hence,

$$\frac{Gr_m^*}{Re_{ss}^2}\oint\rho^* dZ = \frac{pN_G^*}{2Re_{ss}^b} \tag{34}$$

For a loop with horizontal heater and cooler, it can be shown that the $\oint\rho^* dZ = 1$. Hence,

$$Re_{ss} = \left[\frac{2}{p}\frac{Gr_m^*}{N_G^*}\right]^{\frac{1}{2-b}} \text{ or } Re_{ss} = C\left[\frac{Gr_m^*}{N_G^*}\right]^r \tag{35}$$

Where $C=(2/p)^r$ and $r=1/(2-b)$. For laminar flow (b=1, p=64), C=0.03125 and r=1 and for turbulent flow (b=0.25 and p=0.316), C=2.87 and r=0.5714. The same relationship can be obtained for the loop with vertical heater and cooler if we use the elevation difference between the thermal centres of the cooler and heater in place of the loop height in Gr_m. In

case, the value of the LHS in equation (33) is significant, then an explicit equation for Re_{ss} cannot be obtained. Instead, a polynomial in Re_{ss} can be obtained as

$$Re_{ss}^{2-b} = \frac{2Gr_m^*}{pN_G^*} - \frac{2Re_{ss}^2}{pN_G^*}\left[1 - (A_h/A_{sep})^2\right]\rho_L v_{fg} x_{ex} \tag{36}$$

Where x_{ex} is the heater exit quality. Since $x_{ex}=Q/W_{ss}h_{fg}$ without inlet subcooling, Eq. (36) can be rewritten as

$$Re_{ss}^{2-b} = \frac{2Gr_m^*}{pN_G^*} - \frac{2Re_{ss}}{pN_G^*}\left[1 - \left(\frac{A_h}{A_{sep}}\right)^2\right]\frac{\rho_L v_{fg} QD}{A\mu_L h_{fg}} \tag{37}$$

For laminar flow, b=1, an explicit expression for Re_{ss} can be obtained. For turbulent flow, Re_{ss} can be numerically calculated from the above polynomial.

It can be shown that the $\Delta\rho_{ss}$ used in the Gr_m can be estimated as $\alpha_{ex}\rho_{fg}+(\rho_L-\rho_{in})$. For no inlet subcooling, the density at the inlet is ρ_L, then $\Delta\rho_{ss}=\alpha_{ex}\rho_{fg}$ where α_{ex} is the void fraction at the exit of the heater. If we use the homogeneous model for the evaluation of the heater exit void fraction, then $\alpha_{ex}=\rho_L/[(\rho_L-\rho_G)+W_{ss}h_{fg}\rho_G/Q]$. For the evaluation of the $(\phi_{LO})^2$, several homogeneous models are reported in the literature. If we use Owens (1961) model, then $(\phi_{LO})^2=\rho_L/\rho_{tp}=1/[1-\alpha_{ex}(1-\rho_G/\rho_L)]$. Thus knowing the heater exit void fraction both Gr_m and N_G can be evaluated. Although the homogeneous flow assumption was used in the derivation of Eq. (35), the difference in the velocities of the two-phases can be accounted by selecting appropriate models for α_{ex} and $(\phi_{LO})^2$.

5.   TESTING OF SCALING LAWS

The scaling laws presented in section 3 are tested against experimental data for both steady state and stability behaviour.

5.1.   Steady state behaviour of single-phase natural circulation

The steady state scaling laws were tested with data obtained from simple low pressure and high pressure loops. The data included both in-house experimental data and those compiled from literature.

5.1.1. In-house data

For testing of the scaling laws, experiments were carried out in three uniform diameter rectangular loops with horizontal heater and horizontal cooler (Vijayan et al. (1992)). These loops (see Fig. 3) had the same length and height but different internal diameters. These experiments helped to establish the adequacy of Gr_m/N_G as the scaling parameter for the steady state flow as the data from the three loops could be expressed in the form of Eq. (14) with the same value of C and r. Subsequently, experiments were conducted to study the effect of the orientation of the heater and the cooler as different types of nuclear reactors have different orientations of the heat source (core) and the heat sink (steam generator). For example, PHWRs have horizontal core and vertical steam generators, PWRs have vertical

core and vertical steam generators and WWERs have vertical core and horizontal steam generators. In view of this, the heater and cooler orientations studied included the horizontal heater horizontal cooler (HHHC), horizontal heater vertical cooler (HHVC), Vertical heater horizontal cooler (VHHC) and vertical heater vertical cooler (VHVC). Further details of the experimental loop (see Fig. 4) and data generated can be obtained from Bade (2000) and Vijayan et al. (2000). The steady state data collected for different orientations of the heater and cooler are plotted without and with consideration of local pressure losses in Figs. 5a and b respectively. The experimental data is observed to be very close to the theoretical correlations for all orientations of the heater and cooler confirming the validity of the correlations (15) and (16). Considering the local pressure losses improves the agreement with the theoretical correlations (see Fig. 5b).
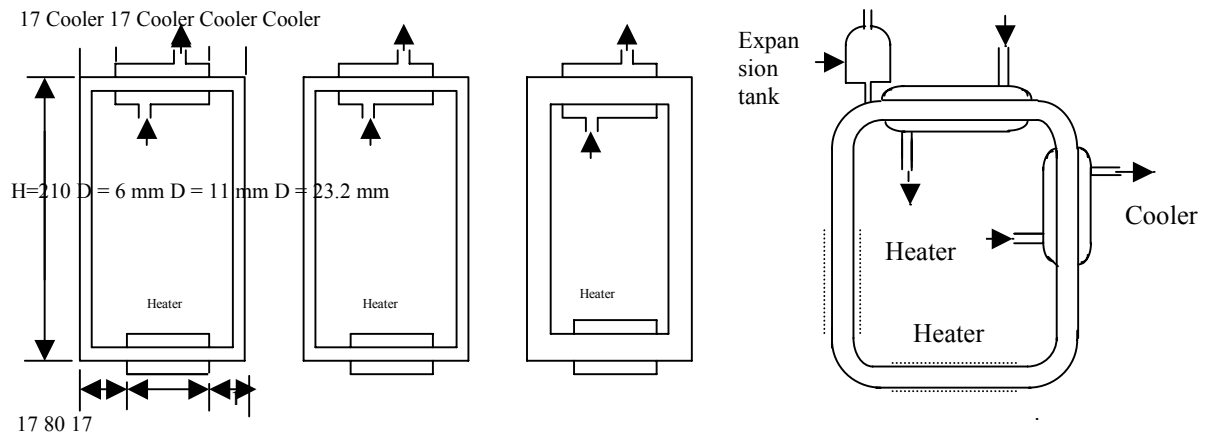
FIG. 3. (left) Uniform diameter loops with different external diameters & identical lengths.
FIG. 4. (right) Experimental loop to study the effect of orientation.
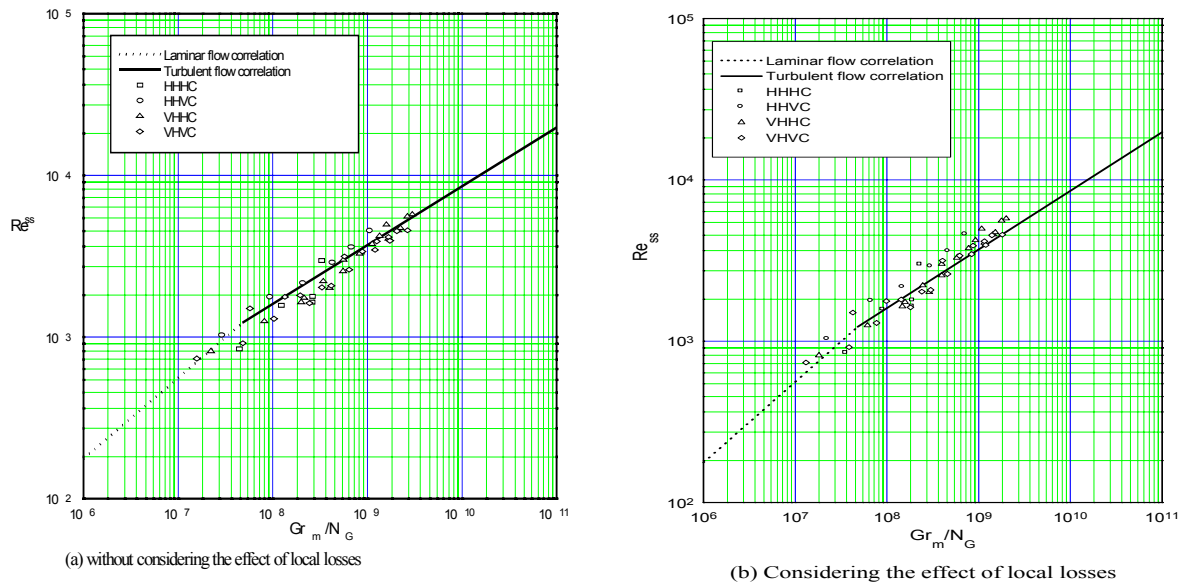
FIG. 5. Effect of heater and cooler orientations on steady state flow.
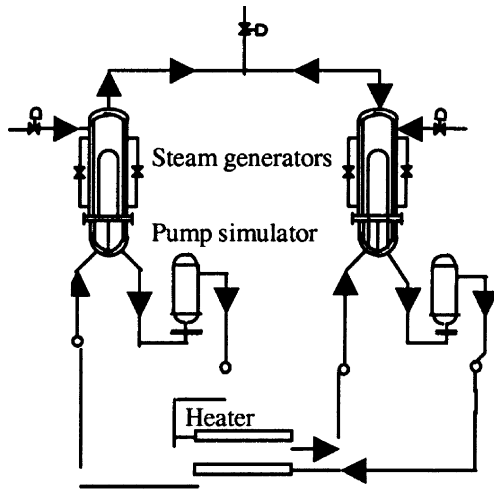
FIG. 6. Schematic diagram of FISBE.
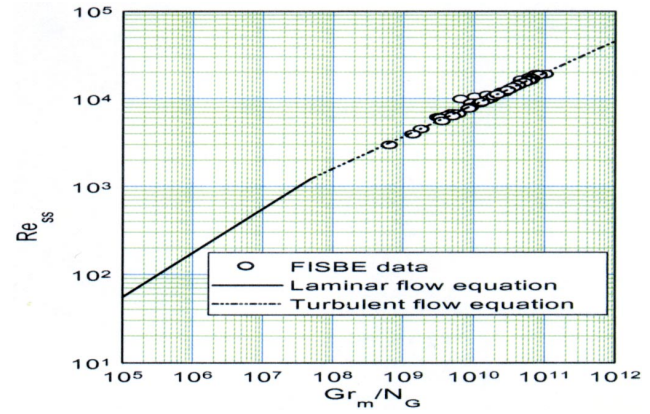
FIG. 7. Comparison of FISBE data with the theoretical correlation.

Subsequent to this, experiments were carried out in the high pressure nonuniform diameter figure-of-eight loop FISBE (Facility for the Integral System Behaviour Experiments, see Fig. 6), which simulates the Narora Atomic Power Station. Steady state data from FISBE are compared with the present correlation in Fig. 7, which shows good agreement. It may be noted that for these tests the loop was an all pipe loop with a tubular heater section, a single U-tube steam generator and pumps replaced by pipe sections. Since the SG used only one U-tube, more than 95% of the loop hydraulic resistance was due to this. Although the loop had several elbows, bends, Tees and other fittings, these were mainly concentrated in the large diameter pipe sections. Hence the contribution of the local pressure losses to the total hydraulic resistance became negligible giving good agreement with the turbulent flow correlation.

5.1.2. Comparison with literature data

Several experiments on single-phase natural circulation loops are reported in the literature. The loops studied can be categorised as Uniform Diameter Loops (UDLs) and Nonuniform Diameter Loops (NDLs).

5.1.2.1. Uniform diameter loops (UDLs)

The UDLs experimentally studied include both closed-loop and open-loop thermosyphons. Considering the shape of the loop, the closed loops can be further classified into rectangular, toroidal and figure-of-eight loops. Holman-Boggs (1960), Huang-Zelaya (1988), Misale et al. (1991), Bernier-Baliga (1992), Vijayan et al. (1992), Ho et al. (1997) and Nishihara (1997) obtained experimental natural circulation data in UDLs of rectangular shape. Uniform diameter open-loops were investigated by Bau-Torrance (1981, 1981a) and Haware et al. (1983).

Fig. 8 shows a comparison of the data with the theoretical correlations for laminar and turbulent flow for uniform diameter loops. The experimental data reported by Misale et al. (1991), Bernier-Baliga (1992) and Ho et al. (1997) are well predicted by the theoretical correlation. Most of these data points are from laminar flow region where the total local loss coefficient is negligible compared to L_t/D due to the large value of the friction factor. For the

150

range $2 \times 10^7 < Gr_m D/L_t < 3 \times 10^8$ significant deviation is observed between the data and the correlation. Beyond $Gr_m D/L_t$ of 3×10^8, the agreement is found to be better.

For all the steady state data reported in Fig. 8, it is assumed that $\Sigma l_{eff} = 1$. But for all practical configurations of loops, local losses are present so that $\Sigma l_{eff} > 1$. Hence, the observed deviations with the theoretical correlation may be attributed partly to the unaccounted local pressure losses in these loops. To study its effect, the local pressure loss coefficients due to elbows, bends, Tees, orifices, etc. given in Streeter and Wylie (1983) were used. The results are shown in Fig. 9. The turbulent flow data is now closer to the theoretical correlation indicating the significance of the local pressure losses at high Reynolds numbers where the friction factor is very low. The laminar region data is practically unaffected. The data for the transition region $2 \times 10^7 < Gr_m/N_G < 3 \times 10^8$ is now closer to the theoretical correlation, but the deviation is still significant. This is the region where the correlation is not applicable as the loop is neither fully laminar nor fully turbulent. Instead the loop is partly in the laminar region and partly in either transition or turbulent regions.
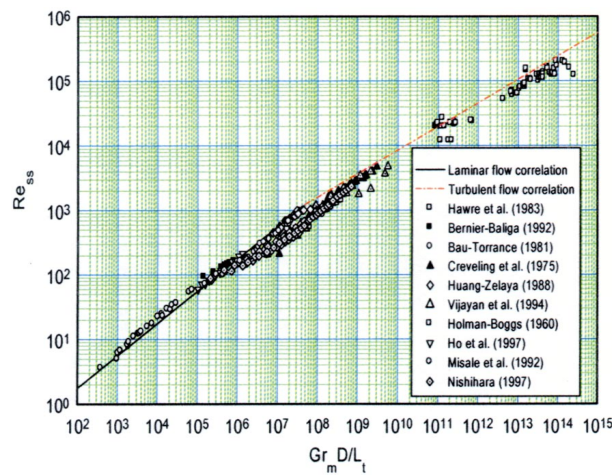
FIG. 8. Steady state natural circulation flow in UDLs without considering local losses.
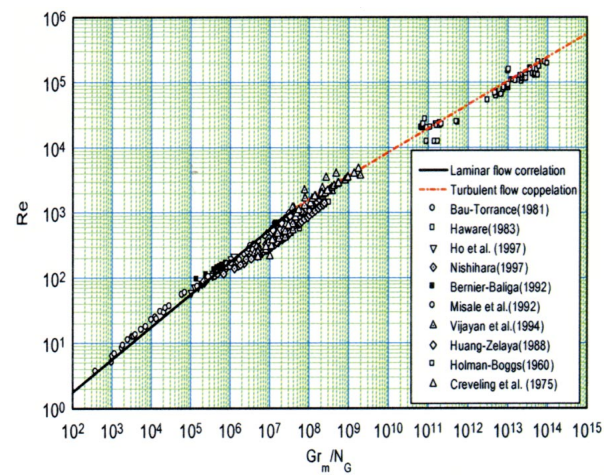
FIG. 9. Steady state natural circulation flow in UDLs with local losses.

5.1.2.2. Nonuniform diameter loops (NDLs)

Most practical applications of natural circulation employ non-uniform diameter loops. Common examples are the nuclear reactor loop, solar water heater, etc. Most test facilities simulating nuclear reactor loops also use non-uniform diameter loops. Depending on the operating pressure, the non-uniform diameter loops can be categorised as High pressure loops and Low pressure loops. Most studies are conducted in the high-pressure test facilities simulating nuclear reactor loops. Typical examples are the SEMISCALE, LOBI, PKL, BETHSY, ROSA, RD-14, FISBE, etc. Some studies, however, are carried out in low-pressure facilities. Examples are the experiments carried out by Zvirin et al. (1981), Jeuck et al. (1981), Hallinan-Viskanta (1986), Vijayan (1988) and John et al. (1991). Most of the available experimental data in a usable form (i.e. full geometrical details are known) are from the low-pressure test facilities. High-pressure test data in a usable form was available only from FISBE. The data from NDLs are plotted in Fig. 10, which shows reasonable agreement with theoretical correlation in the laminar and the turbulent flow regions. Significant deviation is observed for the intermediate values of Gr_m/N_G where the flow is neither fully laminar nor fully turbulent. Similar trend was observed in the case of UDLs. Interestingly, the parallel channel data of John et al. (1991) and parallel loop data of Jeuck et al. (1981) are also found to be in reasonable agreement with the theoretical correlation.
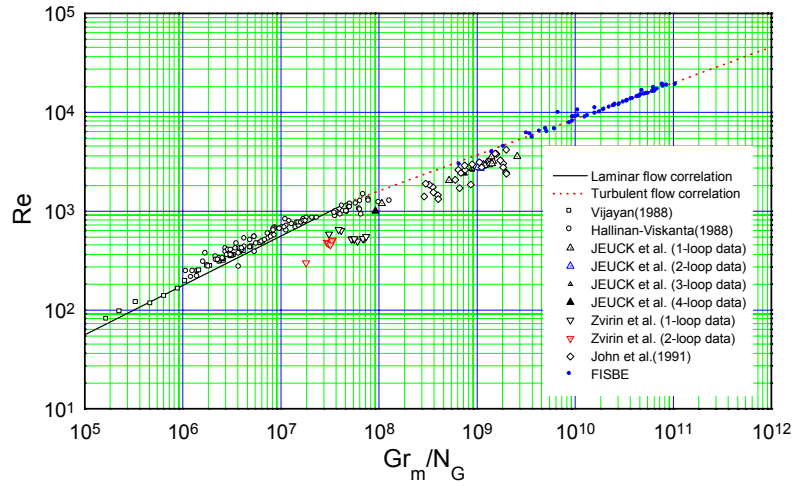
FIG. 10. Steady state flow in NDLs without considering local losses.

5.2. Steady state behaviour of two-phase systems

For testing the scaling laws, a two-phase natural circulation loop as shown in Fig. 11 was constructed. The loop was made of 50 mm NB (2" Sch 80) pipes except for the separator which is 150 mm NB (6" Sch 120) pipe. The separated steam is condensed and the condensate is returned to the separator. The vertical heater is direct electrically heated with a high current source. The loop was extensively instrumented to measure temperature, pressure, differential pressure, level and flow rate. Further details of the loop are available in Naveen et al. (2000). Prior to the actual experiments, pressure drop across one pipe segment was measured under forced flow conditions. This gave the following equation for the friction factor

$$f = 0.05042 / Re^{0.03768} \tag{38}$$

Fig. 12 shows a comparison of the experimental data with equation (35). The p and b values used for the solid line corresponded to the friction factor correlation given by Eq. (38). The experimental flow rate, although shows similar trend as expected, is significantly lower for our data, and is somewhat better for the data of Mendler (1961). This is attributed to the approximate nature of Eq. (35). A better agreement can be expected if we use Eq. (36).
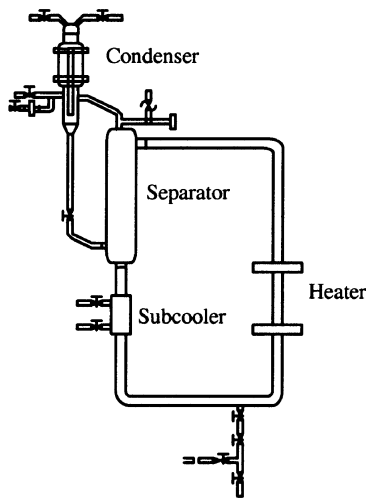
FIG. 11. Experimental two-phase natural circulation loop.
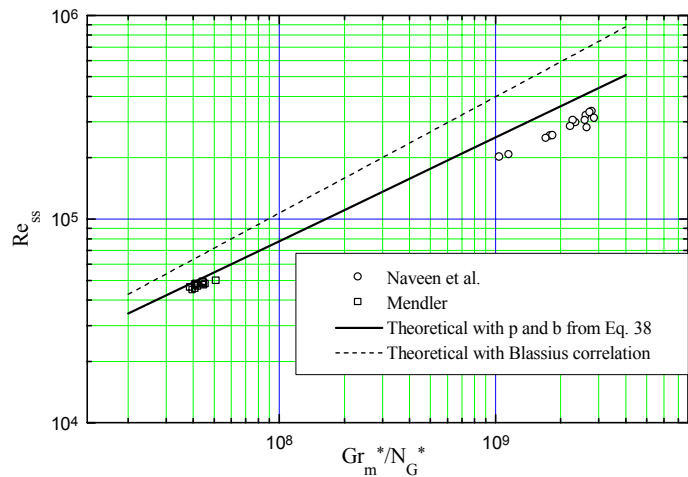
FIG. 12. Steady state flow in a two-phase natural circulation loop.

152

5.2. Stability behaviour

Experimental data on stability behaviour are few. Even with the available data, it is often not possible to accurately estimate the parameters (see Eq. 21) affecting the stability behaviour. This is often caused by the fact that the heat transfer coefficient U used in the St_m is flow dependent, which makes it difficult to estimate it accurately. Due to this, the predicted stability behaviour is compared for different loops to test the validity of the scaling laws used. Figs. 13a and b show the predicted stability maps for laminar and turbulent flow respectively for different loops having the same length scale ratios, but with different diameters. As expected, the curves for all the loops merge giving a single curve for the stability behaviour. A prediction was also made for the different orientations of the heater and cooler for the loop shown in Fig. 4. The results are given in Fig. 14. As expected the results are found to be different for the different orientations, as the length scales are different even though the total circulation length and diameter are the same. This emphasises the fact that simulation of the stability behaviour requires preservation of the length scales in addition to the physical parameters of St_m, Gr_m and N_G. This is because the feedback effects are a strong function of the residence time, which depends on the length scale.

(a) Laminar flow   *(b) Turbulent flow*
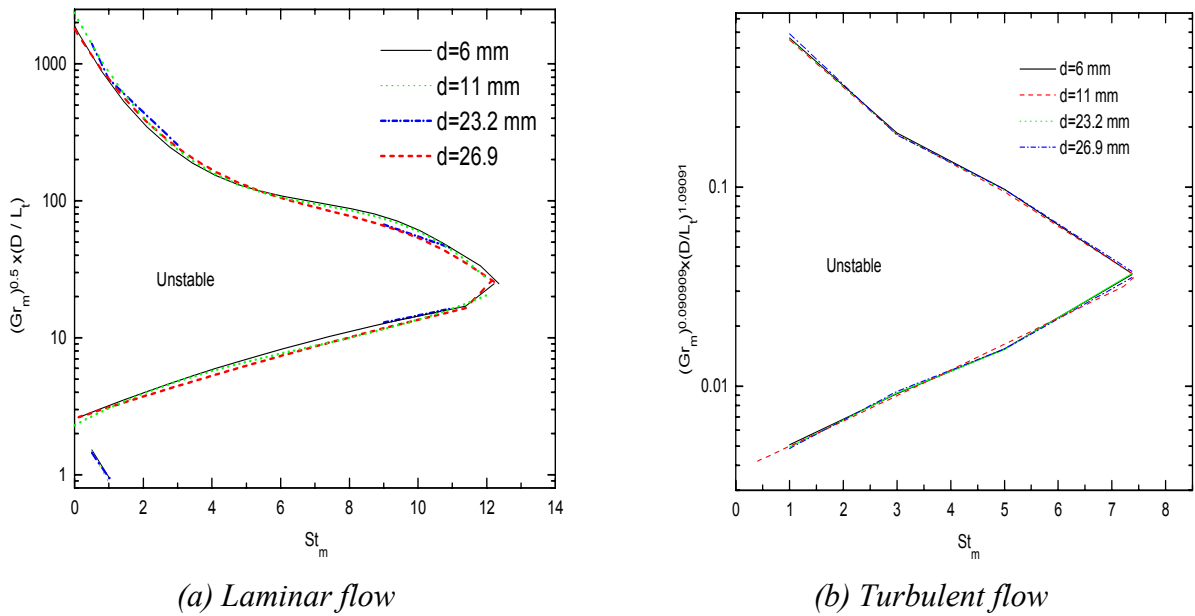
FIG. 13. Stability map for loops of different diameter.
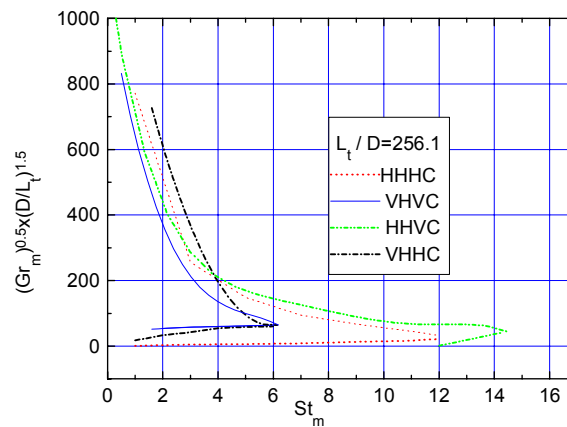
FIG. 14. Effect of heater and cooler orientations on the stability map.

6. CONCLUSIONS

Scaling laws for single and two-phase natural circulation systems have been presented. For single-phase systems, the steady state behaviour can be simulated by preserving Gr_m/N_G same in the model and prototype. Uniform diameter two-phase systems can be simulated by preserving Gr_m^*/N_G^* defined by Eq. (30). Simulation of the stability behaviour of uniform diameter loops requires preservation of the length scales in the model and prototype in addition to the similarity parameters appearing in the nondimensional governing equations.

NOMENCLATURE

A   - flow area, m^2
a   - dimensionless flow area, A/A_r
b   - constant in equation (9)
Cp   - specific heat, J/kgK
D   - hydraulic diameter, m
d   - dimensionless hydraulic diameter
f   - Darcy-Weisbach friction factor
g   - gravitational acceleration, m/s^2
Gr_m - modified Grashof number
h   - enthalpy, J/kg
h_{fg} - latent heat, h_G-h_L, J/kg
H   - loop height, m
k   - thermal conductivity, W/mK
K   - local pressure loss coefficient
l   - dimensionless length, L_i/L_t
L   - length, m
N   - total number of pipe segments
N_G - dimensionless parameter defined
         by Eq. (11)
Nu   - Nusselt number, UD/k
p   - constant in Eq. (9)
P   - perimeter, m
Pr   - Prandtl number, $Cp\mu/k$
q   - heat flux, W/m^2
Q   - total heat input rate, W
Re   - Reynolds number, $DW/A\mu$
s   - co-ordinate around the loop, m
S   - dimensionless co-ordinate around
         the loop, s/L_t
St_m - modified Stanton number
t   - time, s
T   - temperature, K
ΔT_r - reference temperature difference in
         Gr_m defined as $(QH/A_r\mu Cp)$
U   - heat transfer coefficient, W/m^2K
v   - specific volume, m^3/kg
v_{fg} - v_G-v_L, m^3/kg
V_t - total loop volume, m^3
W   - mass flow rate, kg/s
X   - quality

z   - elevation, m

Z   - dimensionless elevation (z/H) or

 (z/Δz)

Δz   - centre line elevation difference

 between cooler and heater, m

Greek Symbols

α - void fraction

β - thermal expansion coefficient, K^{-1}

μ - dynamic viscosity, Ns/m^2

ϕ_{LO}^2 - two-phase friction multiplier

θ - dimensionless temperature

ρ_{fg} - ρ_G - ρ_L, kg/m^3

ρ_r - reference density, kg/m^3

τ - dimensionless time

ω - dimensionless mass flow rate

Subscripts

c   - cooler

cl   - cold leg

e   - equivalent

eff   - effective

ex   - exit

G   - vapour

h   - heater

hl   - hot leg

i   - ith segment

in   - inlet

L   - liquid

p   - pipe

r   - reference value

s   - secondary

sat   - saturated

sep   - separator

sp   - single-phase

tp   -two-phase

BIBLIOGRAPHY

BADE, M.H., Development of generalised correlation for steady state behaviour of single-phase natural circulation loops and investigations on the suppression of instability using helical wire inserts, M.E. Thesis, Shivaji University, Sangli, Maharashtra, India.

BAU, H.H., TORRANCE, K.E, Int. J. Heat Mass Transfer 24 (1981) 597-609.

BERNIER, M.A., BALIGA, B.R, Int. J. Heat Mass Transfer 35 (1992) 2969-2982.

CREVELING, H.F. DE PAZ, J.Y. BALADI, R.J. SCHOENHALS, J. Fluid Mech. 67 (1975) 65-84.

HALLINAN, K.P., VISKANTA, R. Heat Transfer from a rod bundle under natural circulation conditions, NUREG/CR-4556.

HAWARE, S.K. GROVER, R.B., VENKAT RAJ, V. HMT-D2-83, Proc. VIIth National Heat and Mass Transfer Conference, Indian Institute of Technology, Kharagpur, India, 1983.

HEISLER, M.P, Nucl. Sci. Eng. 80 (1982) 347-359.

HO, C.J, CHIOU, S.P., HU, C.S, Int. J. Heat Mass Transfer, Vol. 40 (1997) 3553-3558.

HOLMAN J.P., BOGGS, J.H, J. Heat Transfer 82 (1960) 221-226.

HUANG, B.J., R. ZELAYA, J. Heat Transfer 110 (1988) 487-493.

ISHII, M., KATAOKA, I. NUCL. ENG. DES. 81 (1984) 411-425.

JOHN, B., KANNAN IYER, Proceedings of 24th National Fluid Mechanics Conference, 1991.

JEUCK III, P., LENNERT AND KIANG, R.L, Rep. EPRI-NP-2006, 1981.

MENDLER O.J. ET AL. 1961 J. Heat Transfer, 261-273.

MISALE, M. TAGLIAFICO, L., TANDA, G. Proceedings of the fourth International Symposium on Transport phenomena in heat and mass transfer, Sydney, 14-19 July (1991) p.203-211.

NAHAVANDI, A.N, CASTELLANA, F.S, MORADKHANIAN, E.N, Nucl. Sci. Eng. 72(1979) 75-83.

NAVEEN KUMAR, RAJALAKSHMI R., KULKARNI R. D., SAGAR T. V., VIJAYAN P.K, SAHA D., Experimental investigations in high-pressure natural circulation loop: Progress report for the period January – June, 1999, BARC/2000/E/002, Feb., 2000.

NAYAK A.K, VIJAYAN P.K, SAHA D., VENKAT RAJ V, ARITOMI M, J., Nuclear Science and Technology, 35, 712-722, 1998.

NISHIHARA, T., Proceedings of NURETH-8, Kyoto, Sept. 30-Oct. 4, (1997) 839-847.

OWENS, W.S. 1961, Int. Developments in Heat Transfer, part II, ASME.

STREETER, V.L., WYLIE, E.B, 1983 Fluid Mechanics, p.243-45, McGraw-Hill Book Company, Singapore.

VIJAYAN, P.K. Investigations on the single-phase thermosyphon phenomenon in a figure-of-eight loop relevant to pressurised heavy water reactors, Ph. D. thesis, Indian Institute of Technology, Bombay, 1988.

VIJAYAN P.K, BADE, M.H, SAHA, D, SINHA, R.K., VENKAT RAJ, V., A generalized correlation for the steady state flow in single-phase natural circulation loops, BARC report, June 2000.

VIJAYAN, P.K, NAYAK, A.K, PILKHWAL, D.S, SAHA, D., VENKAT RAJ, V, NURETH-5, Salt Lake City, UT, Vol.1, (1992) 261-267.

VIJAYAN, P.K., AUSTREGESILO, H., Nuclear Engineering and Design 152 (1994) 331-347.

VIJAYAN, P.K, Invited talk, M. Misale and F.Mayinger, (Eds.) 3-16, 1999, Proceedings of EUROTHERM SEMINAR N^{O}. 63 on Single and Two-Phase Natural Circulation, 6-8 September 1999, Genoa, Italy.

ZVIRIN, Y. JEUCK III P, SULLIVAN, C.W, DUFFEY, R.B, J. Heat Transfer 103, (1981) 645-652.

ZUBER, N, Problems in modelling of small break LOCA, Rep. NUREG-0724, October 1980.

Influences of buoyancy and thermal boundary conditions on heat transfer with naturally-induced flow

J.D. Jackson, J. Li

University of Manchester, United Kingdom

Abstract. A fundamental study is reported of heat transfer from a vertical heated tube to air which is induced naturally upwards through it by the action of buoyancy. Measurements of local heat transfer coefficient were made using a specially designed computer-controlled power supply and measurement system for conditions of uniform wall temperature and uniform wall heat flux. The effectiveness of heat transfer proved to be much lower than for conditions of forced convection. It was found that the results could be correlated satisfactorily when presented in terms of dimensionless parameters similar to those used for free convection heat transfer from vertical surfaces provided that the heat transfer coefficients were evaluated using local fluid bulk temperature calculated utilising the measured values of flow rate induced through the system. Additional experiments were performed with pumped flow. These covered the entire mixed convection region. It was found that the data for naturally-induced flow mapped onto the pumped flow data when presented in terms of Nusselt number ratio (mixed to forced) and buoyancy parameter. Computational simulations of the experiments were performed using an advanced computer code which incorporated a buoyancy-influenced, variable property, developing wall shear flow formulation and a low Reynolds number k~ε turbulence model. These reproduced observed behaviour quite well.

1. INTRODUCTION

Convective heat transfer from the outside surface of the steel containment vessel of a pressurised water reactor to a flow of air induced upwards by buoyancy through the space between the vessel and an external concrete shell has been proposed as a passive method of removing heat from the containment following a severe accident. Whilst there is no doubt that conditions of turbulent flow could be produced by this means, it is probable that the effectiveness of the heat transfer process would be poor. In view of the limited flow rate likely to be achieved, the heat transfer process within the passage will be buoyancy-influenced as well as buoyancy-driven. The mechanism of heat transfer will therefore be mixed free and forced convection. Published work on mixed convection heat transfer in vertical passages has been reviewed in a number of papers (see, for instance, Reference [1]). Some surprising trends have been identified. In the case of upward flow in a heated vertical passage, buoyancy aids the motion but contrary to expectation the values of heat transfer coefficient achieved can be lower than for conditions of turbulent forced convection. This is because the turbulence in the boundary layer is modified through the action of buoyancy with the result that the flow takes on the characteristics of one at lower Reynolds number. Impairment of heat transfer builds up gradually as the buoyancy influence is caused to become stronger, either by increasing the heat loading or reducing the flow rate. Eventually a very sharp reduction in the effectiveness of heat transfer is found to occur. With further increase of buoyancy influence, the process of heat transfer recovers. In contrast, for downward flow in a heated tube buoyancy opposes the motion, turbulence is increased and heat transfer is enhanced. The physical mechanism by which turbulent heat transfer is modified through the action of buoyancy influences in vertical passages was first identified by Hall and Jackson [2]. The contrasting influences on heat transfer for upward and downward flow are well described by a simple semi-empirical model of mixed convection developed by Jackson and Hall [3]. Figure 1 shows the predictions of that model for the case of a uniformly heated tube. These are found to be in good agreement with observed behaviour (see Reference [1]).
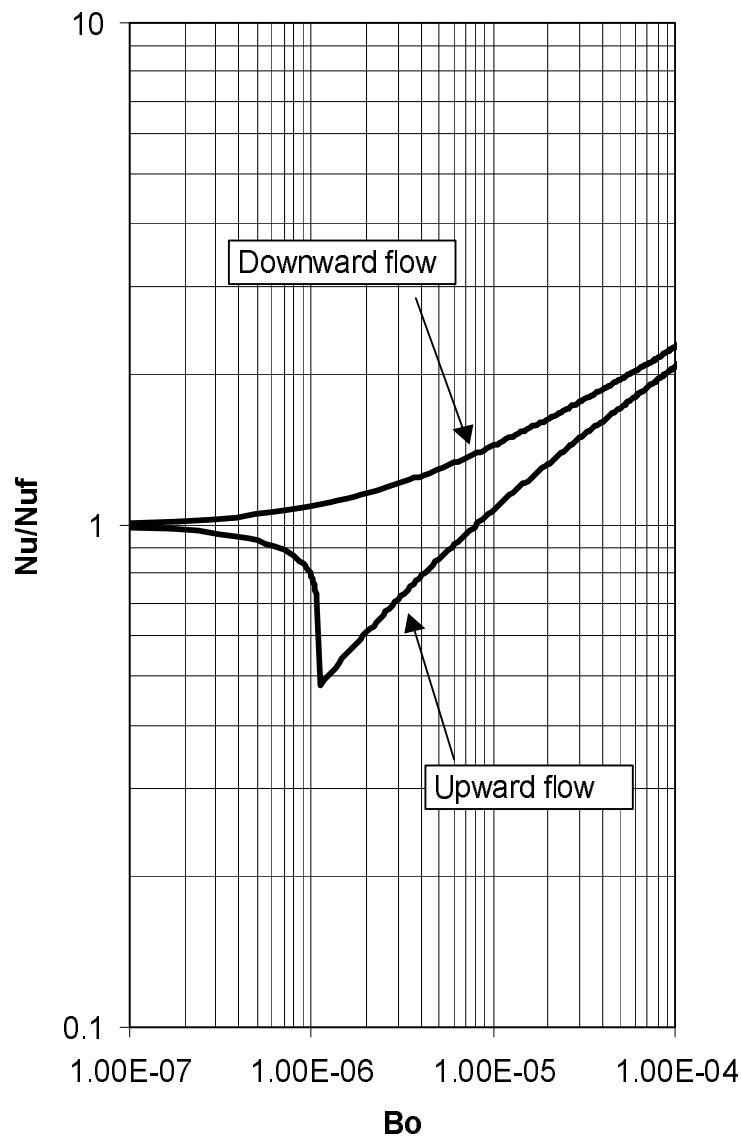
FIG. 1. Description of mixed convection using the semi-empirical model of Jackson and Hall

It is of interest to consider whether impairment of heat transfer would be encountered under the conditions likely to be achieved in a buoyancy-driven flow system of the kind which has been proposed for passively cooling a nuclear reactor containment vessel. In this connection, a further matter needs to be considered. Most of the experimental studies of mixed convection reported to date have been carried out with a thermal boundary condition of uniform wall heat flux. However, in the case of a severe accident in a pressurised water reactor, where steam is released from the core into a steel containment vessel and is condensing on its inside surface, the vessel will take up a uniform temperature. Since the nature of the thermal boundary condition could certainly affect the process of heat transfer to the air, there is a need to consider whether the behaviour with uniform wall temperature will be similar to that with uniform wall heat flux.

The study reported here using a non-uniformly heated test section which can operate at uniform temperature was undertaken to clarify these matters. This naturally-induced cooling experiment (NICE) formed part of the DABASCO project funded by the European Commission to provide an experimental data base for containment thermal hydraulic analysis (see Reference [4]).

2. EXPERIMENTAL FACILITY

The experimental facility used in the present study is shown in Figure 2. The test section, which was made from stainless steel tube of inside diameter 72.9 mm and wall thickness 1.63 mm, is suspended vertically in a space of height 15 m. It can be used for experiments with either naturally-induced flow or pumped flow.
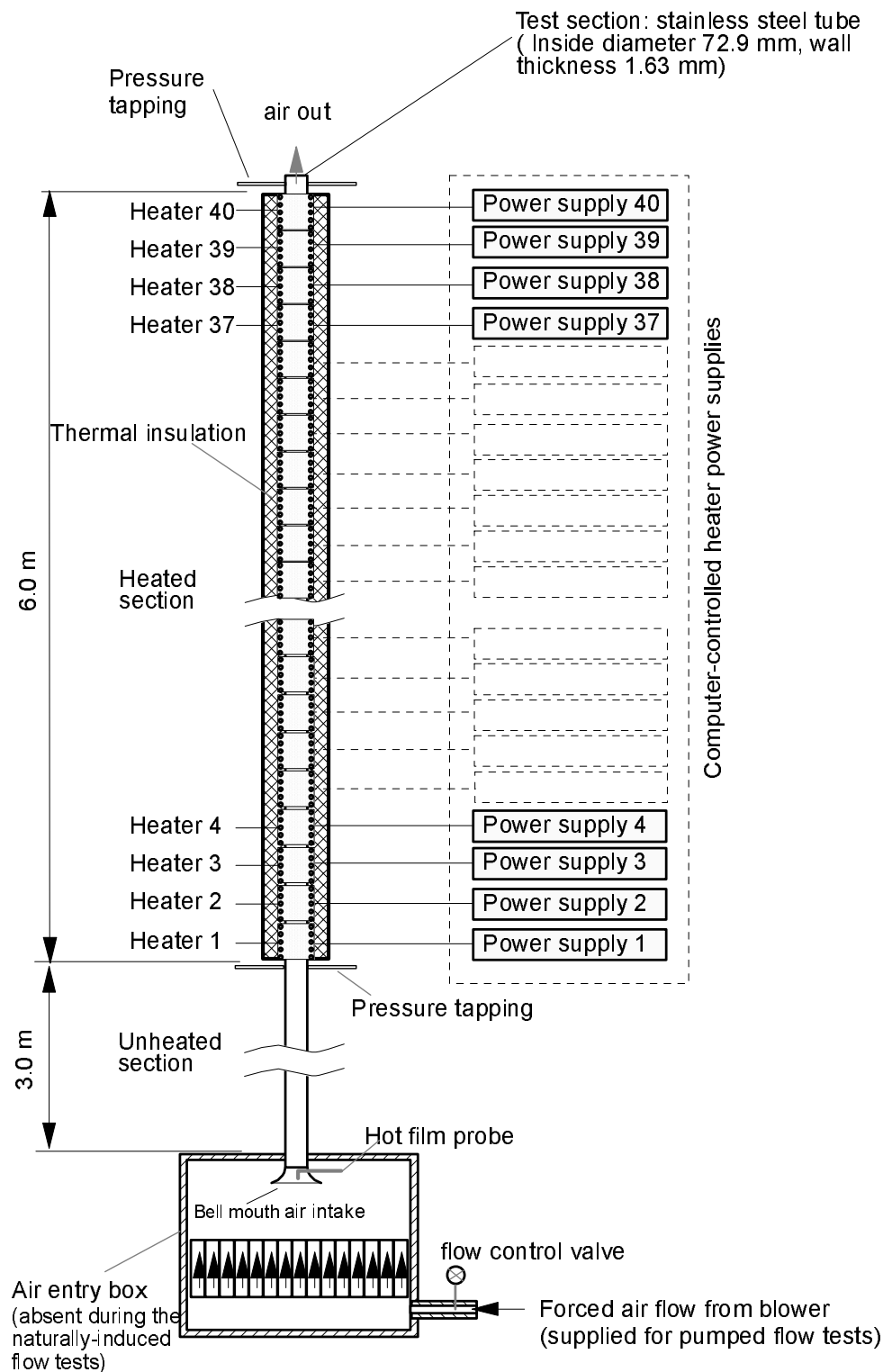
FIG. 2. General arrangement of the test facility

In the case of naturally induced flow, the entry box is absent and air passes from the laboratory into the bellmouth intake and upwards through an unheated flow development section of length 3 m and a heated section above it of length 6 m before discharging at the top. Motion occurs simply as a result of heat being applied to the test section. The velocity at inlet is measured using a calibrated hot film probe mounted in the centre of the bellmouth intake.

In the case of pumped flow, air is supplied to the entry box at the bottom of the test section by a blower and then flows upwards through the test section. The mass flow rate can be measured using a metering nozzle installed at the exit. The hot film probe was calibrated against this flow metering nozzle. Wall static pressure tappings are provided at the top and bottom of the heated section. The pressure difference is measured using a high precision electronic micro-manometer.

Numerous thermocouples attached to the outside of the heated length of the test section enable the wall temperature distribution to be measured in detail. The heated length is well lagged on the outside with pre-formed thermal insulation of low thermal conductivity to minimise heat transfer to the surroundings. The small loses which do occur can be accurately accounted for using data from calibration experiments which were performed at the commissioning stage. Heat can be applied to the test section either uniformly or non-uniformly by means of 40 separate, individually-controlled heaters distributed along its length. These were made using proprietary heater cable which was wound tightly around the outside of the stainless steel tube. Electrical power is supplied to the heaters from the mains via variable auto-transformers through the specially designed computer-based power control and measurement system shown in Figure 3. This supplies power to each heater at a rate needed to maintain the tube at a specified temperature at that location and also enables the power to be measured. The power is controlled by allowing a proportion of the half cycles of the incoming AC supply to pass to the heater. For each of the 40 heaters there is a control signal generator and a zero-crossing solid state relay. The former generates a control signal which enables the latter to pass a programmable number of half cycles from the supply to the heater during a specified time interval of 0.16 s. The signal generators are connected to a computer via a PC interface. The computer can write a number to each of the 40 signal generators under the action of software. The power to each heater is controlled by these numbers. Knowing this number, the voltage of the incoming supply and the electrical resistance of the heater, the power generated can be calculated. In operation, the computer reads temperatures using the Intercole data acquisition system. It then compares each wall temperature with a pre-set value, calculates a new number using the PID technique and sends it to the corresponding signal generator. The power supply system can also be operated in such a manner that a specified distribution of heat input is applied to the test section. A Pentium PC connected to a 208 channel data acquisition system is used for signal collection and processing. The software package which is used to drive the data logger and the power control and measurement system was developed and tested 'in house' using Visual Basic under the Windows 95 environment.

Initially, commissioning tests were performed on the test facility using the pumped flow arrangement to demonstrate that everything was operating satisfactorily. Friction factors determined from pressure drop measurements made under conditions of isothermal flow through the test section were compared with values calculated using the well-established correlation equation of Blasius for fully developed turbulent flow in a smooth tube. The maximum discrepancy was less than 6%.
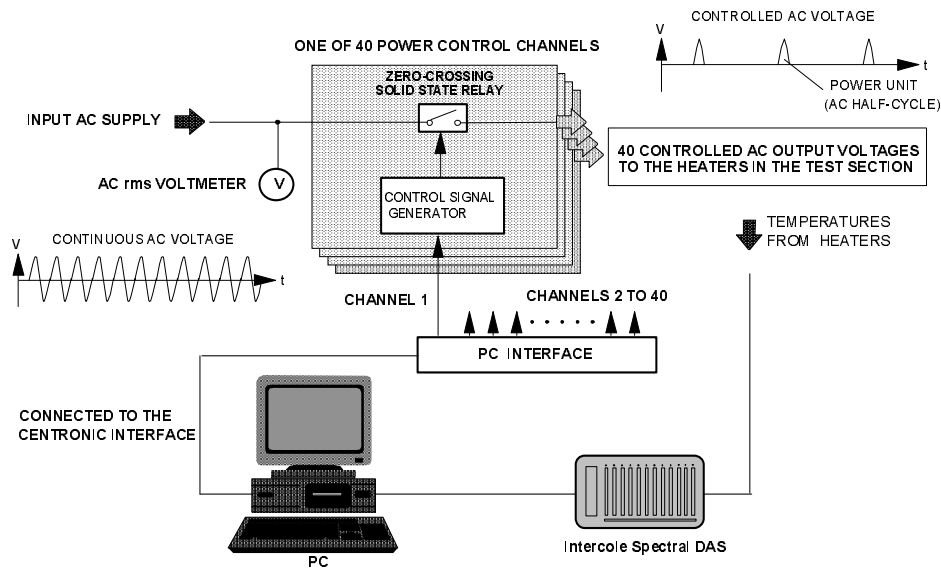
160

FIG. 3. Computer-based heater power control and measurement system

Local values of Nusselt number were determined at various locations along the tube from experiments performed under conditions of forced convection with uniform heating. In Figure 4(a) the results are compared with the distribution of Nusselt number calculated using the established empirical correlation equation of Petukhov et al [5]. As can be seen, the agreement is very satisfactory.

Results from a mixed convection experiment with uniform wall heat flux are shown in Figure 4(b). The Reynolds number was about 10,000. Under such conditions heat transfer was found to be strongly impaired due to the influence of buoyancy. It can be seen that the local values of Nusselt number lie well below the curve for forced convection calculated using the Petukhov equation. The observed behaviour is very similar to that found in an earlier study by Li [6] using a uniformly heated test section of similar dimensions (see Jackson and Li [7]).

3. EXPERIMENTAL INVESTIGATION

3.1. Experiments with naturally-induced flow

From the results of the commissioning tests with pumped flow presented in preceding section, it was clear that the test facility was operating satisfactorily. Accordingly, a detailed programme of experiments was carried out with naturally-induced flow and uniform wall temperature. The power control and measurement system was used to achieve uniform values of wall temperature ranging from 60 to 300°C. Corresponding experiments with uniform wall heat flux were also performed keeping the total heat input the same as in the uniform wall temperature experiments. The matrix of conditions covered was as follows.

Wall temperature Tw (°C)	60	80	100	150	200	250	300
Corresponding wall heat flux q_w (W/m^2)	91.0	171.4	229.7	428.0	640.0	899.4	1130.0

Uniform heat flux boundary condition
Re=29085 Qw=1910 W/m^2
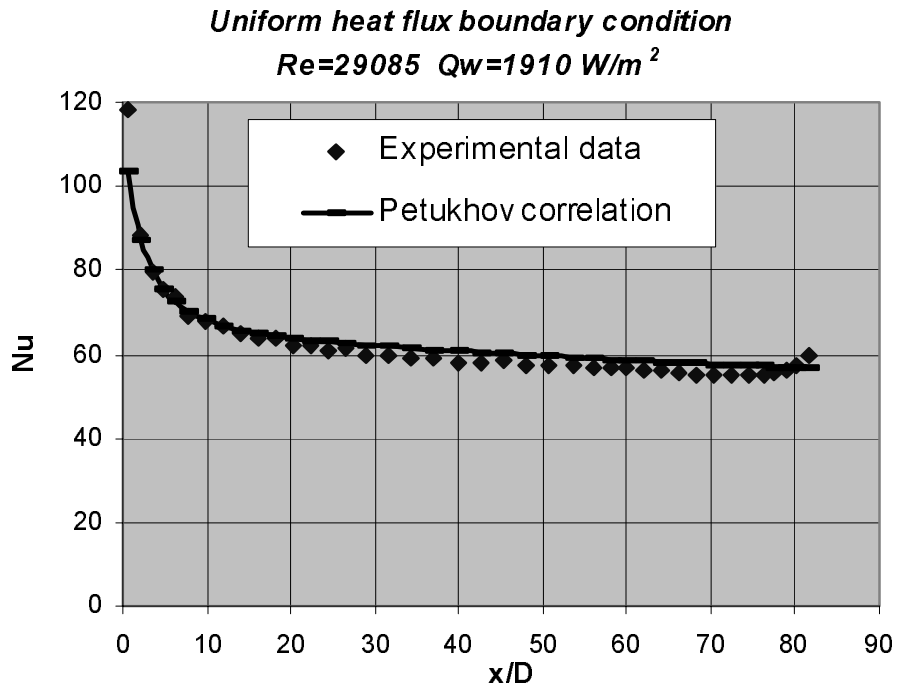
FIG. 4(a). Commissioning test results with uniform heating for forced convection

Uniform heat flux boundary condition
Re=10261 Qw=913 W/m^2
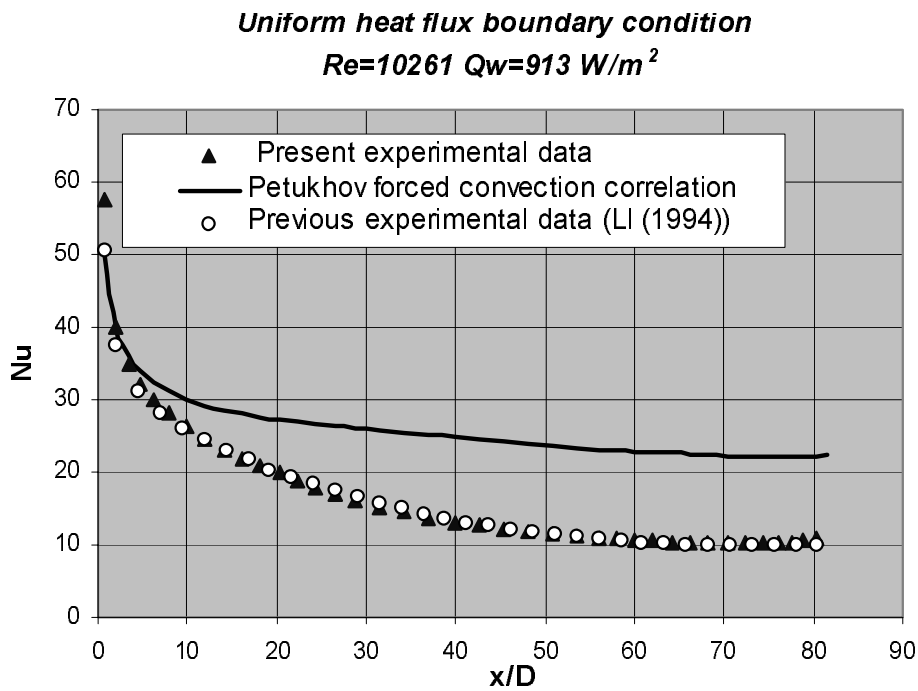
FIG. 4(b). Commissioning test results with uniform heating for mixed convection with impaired heat transfer

In these experiments the flow rate induced through the system increased systematically as the thermal loading was increased. The variation of dimensionless flow rate (characterised by Reynolds number) with dimensionless heat loading (characterised by Grashof number) is shown in Figures 5(a) and 5(b) for the uniform wall heat flux and uniform wall temperature cases, respectively. The physical properties in these dimensionless parameters were evaluated at the inlet temperature and the characteristic dimension used was the tube diameter.

162
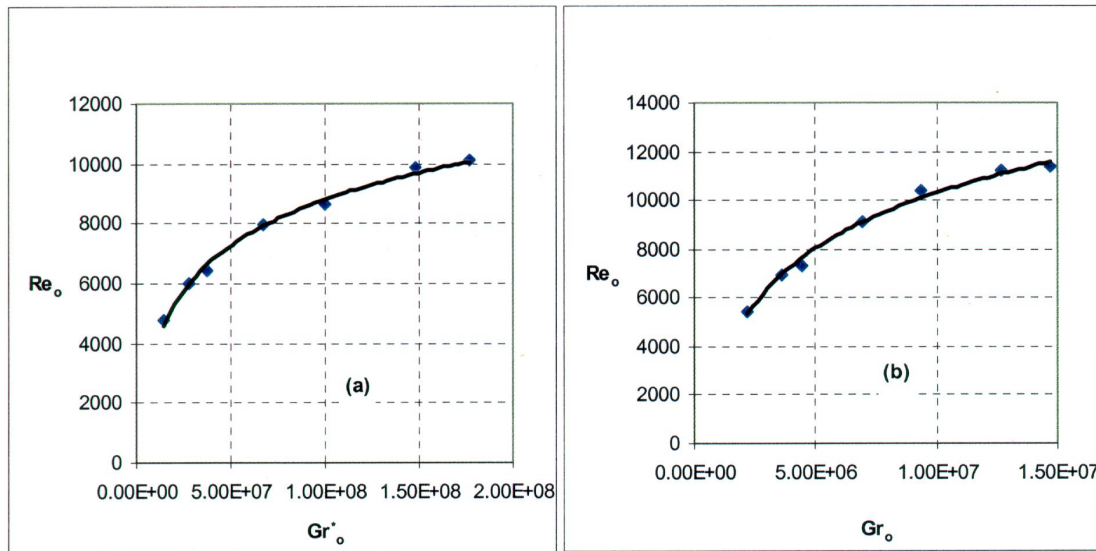
FIG. 5. Relationship between flow rate and thermal loading for naturally induced flow with (a) uniform heat flux, (b) uniform wall temperature

Figures 6(a) to 6(f) show the axial distributions of Nusselt number obtained in these experiments. The flow rates induced through the test section were used to determine the Reynolds numbers shown on the figures. In each case a curve is presented for forced convection with uniform heat flux evaluated at the Reynolds number for that case using the equation of Petukhov et al [5]. The main points to note are:

(i)   The experimental values of Nusselt number all follow a similar general pattern. They lie well below the curves for forced convection calculated using the Petukhov equation.

(ii)   The values of Nusselt number for the uniform wall temperature case are slightly lower than those for uniform wall heat flux in spite of the fact that the flow rates induced through the system are greater.

(iii)   The Nusselt number curves for forced convection calculated using the Petukhov equation decrease slowly at a steady rate in the thermally fully developed region. This is due to the fact that the Reynolds number decreases as the bulk viscosity increases due to the rise of bulk temperature.

Figures 7(a) and 7(b) show the experimental results plotted in terms of local values of local Nusselt number, Nu_x , and Grashof number, Gr_x (evaluated using the distance x from the start of heating as the characteristic dimension). The fluid properties were evaluated at the local bulk temperature, calculated knowing the air temperature at inlet, the heat input and the flow rate of air induced through the system. As can be seen, this method of presenting the results does enable a good correlation of the data to be achieved.

The main conclusions which can be drawn from the naturally-induced flow tests are as follows:

Even though the flow rates achieved were such that in the absence of buoyancy influences the flow would have been turbulent, the effectiveness of heat transfer was seriously impaired in relation to that expected for conditions of turbulent forced convection at those flow rates. It is clear that under the conditions of all the experiments performed the turbulence structure was

significantly modified by buoyancy. In the experiments with uniform wall temperature the heat transfer behaviour did not change much as the temperature was increased. Furthermore, the behaviour was very similar in the corresponding experiments with uniform wall heat flux. Clearly, the results obtained in this study highlight the need for care to be exercised in the design of systems for cooling a steel containment shell by naturally-induced flow of air so as to ensure that the kind of buoyancy-influenced conditions which prevailed in the present experiments are avoided.
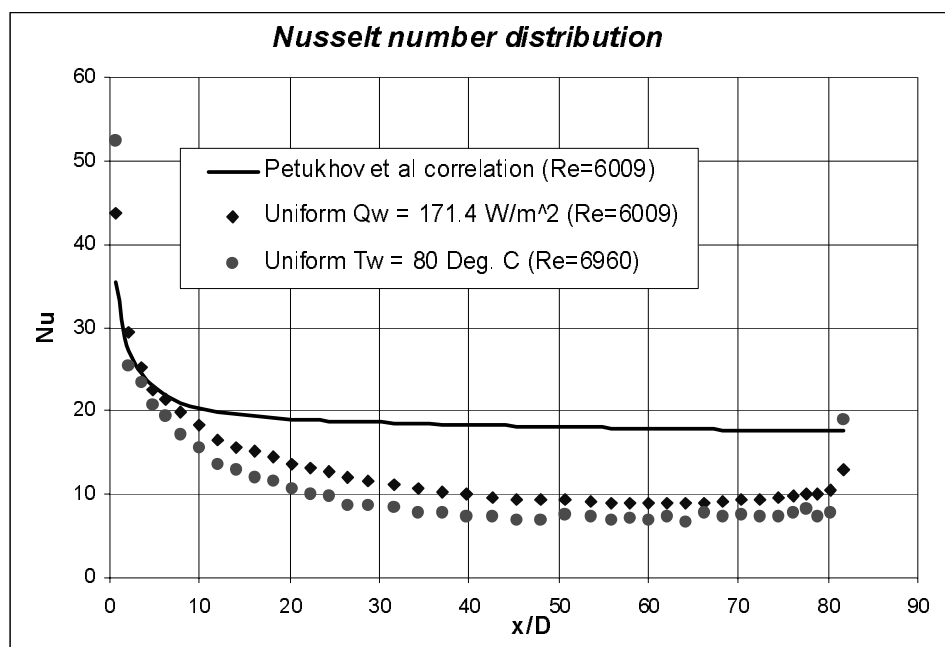
FIG. 6(a). Heat transfer results for naturally-induced flow with Tw = 800C.
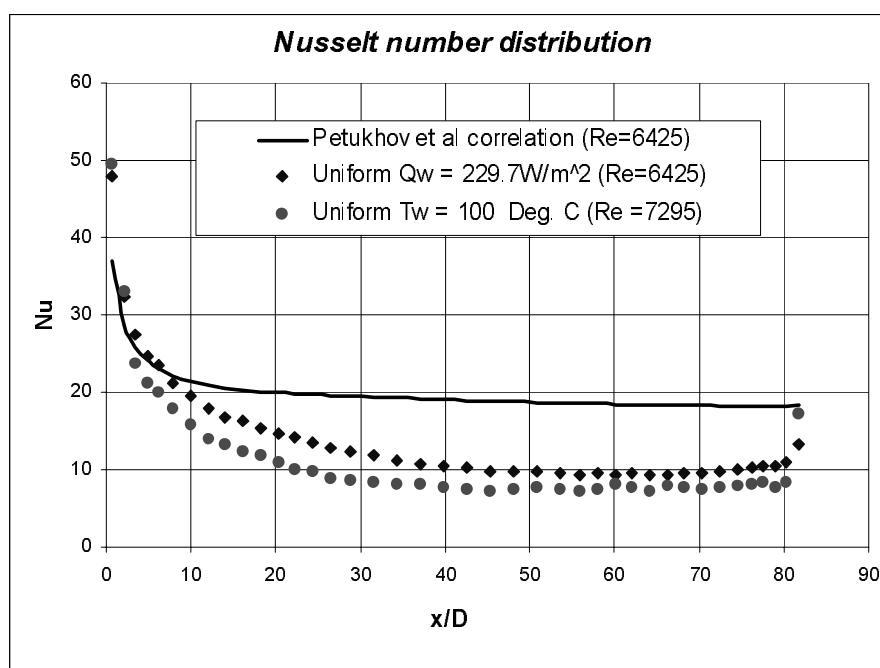
FIG. 6(b). Heat transfer results for naturally induced flow with Tw = 100^0C

164
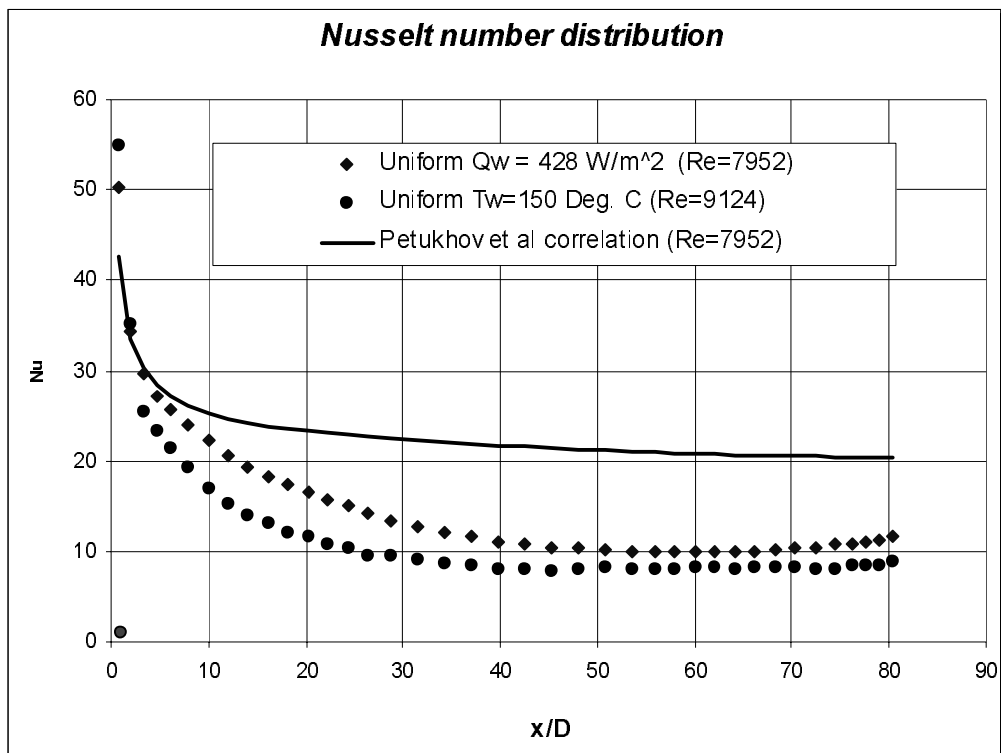
FIG. 6(c). Heat transfer results for naturally-induced flow with Tw = 150⁰C
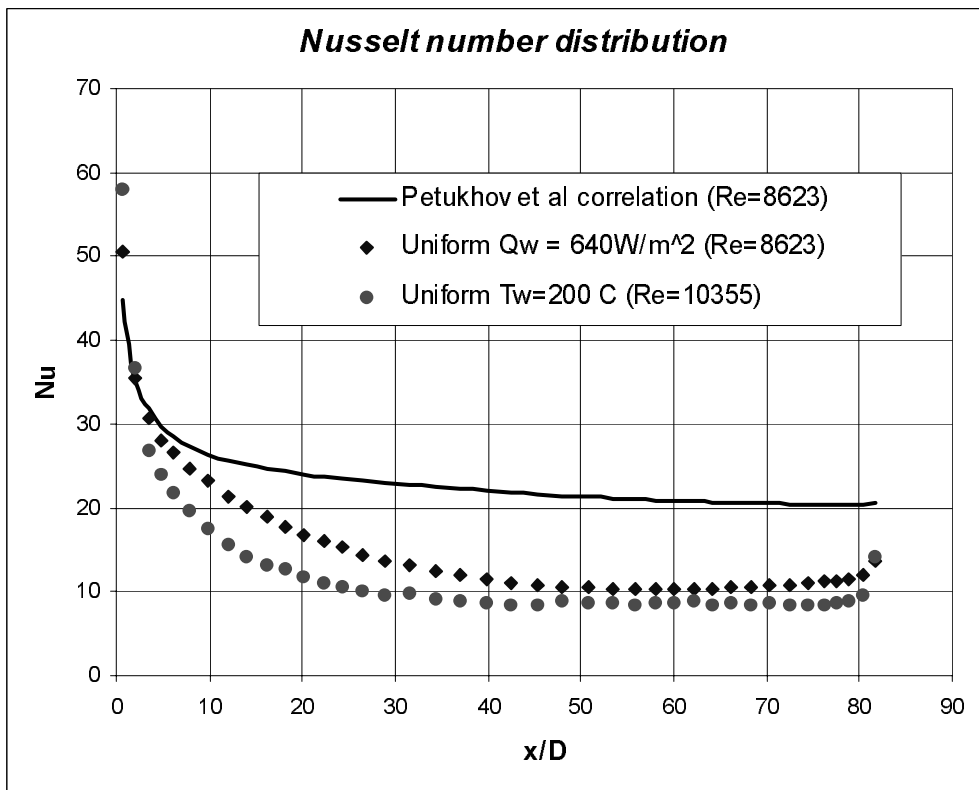
FIG. 6(d). Heat transfer results for naturally induced flow with Tw = 200⁰C

3.2. Experiments with pumped flow

After completing the naturally-induced flow experiments reported in the preceding sub-section, a programme of pumped flow experiments with uniform wall temperature was carried out. The conditions of heat transfer achieved in those experiments varied from forced convection with negligible influences of buoyancy to mixed convection with very strong influences of buoyancy. Inlet Reynolds number was varied in steps from about 30,000 down to 3,500 and values of wall temperature from 75°C to 300°C were covered. Again, corresponding experiments were performed with uniform heat input.
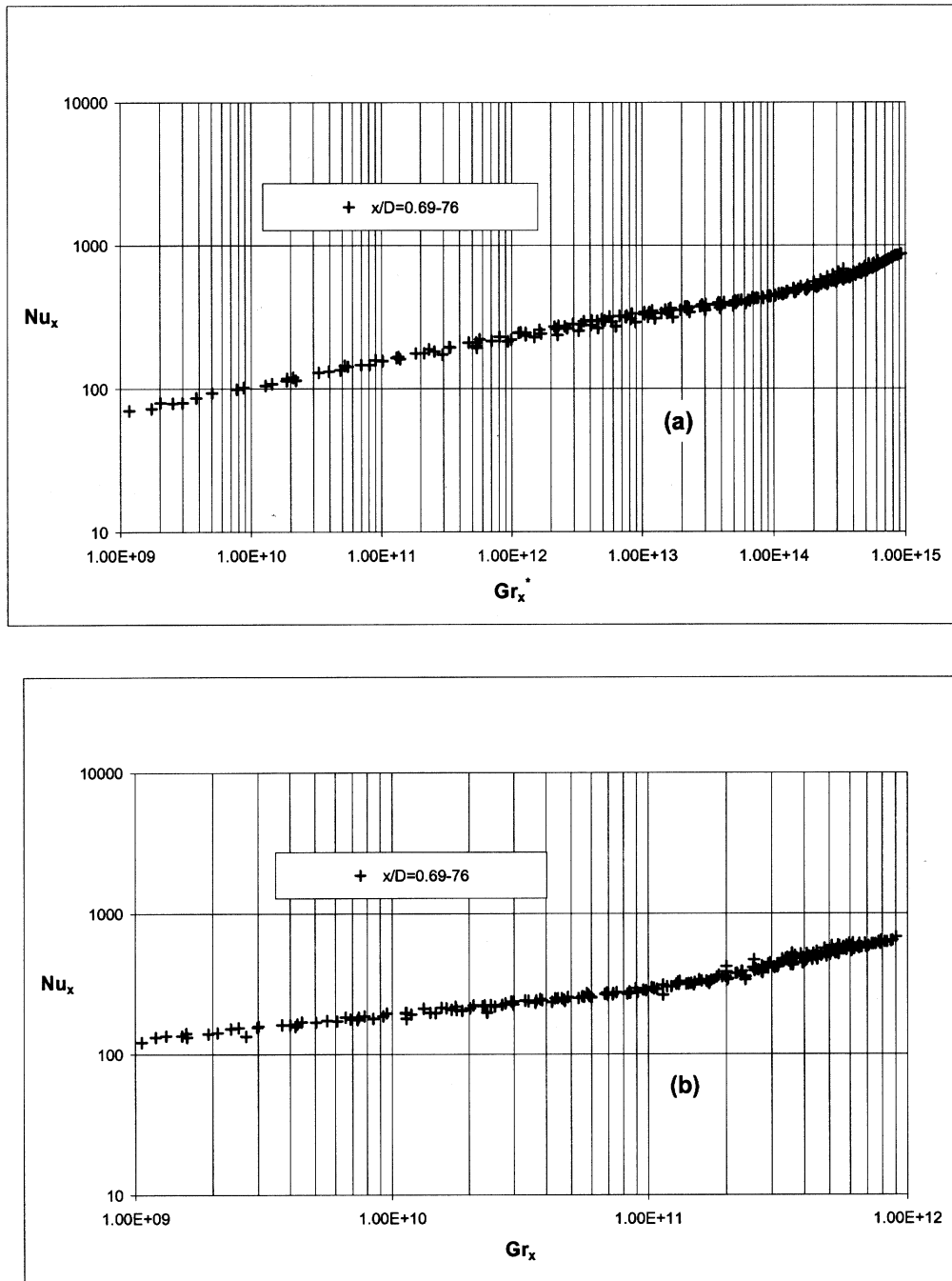
FIG. 7. Correlation of heat transfer results for naturally induced flow with
(a) uniform wall heat flux, (b) uniform wall temperature

Some sample results for a wall temperature of 150°C are shown in Figures 8(a) to 8(d) along with the corresponding ones for uniform heat flux. The Reynolds numbers at inlet were about 29,000, 10,500, 5100 and 3500. The main points to note are:

(i)   The heat transfer mechanism at the highest Reynolds number is turbulent forced convection. As can be seen from Figure 8(a), the results for the uniform heat flux case lie very close to the curve calculated using the Petukhov equation. Thus there are no significant influences of buoyancy. As expected, the results for uniform wall temperature lie slightly below those for uniform wall heat flux.

(ii)   At the Reynolds number of 10,500, Figure 8(b), the mechanism of heat transfer is mixed convection with serious impairment of heat transfer due to influences of buoyancy on turbulence. The effect is much greater for uniform wall temperature than for uniform heat flux. The results for uniform wall temperature are similar to those obtained for naturally-induced flow with a wall temperature of 200°C (Figure 6(d)).

(iii)   In the case of the experimental results shown in Figures 8(c) and 8(d) the conditions are those of mixed convection with progressively stronger influences of buoyancy leading to recovery and enhancement of heat transfer. Concentrated non-uniformities appear in the distributions of Nusselt number as a consequence of the development of the flow along the tube under the influence of strong buoyancy forces.

Figures 9(a) and 9(b) shows results from the pumped flow experiments for a large value of x/D presented in terms of Nusselt number ratio and buoyancy parameter. Experimental data for naturally induced flow are also included (in these cases the Reynolds number was evaluated using the value of flow rate induced through the system). The impairment of heat transfer which develops with increase of buoyancy parameter is strikingly apparent in both cases, as also is the recovery of heat transfer (in relative terms) when buoyancy influences become strong enough to restore turbulence production. As can be seen, when presented in this form the naturally-induced flow results map directly onto the pumped flow results.

Although the results obtained in the pumped flow experiments confirm that the general pattern of behaviour in buoyancy-aided mixed convection is the similar with uniform wall temperature and uniform wall heat flux, the impairment of heat transfer which develops with onset of buoyancy influences does occur more readily in the case of uniform wall temperature. The results highlight the fact that care is needed in the design of containment cooling systems to avoid conditions under which buoyancy-induced impairment of heat transfer might occur.

4.   COMPUTATIONAL SIMULATIONS OF THE EXPERIMENTS

An advanced computer code CONVERT, developed and validated earlier at the University of Manchester for buoyancy-influenced flow in uniformly heated vertical tubes, was used to perform simulations of the present experiments. This code uses a buoyancy influenced, variable property, developing wall shear flow formulation for turbulent flow and heat transfer in a vertical tube in conjunction with the Launder-Sharma low Reynolds number k-ε turbulence model [9]. The conditions covered in the simulations ranged from forced flow with negligible influence of buoyancy to buoyancy-dominated mixed convection. In each case, simulations were made for thermal boundary conditions of both uniform wall temperature and uniform heat flux. These show that the computational formulation used does enable observed heat transfer behaviour in the mixed convection region to be reproduced. Buoyancy-induced impairment of

heat transfer is predicted and satisfactory agreement with experiment is found for such conditions. The non-uniformities which develop in the distributions of Nusselt number under such conditions are well reproduced. It is known from earlier work done by the present authors that other turbulence models are generally less successful than the Launder Sharma model in reproducing the influences of buoyancy on turbulence and heat transfer found in mixed convection. Thus, it is important in the computational modelling of containment cooling systems that an appropriate turbulence model is used.
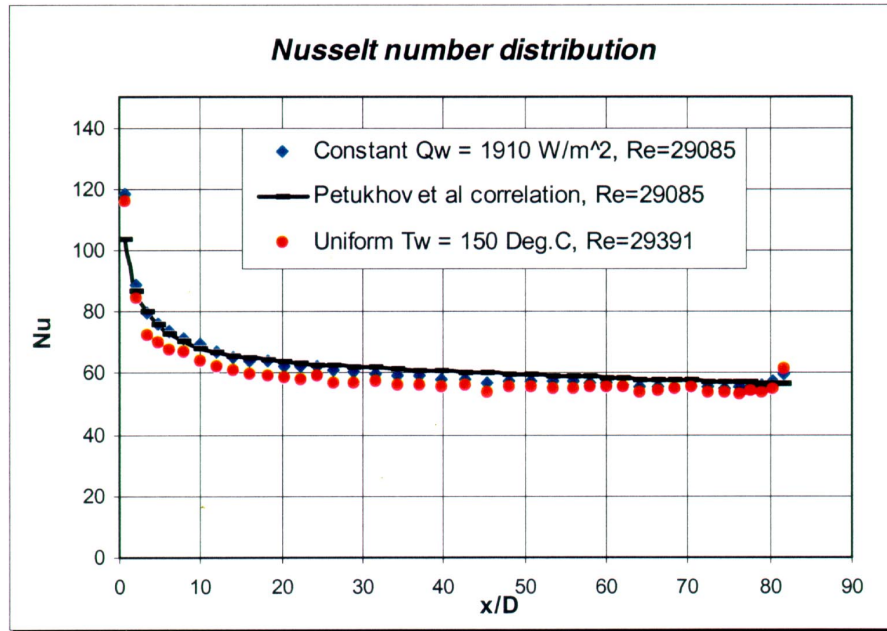
FIG. 8(a). Heat transfer results for pumped flow with Tw = 150^{0}C at Re = 29,000
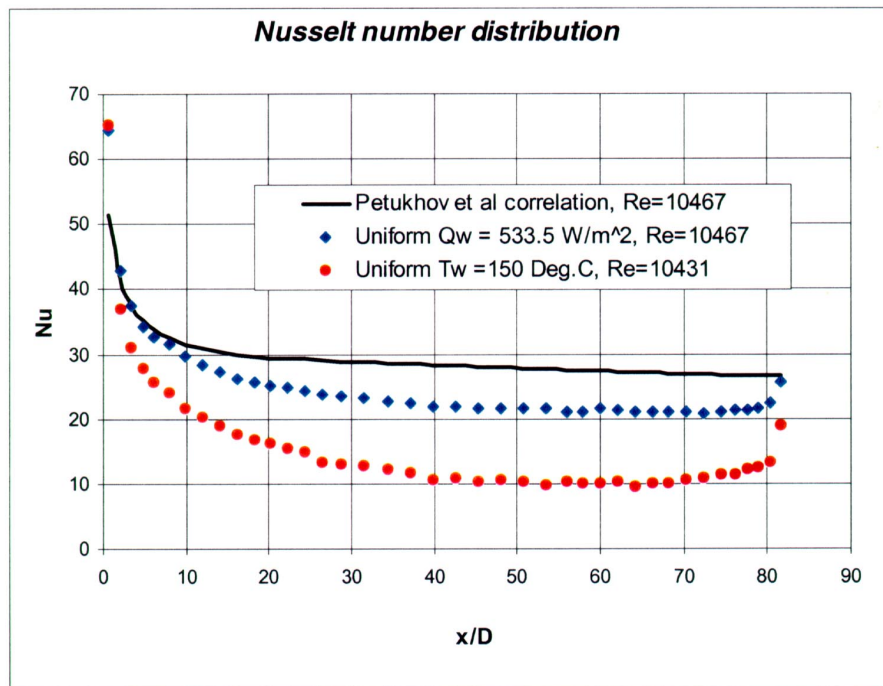
FIG. 8(b). Heat transfer results for pumped flow with Tw = 150^{0}C at Re = 10,000

168
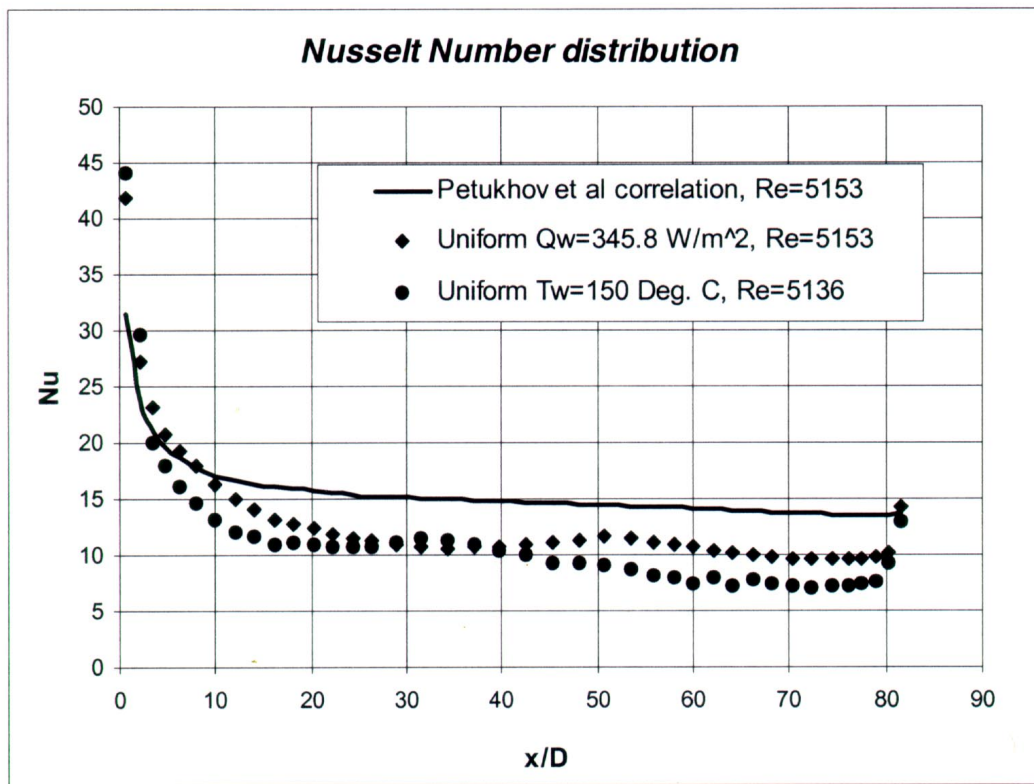
FIG. 8(c). Heat transfer results for pumped flow with Tw = 150^{0}C at Re = 5,400
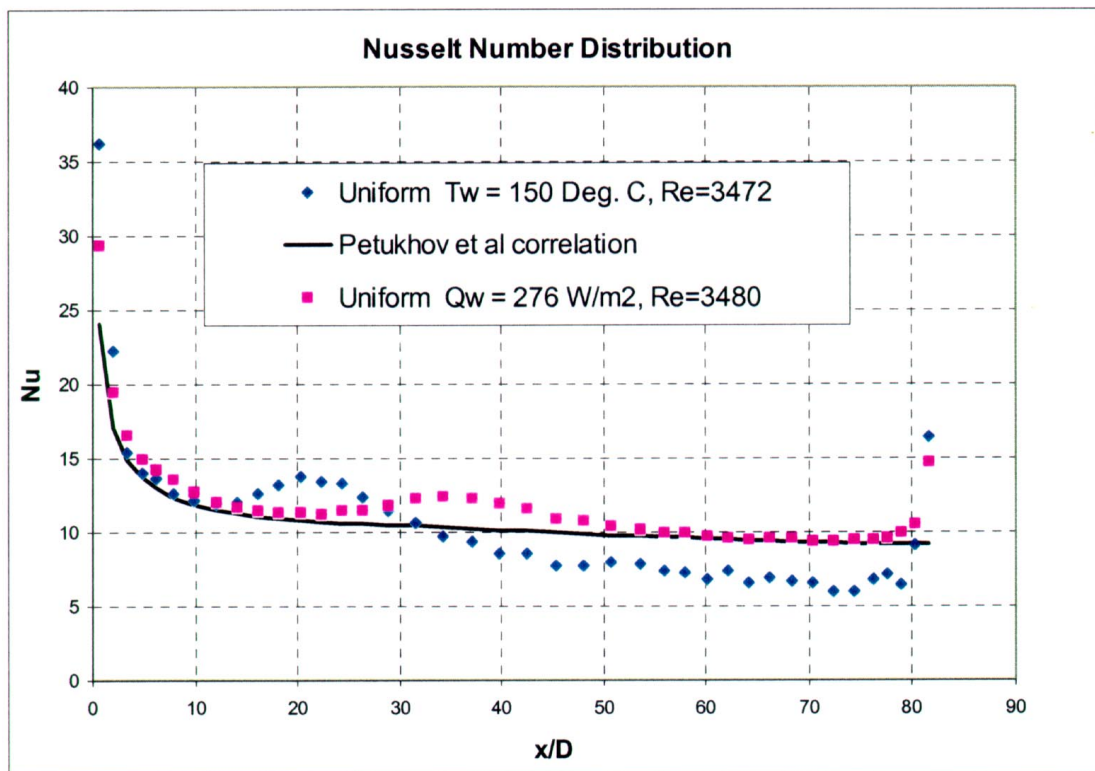
FIG. 8(d). Heat transfer results for pumped flow with Tw = 150^{0}C at Re = 3,500
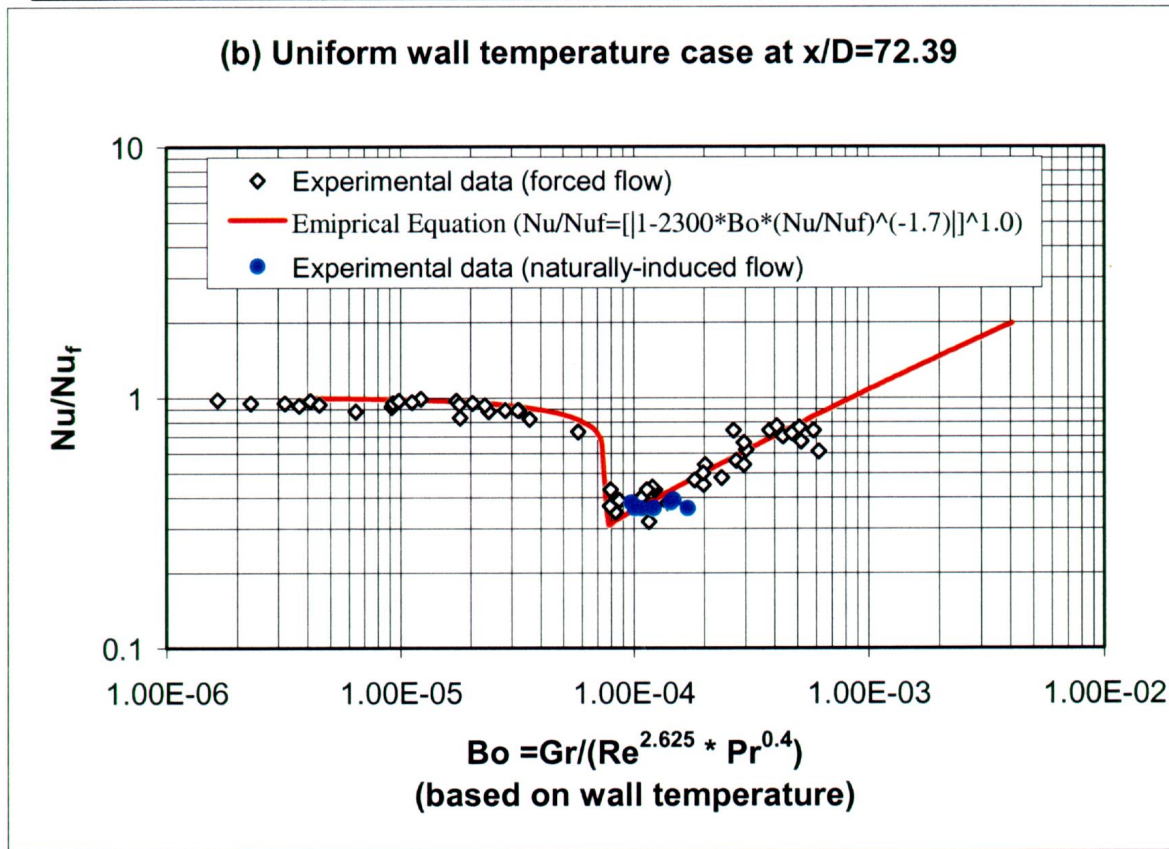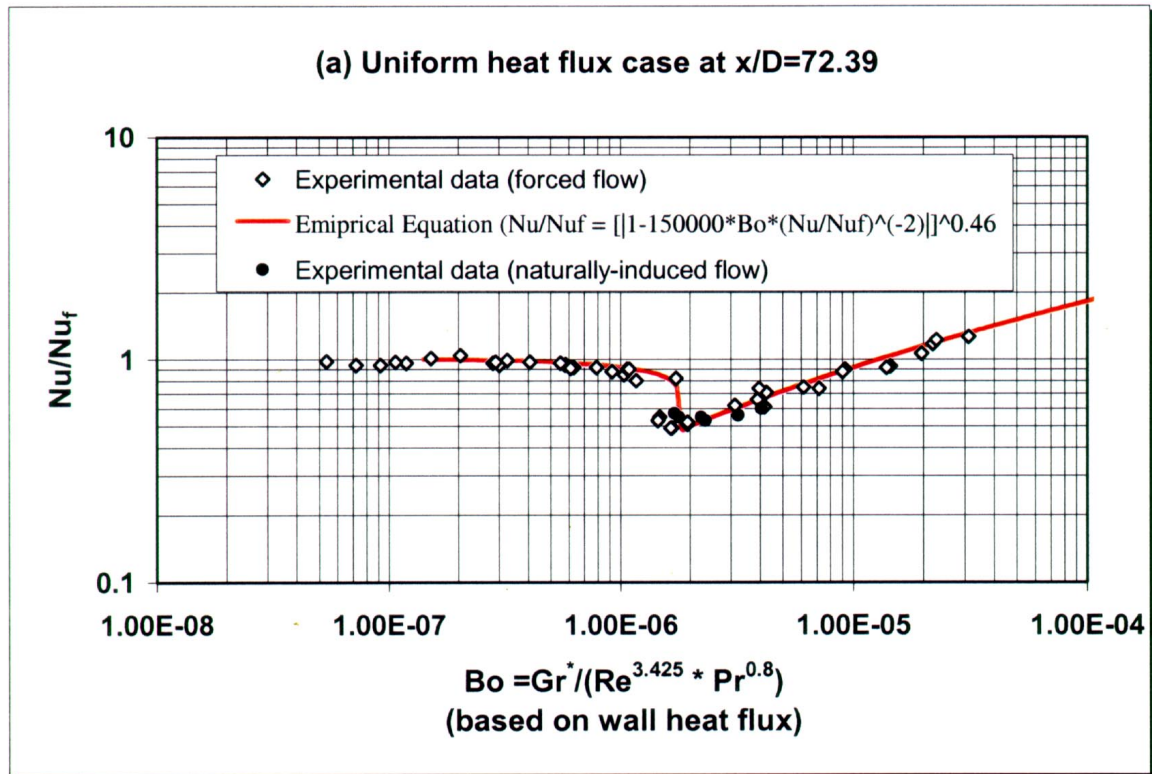
FIG. 9. Correlation of heat transfer data for large x/D in terms of Nusselt number ratio and buoyancy parameter for (a) uniform wall heat flux, (b) uniform wall temperature

5. CONCLUSIONS

Even though the flow rates achieved in the naturally-induced cooling experiments with uniform wall temperature were such that the flow would have been turbulent in the absence of buoyancy influences, the effectiveness of heat transfer was seriously impaired in relation to that for turbulent forced convection. It is clear that under the conditions of all the experiments performed in this study turbulence was strongly impaired as a result of the influence of buoyancy. The heat transfer behaviour did not change very much as wall temperature was raised and was very similar in corresponding experiments with uniform wall heat flux. The results obtained highlight the need for care to be taken in the design of systems for cooling a steel containment shell by a naturally-induced flow of air over it so as to ensure that the buoyancy-influenced conditions which prevailed in the present experiments are avoided.

Although the results obtained in the pumped flow experiments confirm that the general pattern of behaviour in buoyancy-aided mixed convection with uniform wall temperature is similar to that with uniform wall heat flux, impairment of heat transfer with onset of buoyancy influences was found to occur more readily with uniform wall temperature.

The computational simulations showed that the formulation used does enable observed heat transfer behaviour to be satisfactorily reproduced throughout the mixed convection region. It is known from earlier work (Reference [10]) that other turbulence models are generally less successful in reproducing the influences of buoyancy on turbulence and heat transfer found in vertical passages. Thus, in the computational modelling of containment cooling systems it is important to use an appropriate turbulence model and to be aware of the limitations of such models.

REFERENCES

[1] JACKSON, J.D., COTTON M.A. and AXCELL B.P., "Studies of mixed convection in vertical tubes", Int.J. Heat Fluid Flow, Vol. 10, 2-15, (1989).

[2] HALL, W.B. and JACKSON, J.D., "Laminarisation of a turbulent pipe flow by buoyancy forces", ASME, Paper No. 69-HT-55, (1969).

[3] JACKSON, J.D. and HALL, W.B., "Influences of buoyancy on heat transfer to fluids flowing in vertical tubes under turbulent condition". Turbulent Forced Convection in Channels and Bundles Theory and Applications to Heat Exchangers and Nuclear Reactors, 2, Advanced Study Institute Book (eds. Kakac, S. and Spalding, D.B.), 613-640, (1979).

[4]   JACKSON, J.D. with CHENG, X., BAZIN, P., CORNET, P., HITTNER, D., LOPEZ JIMENEZ, NAVIGLIO, J., ORIOLO, A., F. and PLANK, H., "Experimental data base for containment thermal hydraulic analysis". The NURETH 9 Conference, San Francisco, California, USA, October 3-8, (1999) and the Journal of Nuclear Engineering and Design, March (2000).

[5]   PETUKHOV, B.S., KURGANOV, V.A. and GLADUNTSOV, A.I., "Turbulent heat transfer in tubes to gases with variable physical properties". Heat and Mass Transfer, Izd. ITMO AN BSSR, Minsk, Vol. 1, pp117-127, (1972).

[6]   LI, J., Studies of buoyancy-influenced convective heat transfer to air in a vertical tube. Ph.D. Thesis, Unviersity of Manchester, (1994).

[7]   JACKSON, J.D. and LI, J., "Buoyancy-influenced variable property turbulent heat transfer to air flowing in a uniformly heated vertical tube", (Proc. 2nd EF International Conference on Turbulent Heat Transfer, Manchester), Vol. 1, 2.31-2.49, June (1998).

[8]   JACKSON, J.D., LI, J. and AN, P., "The Influence of thermal boundary conditions on mixed convection heat transfer in vertical tubes", Invited Lecture, Proceedings of the 3rd Baltic Heat Transfer Conference, Sopot, Poland, Progress in Engineering Heat Transfer, pp 197-207, 22nd – 25th September (1999).

[9]   LAUNDER, B.E. and SHARMA, B.I., "Application of the energy-dissipation model of turbulence to the calculation flow near a spinning disc". Lett. Heat Mass Transfer 1, 131-138, (1974).

[10]   JACKSON, J.D. and MIKIELEWICZ, D.P., "Computational studies of buoyancy-influenced flow of air in a vertical pipe", Proceedings of the Third International Symposium on Engineering Turbulence Modelling and Measurements, Heraklion, Crete, 27-29 May (1996).

Finnish facilities for studies on innovative nuclear power plant designs

J. Vihavainen, J. Bánáti,
Lappeenranta University of Technology, Finland

H. Purhonen,
VTT Energy, Finland

Abstract. Several series of experiments has been carried out at Lappeenranta University of Technology (LTKK) in co-operation with VTT Energy in Finland to investigate systems to be used in advanced and innovative reactors. The integral and separate effects test facilities and the flexibility to use and modify existing instruments enables the variety of the possible applications. The main goal of the experimental work is to provide test data for validation of computer codes used for nuclear safety analysis. VTT Energy started the studies on Innovative Nuclear Power Plant designs by investigating the Core Make-up Tank (CMT) behaviour on the Parallel Channel Test Loop (PACTEL) facility. The main objective was to provide new and independent information about Passive Safety Injection System (PSIS) performance. The latest project on the PACTEL test facility in European Commission 4th Framework Programme *"Assessment of Passive Safety Injection Systems of Advanced Light Water Reactors"* involved 15 experiments in three series. The purpose of these experiments was to increase information about condensation and heat transfer processes in the CMT, thermal stratification of water in the CMT, and natural circulation flow through the PSIS lines. The PACTEL facility was modified for investigations of the WWER-640 emergency cooling system for reducing primary pressure in Loss-of-Coolant Accident by equalising the primary-system and containment pressures and removing the residual heat from the core by natural circulation to the emergency cooling pool. The results of the experiments have been used for computer code validation in low pressure and low power conditions. Another innovative experimental project is a hydraulic scram system for SWR-1000 power plant concept by Siemens-KWU. The system was studied in the series of separate effect experiments. The system uses pressurised water and steam as a driving force of the hydraulic scram system. Electric heaters located below the water level generate and maintain the steam volume and a layer of saturated water in the tank. After the scram signal the energy of the steam volume is used to move the control rods into the core. In the experiments orifices simulated the response of the control rods.

1. INTRODUCTION

PACTEL (**Pa**rallel **C**hannel **Te**st **L**oop) [1] is a full height, medium-scale integral test facility (volumetrically scaled 1:305) designed to simulate the thermal-hydraulic phenomena characteristic of the Finnish Loviisa PWR. VTT Energy together with the Lappeenranta University of Technology run the facility. PACTEL has three primary coolant loops with pressurizer, primary coolant pumps and horizontal steam generators, high-pressure emergency core cooling system (ECCS), and low pressure ECCS with two accumulators. The peak operating pressures in the primary and secondary sides are 8 MPa and 4.6 MPa, respectively. The reactor vessel is simulated with a U-tube construction consisting of separate downcomer and core sections. The core comprises of 144 full length, electrically heated fuel rod simulators with a heated length of 2.42 meters. The maximum total core output is 1 MW, or 22% of scaled full power. The three coolant loops with double capacity steam generators model the six loops of the reference power plant. Each steam generator has 118 U-tubes with an average length of 2.8 m.

The passive safety injection experiments in Lappeenranta started already in 1992 with a series of five experiments. These experiments simulated hot leg SBLOCA's. The PSIS included a CMT and two PBL's. The second series included four cold leg SBLOCA experiments in 1993. These experiments used similar PSIS as in the first series. In 1996, a new project of passive safety injection experiments with a CMT and one PBL started. The new experiments

are a part of the European Commission 4th Framework Programme Nuclear Fission Safety program. Within this new project, three series of five experiments were completed, project continued until September 1998.

The PACTEL facility was modified for investigations of the WWER-640 emergency cooling system for reducing primary pressure in Loss-of-Coolant Accident by equalising the primary-system and containment pressures and removing the residual heat from the core by natural circulation to the emergency cooling pool. The results of the experiments are not yet finally analysed but they are being used for computer code validation in low pressure and low power conditions.

Another innovative experimental project has been a hydraulic scram system for SWR-1000 power plant concept by Siemens-KWU. The system was studied in the series of seven separate effect experiments during December 1999. The project was a part of VTT's Advanced Light Water Reactor (ALWR) technology programme. It was funded by Siemens, Teollisuuden Voima Oy (TVO), TEKES and VTT. The system uses pressurised water and steam as a driving force of the hydraulic scram system.

2. PASSIVE SAFETY INJECTION EXPERIMENTS

A separate paper is given in this meeting to describe the passive safety experiments in more detail. Here is only a short overview of the experiments.

2.1. Experiments with CMT and two PBL's

The main objective of the tests was the overall simulation of the PSIS behaviour. The experiments demonstrated the capability of PACTEL for the simulation of PSIS's [2, 3, 4, 5]. The data did not provide very detailed information about phenomena in the CMT. The instrumentation of the CMT in the first test series was limited. The tests were partially aimed for investigation of possibilities to run passive safety injection tests on PACTEL. The experience gathered during this first series was then used in the specification of the test parameters and instrumentation of the second series.

2.1.1. The first series of passive safety injection experiments (GDE-01 through GDE-05)

The first experiment series included five SBLOCA tests with break in one hot leg of PACTEL. Three break sizes were used. Three tests included secondary system depressurization as an accident management measure. In all tests, only PSIS provided ECC water to the core. The primary pressure used in the tests was lower than the nominal operation pressure of PACTEL. Maximum operation pressure of the passive accumulators determined the upper limit of the experiment pressure (3.8 MPa).

Although some problems with condensation in the CMT occurred no core heat-up was detected. It should be mentioned here that the CMT used in the test was very large, about twice as large as the scaled volume of four accumulators of the reference plant. On the other hand, the volume of the CMT is about the same as the volume of the rest of the loop. All the tests in this first series were terminated before the CMT was totally empty.

2.1.2. The second series of passive safety injection experiments (GDE-11 through GDE-14)

The second experiment series included four SBLOCA tests with break in one cold leg of PACTEL. Two break sizes were used. The tests also included studies of primary system depressurization and reproducibility of the phenomena. In all tests, only the CMT provided ECC water to the primary loop.

The primary pressure used in the tests was again lower than the nominal operation pressure of PACTEL. The maximum operation pressure of the passive accumulator limited the maximum experiment pressure to 3.8 MPa. Since one loop of PACTEL was equipped with a different steam generator model the tests run with only two loops in operation. There was still water in the CMT when the tests were terminated. During the rapid condensation period, water level in the core simulator dropped close to the top of the core. However, also in these test no core heat-up occurred.

2.2. Experiments with CMT and one PBL [6]

In 1996, a new project for the investigation of passive safety injection systems of ALWR's begun. The new project, entitled "Investigation of Passive Safety Injection Systems of Advanced Light Water Reactors", is a part of the INNO cluster of the European Commission Nuclear Fission Safety (NFS-2) Programme. The project received funding from the European Commission. The general objectives of the new project are:

- to provide new and independent information about passive safety injection system performance,
- to contribute to a public data base for the users and developers of thermal-hydraulic computer codes on the phenomenological behaviour of PSIS's in LOCA conditions, and
- to identify the accuracy, uncertainties and limitations of thermal-hydraulic computer codes in the modelling of passive safety injection system behaviour.

2.2.1. The third series of passive safety injection experiments (GDE-21 through GDE-25)[7]

The main problem in the first two test series in PACTEL was the rapid condensation in the CMT, which temporarily stopped the ECC water injection. The condensation took place when the saturated water layer in the CMT broke down, and the steam got into contact with cold ECC water. This happened when water flowed to the CMT after the level in the tank has already dropped. In the tests the water level in the CMT started to drop almost immediately after the opening of the break and the period of single phase natural circulation through the cold leg pressure balancing line to the CMT was very short. Due to this the saturated water layer in the CMT separating cold water from steam remained thin. For the third series, a flow distributor called sparger has been added to the CMT. The purpose of the sparger is to diminish possibilities of rapid condensation in the CMT. Further, the experiment procedure included filling of the PBL with hot water before the break opening. The CMT and the IL was full of cold water. All the earlier experiments begun with cold water in the CMT, PBL and IL.

The main objective of the third series was to investigate the influences of break size and the removal of the pressurizer PBL on the CMT behaviour in cold leg SBLOCA's. The tests run with four different break sizes (from 1 to 5 mm in diameter) including reproducibility studies. Like in the earlier tests the main objective of the tests was to simulate the PSIS behaviour and not to try to simulate any proposed ALWR reactor concept in particular.

In all experiments the CMT ran as planned. There were no problems with rapid condensation in the CMT, such as was seen in the earlier passive safety injection experiments in PACTEL. The main reason was the new CMT arrangement, with a flow distributor (sparger) installed to the CMT. The sparger spread incoming flow to the CMT horizontally, and the breakdown of the saturated water layer due to incoming water was not possible. The hot liquid layer between the steam and cold water in the CMT remained stable, even in the experiments where the hot liquid layer was less than 5 cm thick.

2.2.2. The fourth series of passive safety injection experiments (GDE-31 through GDE-35)

- The second series of the EC funded project included five experiments for the investigation of the break location and CMT scaling (smaller CMT) on the PSIS behaviour. PACTEL operators made small changes to the CMT instrumentation to better detect CMT level and thermal stratification behaviour. The PSIS consisted of a Core Make-up Tank, which had connections to downcomer through an injection line and to one cold leg through a pressure balancing line.

The experiment series also investigated the CMT behaviour in a situation where the CMT is initially full of hot water. This may happen in the AP600 plant if the injection line check valve leaks. The programme also included an experiment without flow distributor (sparger) in the CMT.

2.2.3. The fifth series of passive safety injection experiments (GDE-41 through GDE-45)

The last series of the EC funded project included additional five SBLOCA experiments. VTT Energy and LTKK ran the experiments in August and September 1997. Based on the experiences from the previous series, the new experiments were performed in the third and final series of the EC funded programme.

In this series the CMT position was moved to a 1 m higher elevation than in previous experiments. The purpose was to increase the driving head of the passive safety system. The result was about 10% higher flow rate during the recirculation phase of the system. Also, a very small break size was used to investigate if the driving force could disappear due to filling of the CMT with warm water. As a result, the experiment showed this phenomenon.

3. WWER-640 EXPERIMENTS

Studying the removal of the residual heat of the reactor in a final stage of an accident with loss of coolant is very important for proving that a nuclear power plant is safe. In this stage of the accident with WWER-640 reactor, the tanks of the emergency core cooling system are empty and the emergency pool is filled with water. At this time of emergency cooling of the reactor, a rather complex heat transfer mechanism based on natural circulation of the coolant is realized. Key elements and systems of the reactor installation are involved in this process. The natural circulation circuit is a system of three vessels with a free liquid surface. These vessels are the reactor, the fuel pool, and the emergency pool. Several pipes connect them to each other, in accordance with a plan, by which the residual heat of the reactor is to be removed by using the emergency pool. The steam generated in the core during natural circulation of the coolant through the reactor enters the pressurized containment space. In this way, the steam bubbles through the liquid layer in the pools. The heat from the pressurized volume is removed by cooling the outer surface of the metallic protective shell of the containment. This is done by using a system of passive heat removal from the pressurized

shell (SPHR PS), which also utilizes the principle of natural circulation of the corresponding coolant. The condensate formed on the cooled internal surface of the protective shell is returned to the emergency pool. Thus, the necessary amount of water is maintained in the emergency pool. Therefore, during the stage of pool cooling of the reactor, the thermal-hydraulic processes that take place in the reactor, the containment, and the emergency system, are interrelated. So, to substantiate measures taken in the design for ensuring safety of the nuclear power unit, we will have to comprehensively simulate the processes mentioned above.

In order to carry out the proposed experiments connected with the WWER-640 reactor, the PACTEL was reconstructed (Fig. 2). The main parts of the PACTEL have been kept in the experiments; such as the instrumented pressure vessel, the downcomer, the lower plenum, the core, and upper plenum. The remaining components and systems were excluded.
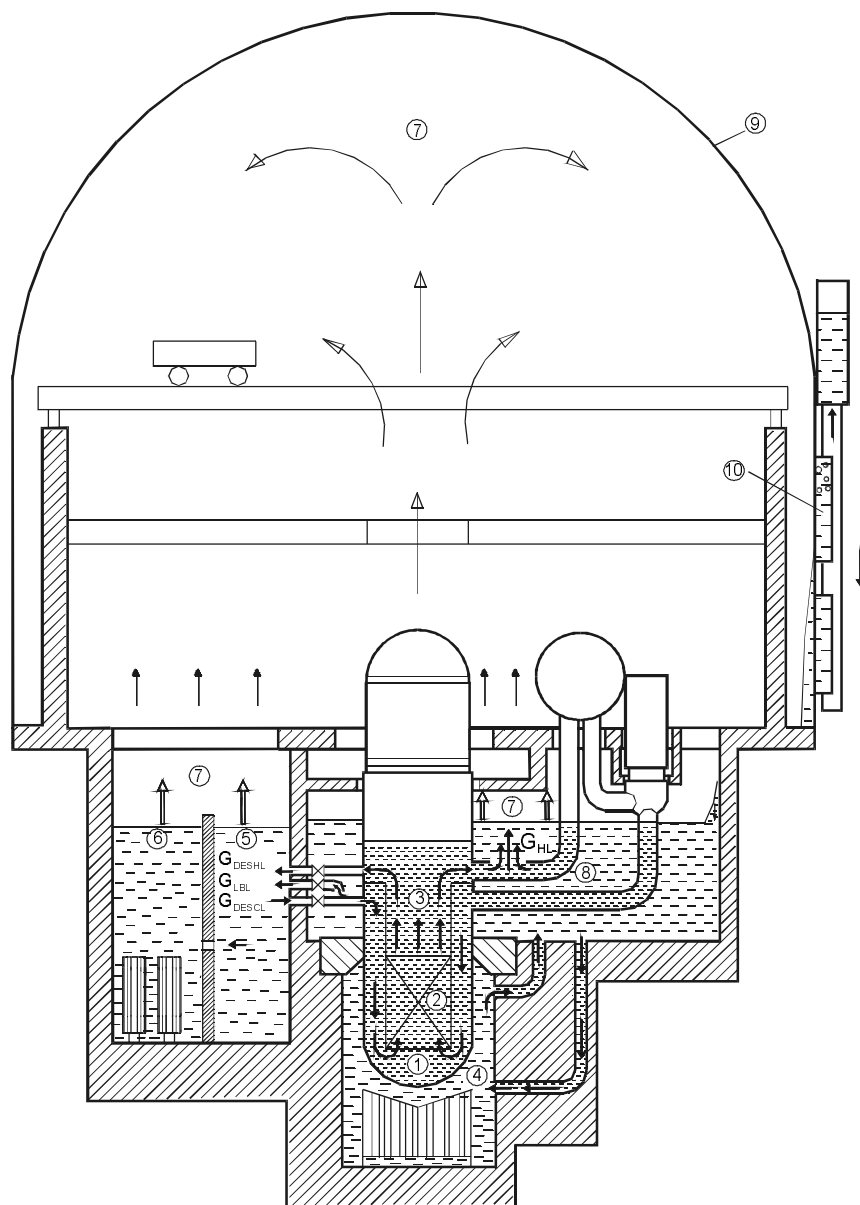
FIG. 1. Safety systems of the reactor WWER-640 1: Lower plenum, 2: Reactor core, 3: Upper plenum 4: Reactor cavity, 5,6: Fuel storage pools, 7: Steam and non-condensable gases, 8: Emergency pool, 9: Containment shroud, 10: Heat removal system.

Two water tanks installed into the PACTEL, simulating the emergency cooling and fuel storage pools. These vessels are open to atmosphere at the top. The larger diameter of the two water tanks models the emergency cooling pool, the smaller one models the fuel storage pool. Geometrical characteristics are presented in the Table I. Each tank has a hydraulic link to the downcomer of the PACTEL with a single horizontal pipe. Similarly, each tank is linked to the upper plenum of the PACTEL with hot-leg connections. The level balancing line (LBL) interconnects the two water tanks (Fig. 3). All of the added pipelines provided with isolation valves to form a circulation loop for each scenario of the performed test series.
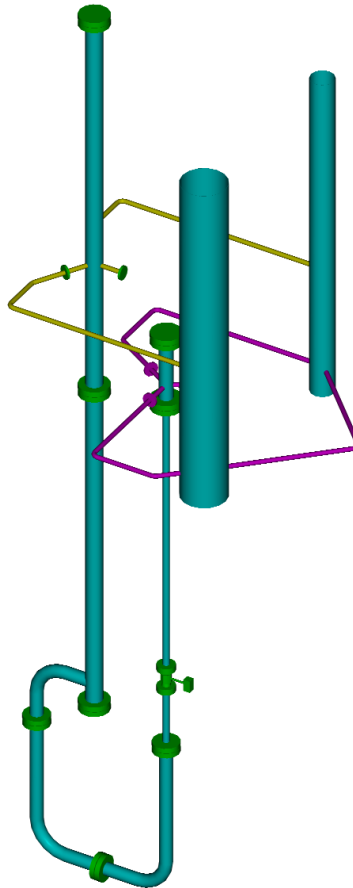
FIG. 2. Modified PACTEL.

3.1. Experimental procedures

Boundary conditions were set as follows: room temperature of 293 K (20°C) in each part of the facility and atmospheric pressure of 1 bar. The level in the pools is at the elevation of 10 m, which is the equivalent of 2.85 m measured from the bottom of the pool. The initial velocity of the fluid is 0 m/s everywhere in the facility. The input heating power was 99 kW in equal radial distribution in the 3 heated channels of the core. Upper plenum was filled with water totally. Table II shows the performed scenarios and status of the isolation valves. The initial condition of the experiments did not fully correspond the condition of the reference reactor in a LOCA situation after the depressurization period. The initial temperature is close to room temperature when density differences, which create the natural circulation, doesn't exist yet.
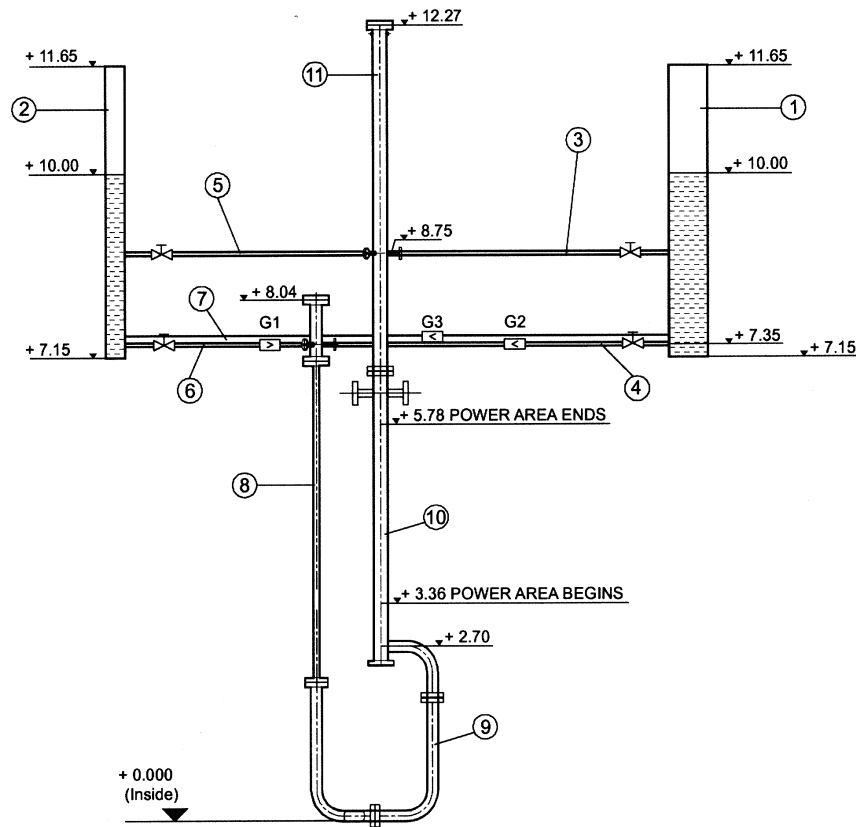
1: Emergency pool, 2: Fuel storage pool, 3: Hot leg, 4: Cold leg, 5: DES hot leg, 6: DES cold leg, 7: Level balancing line, 8: Downcomer, 9: Lower Plenum, 10:Core

FIG. 3. Layout of the PACTEL facility.

TABLE I. THE GEOMETRICAL CHARACTERISTICS OF THE MODIFIED PACTEL FACILITY

Component	D, mm	Wall width, mm	Length, mm
Level Balancing Line	54.3	3.0	3.2
DES Hot Leg	54.3	3.0	3.8
DES Cold Leg	54.3	3.0	3.8
Hot Leg	54.3	3.0	3.7
Cold Leg	54.3	3.0	2.7
Fuel Pool	317.9	3.0	4.5
Emergency Pool	600.0	3.0	4.5

3.2 Experiment results

Experiments ran as expected. The main objective of the experiments was to assure that natural circulation begins when core is heated despite of initially non-existent density differences. On the other hand the experiments were planned to prove that natural circulation is efficient enough to remove the heat from core even though vessel level decreases continuously andflow changes into two-phase flow. Experiments 1-4 were clearly for varying the position of the leak and radial distribution of the core power. Test number 5 was known to be difficult to perform already during the planning of the experiments. The purpose of this experiment

was to investigate a situation, when the valves both in depressurizing and in level control system would not open. In this case the coolant flow path is only through the leakage. The objective was to find out a certain power level, which can generate a steam flow large enough to prevent the coolant flow back to the reactor vessel through a horizontal pipeline. The power control system in PACTEL is designed to operate up to 1 MW power level, so the power below 50 kW was expected to give difficulties. Table III describes the power variation used in the experiment.

TABLE II. VALVE STATUS (+ OPEN, – CLOSED) AND POWER DISTRIBUTION

Test	Scenario	Valve status					Radial power profile in the core, (channels A,B,C), [kW]		
		DES hot leg	DES cold leg	Broken hot leg	broken cold leg	level balancing line	N_A	N_B	N_C
1	break in hot leg	+	+	+	–	+	31.4	31.4	31.4
2	break in hot leg	+	+	+	–	+	0	50	50
3 *)	break in cold leg	+	+	–	+	+	31.3	31.3	31.3
4 *)	break in cold leg	+	+	–	+	+	0	48.7	48.7
5	break in hot leg, failure of all DES valves	–	–	+	–	–	See Table 5		

*) Note: Due to position of the void measurement device, the roles of the pools were switched vice versa.

TABLE III. TIME VARIATION OF POWER IN EXPERIMENT 5

Time [s]	Total Power [kW]	Radial distribution in channels A, B and C [%]
0	0	0
600	28	6+6+6
8100	75	8+8+8
8250	28	6+6+6
8400	0	0
8460	28	6+6+6
8830	37	6+6+7
8940	46	7+6+7
9060	55	7+7+7
9250	28	6+6+6
9600	0	0
9660	28	6+6+6
10500	18.8	6+6+0
10800	9.4	6+0+0
12675	0	0
12700	9.4	6+0+0
13088	18.8	6+6+0
13605	0	0

4. SCRAM-SYSTEM EXPERIMENTS

The facility for SCRAM-system experiments consists of a scram tank, a blowdown tank, electric heaters, piping, valves and measurement instrumentation [9]. The main interest focused on the scram tank. Electric heaters located below the water level generate and maintain the steam volume and a layer of saturated water in the tank. After the scram signal the energy of the steam volume is used to move the control rods into the core. In the experiments orifices simulated the response of the control rods. High design pressure leading to a high steam temperature and high temperature differences in the facility during the system operation challenges the integrity of the whole scram system.

5. CONCLUSIONS

Lappeenranta University of Technology in co-operation with VTT Energy has carried out several experiments to investigate advanced light water reactor safety systems. The experiments studied passive safety injection system with PACTEL facility, long-term cooling of the WWER-640 reactor concept also with PACTEL and new SCRAM system of the SWR-1000 reactor concept with separate test facility. Experiments have been successful and given useful information of different safety systems proposed for innovative reactor designs. Experiments have also proved that PACTEL integral test facility is flexible to use and to modify for various possible applications.

REFERENCES

[1]   TUUNANEN, J., et al., General description of the PACTEL facility. VTT Research Notes 1929. Espoo, Finland, 1998.

[2]   MUNTHER, R., VIHAVAINEN, J., KOUHIA. 1995. Analyses of PACTEL Passive Safety Injection Tests with RELAP5 Code. IAEA Technical Committee Meeting" Progress in Design, Research & Development and Testing of Safety Systems for ALWRs". Piacenza, Italy, May 16-19, 1995.

[3]   MUNTHER, R., VIHAVAINEN, J., KOUHIA. 1995. Simulation of PACTEL Gravity Driven Core Cooling Tests with APROS(2.11) and RELAP5 MOD3.1 Codes. Proceedings of the ANS International Topical Meeting of Safety of Operating Reactors, September 17-20, 1995, Seattle, USA.

[4]   TUUNANEN, J., MUNTHER, R., VIHAVAINEN, J. 1996. PACTEL Experiments for Investigation of Passive Safety Injection Systems of Advanced Light Water Reactors. The 4th International Conference on Nuclear Engineering (ICONE-4). New Orleans, Louisiana, USA, March 10-14, 1996.

[5]   MUNTHER, R., VIHAVAINEN, J., KALLI, H., KOUHIA, J., RIIKONEN, V. RELAP5 Analysis of Gravity Driven Core Cooling Experiments with PACTEL Nuclear Technology. September 1997.

[6]   TUUNANEN, J., VIHAVAINEN, J., D'AURIA, F., KIMBER, G., Assesment of Passive Safety Injection Systems of ALWRs, Final Report of the European Commission 4th Framework Programme Project FI4I-CT95-0004 (APSI), VTT Research Notes No: 1957, Espoo 1999.

[7]   TUUNANEN, J., RIIKONEN, V., KOUHIA, J. AND VIHAVAINEN, J., Analyses of PACTEL passive safety injection experiments GDE-21 through GDE-25, Nuclear Engineering and Design, Volume 180, Issue 1, 1 March 1998, pages 67-91. ISSN 00295493.

[8]   ALEXEEV. A., BÁNÁTI, J., VIRTANEN, E., RELAP5 and CATHARE Analyses of the PACTEL Experiments on the Long Term Cooling of the WWER-640 Power Plant after a Large Break LOCA. International Youth Nuclear Congress, Bratislava, Slovakia, April 9-14, 2000.

[9]   TOLONEN, P., SCRAM Experiments: Experimental Simulation of the Hydraulic Scram System in SWR-1000, VTT Research Report ENE4/47/99, 1999 (confidential).

PACTEL passive safety injection experiments and APROS code analysis

J. Vihavainen
Lappeenranta University of Technology

J. Tuunanen
VTT Energy

Finland

Abstract. VTT Energy in Finland and Lappeenranta University of Technology (LTKK) have run several experiments with the PACTEL (Parallel Channel Test Loop) facility to investigate the performance of Passive Safety Injection System (PSIS) of Advanced Light Water Reactors (ALWRs) in Small Break Loss-Of-Coolant Accident (SBLOCA) conditions. PACTEL is full-height medium scale (1:305) integral test facility originally designed to simulate thermal-hydraulic phenomena of the Finnish Loviisa PWR of VVER-440 type. The passive safety injection experiments in Lappeenranta started already in 1992 with a series of five experiments. These experiments simulated hot leg SBLOCA's. The PSIS included a Core Make-up Tank (CMT), two pressure balancing lines (PBL) and an injection line (IL). The second series included similar PSIS as in the first series. The European Commission 4th Framework Programme project *"Assessment of Passive Safety Injection Systems of Advanced Light Water Reactors Reactors"* involved experiments on the PACTEL test facility and computer simulations of selected experiments. The project involved 15 experiments in three series. The experiments provided information about condensation and heat transfer processes in the CMT, thermal stratification of water in the CMT, and natural circulation flow through the PSIS lines. The EC project included validation of three thermal-hydraulic computer codes. The APROS analyses were performed at LTKK. The analyses showed that the codes are capable of simulating the overall behaviour of the transients. The codes predicted accurately the core heat-up, which occurred when the primary coolant inventory was reduced so much that the core top became free of water. The detailed analyses of the calculation results showed that some models in the codes still needed improvement. Especially, further development of models for thermal stratification, condensation and natural circulation flow with small driving forces would be necessary for accurate simulation of the phenomena in the PSIS. The modelling of thermal stratification has already been improved and also tested with the APROS code. The new calculation results have showed significantly better behaviour in PSIS operation.

1. INTRODUCTION

PACTEL (Parallel Channel Test Loop) [1, 2] is a full height, medium-scale integral test facility (volumetrically scaled 1:305) designed to simulate the thermal-hydraulic phenomena characteristic of the Finnish Loviisa PWR. VTT Energy together with the Lappeenranta University of Technology run the facility. PACTEL has three primary coolant loops with pressurizer, primary coolant pumps and horizontal steam generators, high-pressure emergency core cooling system (ECCS), and low pressure ECCS with two accumulators. The peak operating pressures in the primary and secondary sides are 8 MPa and 4.6 MPa, respectively. The reactor vessel is simulated with a U-tube construction consisting of separate downcomer and core sections. The core comprises of 144 full length, electrically heated fuel rod simulators with a heated length of 2.42 meters. The maximum total core output is 1 MW, or 22% of scaled full power. The three coolant loops with double capacity steam generators model the six loops of the reference power plant. Each steam generator has 118 U-tubes with an average length of 2.8 m.

The passive safety injection experiments in Lappeenranta started already in 1992 with a series of five experiments. These experiments simulated hot leg SBLOCA's. The PSIS included a

CMT and two PBL's. The second series included four cold leg SBLOCA experiments in 1993. These experiments used similar PSIS as in the first series. In 1996, a new project of passive safety injection experiments with a CMT and one PBL started. The new experiments are a part of the European Commission 4th Framework Programme Nuclear Fission Safety program. Within this new project, two series of five experiments have been completed so far, and the third series is scheduled on September 1997. The project continues until September 1998. See Fig. 1 for a general view of PACTEL and Fig. 2 in the passive safety injection system in the fourth experiment series.
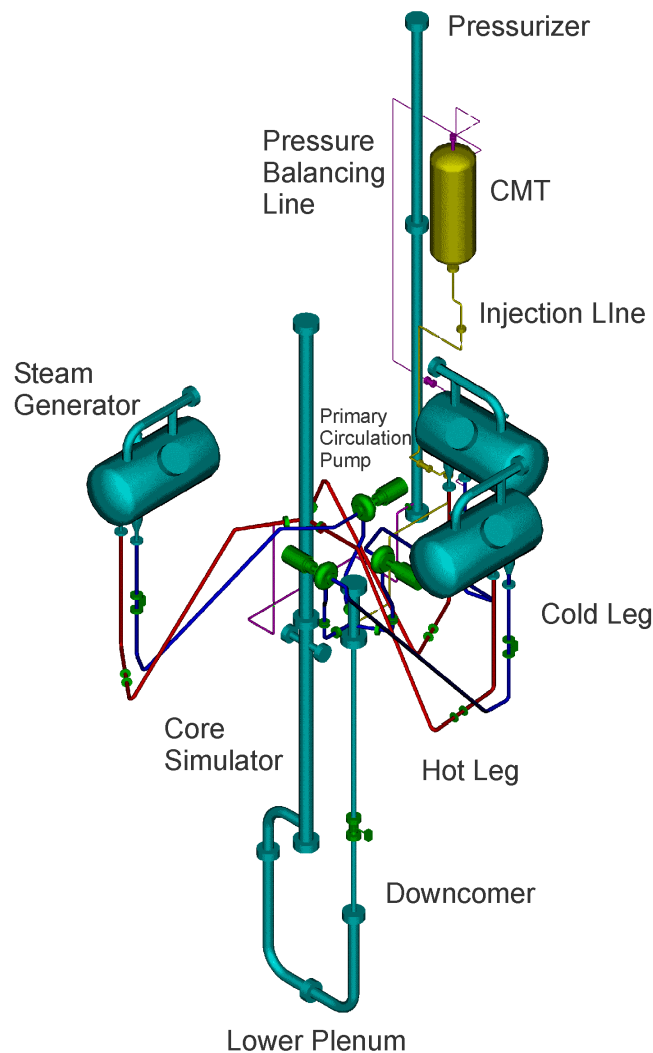
FIG. 1. General view of PACTEL.

2. EXPERIMENTS WITH CMT AND TWO PBL'S

The main objective of the tests was the overall simulation of the PSIS behaviour. The experiments demonstrated the capability of PACTEL for the simulation of PSIS's. The data did not provide very detailed information about phenomena in the CMT. The instrumentation of the CMT in the first test series was limited. The tests were partially aimed for investigation of possibilities to run passive safety injection tests on PACTEL. The experience gathered during this first series was then used in the specification of the test parameters and instrumentation of the second series.
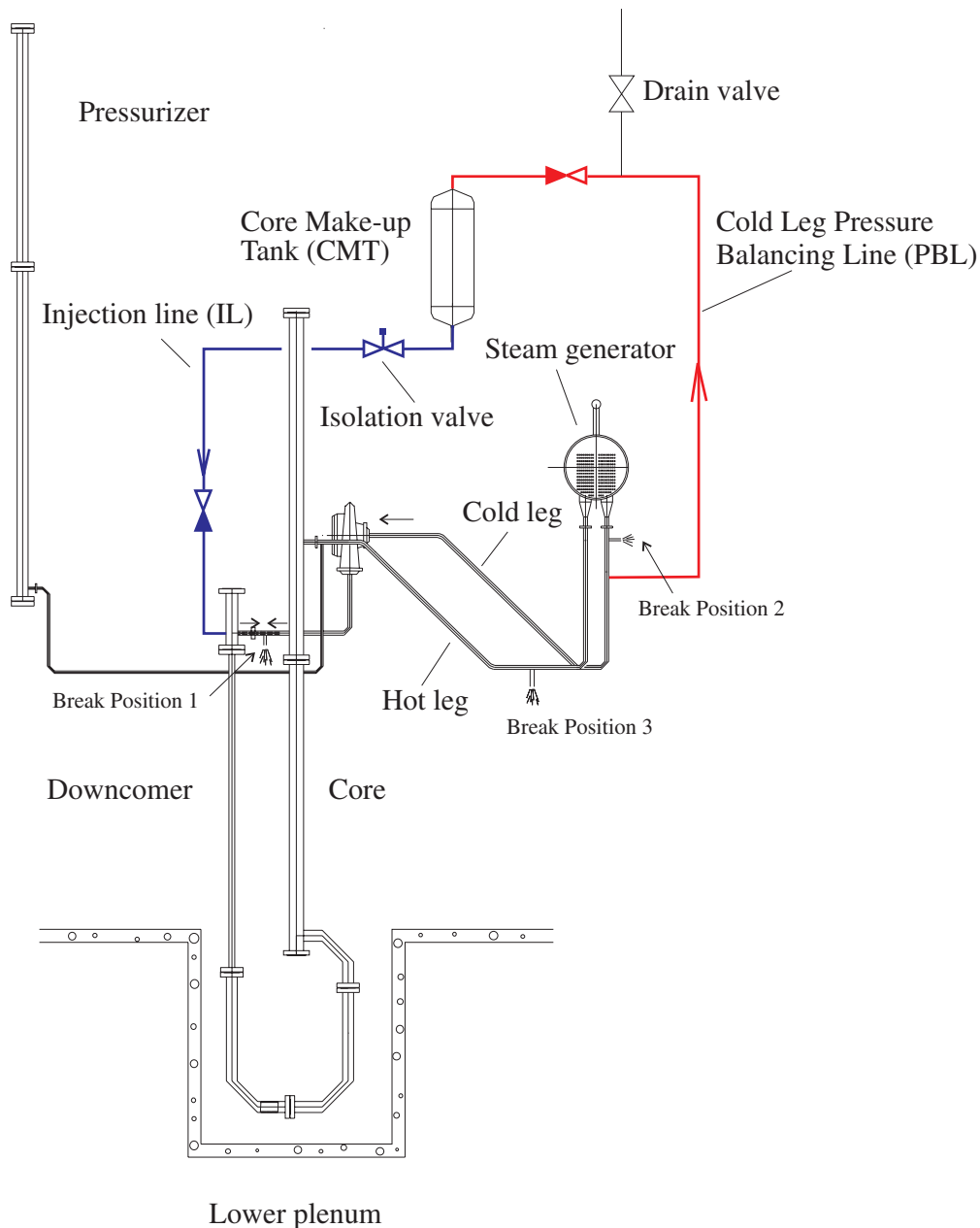
FIG. 2. General view of the PACTEL experiment facility and the passive safety injection system in the fourth experiment series.

2.1. The First Series of Passive Safety Injection Experiments (GDE-01 through GDE-05)

The first experiment series included five Small Break LOCA tests with break in one hot leg of PACTEL. Three break sizes (2, 4 and 6 mm or 0.5, 2 and 4.4%, respectively) were used. Three tests included secondary system depressurization as an accident management measure. The operators of the loop also depressurized the secondary system by opening a steam generator relief valve. The core power in the tests was 80 kW corresponding to 1.8% of the scaled thermal power of the reference reactor. In all tests, only PSIS provided ECC water to the core. The initial temperature of the water in the CMT was 40°C. The primary pressure used in the tests was lower than the nominal operation pressure of PACTEL. Maximum operation pressure of the passive accumulators determined the upper limit of the experiment pressure (3.8 MPa).

Munther [4] and Munther et al. [5, 6, 7] have published the results of these experiments. The main results of the first test series can be summarised as the following:

- three flow modes of CMT operations were present in the experiments: recirculation mode with water circulating through the PSIS lines, oscillating phase with two-phase flow in to the tank and injection phase with flow of steam in to the CMT.
- the ECC water injection stopped totally several times during injection, due to rapid vapour condensation in the CMT.
- flow reversed in the broken cold leg leading to flow of cold water from the downcomer towards the break
-

Although some problems with condensation in the CMT occurred no core heat-up was detected. It should be mentioned here that the CMT used in the test was very large, about twice as large as the scaled volume of four accumulators of the reference plant. On the other hand, the volume of the CMT is about the same as the volume of the rest of the loop. All the tests in this first series were terminated before the CMT was totally empty.

2.2. The Second Series of Passive Safety Injection Experiments (GDE-11 through GDE-14)

The second experiment series included four SBLOCA tests with break in one cold leg of PACTEL. Two break sizes (2 and 4 mm or 0.5 and 2%, respectively) were used. The tests also included studies of primary system depressurization and reproducibility of the phenomena (one test was repeated twice with the same initial and boundary conditions). The PACTEL operators depressurized the primary system by opening a pressurizer relief valve. The core power in the tests was 80 kW corresponding to about 1.8% of the scaled thermal power of the reference reactor. In all tests, only the CMT provided ECC water to the primary loop.

The primary pressure used in the tests was again lower than the nominal operation pressure of PACTEL. The maximum operation pressure of the passive accumulator limited the maximum experiment pressure to 3.8 MPa. The experiment loop geometry in the second series have been described in reference [3]. Munther [4] and Munther et al. [7, 8, 9] have published the results of these experiments. Since one loop of PACTEL was equipped with a different steam generator model the tests run with only two loops in operation. The main results of the second test series can be summarised as the following:

- only a limited period of single phase natural circulation through the cold leg pressure balancing line to the CMT was observed,
- the CMT level started to drop immediately after the opening of the break,
- the saturated water layer formed to the CMT remained thin,
- the ECC water injection was stopped totally during injection, due to rapid vapour condensation in the CMT,
- two types of mixing in the CMT during condensation was observed: complete mixing or only the mixing of the uppermost water layer in the tank.

There was still water in the CMT when the tests were terminated after about 2000 seconds from the opening of the break. During the rapid condensation period water level in the core simulator dropped close to the top of the core. However, also in these test no core heat-up occurred.

3. EXPERIMENTS WITH CMT AND ONE PBL

In 1996, a new project for the investigation of passive safety injection systems of ALWR's begun. The project, entitled "Investigation of Passive Safety Injection Systems of Advanced Light Water Reactors", was a part of the INNO cluster of the European Commission Nuclear Fission Safety (NFS-2) Programme. The project received funding from the European Commission. The project had four partners: VTT Energy and Lappeenranta University of Technology from Finland, AEA Technology from the UK and the University of Pisa from Italy. VTT and LTKK were responsible for the experiments in PACTEL and for the APROS simulations of selected experiments. AEA Technology and University of Pisa were responsible for simulation of selected experiments with RELAP5 and CATHARE codes. The general objectives of the new project were:

- to provide new and independent information about passive safety injection system performance,
- to contribute to a public data base for the users and developers of thermal-hydraulic computer codes on the phenomenological behaviour of PSIS's in LOCA conditions, and
- to identify the accuracy, uncertainties and limitations of thermal-hydraulic computer codes in the modelling of passive safety injection system behaviour.

The next sections summarise the main results of the three series (called here the third, fourth and fifth Passive Safety Injection experiment series) of the EC funded programme.

3.1. the third series of passive safety injection experiments (GDE-21 through GDE-25)

The main problem in the first two test series in PACTEL was the rapid condensation in the CMT, which temporarily stopped the ECC water injection. The condensation took place when the saturated water layer in the CMT broke down, and the steam got into contact with cold ECC water. This happened when water flowed to the CMT after the level in the tank has already dropped. In the tests the water level in the CMT started to drop almost immediately after the opening of the break and the period of single phase natural circulation through the cold leg pressure balancing line to the CMT was very short. Due to this the saturated water layer in the CMT separating cold water from steam remained thin. For the third series, a flow distributor called sparger has been added to the CMT. The purpose of the sparger is to diminish possibilities of rapid condensation in the CMT. Further, the experiment procedure included filling of the PBL with hot water before the break opening. The CMT and the IL was full of cold water. All the earlier experiments begun with cold water in the CMT, PBL and IL. The main objective of the third series was to investigate the influences of break size and the removal of the pressurizer PBL on the CMT behaviour in cold leg SBLOCA's. The tests run with four different break sizes (from 1 to 5 mm) including reproducibility studies. Like in the earlier tests the main objective of the tests was to simulate the PSIS behaviour and not to try to simulate any proposed ALWR reactor concept in particular.

The main results of the third series can be summarised as the following:

- the recirculation phase was much longer than in the earlier experiments with two PBL's and without PBL heating,
- the recirculation phase was longer; and the resulting hot liquid layer, thicker in the experiments with smaller break size;

- the analyses of the test data supported using the McAdams correlation for calculating the heat transfer from the hot liquid layer to the CMT wall, as the Westinghouse suggested [11]. The use of the Nusselt film condensation correlation for the condensation in the CMT walls seems correct, although the correlation gave high values for the heat transfer coefficient;
- the oscillation phase between the injection and recirculation phases was longer in the experiments with small break size; and
- local wall heat flux to the CMT wall was higher in the experiments with larger break size.

In all experiments the CMT ran as planned. There were no problems with rapid condensation in the CMT, such as was seen in the earlier passive safety injection experiments in PACTEL. The main reason was the new CMT arrangement, with a flow distributor (sparger) installed to the CMT. The sparger spread incoming flow to the CMT horizontally, and the breakdown of the saturated water layer due to incoming water was not possible. The hot liquid layer between the steam and cold water in the CMT remained stable, even in the experiments where the hot liquid layer was less than 5 cm thick.

3.2. The fourth series of passive safety injection experiments (GDE-31 through GDE-35)

The second series of the EC funded project included five experiments for the investigation of the break location and CMT scaling (smaller CMT) on the PSIS behaviour. PACTEL operators made small changes to the CMT instrumentation to better detect CMT level and thermal stratification behaviour. The PSIS consisted of a Core Make-up Tank, which had connections to downcomer through an injection line and to one cold leg through a pressure balancing line. The break location and CMT scaling influences can be summarised as follows:

- Flow of cold water from downcomer to cold leg of the broken loop occurred in both hot and cold leg break experiments. The cold water did not, however, flow to the CMT through the PBL. So, no condensation problems occurred in the CMT due to flow of cold water to the tank.
- The saturated liquid layer in the CMT was very thin in the experiment where the break located in the cold leg close to downcomer. In the hot leg and cold leg inlet part break experiments, the saturated liquid layer was thick, due to flow of water to the tank during the injection phase. In all experiments, the thickness of thermally stratified region in the CMT increased during the experiments.
- The overall primary loop behaviour was similar in experiments with small and large CMT. As expected, the availability of larger amount of ECC water in the experiment with large CMT delayed the core heat-up.

The experiment series also investigated the CMT behaviour in a situation where the CMT is initially full of hot water. This may happen in the AP600 plant if the injection line check valve leaks. The programme also included an experiment without flow distributor (sparger) in the CMT. The results of these two experiments can be summarised as follows:

- Practically no recirculation flow occurred in the experiment where the CMT was initially full of hot water. The recirculation flow did not begun although there was a small initial density difference between the PSIS lines. This did not, however, cause any problems for the safety injection from the CMT.

- The fact that the CMT was full of cold water influenced the water distribution in the primary loop during the transient. This had affects on the water level formation in the vessel and the timing of the core heat-up.
- The experiment without sparger demonstrated the importance of the flow distributor on the CMT behaviour: the removal of the sparger led to rapid condensation in the CMT, which stopped safety injection from the tank. The PACTEL operators had to terminate the experiment due to condensation problems in the CMT.
- Condensation problems occurred in GDE-35 experiment when water flowing to the CMT broke saturated water layer in the CMT. This did not happen in the experiments with sparger, which distributed the incoming water horizontally into the tank.

3.3. Fifth series of passive safety injection experiments (GDE-41 through GDE-45)

The last series of the EC funded project included additional five SBLOCA experiments. VTT Energy and LTKK ran the experiments in August and September, 1997. Based on the experiences from the previous series, the following new experiments were performed in the third and final series of the EC funded programme:

GDE-41 3,5mm cold leg break close to DC, CMT position; increased driving force for CMT flow

GDE-42 3,5 cold leg break close to DC, additional IL flow orifice

GDE-43 1 mm cold leg break close to DC, long recirculation phase; disappearance of driving force for injection

GDE-44 3,5 mm cold leg break close to DC, cold CMT; PBL heating

GDE-45 3,5 mm cold leg break close to DC, PBL connected to pressurizer (Korean design of PSIS)

The objective of the GDE-43 experiment was to investigate the PSIS behaviour in a situation, when the break size is small and, consequently, CMT recirculation phase is long. If the CMT recirculation phase is long, the whole PSIS may become full of hot water before the CMT begins to inject water, and the driving force for injection disappears. This may have effects on the beginning of safety injection from the CMT. In the GDE-43 experiment, the break was located in the Loop 2 cold leg close to the downcomer, in the similar manner as in the GDE-24 and GDE-34 experiments. The break size was 1.0 mm in diameter, which is clearly smaller than in the two other simulation cases.

In the GDE-45 experiment the PBL connected the top of the pressurizer to the top of the CMT. The CMT sparger design effectively reduced condensation in the tank and no severe condensation occurred in the experiment. The CMT injection flow stagnated once, however, when the water flowing from the pressurizer disturbed the hot liquid layer in the CMT, steam condensed in the tank and CMT pressure dropped slightly. The CMT injection flow rate was oscillating. This was an outcome of the specific loop geometry of PACTEL. PACTEL has loop seals in both hot and cold legs of the primary circuit. The water accumulation to the pressurizer and the PSIS injection line resulted in an earlier core heat-up than in the similar experiments with PBL connection to the cold leg.

4. COMPUTER SIMULATIONS OF PASSIVE SAFETY INJECTION EXPERIMENTS

4.1. APROS analyses of the GDE-11 experiment

The PACTEL experiment GDE-11 was calculated with APROS 2.11 codes. This experiment contained a rapid condensation and long lasting mixing period in the CMT. A steep thermally stratified layer was already formed before the break opening. All simulations used previously created and tested models for PACTEL, which were modified according to the needs of the PSIS. The results of the calculations have been presented in references [6, 12, 13, 14, 15, 16].

The APROS calculation used 5-equation model. The drift flux model was used to describe the velocity difference between phases. The CMT was modelled with five equal sized nodes. Sensitivity analyses with different number of nodes was not performed. With five nodes, it was not possible to model exactly the thermal stratification in the CMT. In the base case calculation, the top node liquid temperature was initiated to 140°C, which corresponds to the average temperature of the upper part of the CMT.

- CMT level did not drain until the top node liquid temperature had reached saturation. Draining stagnated to the level of the node boundary and continued after the liquid in the node next below was in saturation. During the stagnation the injection flow decreased dramatically and started to oscillate.
- This stepwise draining mode was observed also with the initial temperature of 50°C in the CMT top node.
- The CMT behaviour dominated the primary system behaviour.

4.2. APROS analyses of the GDE-24, GDE-34 and GDE-43 experiments

The PACTEL GDE-24 experiment was calculated with APROS 4.02 code [18], [19], [20], [21]. The models of the CMT, PBL and IL were included to the APROS model of PACTEL created for SBLOCA calculations. The CMT was modelled with a standard pipe module of APROS divided in 30 equal length nodes.
- APROS calculated successfully the recirculation phase.
- Due to numeric diffusion the temperature profile was not as steep as in the experiment.
- Problems occurred during the draining mode. Injection flow started to oscillate continuously never reaching the anticipated full magnitude. The vapour entering to the top node condensed directly to the subcooled water and caused a flow stagnation due to rapid pressure drop. The injection was possible only after the water had reached saturation temperature in the boundary node. Hence, the explanation for these flow oscillations was lack of continuous existence of saturated liquid layer, which would prevent direct contact of vapour and cold water.
- Oscillating characteristics caused delay to the timing of main events.
- Important parameters were maximum time step, amount of nodes and hydraulic diameter in the CMT. To reduce the condensation it was possible to manipulate the condensation heat transfer coefficient by giving higher values to the hydraulic diameter in the CMT nodes. To get more accurate calculation results, it was necessary to use dense CMT nodalization (30 nodes) and small maximum time step (0.025 s) during the first 1000 s transient period.

For the calculation of the GDE-34 experiment a smaller CMT model with 30 nodes was created and the CMT water was initiated with warm water. Some minor modifications for the PBL pipework were also made.

- The recirculation mode existed in the calculation though it was not observed in the experiment. Hence, the density difference between PBL and CMT was enough to initiate the flow in the calculation.
- Injection flow oscillated, but with smaller amplitude than in GDE-24, because of less condensation. The average injection flow rate was quite near to the measured one. Also, flow injection stagnated once due to temporary water level increase in the vertical section of cold leg 2, which is connected to the PBL.
- The increase of hydraulic diameter reduced condensation also in this case.
- The calculation was not very sensitive to any other parameters.
- Timing of the main events agreed well with the experiment.

For the calculation of the GDE-43 experiment a smaller CMT model with 30 nodes was also used.

The calculations were performed with APROS version 4.06.

The first pressure peak occurred too early in the APROS calculation and one additional pressure peak was observed after the pressure had already started to drop in the experiment. The code simulated the general trend of the downcomer flow behaviour well until the PSIS stagnated. During the PSIS stagnation period, between 10000 and 12000 seconds, the downcomer flow decreased and stopped completely in the experiment. This did not happen in the APROS simulation. The CMT started to empty too early in the APROS calculations. This happened since too much water flowed into the pressuriser and the steam begun to flow to the cold legs too early. The recirculation flow through the PSIS decreased as the hot water filled the CMT in the APROS calculation, but the flow did not stop completely. The calculated recirculation flow at the end of the recirculation phase was about about 75% of the initial value in the APROS calculation.
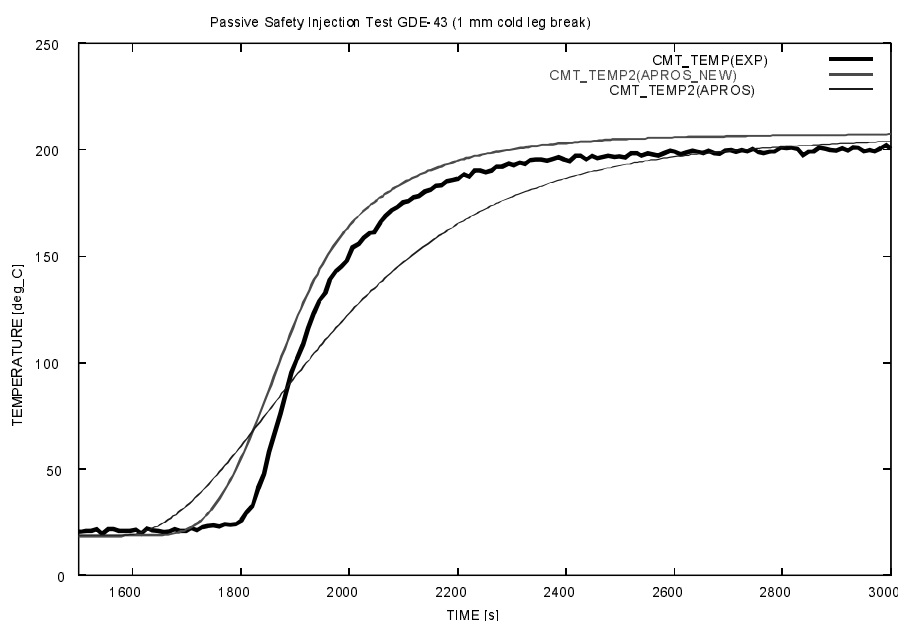
FIG. 3. Water temperature in the CMT. Experiment GDE-43 vs. APROS calculations.

The effects of numerical diffusion were clear in the APROS calculation of CMT water temperature (Fig. 3). The calculated temperature rise was smoother than in experiment. Too much water accumulated in the pressuriser in the all calculations during the primary flow stagnation periods, indicating problems in modelling pressuriser heat losses. At the end of the transient, too much water accumulated in the pressuriser in the APROS simulation. The accumulation of water in the pressuriser partly explains the fact that the PSIS flow stagnation did not occur in the APROS calculation. The core water level dropped too fast in the APROS simulation in the early phase of the transient and the codes did not predict the core water level lowering during the PSIS flow stagnation

4.3. APROS calculation with the new thermal stratification solution model

Due to obvious deficiencies in the calculations with previous APROS versions a new solution model for the thermal stratification of APROS code was developed [23]. The old method used upwind solution for the enthalpy. Due to numeric diffusion the code lost information about the stratified layer. The new higher order numeric method uses information from three consecutive nodes to solve the transported liquid enthalpy. The new enthalpy solution contains a special weight function, which is calculated from liquid enthalpies of the three nodes. The experiments GDE-41 and GDE-43 were recalculated with the new model (Fig. 4). The model was also tested separately with a standalone PSIS [24]. The calculation results were good. The new model eliminated significantly the numerical diffusion and restricted the spreading of the thermal front.
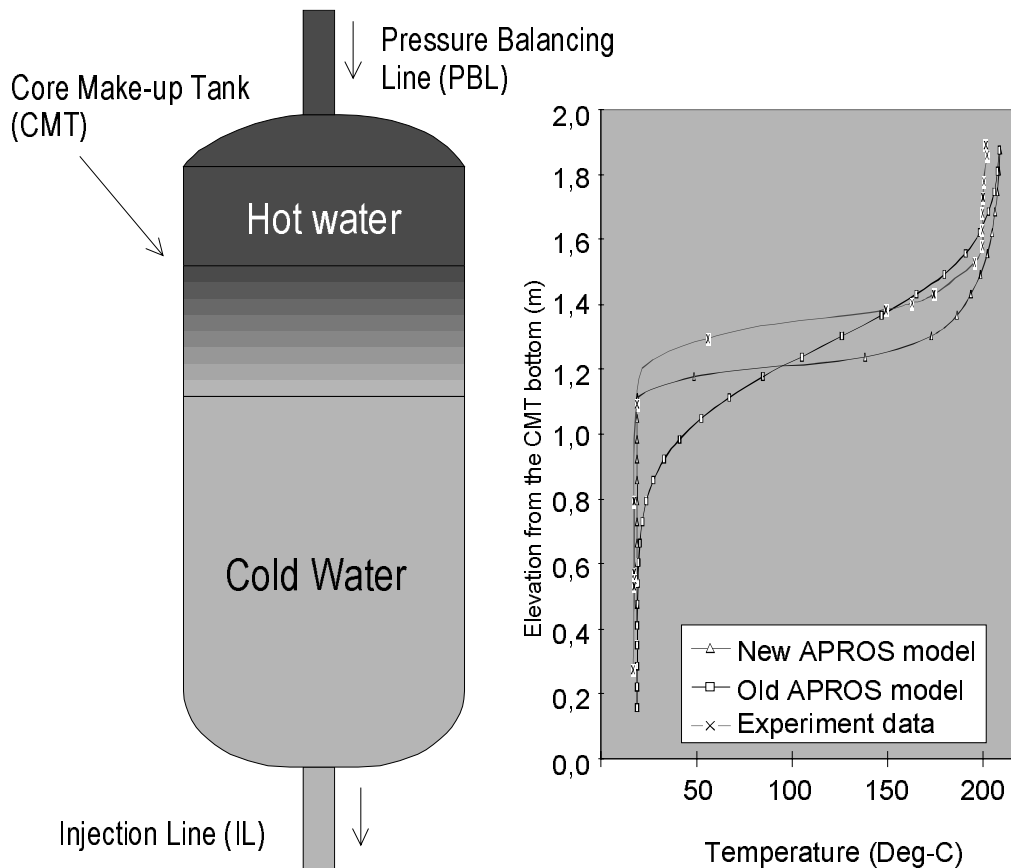
FIG. 4. Temperature distribution in the GDE-43 experiment vs. APROS calculation with the old and new models at time 4000 s.

5. CONCLUSIONS

Lappeenranta University of Technology in co-operation with VTT Energy has performed totally 24 experiments to investigate Passive Safety Injection system with PACTEL facility during past eight years. The experiments in PACTEL have provided valuable information about PSIS behaviour in SBLOCA's. The PSIS system worked as planned when the CMT was equipped with flow distributor (sparger). The main source of disturbances was condensation, which took place when stem met cold water. The experiment data has been and will be used to further develop Finnish thermal hydraulic analyses code APROS. The computer simulations have reproduced the measured transient behavior with good accuracy despite of smoothing of the thermal front generated by numerical diffusion. The code has been improved by developing a new solution model for the thermal stratification, which largely eliminated the effect of numerical diffusion.

REFERENCES

[1]   T. KERVINEN, V. RIIKONEN, J. KOUHIA, "PACTEL, Facility for Small and Medium Break LOCA Experiments," Proceedings of ENC'90 Conference. European Nuclear Society, Lyon, France, September 23-28, 1990

[2]   PURHONEN, H., MIETTINEN, J. 1992. PACTEL - Parallel Channel Test Loop, General Description for ISP. Proceedings of the ISP 33 First Workshop. Lappeenranta, Finland, 18-19 February, 1992.

[3]   TUUNANEN, J., KOUHIA, J., 1995. Modifications of the PACTEL Test Facility for the Gravity Driven Emergency Cooling Tests. Technical Report. TEKOJA 11/95. VTT Energy. September. 1995.

[4]   MUNTHER, R., 1994. Passive Safety Systems of the Future Nuclear Power Plants. Licentiate Thesis. Lappeenranta University of Technology. 117 pages (In Finnish).

[5]   MUNTHER, R., KALLI, H., KOUHIA, J., KERVINEN, T. 1993. Passive Core Cooling Experiments with PACTEL Facility. Proc. of the ENS TOPNUX'93 - Towards the next Generation of the Light Water Reactors -meeting. Hague, Netherlands, April 25-28, 1993.

[6]   MUNTHER, R., VIHAVAINEN, J., KALLI, H., KOUHIA, J., RIIKONEN, V. 1994. RELAP5 Analyses of the Gravity Driven Core Cooling Experiments with PACTEL. Proc. of the ANS ARS'94 - International Topical Meeting on the Advanced Reactor Safety, Pittsburgh, USA, April 17-21, 1994.

[7]   MUNTHER, R., KALLI, H., KOUHIA, 1994. Gravity Driven Core Cooling Experiments with PACTEL. IAEA Advisory Group Meeting on "Technical Feasibility and Reliability of Passive Safety Systems", Julich, Germany, November 21-24, 1994.

[8]   TUUNANEN, J., Experimental Program on PACTEL for the Investigation of Passive Safety Injection Systems of ALWRs. Jahrestagung Kerntechnik '96. Mannheim, Rosengarten, 21.-23. Mai 1996.

[9]   MUNTHER, R., KALLI, H., KOUHIA. 1995. Condensation During Gravity Driven ECC. Proc. of the NURETH-7, 7th Int. Meeting on Nuclear Reactor Thermal Hydraulics, Saratoga Springs, USA, September 10-15, 1995.

[10]   J. MARTIN BERMEJO, G. VAN GOETHEM. 1997. EC-Sponsored Research Activities on Innovative Passive Safety Systems. Post-SMiRT 14 Seminar on "Passive Safety Features in Nuclear Installations", August 25-27th 1997, Pisa University, Italy.

[11]   J P CUNNINGHAM et al. Analysis of the AP600 Core Makeup Tank Tests. Westinghouse Electric Corporation. Paper presented in the 4th International Conference on Nuclear Engineering (ICONE-4). New Orleans, Louisiana, USA, March 10-14, 1996.

[12] MUNTHER, R., VIHAVAINEN, J., KOUHIA. 1995. Analyses of PACTEL Passive Safety Injection Tests with RELAP5 Code. IAEA Technical Committee Meeting "Progress in Design, Research & Development and Testing of Safety Systems for ALWRs". Piacenza, Italy, May 16-19, 1995.

[13] MUNTHER, R., VIHAVAINEN, J., KOUHIA. 1995. Simulation of PACTEL Gravity Driven Core Cooling Tests with APROS(2.11) and RELAP5[MOD3.1 Codes. Proceedings of the ANS International Topical Meeting of Safety of Operating Reactors, September 17-20, 1995, Seattle, USA.

[14] TUUNANEN, J., MUNTHER, R., VIHAVAINEN, J. 1996. PACTEL Experiments for Investigation of Passive Safety Injection Systems of Advanced Light Water Reactors. The 4th International Conference on Nuclear Engineering (ICONE-4). New Orleans, Louisiana, USA, March 10-14, 1996.

[15] MUNTHER, R., VIHAVAINEN, J., KALLI, H., KOUHIA, J., RIIKONEN, V. RELAP5 Analysis of Gravity Driven Core Cooling Experiments with PACTEL Nuclear Technology. September 1997.

[16] VIHAVAINEN, J., KALLI, H. The Applicability of Current Thermal-hydraulic Computer Codes to Simulate ALWR's. Lappeenranta University of Technology. Research Report EN B-103. ISBN 951-764-068-4. 1996 (in Finnish).

[17] MUNTHER, R., RAUSSI, P., KALLI, H., KERVINEN, T. Modelling of the Fluid Dynamics of Decay Heat Removal Through Water Pools. LTKK Research Report EN B-76. 1992. (In Finnish).

[18] HÄNNINEN, M., et al. APROS Code for the Analyses of Nuclear Power Plant Thermal-hydraulic Transients. Proc. of ANS Winter Meeting, Chicago, Illinois, USA, November 15-20, 1992.

[19] VIHAVAINEN, J. Analyses of Passive Safety Injection System with APROS Code. Proceedings of the 2nd French-Finnish Colloquium on PWR Safety, CEA Grenoble, December 2-3, 1996.

[20] TUUNANEN, J., VIHAVAINEN, J., D'AURIA, F., KIMBER, G., Assesment of Passive Safety Injection Systems of ALWRs, Final Report of the European Commission 4th Framework Programme Project FI4I-CT95-0004 (APSI), VTT Research Notes N:o 1957, Espoo 1999.

[21] TUUNANEN, J., RIIKONEN, V., KOUHIA, J. AND VIHAVAINEN, J., Analyses of PACTEL passive safety injection experiments GDE-21 through GDE-25, Nuclear Engineering and Design, Volume 180, Issue 1, 1 March 1998, pages 67-91. ISSN 00295493.

[22] VIHAVAINEN, J., TUUNANEN, J. "Passive Safety Injection during SBLOCA from a Core Make-up Tank with a Pressure Balancing Line to Pressurizer: Experiment in PACTEL and APROS Simulations". Proceedings of the 6th International Conference on Nuclear Engineering, ICONE-6, May 9-14, 1998, San Diego, California, USA.

[23] VIHAVAINEN, J., HÄNNINEN, M., TUUNANEN, J., Improved Thermal Stratification Modeling in Apros Code Simulation of Passive Safety Injection Experiments. Ninth International Topical Meeting in Nuclear Reactor Thermal Hydraulics (NURETH-9), San Francisco, California, October 3-8, 1999.

[24] VIHAVAINEN, J., Calculation of Standalone Passive Safety Injection System with New Thermal Stratification Solution Method of APROS Code, Proceedings of ICONE8, 8th International Conference on Nuclear Engineering, April 2-6, 2000, Baltimore, MD, USA.

Numerical analysis of experiments modeling
LWR sump cooling by natural convection

G. Grötzbach, L.N. Carteciano, B. Dorr

Forschungszentrum Karlsruhe GmbH, Institut für Reaktorsicherheit,
Germany

Abstract. An optional sump cooling concept for the European pressurized water reactor EPR was investigated at the Research Center Karlsruhe. This concept foresees to utilize single phase natural convection in water to remove the decay heat from the core melt. The natural convection was investigated by the SUCOS-2D and -3D scaled experiments. A numerical investigation and interpretation of these experiments was performed by means of the computer code FLUTAN. In this paper, the numerical investigation of SUCOS-3D is summarized. Following the results of the former 2d experiments and the numerical analysis of both experiments, an unexpected temperature distribution is found in this 3d experiment. Basing on the experimental data it had to be postulated that one of the horizontal coolers was slightly tilted against the main flow direction. Additional numerical investigations show that a slope of only one percent would explain the experimental flow field. Conclusions are also drawn on the limits of scalability and transferability of the experimental results to a reactor sump. A detailed transformation will only be possible by applying well validated CFD-codes and experienced code users. As the flow in the reactor sump will be turbulent and this flow is strongly three-dimensional and time-dependent, only the method of Large Eddy Simulation is considered of being an adequate tool for reliable transformation of the gained experience to analyses for the reactor sump at 1:1 scales.

1. INTRODUCTION

The final safety barrier after a core melt down accident is the core catcher in the reactor sump. An optional cooling concept for the European Pressurized water Reactor EPR utilizes passive safety features to remove the decay heat from the sump. After the accident, a dry distribution and stabilization of the core melt in the sump region of the reactor (see Fig. 1) is foreseen. Then cooling of the core melt begins with the water from the in-containment refueling water storage tank. Water cooled heat exchangers and condensers are present in the reactor sump region in order to remove the decay heat from inside the containment. The decay heat is transferred from the core melt to the sump water by evaporation, natural convection, and conduction. In the first days the convection of the sump water is in two-phase conditions; about ten days after the accident, single-phase natural circulation conditions are reached.
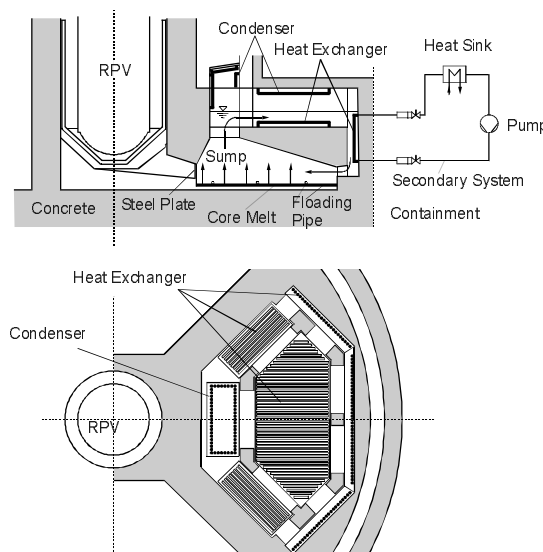
FIG. 1. Schematics of a sump cooling concept.

The single phase natural convection is experimentally and numerically investigated in the Research Center Karlsruhe in the program SUCOS (SUmp COoling Small) (Knebel et al. 1995). The aim of this program is to obtain quantitative results to be transferred to the prototypic condition in order to make a statement on the feasibility of the single phase sump cooling. Two scaled test facilities (1:20) are applied in the program: SUCOS-2D (Fig. 2), which represents a two dimensional plane slab (580 × 275 × 235 mm) of a simplified reactor sump geometry, and SUCOS-3D (Fig. 3), which is a three dimensional scaled geometry (1298 × 580 ×= 275mm) of the sump. Water was heated by a heated copper plate at the bottom of the pool simulating the core melt and cooled by horizontal and vertical heat exchangers in areas where they are protected against vapor explosion consequences.
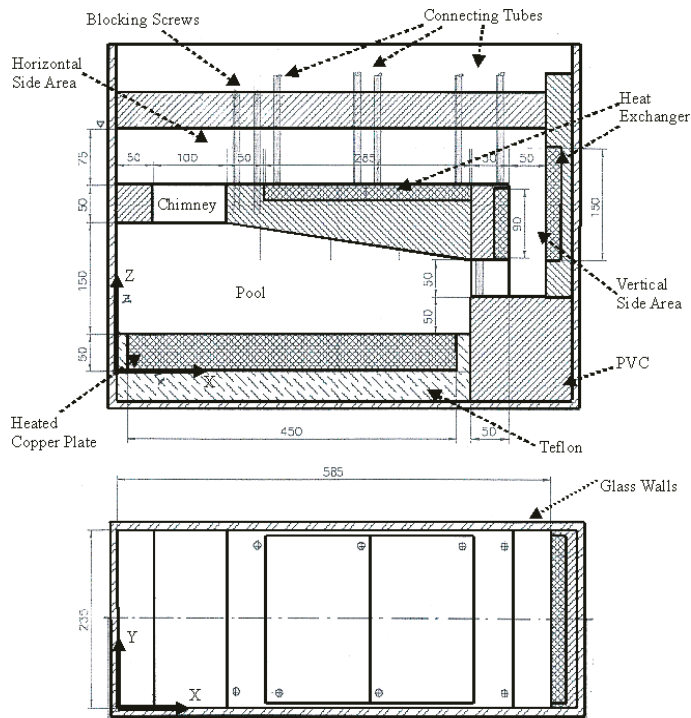
FIG. 2. Schematics of the test geometry SUCOS-2D.
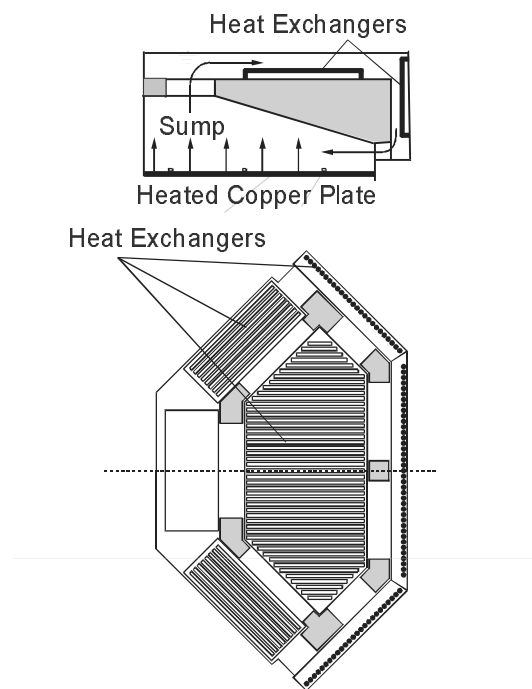
FIG. 3. Schematics of the test geometry SUCOS-3D.

A numerical investigation of this sump cooling concept and the related model experiments is performed by using the FLUTAN code (Willerding at al. 1995). This thermal- and fluid-dynamical computer code is developed in the Research Center Karlsruhe for the numerical analysis of the passive heat decay removal in new reactor systems. It was already extensively validated and applied to analyses of model experiments for the decay heat removal in the fast breeder reactor SNR-300 (Weinberg et al. 1996). It is used here to investigate and interpret numerically the single-phase natural convection in the experiments SUCOS-2D and 3D. The aim of this numerical investigation is to confirm the feasibility of the sump cooling concept and to analyze in more detail the experiments.

The first step of this investigation consisted of the numerical simulation and interpretation of an SUCOS-2D experiment (Carteciano et al. 1999). The most important result was that SUCOS-2D cannot be well reproduced with a two-dimensional calculation whereas three-dimensional calculations reproduce the experiment quite well. The simulations showed that significant

three-dimensional experiment specific phenomena are present in the experiments, but these 3d phenomena are of much less relevance in the reactor sump. Furthermore, the analysis of the calculation of SUCOS-2D gave information on the requirements for the modeling of geometry and boundary conditions for simulations of an experiment of SUCOS-3D which is the second and final step of the numerical investigation of the single-phase sump cooling concept. This step of analyzing the SUCOS-3D experiment in detail is documented in (Carteciano et al. 2000). Here, the most important results of this study are discussed to give at the end an outlook on the current status of methods to transfer all these results of the model experiments by CFD tools to EPR scales.

2. FLUTAN CODE

FLUTAN is a highly vectorized computer code for 3D fluiddynamic and thermal-hydraulic analyses in Cartesian or cylinder coordinates. It is related to the family of COMMIX codes originally developed at Argonne National Laboratory, USA (Shah et al, 1985). FLUTAN was developed in order to simulate single phase flows with small compressibility. The conservation equations for mass, momentum, energy, and turbulence quantities are discretized in a structured grid using a finite volume method. A staggered grid is used for the velocities. The discretization of the diffusive terms is performed by a central difference method (CDS). A first order upwind or one of two second order upwind methods (QUICK (Leonard 1979) and LECUSSO (Günther 1992)) can be chosen for the convective terms. A first order implicit Euler-method is used for time discretization. Several turbulence models are available in FLUTAN. The most important one for buoyant flows is the Turbulence Model for Buoyant Flows (TMBF) which consists of a first order k-ε model in a low-Reynolds number formulation and a second order five-equations turbulent heat flux model (Carteciano et al. 1997). In several benchmarks it turned out that the TMBF in its current development status is at least a powerful tool for forced and mixed convection (Baumann et al. 1997). Special thermal boundary conditions are available in order to simulate different thermal situations like a heat exchanger model and a wall model. A 3d heat conduction model for the structures was developed for the investigation of the SUCOS experiments. This is necessary for simulating solid structures with internal non-uniform transport of heat; it was required to achieve realistic boundary conditions for the fluid domain at the heated copper plate in the SUCOS experiments. The structure temperatures are discretized on an own grid on which the heat conduction equation is solved in all dimensions independent of the solution of the corresponding equation in the fluid domain.

3. SUCOS-3D INVESTIGATION

3.1 The test facility

The test facility SUCOS-3D consists of a tank (1298 × 580 × 275) whose outer walls are 20 mm thick and made of Plexiglas (Fig. 3). The ratio between lengths in the test facility and EPR is 1:20. A 30 mm thick copper plate which is heated by electric heat conductors simulates the core melt; it is isolated from the ground, from the walls, and from outside with Teflon. The heating power is scaled according to the volume of the sump as $(1/20)^3$. Plexiglas structures replace the structures of concrete in the prototype. The heat exchangers are slab heat exchangers made of copper; their cooling tubes have a meander form and use water as a cooling fluid. The horizontal heat exchanger is divided in four separate sections: two small and two large ones. The vertical heat exchangers consist of 8 sections: 4 inner and 4 outer sections respectively. Additional coolers in an upright position are present in the test facility. The space above the heated copper plate is called pool, see Fig. 2. The space above the horizontal heat ex-

changers is called horizontal side area. The space between the vertical heat exchangers is called vertical side area. The vertical channel without heat exchangers connecting the pool and the horizontal side area is called chimney.

Several experiments were performed in SUCOS-3D varying the value of the power input to the copper plate, the arrangement of the heat exchangers, the inlet temperature of the secondary fluid in the heat exchangers, and the level of water. Only temperatures were measured using thermocouples in two planes near the mid section. The experiments are characterized by a so called pool temperature. This is the mean temperature in the pool area which is measured by six thermocouples below the tilted roof of the pool.

In order to perform the numerical simulation and interpretation with FLUTAN, a SUCOS-3D experiment had to be chosen which is consistent with the one already simulated for SUCOS-2D. Therefore, one was chosen in which the horizontal and the outer vertical coolers were in operation, while the internal vertical coolers were not active. The electric heat supply of the heated copper plate amounted to 1,240 W. The inlet temperature of the coolant on the secondary side of the heat exchangers was set to 20^0C and the flow rate was 20 or 40 g/s. The measured pool temperature was 32.6 ^{0}C.

3.2 Specification of the computational model

To reduce the computational effort only half of the complex but symmetric geometry of the test facility is simulated. According to the experience gained from the numerical analysis of SUCOS-2D, all structures have to be modeled in detail and a very fine grid is necessary for a good resolution of the thin boundary layers near walls and coolers. The mesh size of the grid changes from 8 mm to 1 mm. Ratios of the mesh sizes between two neighboring cells are less than or equal to 2. The 3d grid consists of 691,000 fluid cells and 68,000 structure cells. A first order upwind scheme is used to compute the convective fluxes of enthalpy and momentum. No turbulence model is used because the flow was laminar in the experiment.

The connecting tubes of the coolers, which are present in the horizontal side area are spatially recorded and modeled even if it is expected that they would have a minor influence on the natural convection than in the calculation of SUCOS-2D. The heat losses to the outside through the lateral walls are neglected. The active heat exchangers can be modeled by a heat exchanger model or by pre-setting a distribution of surface temperature or of heat flux. The calculation of SUCOS-2D showed that it is not necessary to simulate the coolers with the complex heat exchanger model. It is sufficient to give a distribution for the temperature on the surface between fluid and cooler. A linear distribution for the temperature is approximated by a step function prescribing three values for the vertical right coolers. For the horizontal coolers a constant value of temperature is sufficient because the difference of temperatures between inlet and outlet coolant water is less than 1 K. The prescribed values are determined by means of experimental data.

In former simulations for SUCOS-2D it was found that the heated copper plate needs special attention (Kuhn 1996). Even the developing circulation sense in the complete fluid domain is sensitive to the thermal boundary conditions used at the upper surface of the copper plate (Grötzbach et al. 1997). There, the problem of using an artificial Neumann or Dirichlet boundary condition was analyzed by calculating the heat conduction in the copper plate. 2d tests showed the surprising result that the copper plate does not ensure a constant heat flux to the fluid, but that it redistributes the heat horizontally in such a strong manner, that the heat flux

into the fluid varies along the plate surface by more than +/-50% of its mean value, Fig. 4. Thus, the thermal conduction in the heater plate is also calculated here. A 3d grid is used for the heated plate; the horizontal grid width distribution corresponds to the one of the fluid region; 5 cells are used in the vertical direction with mesh sizes of 6 mm. The electrical heaters below the copper plate are simulated as a heat flux boundary condition with constant horizontal distribution.
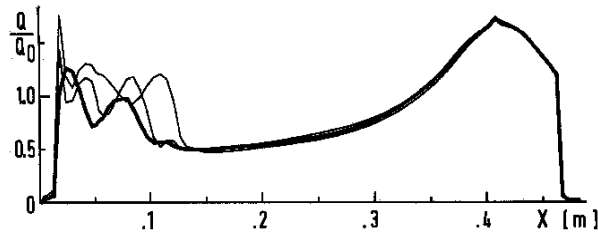

FIG. 4. Horizontal distributions of the calculated heat flux Q divided by its mean value Q_0 from the copper plate to the fluid at three different times in SUCOS-2D.

The simulation was performed on a CRAY J916 with a memory need of 2.7 Gbytes. The transient calculation was preceded by a steady state calculation to obtain an initial flow and temperature field for the transient calculation. The steady state calculation is stopped when an equilibrium in the changes of temperature and in the balance of the heat fluxes is nearly achieved. This happened after 4 h corresponding to 240 h of CPU-time. The transient calculation is performed for a problem time of 227 s with a time step width of 1.0 s. This corresponds to 407 h CPU-time. The system of the pressure equations is solved by the iterative CRESOR method (Borgwaldt 1990), whereas the system of the enthalpy equations is solved by the iterative SOR method.

3.3 Results

All following results are from the transient calculation and are time averaged over two minutes, like in the experiment. The calculated temperature field is shown in Fig. 5. Despite a careful and detailed 3d modeling of the geometrical and thermal characteristics of the SUCOS-3D experiment, the calculated pool temperature ($T_{p,cal} = 29.2^0C$) is lower than the measured one $T_{p,exp} = 32.6^0C$: the corresponding deviation is $(T_{p,cal}-T_{p,exp})/(T_{p,exp}-T_{cool}) = 34\%$.
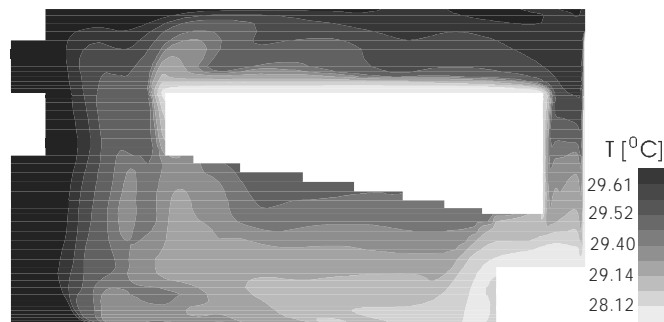
FIG. 5. Calculated temperature field roughly in the mid plane of the computational domain.

In order to find possible reasons for this deviation one should compare the calculated flow field to the experimental one. The calculated flow field for SUCOS-3D is very similar to the experimentally found and calculated one for SUCOS-2D. A stable natural convection loop develops, Fig. 6: the heated fluid rises from the copper plate through the chimney to the covered water level; here the warm flow turns right to the horizontal side area and flows on without an intensive contact to the horizontal cooler; the water is mainly cooled in the vertical side area from where it returns to the pool where it is heated again; part of the cold water from the horizontal coolers moves from time to time in form of cold plumes against the mean flow downwards through the chimney and mixes with the rising heated water. These non-stationary plumes cause the strong time dependence of the heat flux on the copper plate, Fig 4. According to this flow field, the temperatures in the horizontal side area of SUCOS-2D are higher than the ones in the pool under the tilted roof, similar to the temperatures in Fig. 5.

The flow field in the experiment SUCOS-3D must be reconstructed from the measured temperatures because no velocity measurements were performed. Other than in SUCOS-2D here we find in the experiment the highest temperatures not in the horizontal side area, but below the tilted roof, Fig. 7. Therefore, a different behavior of the natural convection has to be deduced: We have at least to expect stronger mixing between cold counter-current downward flow with hot rising fluid in the chimney.
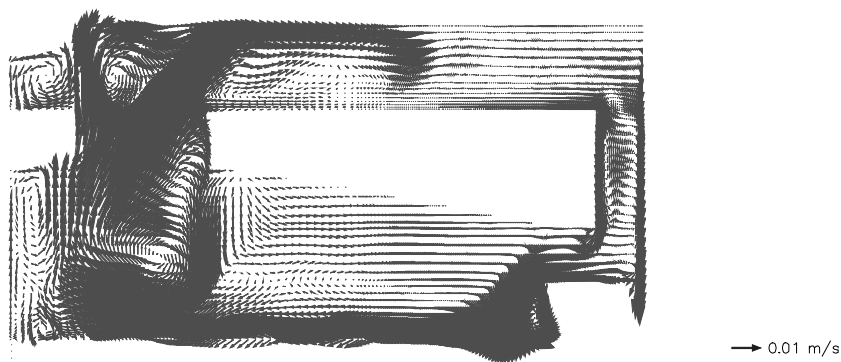
FIG. 6. Velocity vector field roughly in the mid plane of the computational domain. Calculation of SUCOS-3D.
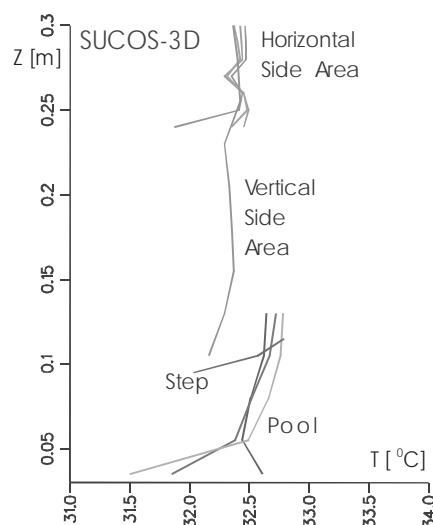
FIG. 7. Distributions of measured temperatures in SUCOS-3D.

Possible reasons for the disagreement in the pool temperature and in the natural convection loop were investigated. Since SUCOS-2D calculations showed a high sensitivity of the natural convection on thermal disturbances, the thermocouple support structure installed in the chimney was additionally modeled as a thermally interacting structure. Unfortunately, the exact position of the movable probe is not known. Nevertheless, the new results with probe support structure are better than the previous ones and bring the calculated pool temperature to the right direction but not yet enough to achieve a satisfactory agreement.

So far, the cooling performance of the vertical coolers was overestimated by all previous calculations. Therefore, a further numerical study was performed changing the kind of the thermal boundary conditions for the active vertical coolers: values for the wall heat fluxes deduced from the experiment were pre-set instead of using surface temperatures. Then, the calculated pool temperature $T_{p,cal} = 32.8\ ^0C$ agrees well with the experimental one, Fig. 8: the deviation is reduced from 34% to only 2%. Despite of this positive result, qualitatively the same natural convection loop is obtained like in the previous calculations. This means, the calculated flow field still shows no agreement with the reconstructed one in the experiment.
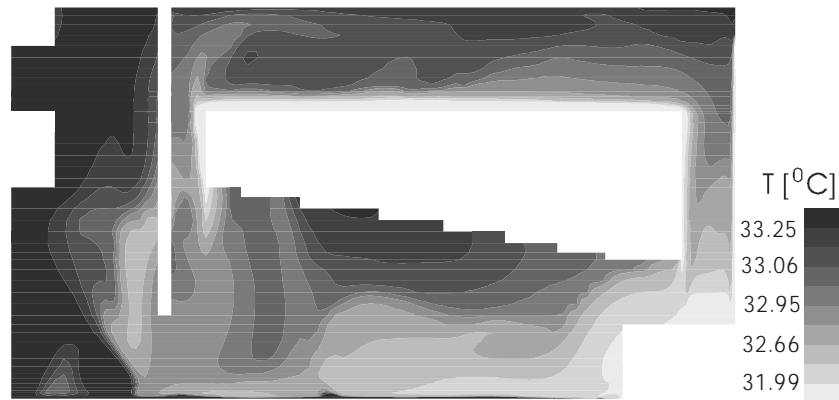
FIG. 8. Temperature field roughly in the mid plane of the computational domain. Calculation with temperature probe support and pre-set wall heat fluxes for the vertical right coolers.

The differences between experiment and calculation in the behavior of the flow field were further analyzed by means of vertical temperature distributions, which were measured in the chimney and in the vertical side area (Carteciano et al. 2000). The amount of water flowing down from the horizontal cooler to the vertical one was much less in the experiment than calculated, which causes reduced heat fluxes at the outermost section of the vertical coolers. An other significant difference between calculation and experiment can also be found in the chimney: recirculation of cold water flowing back from the horizontal cooler to the chimney is calculated, while cold water was registered in the experiment in the plane of measurements only under the tilted roof. The origin of the cold water under the roof in the experiment was reconstructed by analyzing the cooling performance of the horizontal coolers which are divided into two big and two small ones. The cooling performance of one small cooler is in the experiment as high as the one of a big cooler despite the cooling surface ratio of about 1:2. Therefore, a stronger water flow was obviously present over the small cooler. This cold flow returns to the corners of the chimney (Fig. 9) and is recorded only when it reaches the thermocouples at position R below the chimney.
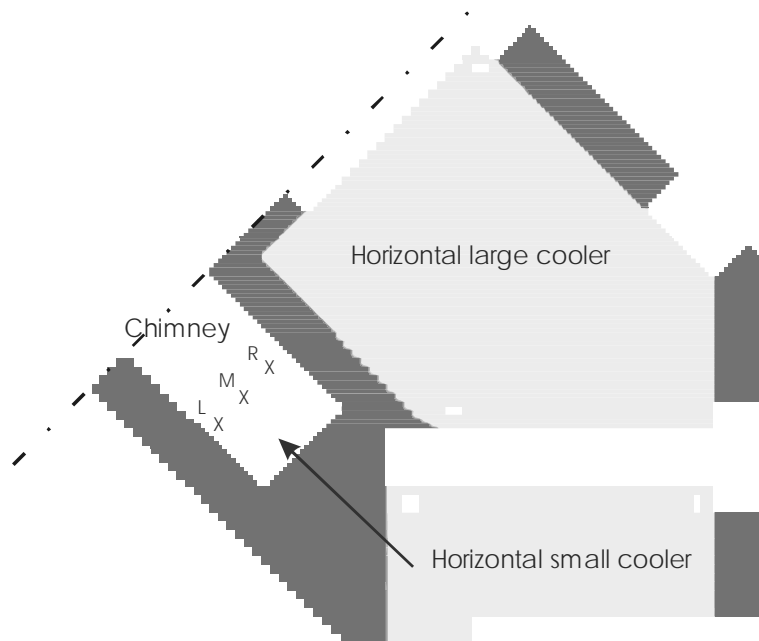
FIG. 9. Arrangement of the horizontal coolers. The arrow indicates the increased cold flow coming back to the chimney.

A decisive conclusion on the disturbance responsible for the experimental flow behavior was not found in all previous calculations and studies. Further deviations in the modeling or boundary conditions used in the simulations from those in the experiments have to be considered. One example, which would explain the unexpected results from the SUCOS-3D experiment, is to postulate that one of the horizontal coolers was slightly tilted against the main flow direction.

Additional calculations with a 2d slab model similar to SUCOS-2D were performed with different inclinations of the horizontal coolers from 0 to 4 mm, corresponding respectively to 0 and 1.04 % slope. The mass flow of the cold water going back to the chimney from the horizontal coolers increases due to this measure by about 70% and the corresponding heat removal by this flow increases by about 55%! Therefore, the mixing between the cold water and the heated water rising through the chimney is strongly increased like in the experiment. These results show that a very small slope of the horizontal coolers can influence the flow behavior in a drastic way and would explain the experimental flow field, but a final check is not possible because the experimental facility is already disassembled.

4. TRANSFER METHODS TO EPR CONDITIONS

Conclusions on the conditions in the reactor sump can in principal be drawn from the experimental results by two means, by applying scaling laws, and by applying CFD methods. Scaling laws were applied by Knebel & Müller (1997) to determine from the 2d experiments that in the first days the temperatures in the water above the core melt will be large enough to achieve boiling. As a consequence, the investigations in SUCOS are only applicable for the long term cooling after about ten days. A condition for applying scaling laws is, that the physical transport phenomena are of similar relevance in the model experiment and in the reactor sump. The analyses of SUCOS-2D in Carteciano et al. (1999) have shown that specific 3d effects, like the

feed water pipes to the coolers, the bolts, and screws going through the fluid domain strongly affect the experimental results. In the small cross section of the SUCOS-2D slab geometry these structures become more important for the heat transfer and for the flow resistance than in the huge reactor sump. Thus, the results of this experiment cannot be used for scaling up to predict accurately the temperatures in the reactor sump. In contrast, the first numerical cases, which did not record those structures, are more feasible as a basis for this extrapolation. The experimental results of SUCOS-3D could be a better basis because there the cross sections occupied by those structures are of relatively less importance, but there the above mentioned strange flow distribution was found which is specific for this experiment and not for the reactor sump.

Scaling up by CFD-tools is also not free of serious problems in this context. On one hand the SUCOS tests could successfully be interpreted with the FLUTAN code. Such CFD codes have the flexibility to tackle all the experiment or reactor specific structures. On the other hand the model experiments showed laminar flows, whereas the reactor sump will have turbulent flow conditions (Knebel & Müller 1997). Hence additional investigations are necessary by experiments of similar flow types to validate the turbulence models and boundary conditions used with the turbulence models. Purely buoyant flows are currently a challenge for any turbulence model, see e.g. Hanjalic (1994, 1999). Also the TMBF, which is explicitly developed for buoyant flows, has up to now only been validated for two-dimensional forced, mixed, and natural convection (Carteciano et al. 1997, 1999b). An additional feature, which is inherent to most purely buoyant flows, is its local time dependence. The cold plumes plunging down through the chimney are a low frequent phenomenon which was also not completely filtered out in the experiment by time-averaging over two minutes. This causes the wall heat flux on the copper plate to change in time, Fig. 4. And also the hot plumes rising from the surface of the copper plate are no stationary phenomenon. The surface temperature on the copper plate, Fig. 10, is very straggly as it is typically found in Rayleigh-Bénard convection in which the hot plumes rise mainly from the knots of those straggly structures (Wörner & Grötzbach 1997).
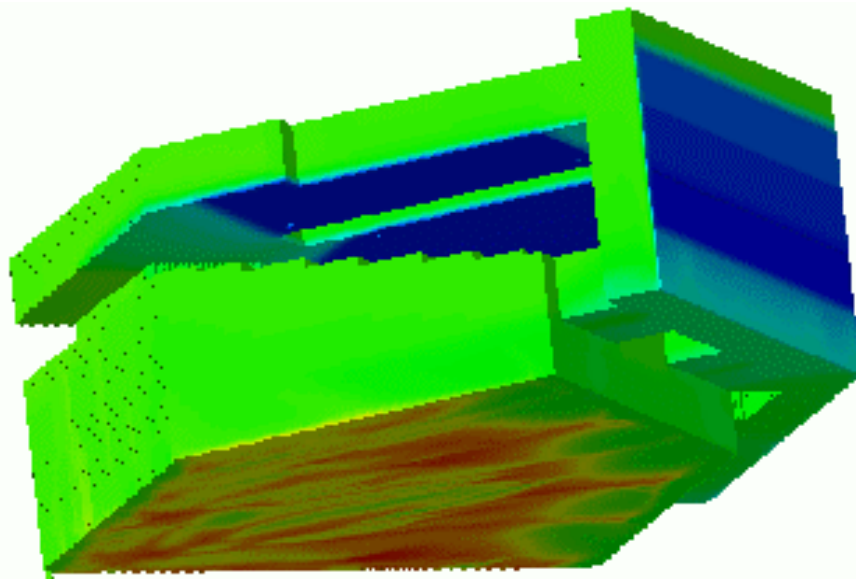
FIG. 10. Calculated temperature field on the surface of the structures of SUCOS-3D. View from below on the fluid domain. The dark areas represent the cooler surfaces.

As a consequence of the 3d and time-dependent nature of buoyant flows and of the current status of development of the standard turbulence models, there is currently no way to achieve reliable results by standard models on the temperature fields in the reactor sump. The only way which is nowadays often considered to give a better solution for 3d time-dependent flows is to apply Large Eddy Simulation methods (LES). Indeed, there exist already several applications of LES to reactor typical flows; for an overview see Grötzbach & Wörner (1999). These show the tremendous potential of the LES method and that its possibilities are going far beyond those of standard Reynolds averaged turbulence models. The main problems which need to be solved for LES methods in this context are e.g. the development of more universal subgrid scale models, of boundary conditions for buoyant flows, and of numerical methods in commercial codes that fulfill LES requirements.

5. CONCLUSIONS

The former numerical interpretation of SUCOS-2D experiments with the FLUTAN computer code showed that good agreement between experiment and calculation can be achieved when local thermal disturbances like the feed water pipes to the coolers are recorded in the simulation. Here, the single phase natural convection experiment SUCOS-3D is interpreted. The numerical results confirm, natural convection in large pools, in which pressure drops are negligible, is very sensitive against small disturbances. Here, some other discrepancies are found by analyzing the experimental results from SUCOS-3D: In these experiments the maximum temperature did not occur far above the horizontal coolers as in SUCOS-2D, but below the tilted roof, and the heat fluxes over the horizontal and vertical coolers were not homogeneously distributed. Comparable pool temperatures could only be achieved numerically by using the measured heat fluxes at the coolers instead of temperature boundary conditions, but the calculated flow pattern was still different. One explanation for this strange result is supported by the experimental data, this is to postulate that one of the horizontal coolers was slightly tilted against the main flow direction. Additional numerical investigations indeed show that a slope of only one percent would explain the experimental flow field. From this problem of the experiment one can learn how to improve this sump cooling concept: Foreseeing a small slope of the horizontal coolers downwards in the expected flow direction would stabilize the flow and would drastically increase the efficiency of the horizontal coolers.

Based on the performed numerical investigations it can be concluded that a transformation of the experimental results from SUCOS-2D and -3D to reactor sump conditions by means of scaling laws is questionable. Such transformation will only be possible by applying well validated CFD-Codes and experienced code users with a sound physical and engineering background. Current standard turbulence models form the working basis for engineers, but they can only be used for approximate predictions, because the statistical models fail for buoyant flows which are locally time-dependent. The only more reliable solution could come from adequate Large Eddy Simulation methods and LES-suitable codes for complex geometries.

REFERENCES

[1] BAUMANN, W., CARTECIANO, L., WEINBERG, D., 1997. *Thermal propagation effects in a vertical turbulent flow behind a jet block - A benchmark exercise*. Journal of Hydraulics Research, Vol. 35, pp. 843-864.

[2] BORGWALDT, H., 1990. *CRESOR, A Robust Vectorized Poisson Solver Implemented in the COMMIX-2(V) Thermal-Hydraulic Code*. Paper AC064. Int. Conf. On Super-computing in Nuclear Application (SNA 90). Mito City, Japan, March 12-16, pp. 346-351.

[3] CARTECIANO L.N., WEINBERG D., MÜLLER U., 1997. *Development and Analysis of a turbulence Model for Buoyant Flows*. Proc. of the 4th World Conf. on Experimental Heat Transfer, Fluid Mechanics and Thermodynamics, Bruxelles, Belgium, June 2-6. Vol. 3, S. 1339-46. Pisa Edition ETS.

[4] CARTECIANO, L.N., DORR, B., GRÖTZBACH, G., 1999. *Theoretical Interpretation of the Single Phase Sump Cooling Experiment SUCOS with the FLUTAN Code*. Proc. 9th Int. Meeting on Nuclear Thermal-Hydraulics NURETH-9, CD-Rom Log107.

[5] CARTECIANO, L. N., WÖRNER, M., GRÖTZBACH, G., 1999b. *Erweiterte Turbulenzmodelle für technische Anwendungen von FLUTAN auf Naturkonvektion*. Jahrestagung Kerntechnik 1999, Karlsruhe, 18. - 20.5.1999, INFORUM Bonn, S. 129-133.

[6] CARTECIANO, L.N., DORR, B., GRÖTZBACH, G., 2000. *Numerical Investigation of the Single Phase Natural Convection in Sump Cooling Experiments with the FLUTAN Code*. The Tenth Int. Conf. On Emerging Nuclear Energy Systems (ICENES 2000), Petten, The Netherlands, 24.-28. Sept.

[7] GRÖTZBACH, G., WÖRNER, M., 1999. *Direct numerical and large eddy simulations in nuclear applications*. Int. J. Heat and Fluid Flow (20), pp. 222-240.

[8] GRÖTZBACH, G., M. WÖRNER, T. AMMANN, A. BLAHAK, L. CARTECIANO, B. DORR, Y. KIMHI, W. OLBRICH, W. SABISCH, Q. YE, M. ALEF, ST. GENZ, A. HENNEMUTH, G. JANßEN, M. LINDER, D. Seldner, 1997. *Entwicklung von Thermofluiddynamikprogrammen und ingenieurtechnische Anwendungen*, Projekt Nukleare Sicherheitsforschung, Jahresbericht 1996, FZKA 5963, pp. 411-427.

[9] GÜNTHER, C., 1992. *Fortgeschrittene Upwind-Differenzen-Verfahren zur numerischen Lösung der Konvektions-Diffusionsgleichung*. Habilitation, KfK 4697.

[10] HANJALIC, K., 1994. *Achievements and limitations in modelling and computation of buoyant turbulent flows and heat transfer*. 10th Int. Heat Transfer Conf., August 14-18, Brighton, U.K.

[11] HANJALIC, K., 1999. *Second-Moment Closures for CFD: Needs and Prospects*. Int. J. Comp. Fluid Dyn. 12, 67-97.

[12] KNEBEL, J. U., MÜLLER, U., 1995. *Experimental and Numerical Simulation of Passive Decay Heat Removal by Sump Cooling After Core Melt Down*. Proc. 8th Int. Meeting on Nuclear Thermal-Hydraulics NURETH-8, Vol. 2, pp. 1059-1066.

[13] KNEBEL, J. U., MÜLLER, U., 1997. *Scaling of passive decay heat removal by sump cool ing*. Jahrestagung Kerntechnik 97, Aachen, 13.-15. Mai, INFORUM Bonn, S.144-47.

[14] KUHN D., 1996. *Numerische und experimentelle Untersuchungen zum Sumpkühlkonzept*. Diplomarbeit, Institut für Angewandte Thermo- und Fluiddynamik (IATF), Forschungszentrum Karlsruhe.

[15] LEONARD, B. P., 1979. *A Stable and Accurate Convective Modelling Procedure Based on Quadratic Upstream Interpolation*. Computer Methods in Applied Mechanics & Engineering, Vol. 19, p. 59.

[16] SHAH et al., 1985. *COMMIX 1-B: A 3d Transient Single-Phase Computer Program for Thermal Hydraulic Analysis of Single and Multicomponent Systems.* NUREG/CR-4348, Vol. I and II.

[17] WEINBERG, D., RUST, K., HOFFMANN, H., 1996. *Overview Report of RAMONA-NEPTUN Program on Passive Decay Heat Removal.* FZKA 5667.

[18] WILLERDING, G., BAUMANN, W., 1996. *FLUTAN 2.0 input specifications.* FZKA 5712.

[19] WÖRNER, M., GRÖTZBACH, G., 1997. *DNS database of turbulent natural convection in horizontal fluid layers.* World Wide Web-site http://www.fzk.de/irs/turbit.

CIRCUS and DESIRE: experimental facilities for research on natural-circulation-cooled boiling water reactors

W.J.M. De Kruijf, T.H.J.J. Van Der Hagen, R. Zboray, A. Manera
Interfaculty Reactor Institute, Delft University of Technology

R.F. Mudde
Kramers Laboratorium voor Fysische Technologie, Delft University of Technology

Netherlands

Abstract. At the Delft University of Technology two thermohydraulic test facilities are being used to study the characteristics of Boiling Water Reactors (BWRs) with natural circulation core cooling. The focus of the research is on the stability characteristics of the system. DESIRE is a test facility with freon-12 as scaling fluid in which one fuel bundle of a natural-circulation BWR is simulated. The neutronic feedback can be simulated artificially. DESIRE is used to study the stability of the system at nominal and beyond nominal conditions. CIRCUS is a full-height facility with water, consisting of four parallel fuel channels and four parallel bypass channels with a common riser or with parallel riser sections. It is used to study the start-up characteristics of a natural-circulation BWR at low pressures and low power. In this paper a description of both facilities is given and the research items are presented.

1. INTRODUCTION

Natural circulation is a key item in the design of innovative natural-circulation-cooled Boiling Water Reactors (BWRs). Instead of using recirculation pumps to provide the cooling flow for the core, the core flow is driven by the density differences between the two-phase mixture in the core and the essentially single-phase flow in the downcomer. The natural-circulation core flow is enhanced by using a riser section on top of the core. Because the core flow cannot be controlled by means of a pump, the recirculation core flow is an internal variable of the system. Natural circulation has been used in the early stages of reactor development. Both the Experimental Boiling Water Reactor (EBWR) [1] and the Vallecitos Boiling Water Reactor [2] could be used with natural circulation. Later, the Humboldt Bay atomic unit and the Dodewaard plant have been operated as commercial BWR/1 plants with natural circulation. More recently the interest in natural circulation as a possibility for the core cooling has been renewed. This can be seen in the design of the Simplified Boiling Water Reactor, based on which new designs such as the ESBWR have been proposed [3]. The trend in these designs with respect to the reactor core is towards larger cores and higher power, combined with larger risers to enhance the natural-circulation core flow.

Because the core flow responds to changes in power the stability of a natural-circulation BWR is somewhat different from the stability of a forced-circulation BWR. Therefore, the stability of a natural-circulation BWR requires special attention. It has been shown that two different instability types exist for such a reactor, denoted by type-I and type-II [4]. Type-I oscillations are typical for natural-circulation BWRs and are driven by the gravitational pressure drop over the core and riser. Type-II oscillations are driven by the interplay between single-phase and two-phase friction in the core. This division in different types is not sharp. The transition from one type to the other occurs gradually. Although the character of both types of oscillations is different one could describe both of them as density-wave oscillations.

The type-I oscillations may occur during the start-up phase of the reactor, because this unstable region broadens as the pressure decreases and because it is associated with low-

power operating conditions. The flashing of water in the riser at low pressures induces this type of oscillation. The neutronic feedback is not important for this type of instability. The core region is essentially single-phase and thus the power oscillations will be small. Moreover, at such a low level power oscillations cannot cause any damage to the fuel. However, large flow oscillations should be avoided in view of their possible effect on structural materials. Different types of oscillations could be possible in view of the different possible configurations of parallel fuel bundles with common or parallel riser sections.

Type-II oscillations may occur during high-power/low-flow conditions in both natural-circulation or forced-circulation BWRs. Because the density in the core region fluctuates, the nuclear feedback is essential in the analysis of these types of oscillations. A division is made between core-wide, regional, and local oscillations. In core-wide oscillations the total power in the core will vary and all fuel bundles oscillate in-phase. This mode is favoured neutronically because of the subcriticality of the regional modes. In regional oscillations the total power will remain nearly constant and the power distribution will vary periodically. This mode is favoured thermohydraulically because the total flow will be nearly constant. A third type of oscillation is a local thermohydraulically unstable fuel bundle which induces small changes in the power and the power distribution.

The pressure dynamics and the feedwater (inlet subcooling) dynamics of the system should also be taken into account; this might especially be important for type-I oscillations in natural-circulation BWRS for which water flashes into large volumes of steam giving rise to large flow oscillations.

At the Delft University of Technology two thermohydraulic test facilities are being used to study the instability types in natural-circulation BWRs: DESIRE for type-II oscillations and CIRCUS for type-I oscillations. A description of DESIRE is given in Section 2, a description of CIRCUS is given in Section 3. Both facilities can be used to produce valuable experimental data needed for further model development in the system codes applied for nuclear power plant analyses[5].

2.   DESIRE

DESIRE is a simulated fuel bundle of a natural-circulation BWR with freon-12 as scaling fluid. Figure 1 shows an overview of the primary loop of the current facility, which is a scaled model of the Dodewaard natural circulation reactor[6]. The fuel bundle consists of 35 fuel rods in a 6 × 6 array. The fuel rods are 958 mm long with an heated length of 880 mm. The diameter is 6.35 mm. The fuel rods have either a chopped cosine or a flat uniform axial profile. Six independent power supplies can be connected arbitrarily with individual fuel rods, facilitating a wide range of radial power distributions. The nominal power is 22.3 kW, but the maximum power is about 50 kW. The pressure ranges from 8 to 13 bar (nominal pressure is 11.6 bar). In this manner, using freon-12 as a coolant, a full 1.8 m BWR bundle is simulated operating at 75 bar and 1116 kW nominal conditions. The inlet friction of the fuel bundle can be varied by means of a valve. The riser section can be varied in length (1.1 m–1.9 m) by means of a telescopic riser section. At the top of the riser a free surface exists at which the vapour is separated from the liquid which returns through the downcomer. Part of the vapour is also drawn into the downcomer, the so-called carry-under. The temperature distribution in the loop is measured with chromel-alumel thermocouples. The absolute pressure is measured at different positions in the loop, and the pressure difference is measured over the upper part of the downcomer tube and part of the steam dome, which gives an indication of the collapsed liquid level above the riser exit. The total recirculation flow as well as the steam flow and the

feedwater flow is measured with vortex flow meters. Gamma transmission is used to determine the average void fraction at a given height in the core region. This void fraction is also being used to implement an artificial feedback on the power of the fuel rods. The fuel rod thermal time constant as well as the void reactivity coefficient can be varied artificially. Gamma transmission can also be used to reconstruct the void-fraction on a subchannel basis, using tomographic techniques. In order to study the stability characteristics of the system, noise-analysis techniques are being used.
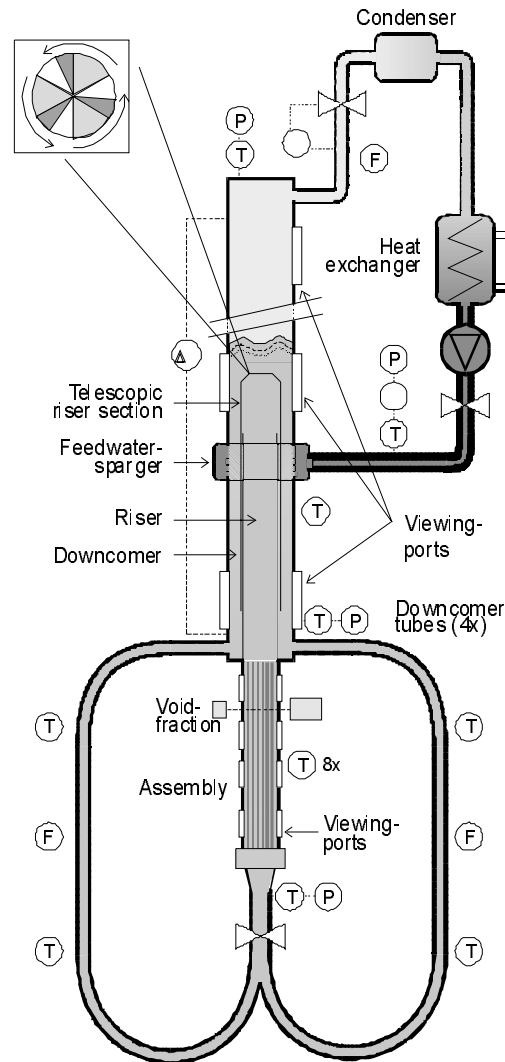
FIG. 1. Overview of the DESIRE facility. The position of the instrumentation is shown as well (T=Temperature, P=Pressure, ΔP=Pressure Difference and F=Flow).

DESIRE has been extensively used to study the natural circulation and stability characteristics of the Dodewaard natural circulation reactor[7,8]. Recently a riser exit restriction has been implemented to be able to destabilize the system in order to study limit cycles and non-linear effects with the facility[9]. With this riser exit restriction the effect of steam separator friction can be studied. In the near future the intention is to use DESIRE in the framework of the European NACUSP project. A large set of thermohydraulic experiments without artificial feedback will be performed covering a wide operational range of the facility (power, feedwater temperature, pressure, riser liquid level, power distribution) for a large range of geometrical settings (inlet friction, outlet friction, riser length). For this purpose the instrumentation of the loop is currently being updated and extended. A dedicated set of

experiments will be performed to study the capability of 3D-codes to calculate the void-distribution in the fuel bundle. The focus of these experiments is at low void fractions. Finally, part of the experiments will be devoted to optimize the artificial nuclear feedback currently being used in the facility. This optimization is needed to be able to extend the facility to multiple "parallel bundles" with which coupled neutronic/thermohydraulic regional oscillations can be simulated.
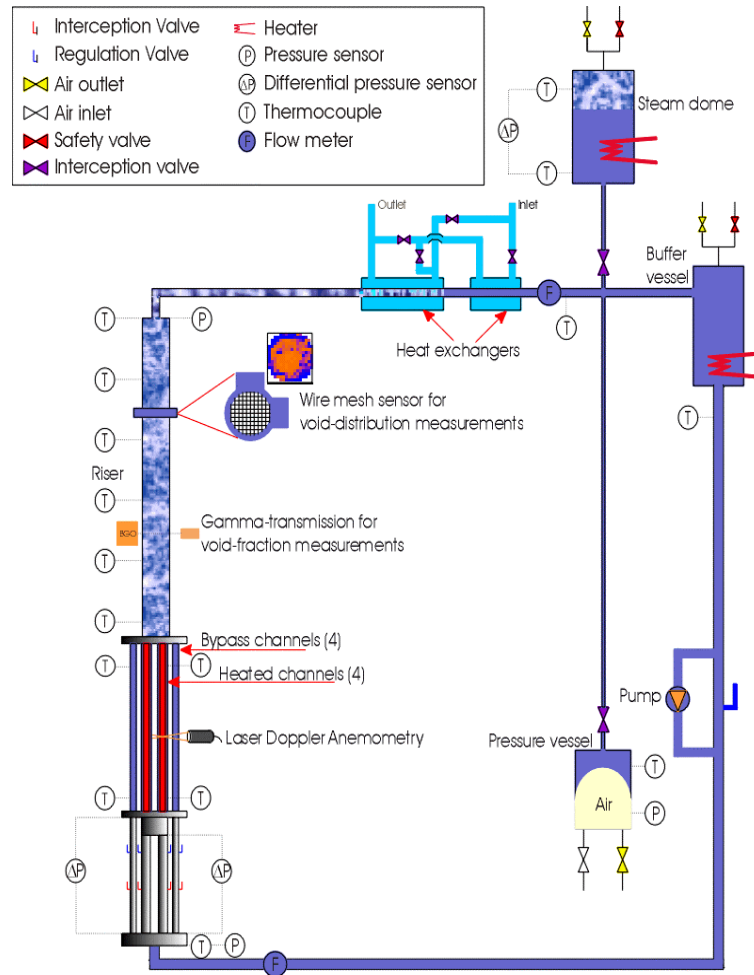
FIG. 2. Scheme of the CIRCUS facility (out of scale). The main instrumentation is also shown. (see legend).

3.   CIRCUS

The CIRCUS-facility is a full-height scaled steam/water loop of the Dodewaard reactor. Figure 2 shows a schematic view of the current facility.The reactor core is simulated by 4 electrically heated fuel rods in coolant channels and by 4 separate bypass channels. The channels are made of glass in order to be able to visualize the flow. This is one of the important features of the CIRCUS facility, which enables the researcher to combine the measurements with observations of the flow. The friction of each individual coolant channel or bypass channel can be varied independently. On the top of the core section a long adiabatic glass tube is used to simulate the riser section. The two-phase mixture is condensed and cooled by means of a heat exchanger. The length and the secondary flow rate of the heat exchanger can be varied. This controls in combination with the heater power in the buffer

vessel the subcooling of the liquid at the core inlet. The system pressure is regulated with a steam vessel, representing the steam dome in a BWR. A pressure vessel is used to pressurize the system. When the level in the steam dome drops below a certain level, the pressure vessel can be disconnected. The pressure vessel can also be used to perform alternative measurements with pressure feedback of the pressure vessel itself instead of pressure feedback of the steam volume in the steam dome. The position of the steam dome will be changed to a place before the heat exchanger to avoid problems with subcooled liquid entering the steam dome. Table 1 shows the main characteristics of the facility.

The temperature distribution in the loop is measured with chromel-alumel thermocouples and two Pt-100 temperature sensors for reference measurements. Absolute pressure is measured at the top of the riser and at the inlet of the core. The liquid level in the steam dome is measured with a differential pressure sensor. The differential pressure over the friction settings of the individual channels is a measure for the flow distribution over the coolant channels and bypass channels. The total flow in the loop is measured at 2 different positions with electromagnetic flow meters. The void fraction at a given height can be measured with gamma transmission techniques. At a fixed height at the top of the riser the radial void distribution is measured with a wire-mesh sensor, which measures the conduction of the two-phase mixture on a two-dimensional grid. Furthermore, laser doppler anemometry is used to study the local liquid velocity in the core or in the riser.

A limited set of experiments has been performed in which large flashing-induced oscillations have been observed[10]. As well as DESIRE, CIRCUS will also be used in the near future in the framework of the NACUSP project. A large set of thermohydraulic experiments will be performed covering a wide operational range of the facility (power, inlet subcooling, pressure, steam dome level, power distribution) for a range of geometrical settings (inlet friction, friction distribution). A dedicated set of experiments will be performed in order to study the flashing effect in the riser in detail. The gamma transmission technique and the wire-mesh sensor are of course important tools for this study. A third extensive set of experiments will be performed with two parallel riser sections instead of one common riser as in the current configuration.

TABLE. I. MAIN CHARACTERISTICS OF THE CIRCUS FACILITY

Power range per rod	0-3 kW
Pressure range	1-5 bar
Fuel channel diameter	20.4 mm
Fuel rod diameter	12.5 mm
Bypass channel diameter	10 mm
Fuel channel length	1.95 m
Riser diameter	47 mm
Riser length	up to 3 m

4. CONCLUSIONS

An overview of the facilities at the Delft University of Technology to study the natural circulation and stability characteristics of natural-circulation cooled BWRs has been given. The results of these studies are not only useful for these types of reactors but also for forced-circulation BWRs, because of the study on type-II instabilities. The results are also useful for LWR-reactors in general, because of the experimental data that will be generated at low

power and low pressure. The experiments in the near future will be performed in the framework of the European NACUSP project in which the natural circulation characteristics and stability performance of natural-circulation cooled BWRs are studied.

REFERENCES

[1]   ARGONNE NATIONAL LABORATORY, "The EBWR experimental boiling water reactor", ANL 5607, (1957).

[2]   KRAMER, A.W., "Boiling Water Reactors", Addison-Wesley Publishing Company, Inc. (1958).

[3]   KHORANA, S.S. *et al.*, "Technology basis for the ESBWR - An overview," Proceedings of ICONE5, 5th International Conference on Nuclear Engineering, May 26-30, 1997, Nice, France.

[4]   FUKUDA, K. and KOBORI, T., "Classification of Two-Phase Flow Instability by Density-Wave Oscillation Model", J. Nucl. Sci. Technol., **16** (1979) 95-108.

[5]   ISHII, M., "Views on the future of thermal hydraulic modeling," Proceedings of the OECD/CSNI Workshop on Transient Thermal-Hydraulic and Neutronic Code Requirements, November 5-8, 1996, Annapolis, Maryland, USA, NUREG/CP-0159, NEA/CSNI/R(97)4,751-759.

[6]   VAN DER GRAAF, R. *et al.*, "Scaling laws and design aspects of a natural-circulation-cooled simulated boiling water reactor fuel assembly", Nucl. Technol., **105** (1994) 190-200.

[7]   KOK, H.V. and VAN DER HAGEN, T.H.J.J., "Modeling the statics of a natural-circulation boiling water reactor loop", Nucl. Technol., **127** (1999) 38-48.

[8]   KOK, H.V. *et al.*, "Measurements of the void-fraction distribution in a simulated fuel assembly and the role of the void-fraction on the dynamics of a natural circulation loop", Ann. Nucl. Energy, **24** (1997) 1333-1347.

[9]   ZBORAY, R. *et al.*, "Experiments on nonlinear density-wave oscillations in the DESIRE facility," Proceedings of the NURETH-9 Conference, October 3-8, 1999, San Francisco, California, USA (on CDROM).

[10]   MANERA, A. *et al.*, "Experiments with the CIRCUS-facility on flashing-induced instabilities during startup of natural-circulation-cooled BWRs ," Proceedings PHYSOR 2000, May 7-11, 2000, Pittsburgh, Pennsylvania, USA (on CDROM).

The NOKO/TOPFLOW facility for natural convection flow

E.F. Hicken, H. Jaegers
Institute for Safety Research and Reactor Technology, Forschungszentrum Jülich

A. Schaffrath, F.-P. Weiss
Institute for Safety Research, Forschungszentrum Rossendorf

Germany

Abstract. For the study of the effectiveness of passive safety systems a high pressure (up to 7 MPa) and high power (up to 4 MW) test facility – named NOKO – has been constructed and operated at the Forschungszentrum Jülich. From 1996-1998 this facility was used for a project within the 4th FP of the EU "European BWR R&D Cluster for Innovative Passive Safety Systems". An overview and selected results are given for the tests with two bundles of the emergency condenser, with the building and plate condenser, with 4 different passive initiators, with a passive flooding system and with decay heat removal tests during shutdown. It has been decided to decrease substantially the safety research at the Forschungszentrum Jülich; to maintain the experimental competence for two-phase flow the NOKO facility will be transferred to the Forschungszentrum Rossendorf by the end of the year 2000 up to the beginning of the year 2001. The facility will be named TOPFLOW; the main objectives of future tests will be oriented towards more generic research: investigation of steady state and transient two-phase flow phenomena especially transient two-phase flow patterns, the development of two-phase flow instrumentation, the generation of a data basis for Computational Fluid Dynamic (CFD)-Code validation and testing of heat exchangers and safety systems. An overview will be given about the modifications and improvements related to the test facility and the planned tests.

1.   INTRODUCTION

It is a good demonstration of safety culture if vendors, utilities and licensing authorities equally make an effort to increase the safety level of Nuclear Power Plants – existing and future ones. Recognising that design and main licensing requirements were developed in the sixties and seventies it is appropriate now to develop new solutions as well as new licensing requirements, evaluate the feasibility of these solutions and possibly test their effectiveness.

The goals for new safety systems are evident: effective, simpler, more reliable, cheaper and licensable. Without major efforts, it can be stated that passive safety systems proposed up to now are simpler and are expected to be more reliable. They also seem to be licensable if the remaining uncertainties with respect to requirements for redundancy and diversity have been solved. An assessment of the costs is complex and cannot be discussed here.

During recent years and still ongoing are efforts to experimentally study the effectiveness of passive safety systems and compare the results with code calculations; due to the different operating conditions (e.g. small driving forces) as compared with active systems, some models in computer codes have to be improved. Therefore, it was decided to plan, construct and operate a facility at Forschungszentrum Jülich to study experimentally and analytically the effectiveness of the emergency condensers planned to be installed in the SWR 1000. This facility was named NOKO.

Due to the decision by the board of directors of the Forschungszentrum Jülich to reduce substantially the safety research for Nuclear Power Plants at Jülich and the decision to maintain the experimental competence for two-phase flow relevant to reactor safety it has been decided to transfer the NOKO facility from the Forschungszentrum Jülich to the Forschungszentrum Rossendorf by the end of the year 2000/the beginning of the year 2001. This facility will be named TOPFLOW.

2. THE NOKO TEST FACILITY

2.1. History

In 1993 it was decided by the Ministry for Research and Technology, SIEMENS, the German Utilities and the Forschungszentrum Jülich to build a test facility to study the effectiveness of the SWR 1000 emergency condensers; the facility was built in only 18 months.

From 1996-1998 the facility was used for a project within the 4th FP of the EU "European BWR R&D-Cluster for Innovative Passive Safety Systems"; seven partners participated. In 1997, in addition, seven partners of a EU-Concerted Action "BWR CA" took part in this project.

2.2. The NOKO facility imbedded in the matrix of two-phase-flow facilities in western Europe

In Fig. 1, some European test facilities capable to perform thermal-hydraulic tests with passive safety systems are shown. It is evident that the wide spread of power and pressures will allow the testing of the same component in several facilities of different size and thus increasing the confidence in the assessment of the effectiveness of this component. It has to be mentioned that the PANDA test facility has a larger volume than the other test facilities.
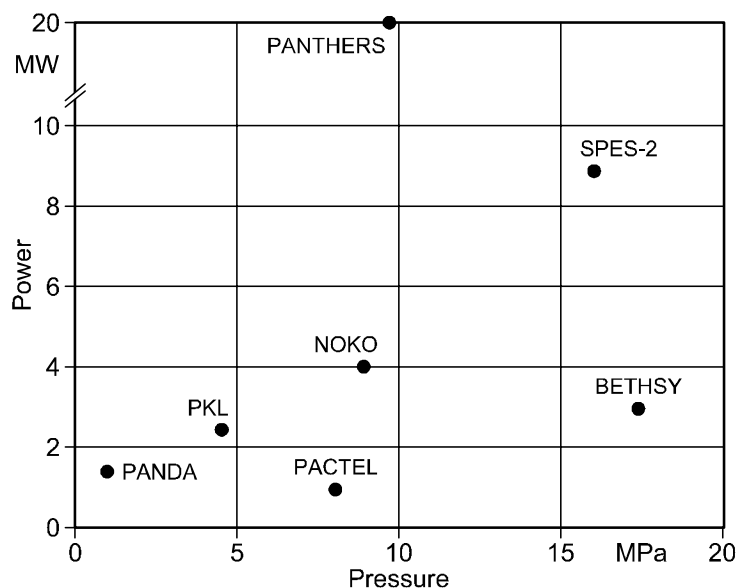
FIG. 1. European test facilities to perform thermal-hydraulic tests with passive safety systems.

2.3. The Facility

In Fig. 2, the layout of the NOKO facility is shown [4]. In principle, the facility consists of three loops:

1) The high pressure (<10 MPa) "primary" loop with the electrically heated boiler (<4 MW), the recirculation pump, the steam-water separator, the pressure vessel and the test object (passive initiator, emergency condenser, building condenser or plate condenser).

2) The medium pressure (<1-1.5 MPa) "secondary" loop with the condenser tank with inlet and outlet pipes for the different fluids (water, steam, non-condensables).

3) The ambient pressure "auxiliary" loop with condensation tank and heat exchanger which is cooled by river water or via a cooling tower.

A commonly used instrumentation is installed.
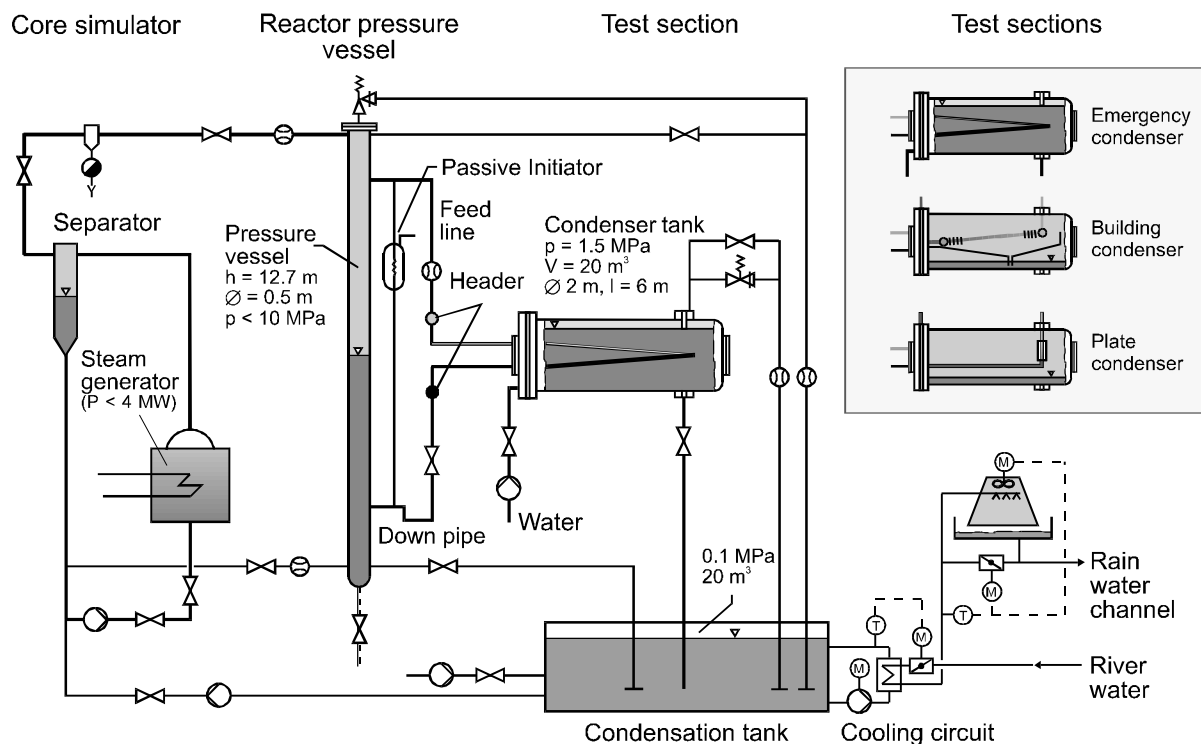
FIG. 2. Schematic of the NOKO test facility.

2.4. The NOKO Data Bank

Data as well as drawings, calculations and reports are stored in a data bank; all information are available through the Internet – protected by a password. In Fig. 3 an overview is given.

2.5. Energy Balances

In Section 2.3 it was shown that - in principle - 3 different loops exist in the NOKO facility. For the tests with the emergency condenser as the test section this configuration allowed the

evaluation of the energy transferred by the emergency condenser by three different and independent balances:

I)   The steam flow to the condensers was measured with an orifice.

II)   The steam flow to the condensers was calculated from the power input by the boiler and pumps, the heat losses and the energy removal by cooling.

III)   If the water pool was at saturation temperature, the steam was measured using an orifice.

The comparison of these three balances increased the confidence in accuracy of the results.
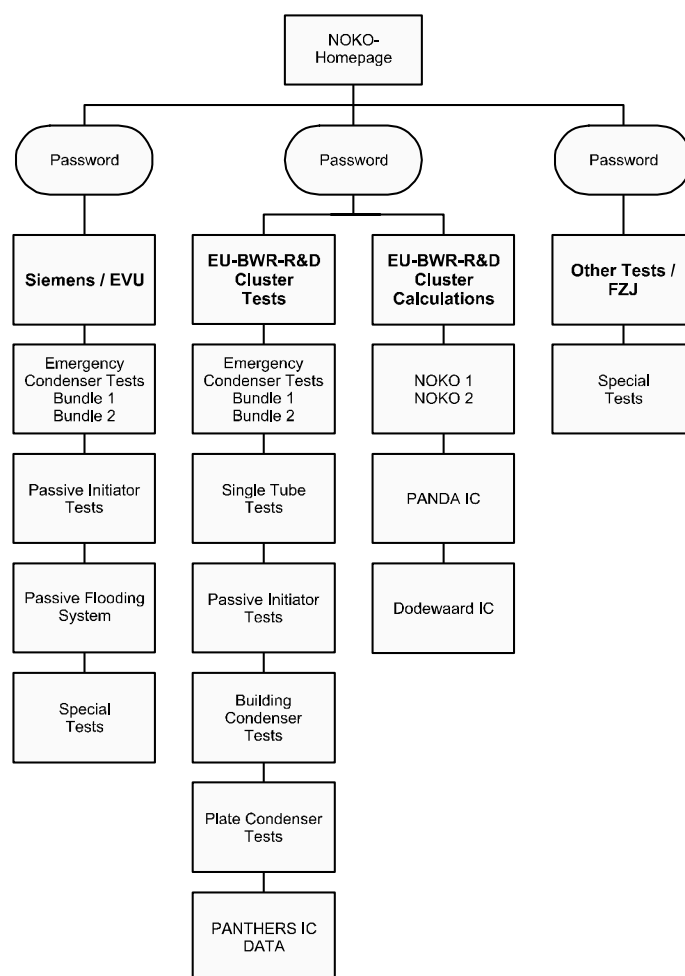
FIG. 3. Structure of the NOKO-Data in the Internet.

3.   TEST CONFIGURATION AND SELECTED RESULTS

Original dimension and material – but not the original number or area – were used for the test sections Emergency Condenser, Building Condenser, Plate Condenser and Passive Initiator. For all tests the thermal hydraulic boundary and initial conditions were equivalent to these of the SWR 1000; the only exception was that Helium instead of Hydrogen was used for related tests.

3.1. Emergency Condenser 1. Bundle

In Fig. 4 the configuration with the first Bundle is shown; the geometrical data for one tube are:

average length   10 m
inner diameter   38.7 mm
wall thickness   2.9 mm.

In Fig. 5 the experimental data (solid lines) are compared with calculations with 4 different codes; the agreement is good.

3.2. Emergency Condenser 2. Bundle

It could be calculated that the tube wall is responsible for more than 50 percent of the total heat transfer resistance. Therefore, a second bundle was used with the geometrical data.

total length: about 10 m
inner diameter: 44.3 mm
wall thickness: 2.0 mm.
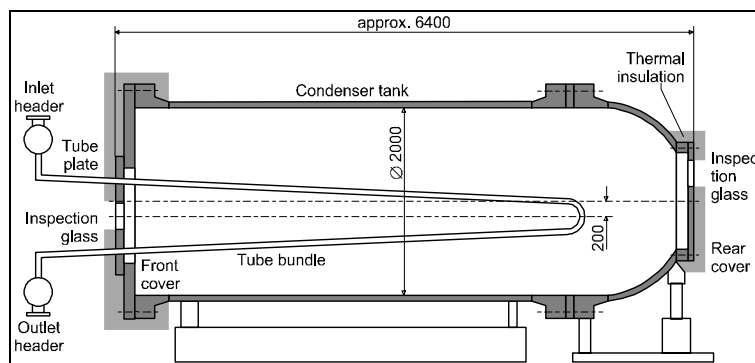
FIG. 4. The design of the Emergency Condenser (EC).
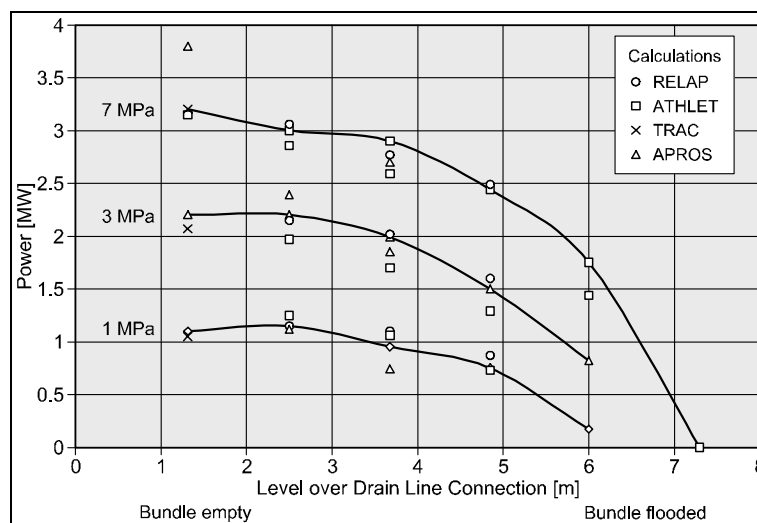
FIG. 5. Power transfer to the water pool with the EC with four tubes.

217

In addition, the bundle was oriented in a vertical position, under an angle of 40.9° and in a horizontal position.

The experimental results and a comparison with ATHLET calculations are shown in Fig. 6. From sensitivity studies it has been evaluated that the thermalhydraulic codes like ATHLET or CATHARE are calculating well the integral power transferred, but deviate substantially in the in-tube heat transfer by condensation processes. Therefore, special tests with a single tube only and an improved instrumentation were performed. In addition, special tests and measurements for 3D-temperature fields in the water pool have been performed, see the isothermes in Fig. 7 for one of the tests.

3.3 Building Condenser

The NOKO facility has also been used to study the effectiveness of systems removing the decay heat from the containment.
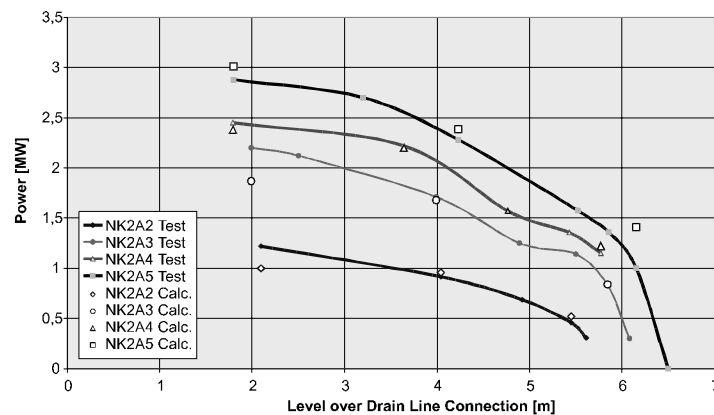
FIG. 6. NOKO-2 power levels from test and calculations with ATHLET for the bundle in vertical position and three tubes.
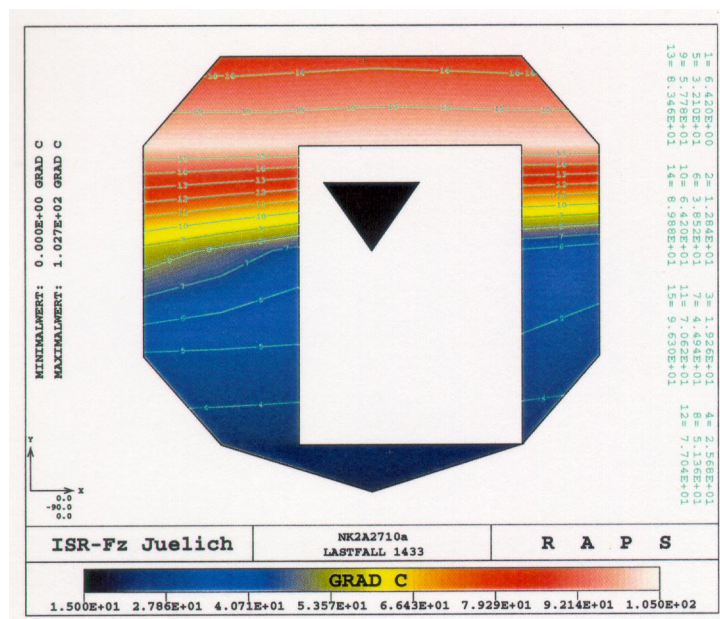
FIG 7. Isoterms in pool with the vertical bundle heated only in the upper part.

218
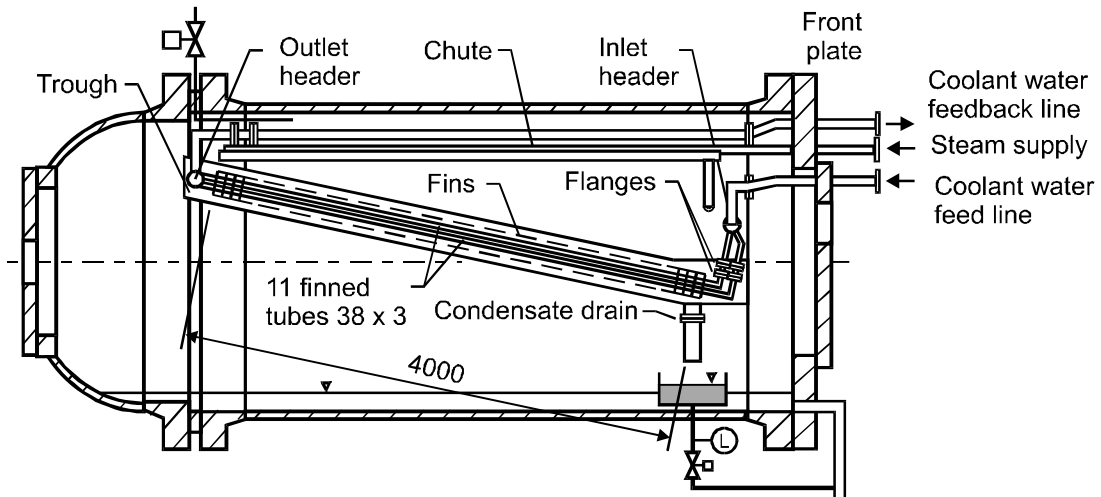
FIG. 8. Building condenser in NOKO without trough and fall pipe.
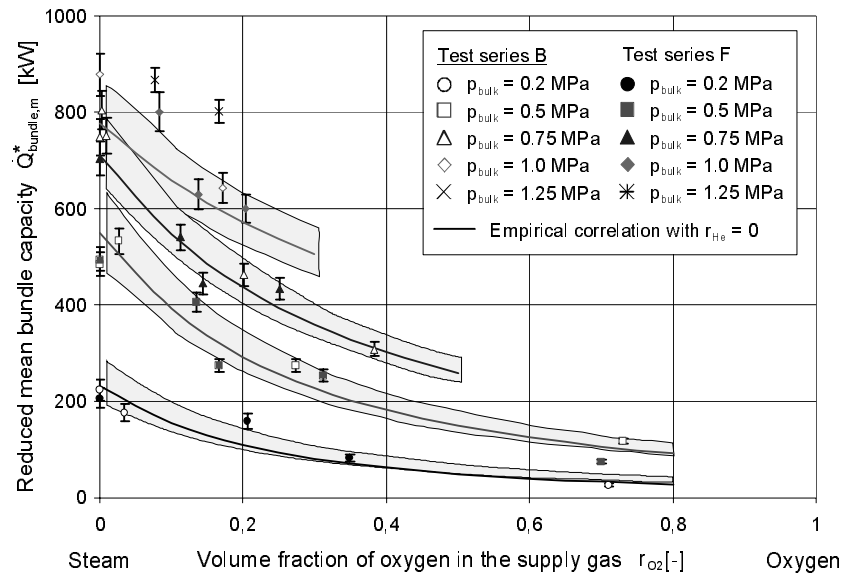
FIG. 9. Bundle capacity as a function of the total pressure and the volume fraction of oxygen.

In Fig. 8 the configuration of the building condenser within the condenser tank is shown.

In Fig. 9 test results showing the influence of non-condensables on the energy transport from the building condenser to the environment are shown.

3.4   Plate Condenser

Tests have been performed with a Plate Condenser, which was installed within the Condenser Tank, see Fig. 10. The atmosphere tested was pure steam, a mixture of steam and oxygen, a mixture of steam and helium and a mixture of steam, oxygen and helium.

In Fig. 11 the influence of the non-condensables on the transferred power is shown. Fig. 12 shows one test with steam and oxygen, showing an accumulation in the lower part of the tank.
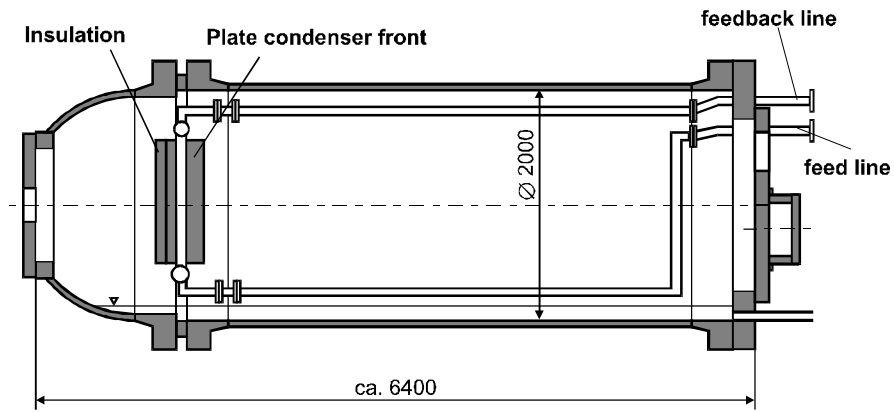
FIG. 10. Condenser vessel.
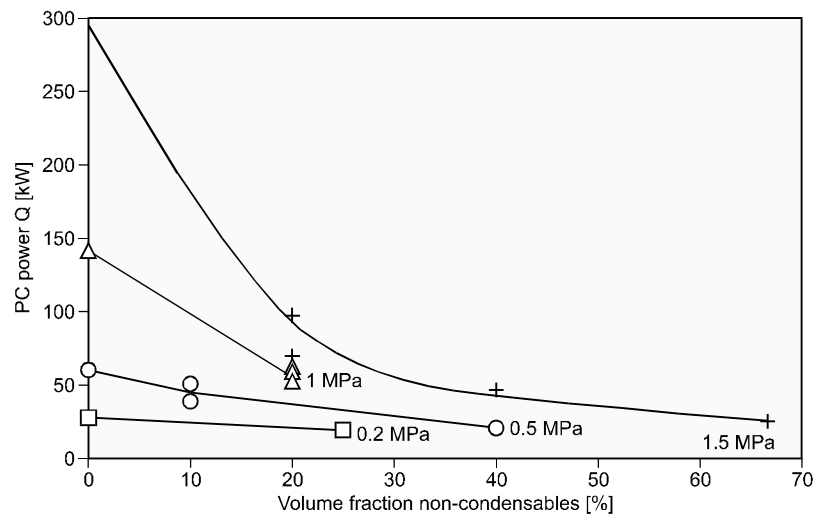
FIG. 11. Normalized power of the plate condenser calculated with RALOC as a function of the inert gas volume fraction.
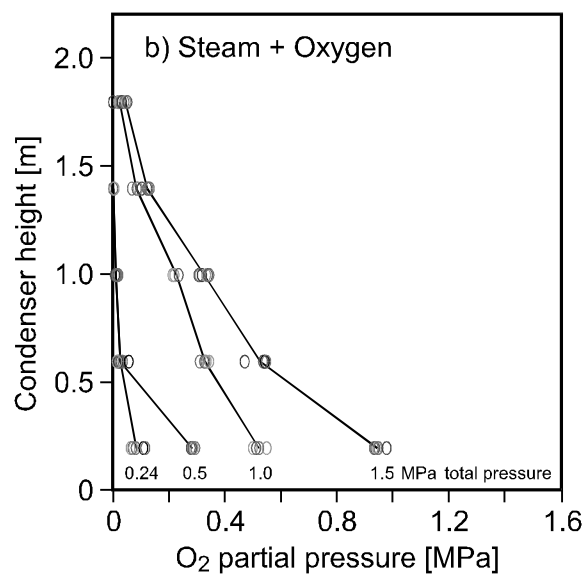
FIG. 12. Vertical concentrations.

3.5 Passive Initiators

Passive Initiators (PI) are small heat exchangers outside the Reactor Pressure Vessel (RPV); one line of this heat exchanger is connected to the RPV well above the normal water level and the other line well below the water level. Both lines are always open to the RPV. The secondary side of the Passive Initiators is filled with water. In case of a substantial water level decrease in the RPV steam will condense inside the PI and heat up the secondary side resulting in a pressure build-up. This can be used for control purposes. In Fig. 13a the four designs tested are schematically shown. In Fig. 13b the pressure build-up on the secondary side and the outflow is given for water and ethylacetate (ESEE), which has a lower boiling point than water.
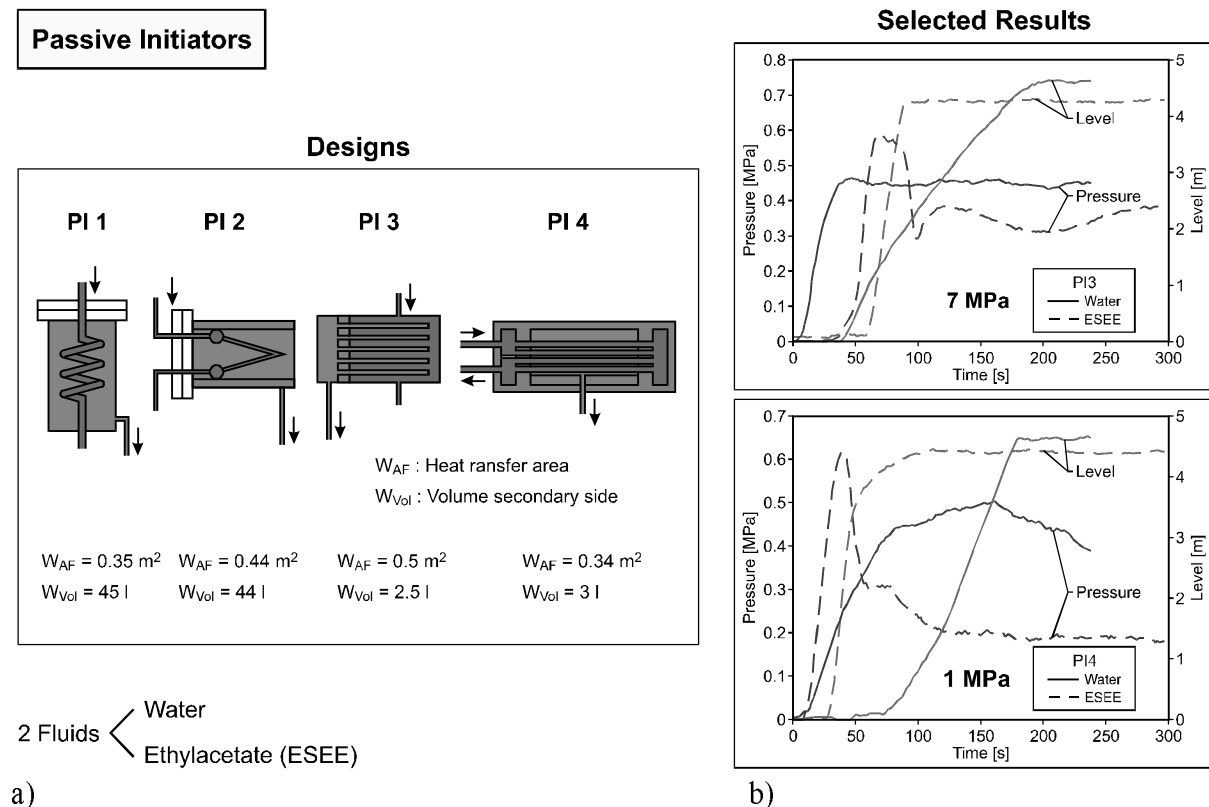
FIG: 13. Designs (a) and experimental results (b) of the different passive initiators.

3.6 A Passive flooding system

Tests have been performed with a passive flooding system. The objective was the experimental verification of the flooding of a pressure vessel with water from an outside water pool, using a special check valve.

3.7 Passive decay heat removal during shutdown

With a flooded pressure vessel it could be shown that it is possible to remove decay heat from the core region to an outside pool by natural convection, see [3].

4. THE TOPFLOW FACILITY

A Saxony collaboration consisting of the Institut für Sicherheitsforschung of the Forschungszentrum Rossendorf (FZR) e.V., the University of Dresden (TUD) and the Hochschule für Technik, Wirtschaft und Sozialwesen Zittau-Görlitz (HTWS) are going to take over the NOKO facility, which will be reconstructed as TOPFLOW (Transient Two Phase Flow Test Facility) at FZR. TOPFLOW will mainly be used for the investigation of generic and applied steady state and transient two-phase flow phenomena in power and process industries. Main fields of activities are the investigation of:

- transient flow regimes in horizontal, vertical and inclined tubes,

- critical mass flows and oscillations during depressurization,

- natural convection in parallel channels and feed pipes,

- condensation phenomena in horizontal tubes,

- dynamic behaviour of interphase area in bubble columns,

- non-equilibrium effects.

The philosophy of the facility is, that working groups throughout Europe shall be invited to come to Rossendorf with their ideas and to perform their experiments here making use of the wide range of parameters (power, water and steam mass flow, pressure range, measuring instrumentation) offered by TOPFLOW.

4.1   Main modifications

The flow diagram of the TOPFLOW facility is given in Fig. 14; a front and a side view is shown in Fig. 15.
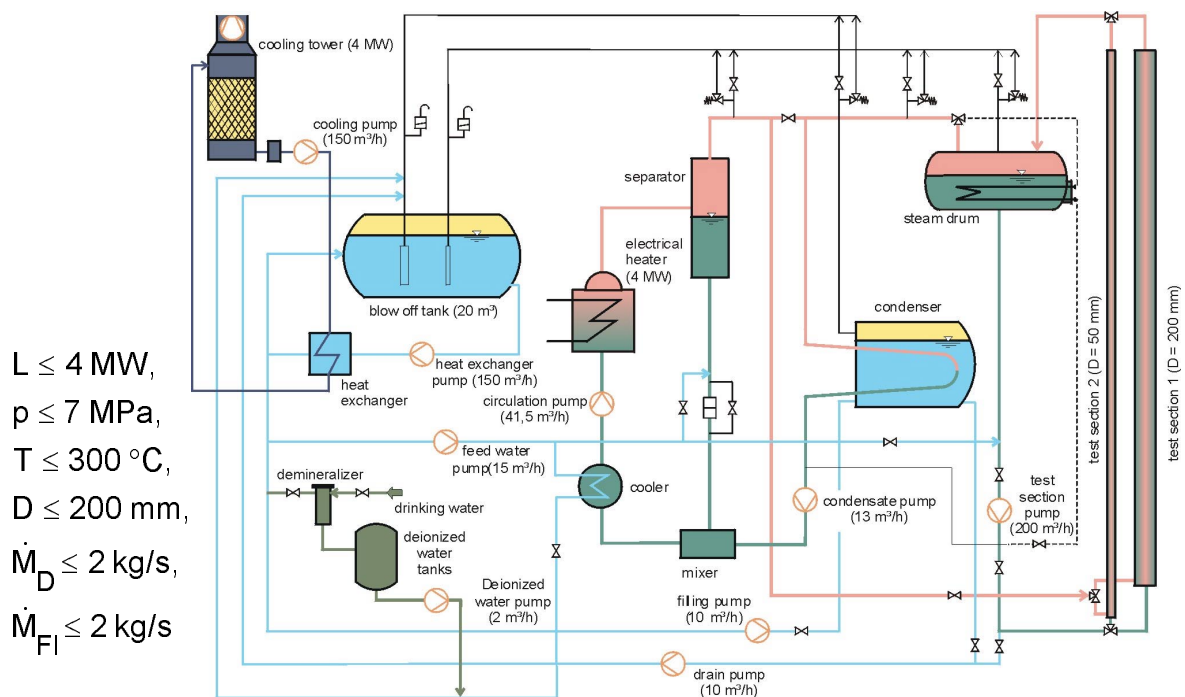
FIG: 14. Flow diagram of the TOPFLOW test facility.

The main additional test sections are the steam drum (L = 5 m, D = 1.5 m, V = 8 m³) and two vertical pipes (D = 50 and 200 mm, L = 10 m) to be used for the instrumentation development, evaluation of flow profiles, WWER steam generator behaviour during small break LOCA and the investigation of heat up, local steam production and temperature stratification in large water pools and turbulence. Additionally several junctions are foreseen for the connection of further test sections like a PWR hot leg model [4]. The pressure vessel has been removed but is still available if needed.

The data acquisition systems will be replaced and extended, e.g. the number of the measurements as well as the acquisition rate are increased. Additionally the balance of plant system will be replaced and is now computer controlled.
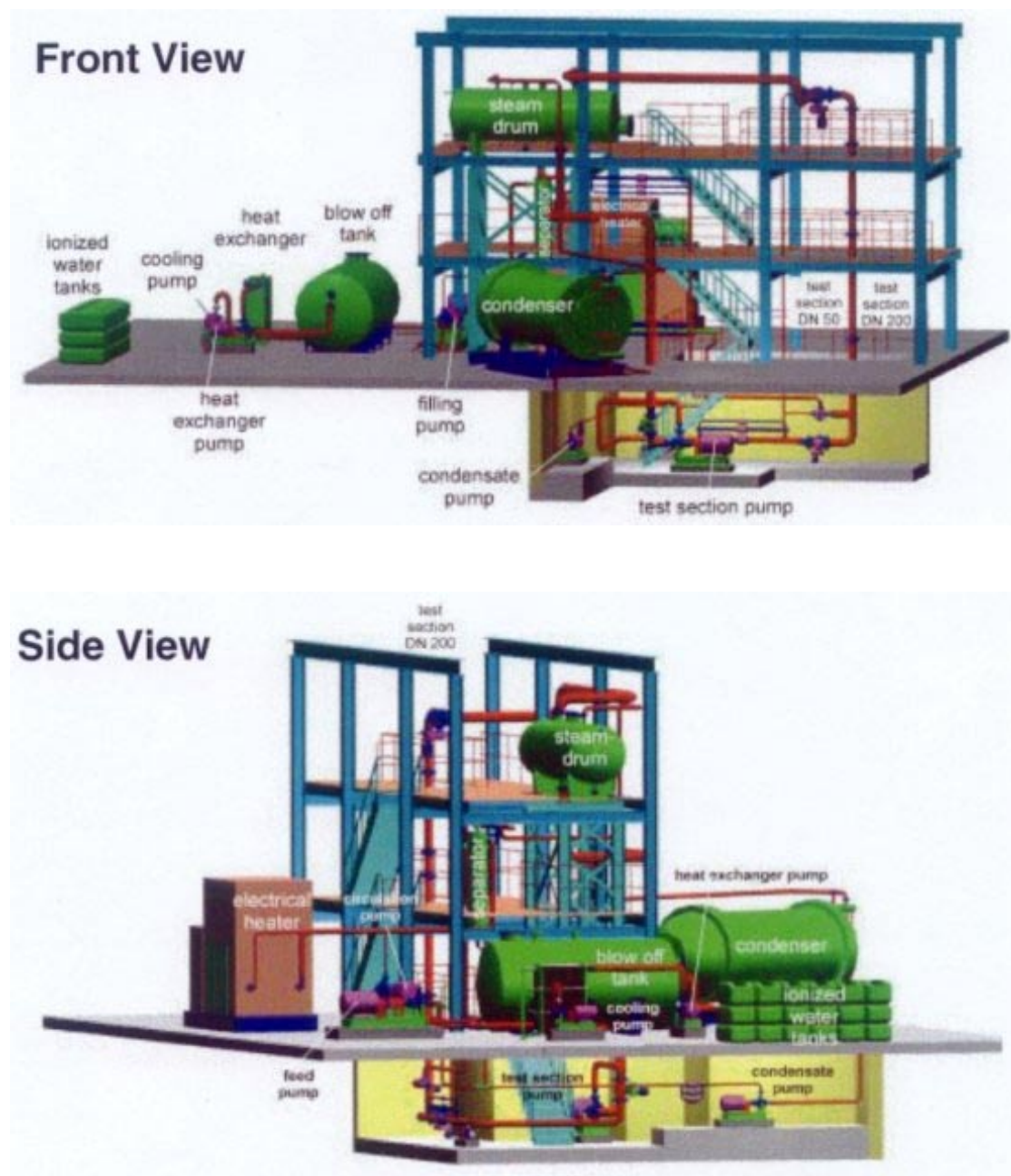
FIG. 15. Front and side view of the TOPFLOW test facility.

4.2 The Instrumentation Development

TOPFLOW will be equipped with advanced two-phase instrumentation mainly and adapted and developed in Rossendorf, such as wire-mesh sensors, needle-shaped conductivity probes with integrated thermocouple, gamma and X-ray tomography and passive ultrasonic droplet probes. Additionally, laser-doppler anemometry and a phase-doppler particle analyser are available. Two of these devices, the needle-shaped conductivity probes with integrated thermocouple and the wire-mesh sensors will be described in detail.

Advanced needle probes are equipped with a micro thermocouple substituting the traditional electrode. These probes combine a local phase indication with a fast temperature measurement, so that the temperature can be correctly related to the instantaneous phase state. This allows to distinguish between steam and non-condensable gas in the gas phase and can be used to measure the sub-cooling in the liquid phase and temperature gradients at the inter-phase boundary [5].

FZR has developed wire-mesh sensors for gas-liquid flows, which allow a fast visualisation of transient gas fraction distributions in a tube [6]. The function is based on the measurement of the local instantaneous conductivity of the two-phase mixture. The sensor consists of two electrode grids with 16 electrodes each, placed at a small axial distance behind each other. The conductivity is measured at the crossing points of the wires of the two grids. One plane of electrodes is used as transmitter, the other as receiver plane. During the measuring cycle, the transmitter electrodes are activated by supplying with voltage pulses in a successive order. The currents arriving at the receivers are recorded. This procedure is repeated for all transmitter electrodes.

Sensors of this kind were applied at FZR to an air-water flow test loop in a vertical pipeline (inner diameter D = 51.2mm) as well as to a cavitating flow behind a fast acting valve. The high resolution of the sensor allowed to obtain bubble size distributions and to study the evolution of the flow structure along the pipe [7]. The maximum time resolution available to perform these experiments was 1200 measurements per second. Recently, the measuring rate was increased to 10 000 frames per second with sensors of 16 × 16 measuring points. In the result it is possible to visualise and quantify individual bubbles or droplets at a much higher flow velocity, than before.

It is planned to apply this type of fast flow visualisation to different test sections of the TOPFLOW facility. In the first experiments, the flow pattern in a vertical pipeline of 200 mm diameter will be studied. A special developed sensor will allow to achieve a spatial resolution of 3 mm at a measuring rate of 2 500 frames per second. For this purpose, the sensor must consist of 64 transmitter and 64 receiver wires (64 × 64 measuring matrix).

4.3 Potential test series

The following test series related to natural convection are under consideration:

- boiling in large water pools
- WWER steam generator behaviour with out/with non-condensables
- two phase flows in typical reactor geometries (e.g. hot leg, downcomer)
- operational mode and effectiveness of passive safety systems.
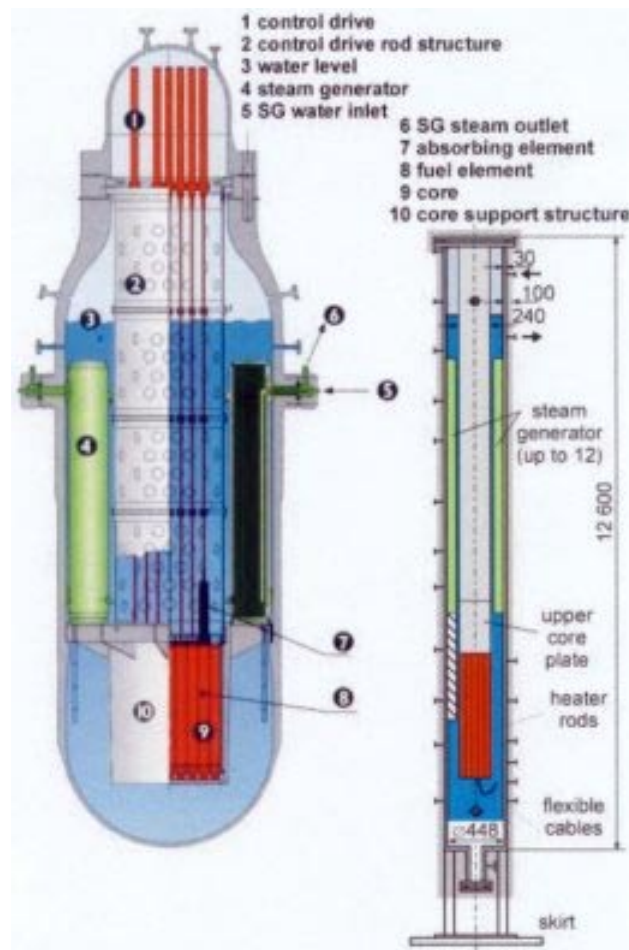
FIG. 16. Selected Convection Phenomena related to the Argentinean CAREM PWR Project.

A first feasibility study has been performed regarding a reactor with internal circulation flows. The Argentinean CAREM PWR Project has been used as a model. In Fig. 16 a comparison between the CAREM Reactor and its modelling in TOPFLOW is shown.

5. CONCLUSIONS

With the NOKO facility high quality data have been produced. They were used to study phenomena and used as a basis for comparison with code calculations.

Based on the experience gained with the NOKO facility the TOPFLOW facility will be improved and its test spectrum extended. Especially the development of two-phase instrumentation will be a major goal.

REFERENCES

[1]   A. SCHAFFRATH, H. JAEGERS. Allgemeine Beschreibung des NOKO-Versuchsstandes, Jül-3167, Forschungszentrum Jülich, Januar 1996.
[2]   A. SCHAFFRATH. Experimentelle und analytische Untersuchungen zur Wirksamkeit des Notkondensators des SWR 600, Abschlussbericht zum Forschungsvorhaben BMBF 15 NU 09485, Ruhr-Universität Bochum, RUB ISR-01, Bochum, März 1997.

[3]   H. JAEGERS, E. HICKEN, P. DAVID, R. KOSCHMIEDER. Decay Heat Removal during Shut-down, INNO-IPSS(00)-D-2.1.9, Research Center Jülich, June 2000.

[4]   A. SCHAFFRATH, A.-K. KRÜSSENBERG. Investigation of multiphase and multicomponent flows - experiments and measurement devices. Seminare Politecnico di Milano, Dipartimento di Ingegneria Nuclerare, Milano, March 13, 2000.

[5]   A. SCHAFFRATH, H.-M. PRASSER. Theroretical support to the NOKO experiments, Final report of Workpackage 2 of the "BWR Physics and Thermohydraulic Complementary Action (BWR-CA), FZR-224, June 1998.

[6]   H.-M. PRASSER, A. BÖTTGER, J. ZSCHAU. A new electrode tomograph for gas-liquid flows, Flow measurement and instrumentation 9 (1998), p. 111-119.

[7]   A.-K. KRÜSSENBERG, H.-M. PRASSER, A. SCHAFFRATH. A new criterion for the identification of the bubble slug transition in vertical pipes, Kerntechnik 65 (2000), No. 1, p.7-13.

Passive decay heat removal from the core region

E.F. Hicken, H. Jaegers

Institute for Safety Research and Reactor Technology, Forschungszentrum Jülich
Germany

Abstract. The decay heat in commercial Light Water Reactors is commonly removed by active and redundant safety systems supported by emergency power. For advanced power plant designs passive safety systems using a natural circulation mode are proposed; several designs are discussed. New experimental data gained with the NOKO and PANDA facilities as well as operational data from the Dodewaard Nuclear Power Plant are presented and compared with new calculations by different codes. In summary, the effectiveness of these passive decay heat removal systems have been demonstrated; original geometries and materials and for the NOKO facility and the Dodewaard Reactor typical thermal-hydraulic inlet and boundary conditions have been used. With several codes a good agreement between calculations and experimental data was achieved.

1. INTRODUCTION

The decay heat in commercial Light Water Power Reactors is commonly removed by active safety systems which require redundant systems as well as emergency power. This is expensive and requires time for maintenance and testing.

Therefore – when studying advanced power plant designs – the decay heat removal by passive safety systems was re-evaluated. In Fig. 1 some passive safety systems under consideration are shown.
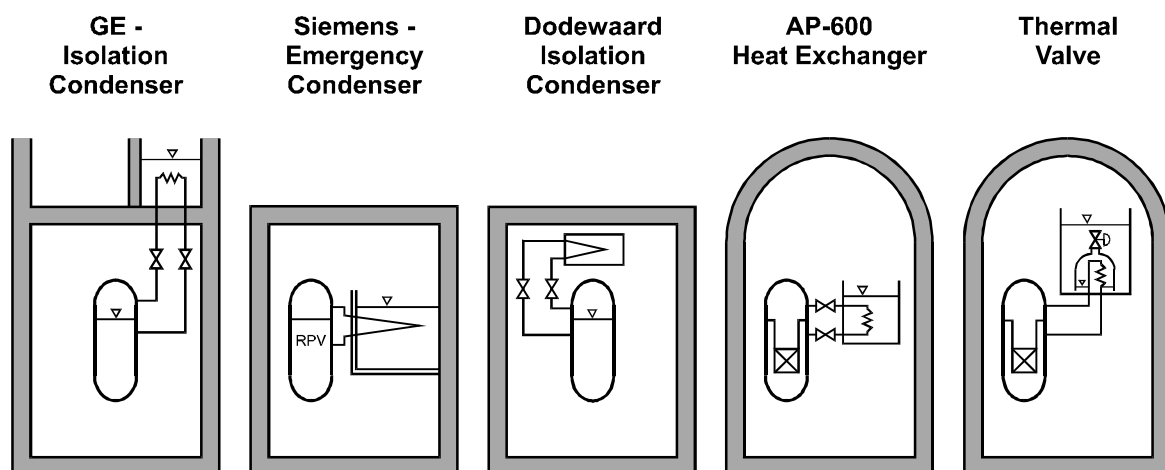
FIG. 1. Design for passive decay heat removal.

For PWR the use of heat exchangers submerged in a large water pool (up to several thousand m³) is evident. The working principle is well known and can be calculated with well validated codes. However, to avoid heat losses during normal operation in the range of several per cent of the total thermal power valves have to be installed in the pipes to and/or from the heat exchanger. This definitely reduces the reliability of the decay heat removal as well as it results in additional costs. The expensive valves can be avoided if the principle used for the so-called

"Thermal Valve" is applied: the heat exchanger – now without valves in the high-pressure lines – is installed within a bell-shape volume. On signal by the reactor protection system or by manual operation a valve at top of the volume opens allowing heat removal by water circulation. This proposed design, however, has to be validated against experiments and related code calculations.

The principle already used in BWR's and again proposed for advanced BWR designs is the Evaporation – Condensation mode: water in the core region is evaporated by decay heat and condensed within a heat exchanger placed in a water pool, the condensate returns to the core region.

This principle has been used in the Dodewaard Reactor and some other reactors already decommissioned. This principle has been proposed for the advanced BWR, the SBWR and the SWR 1000. Experimental results and comparison with code calculations will be given below.

The two new designs – for the SBWR and the SWR 1000 – show some remarkable differences; some will be discussed below.

1)   Both designs need a large water pool. Due to the fact that the heat exchanger for the SWBR can be placed above the Reactor Pressure Vessel (RPV) – thus allowing more flexibility in the design – valves are needed in the lines to and from the heat exchanger. Therefore, the heat exchanger can also be placed outside the containment. The heat exchanger and the water pool of the SWR 1000 have to be placed at the elevation of the core and within the containment.

2)   The operation of both designs is quite different. When opening the valves in the connecting lines the full heat exchanger capacity is available from the beginning while the heat exchanger of the SWR 1000 will start slowly from zero to full capacity.

3)   These passive heat exchangers are mainly designed to be used for a decay heat removal without a loss-of-coolant sequence; for some time they assist the heat removal in case of small breaks – for large break LOCA they are of no benefit.

4)   The modelling of the phenomena and system behaviour with these designs is not always easy as it will be shown below, because the condensation behaviour inside the heat exchanger tubes – including the presence of non-condensables – as well as the heat transfer from these tubes to the water pool has to be considered.

5)   Heat exchangers using condensation of steam are always sensitive to the accumulation of non-condensables. If no venting capability is installed the concentration has to be kept below a value, where the non-condensables can be dissolved in the condensate.

6)   There exists some operating experience mainly in the Dodewaard Reactor.

2.   EXPERIMENTAL   AND   ANALYTICAL   RESULTS   REGARDING   THE EFFECTIVENESS OF CONDENSERS

The results presented in the following chapters were gained within the project "European BWR-R&D Cluster for Innovative Passive Safety Systems (INNO-IPSS)" supported by the EU within the 4th framework programme.

228

2.1. The Emergency condenser

The design of the Emergency Condenser, as already used in the Gundremmingen Unit A Power Plant, is shown in Fig. 2. The tubes are about 10 m long. The tube inner diameter is 38.7 mm and the wall thickness 2.9 mm. Because the wall thickness resulted in a thermal conductivity of about two thirds of the total thermal conductivity a second bundle was designed with an inner diameter of 44.3 mm and the minimum acceptable wall thickness of 2 mm. Tests with the second bundle were performed with the bundle oriented in a vertical position, under an angle of 40.9° and in a horizontal position. The orientation under an angel of 40.9° should decrease the height between a flooded bundle (with zero energy transfer) and an empty bundle (with maximum energy transfer to the pool); in addition the mixing within the pool should be enhanced.

FIG. 2. Bundle of the emergency condenser with dimensions

The tests have been performed under the same thermal conditions as in a real BWR; the pressures chosen were 7, 5, 3 and 1 MPa. The tests were performed in the NOKO facility, see Appendix A. The test procedure started with a flooded bundle, then the water level in the pressure vessel was decreased stepwise until the bundle was empty.

In Fig. 3 and 4 the experimental results are given. It should be added that the accuracy of the results ranged between less than 10 per cent for high powers and several ten per cent for power levels below 1 MW; the conditions for a flooded bundle are - on the other hand – relatively accurate.

In principle, the dependence of the transferred power on the water level in the pressure vessel is similar for both bundles. The influence of the orientation of the bundle is only minor, see Fig. 4.

Post-test calculations with ATHLET are shown in Fig. 3 for the first bundle and in Fig. 5 for the second bundle; the agreement is good. The distortion at about 5 m is due to the vertical part of the bundle.

It was shown that despite the good agreement for the (integral) transferred power the local deviations in the heat transfer during condensation as calculated by the ATHLET and CATHARE, see Fig. 6, are large.
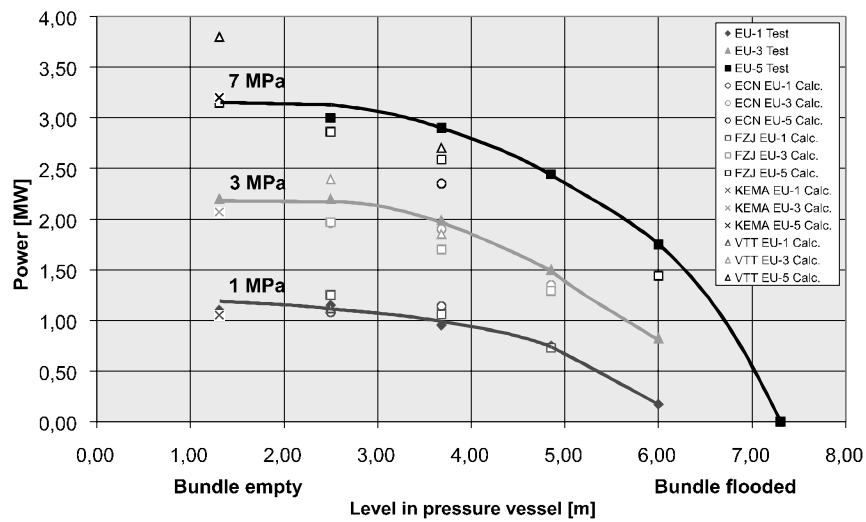
FIG. 3. Results of the first NOKO-EC bundle tests (4 tubes).
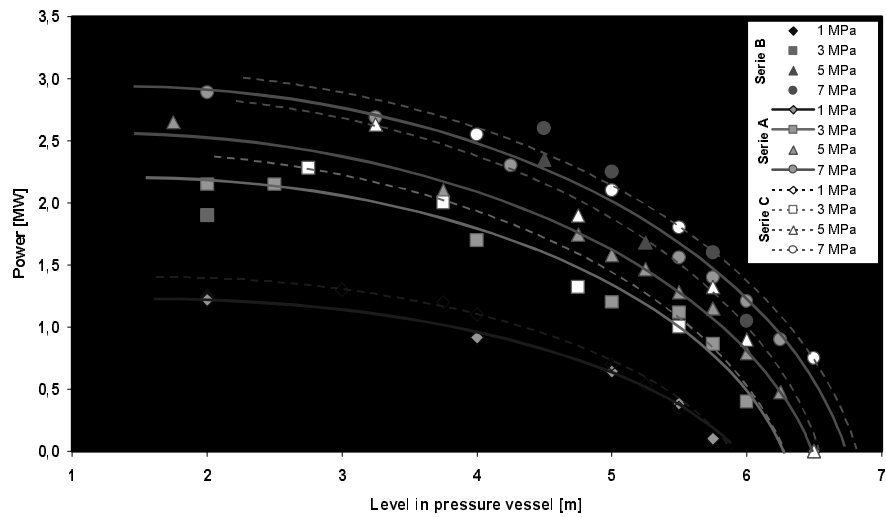

FIG. 4. Results of the second NOKO-EC bundle tests (3 tubes, for horizontal bundle 4 tubes).
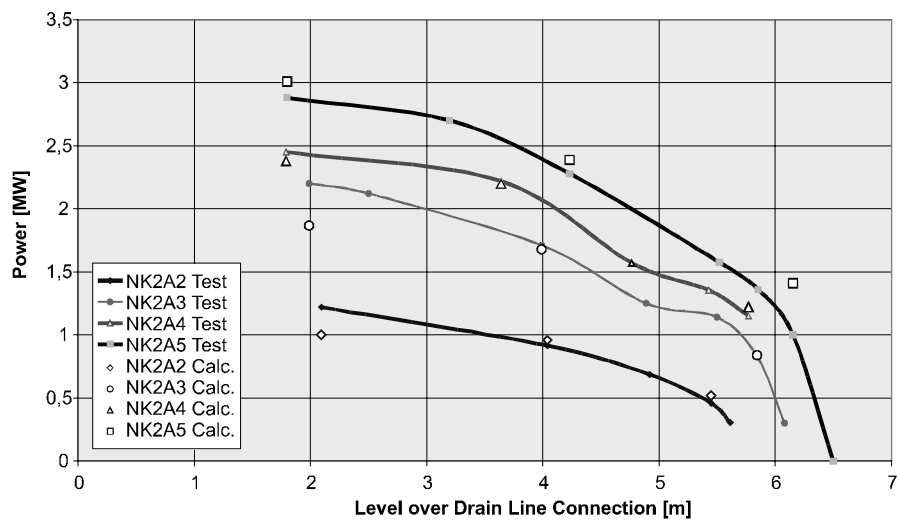

FIG. 5. NOKO-2 power levels from tests and calculations for the bundle in vertical position
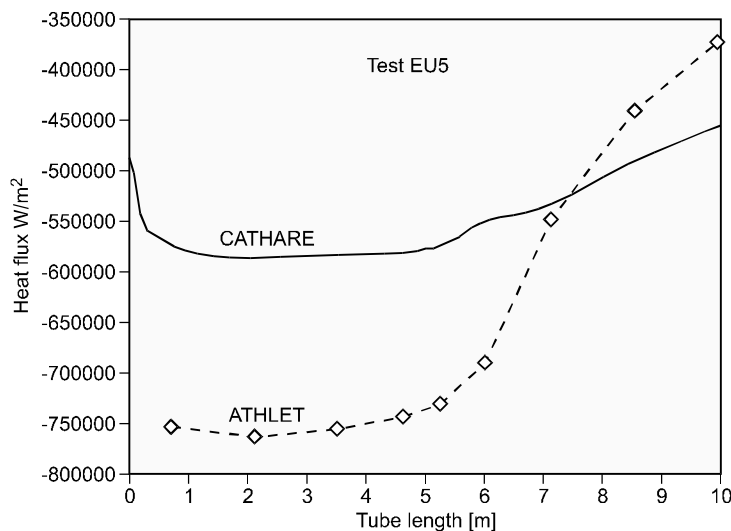
230

FIG. 6. Comparison between ATHLET and CATHARE calculation results.

Therefore, for orientation tests were performed with a single tube (dimensions of the first bundle) instrumented with needle probes for the identification of the film thickness. To better study the film thickness a test tube with a tube of the second bundle and movable film probes are underway.

It was a result of the single tube tests that non-condensables were accumulated in front of the condensed water rather than been distributed along the tube.

2.2. The isolation condenser

Fullscale tests with an Isolation Condenser (IC) as proposed for the SBWR from GE have been performed in the PANTHERS facility. Because the results are proprietary special tests have been performed in the PANDA facility, see Appendix B.

The design of an IC is schematically shown in Fig. 7; vertical tubes are connected to an upper (inlet-) header and a lower header.

Tests with pure steam as well as tests with a mixture of steam and helium (up to about 14 per cent) were performed.

In Fig. 8 test results with pure steam and calculated results with ATHLET are shown.

2.3. The Isolation Condenser in Dodewaard

The design of the Isolation Condenser in the Dodewaard Reactor is shown in Fig. 9. Some operational tests have been performed as well as some sequences occurred where the isolation condenser was used to cope with transients.

Because the operational instrumentation did not completely cover the phenomena needed for a detailed analysis and because some manual operation (not documented in detail) was used to cope with the transient a detailed evaluation of the operational data is not possible. Therefore, in Fig. 10 calculated values for the Dodewaard Isolation Condenser is given. One power level could be compared with a TRAC calculation; the agreement is good.
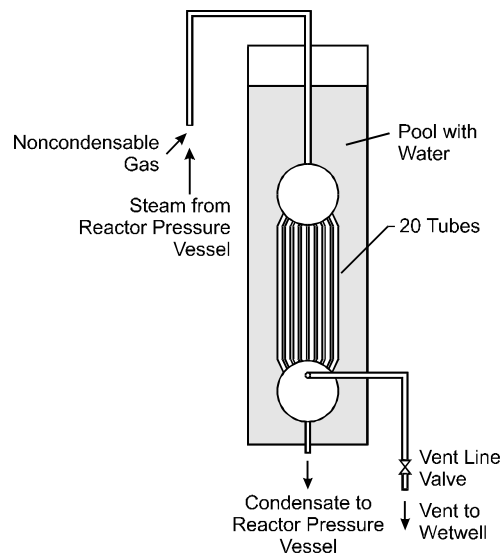
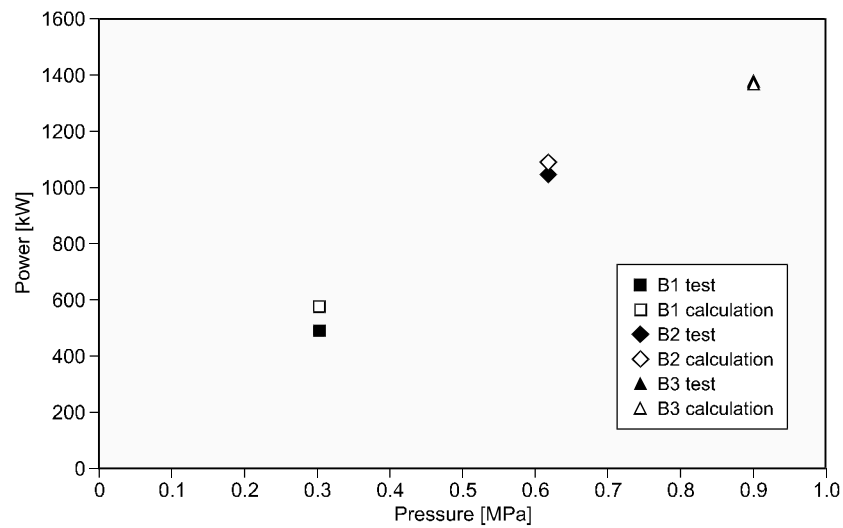FIG. 7. Arrangement of the PANDA-IC in the pool.

FIG. 8. Power levels of the PANDA-IC calculated with ATHLET as a function of pressure for the pure steam tests.
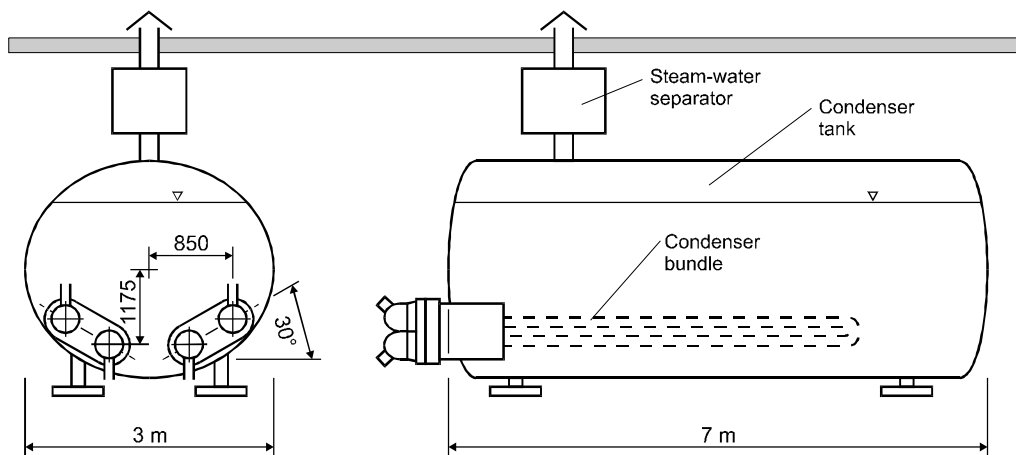

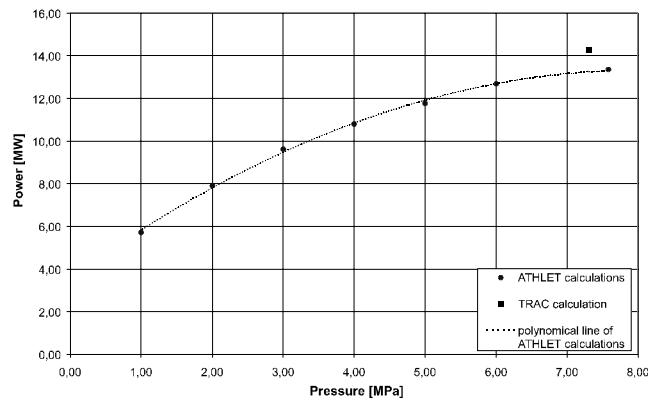FIG. 9. Arrangement of the isolation condenser in the condenser tank of the Dodewaard nuclear power plant.

FIG. 10. Power levels of the Dodewaard Isolation Condenser calculated with ATHLET as a function of pressure

3.   DISCUSSION AND CONCLUSIONS

The requirements from licensing bodies for the acceptance of experimental and analytical data in a licensing process are quite higher now than 10 or 20 years ago.

To the extend possible original geometries and materials should be used; if this is not possible, reliable scaling rules should exist.

> For the Emergency Condenser (EC) and the Dodewaard Isolation Condenser (IC) original geometries and materials were used. The Isolation Condenser in PANDA is a scaled-down test section. However, the components with original geometries and materials have been tested in the PANTHERS facility; the data are not publicly available except for the licensing bodies.

The equivalent thermal-hydraulic initial and boundary conditions should be used.

> This is the case for the EC and the Dodewaard IC. The PANDA IC was limited to 1 MPa, but the full pressure has been used in PANTHERS.

To the extend possible the components should be tested also with beyond-design thermal-hydraulic conditions and for low-power or shutdown situations.

> The EC and PANDA IC have also been tested with non-condensables in the inlet flow. The EC has been tested with shutdown situations.

The data and procedures should be documented; an uncertainty analysis should be available.

> With the exception of the Dodewaard IC those requirements could be met.

The sequences tested should be simulated with at least one computer code and the results compared with the experimental data.

> This has been extensively done for the EC and PANDA IC test series.

In conclusion, tests as well as related calculations with several computer codes have been performed for passive decay heat removal systems. The spectrum tested and the quality should allow its use in a licensing process.

Appendix A

NOKO Facility

The NOKO test facility located at the Institute for Safety Research and Reactor Technology of the Research Center Jülich is a thermal hydraulic test rig, which was constructed within the framework of a research task in a joint project of the Research Center Jülich (FZJ) and SIEMENS AG, Power Generation Division (KWU), with support from the German Federal Ministry of Education, Science, Research and Technology and German utilities. The facility is suited for a broad spectrum of experiments in the field of thermodynamics and fluid dynamics of water, water vapor and non-condensable gases. Different passive safety systems can be investigated with only minor modifications.

The parameter limits given by the design are:
- maximum primary pressure: 7 MPa;
- maximum secondary pressure: 1 MPa;
- maximum power: 4 MW.

The maximum temperatures are the corresponding saturation temperatures.

The NOKO facility is composed of three sections. The first section is the primary circuit with the pressure vessel, the bundle of the emergency condenser and the associated connecting lines. The second section is the secondary side with condenser tank, relief lines and relief tank. The system of steam generation with electric boiler, separator and the associated lines forms the third section. The arrangement and linkage of the individual sections can be seen from Figure A1.
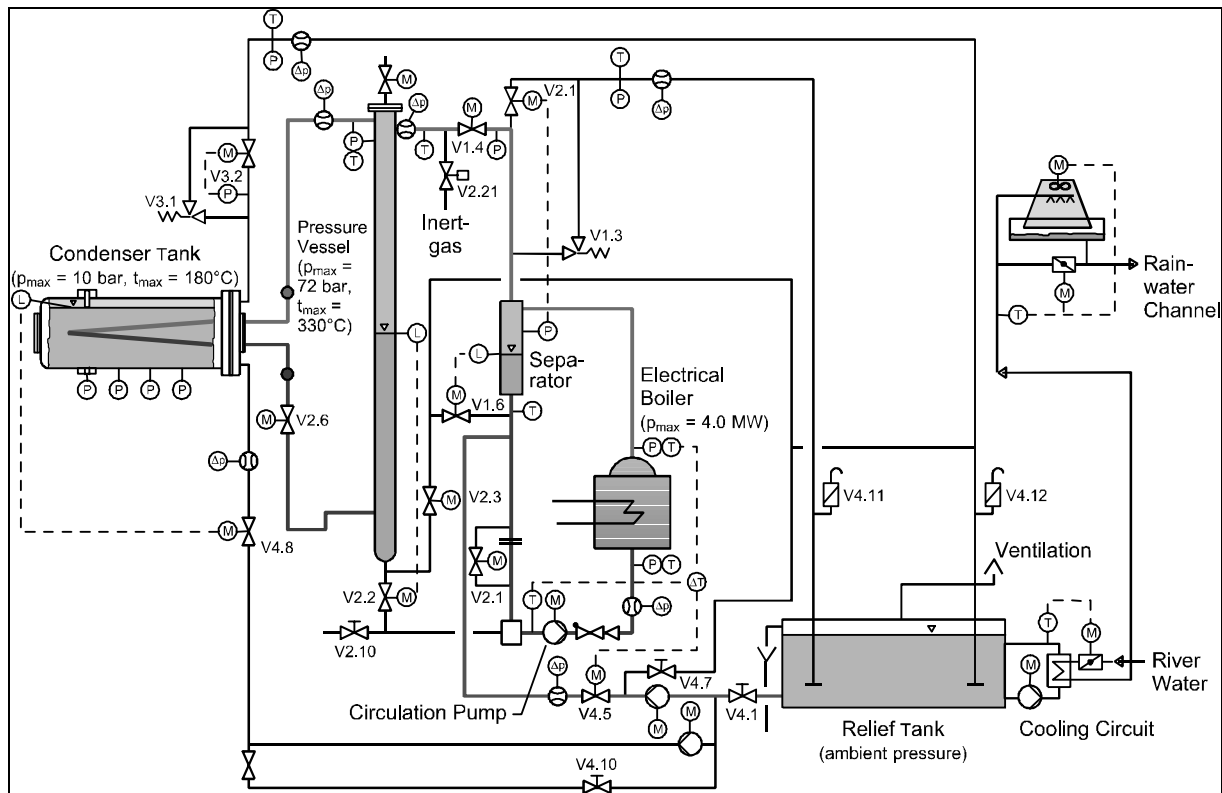

Fig. A1. System diagram of the NOKO facility.

The steam-water mixture produced in the electric boiler is passed into the water - steam separator where the steam is separated from the water. The water is pumped back into the electric boiler. The separated steam is either passed into the pressure vessel or - if more steam was produced than is needed - the excess steam blown off into the relief tank. The steam is condensed in the relief tank which is cooled by an external cooling circuit. The components are made of austenitic steel. An exception is the condenser tank, which consists of ferritic steel and is internally coated with XYVADUR 569 for reasons of corrosion protection. This coating is resistant up to 200°C.

Appendix B

PANDA facility

The PANDA test facility was erected in the early 1990s within the framework of the so-called ALPHA Program (Advanced Light Water Reactor Passive Heat Removal and Aerosol Retention Program) at the Paul Scherrer Institute. The PANDA test facility is a large-scale thermal hydraulic low-pressure test facility for investigating passive decay heat removal systems for the next generation of Light Water Reactors. In the first instance, PANDA is used to examine the integral long-term performance of the Passive Containment Cooling System for the Simplified Boiling Water Reactor (SBWR). The facility is an approximately 1:25 volumetric, full-scale height simulation of the SBWR containment system.

Within the project here, experiments with newly developed components were carried out in the PANDA test facility. This included the PANDA isolation condenser, the SWR-1000 building condenser and a plate condenser. All three components serve for heat removal from the containment after a serious accident.
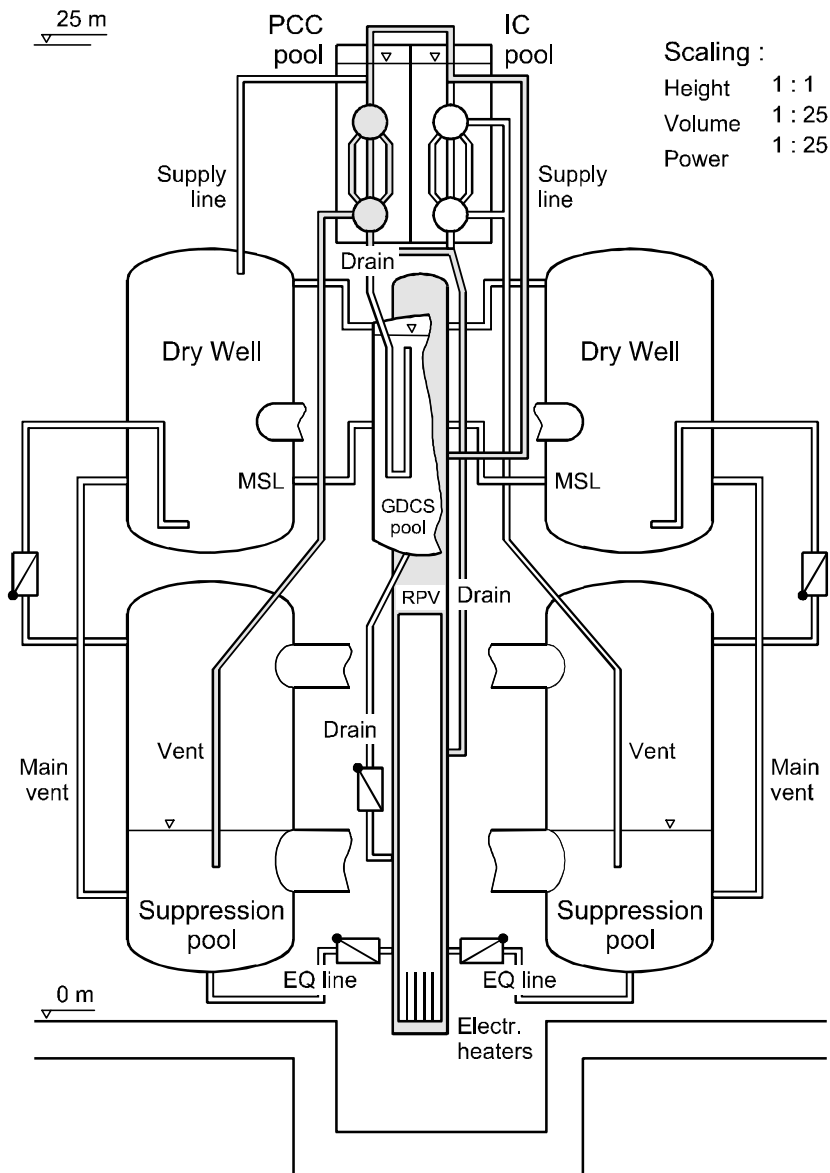
FIG. B1. Schematic setup of the PANDA test facility.

The PANDA test facility is of modular design. It consists of a pressure vessel simulating the reactor pressure vessel, two dry-well and two wet-well containers as well as a Gravity Driven Cooling System (GDCS) pool. The facility has two separated water pools. In a water pool two passive containment coolers (PCC) are installed. In the other pool one PCC which was also used as an isolation condenser (IC) was placed. The condensers are full-scale mock-ups which only differ from those projected for the SBWR by the number of tubes. The setup of the facility is shown in Figure B1 comprising also the connections between the containers, which are not described here in detail.

The PANDA-PCC consists of 20 vertically arranged tubes connected at their ends with drum-type headers. The upper header has a connection for steam supply, the bottom header has a drain for the condensate produced and a drain for non-condensable gases. The tubes of the PCC have an outside diameter of 50.8 mm and a wall thickness of 1.65 mm. They are made of austenitic steel.

The PCC as well as the IC are passively acting components. They are heat exchangers serving to condense steam. The gas flows to the condensers without the use of pumps. It enters into the upper drum and most of the steam is condensed in the vertical tubes. The condenser pool has a ground surface of 1.5 m × 2 m and a height of 5 m. The water level is approx. 4.50 m.

Passive decay heat removal during shutdown

E.F. Hicken
Institute for Safety Research and Reactor Technology,
Forschungszentrum Jülich, Germany

H. Jaegers
Institute for Safety Research and Reactor Technology,
Forschungszentrum Jülich, Germany

Abstract. During shutdown the decay heat in commercial Boiling Water Reactors is removed from the core region by active and redundant pump/heat exchanger–systems which are, in addition, supported by emergency power. To study the capability of the newly developed emergency condensers to remove energy produced within the core region to a large water pool outside the Reactor Pressure Vessel by natural convection, a related test in the NOKO facility as performed. The pressure vessel in the NOKO facility has been flooded above the inlet line to the emergency condenser and heated up to about 100°C. The natural circulation resulted in a cool down of the water within the pressure vessel. With two specially designed grids equipped with up to 12 thermocouples the temperature fields in two cross sections were measured; no plume-effect was identified. The vertical temperature profile was measured with thermocouples. The test showed that decay heat could be removed some time after scram to an outside pool by natural convection processes; the time after scram depends on the emergency condenser heat exchange area.

1. INTRODUCTION

It is well known that also after scram decay heat in the range of 30 to 40 MW for a LWR with 1000-1300 MW(e) is produced within the reactor core. To avoid an evaporation of fluid active and redundant heat removal systems are mandatory; usually diesel generators are installed, in addition, to maintain the heat removal capability also in case of the Loss-Of-Outside-Power (LOOP).

The SWR 1000 is equipped with emergency condensers for the removal of decay heat mainly for transients without loss of coolant; for loss-of-coolant accidents these condensers will assist the decay heat removal for some time.

These emergency condensers do not need any power and no valves are needed to start the operation; they are "passive" by definition. Therefore, a test should be performed to evaluate the capability of these condensers to remove heat produced in the core region to the outside pool by natural convection and, in addition, at ambient pressure, as it will be during long term shutdown.

Although the removal of the decay heat cannot be expected from the beginning it would be beneficial if the decay heat could be removed after some time. This capability would then be diverse to the active heat removal systems.

2. THE CONFIGURATION IN THE NOKO FACILITY AND INSTRUMENTATION

In Fig. 1 the configuration in the NOKO facility is shown; for more details about the facility and the effectiveness of the emergency condensers see [1], [2] and [3]; three tubes from the emergency condenser were used. At distances of about 1000 mm thermocouples were installed along the height of the vessel using existing flanges, see Fig. 2.

At two positions, 800 mm and 2000 mm above the return line, see Fig. 1, special grids equipped with up to 12 thermocouples were installed. The position of the thermocouples is

shown in Fig. 3; in Fig. 4 a photo of this grid is shown. The objective was the evaluation if cold or hot water plumes would develop inside the vessel.

The flooding of the reactor vessel to a level above the upper line of the emergency condensers is mandatory.

Before the start of the test the fluid in the pressure vessel was heated up to a – uniform – temperature of about 100°C while the condenser tank was at a temperature of about 30°C.
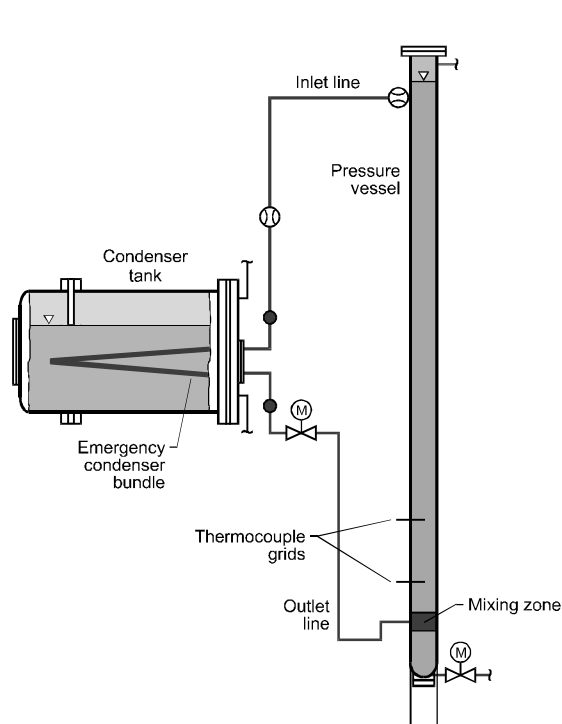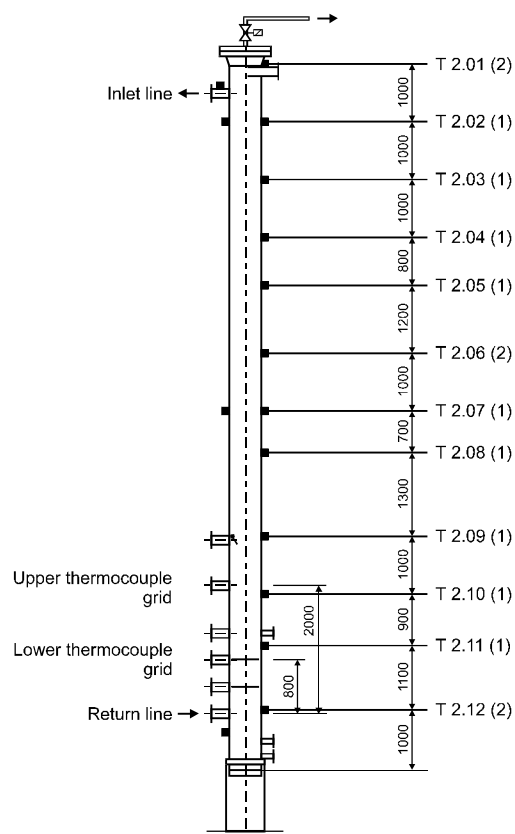

FIG. 1. The configuration in the NOKO-test facility.

FIG. 2. Pressure vessel with instrumentation.
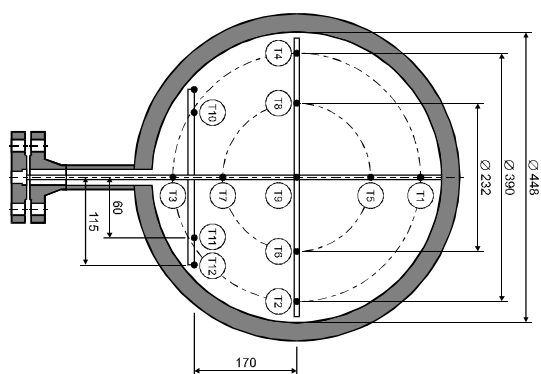
Fig. 3. Thermocouple grid.
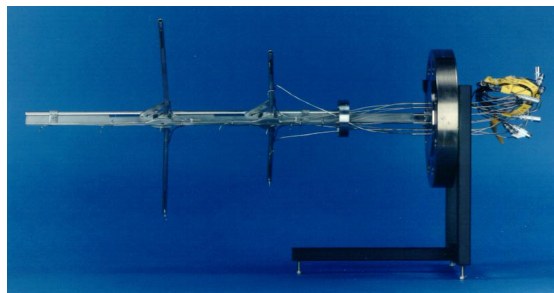
Fig. 4. Photo of the thermocouple grid.

3. TEST RESULTS

The test was started by opening the valve in the outlet line, see Fig. 1.

The outlet line has an inner diameter of 65 mm. The velocity of the fluid entering the pressure vessel (inner diameter 448 mm) is about 0.2–0.3 m/s at the beginning. Analysing the thermocouple readings a mixing zone of about 70-100 mm in the lower part of the vessel can be evaluated; this is plausible. From the temperature distribution at the highest level (T2.02) it can be concluded that the length of the mixing zone did not change along the height of the vessel.

The two special grids have been installed to evaluate the possibilities of plumes. Fig. 5 and 6 show the temperature deviations from the mean temperature for the lower and upper grid, resp. With the exception of time period during which the mixing zone passes the grid the deviations are about ≤ 0.2 K.

In Fig. 7 the temperature curves measured with the thermocouples are given. In Fig. 8 the time when the mixture zone passes a level is shown. Differentiating the curve (spline-approximation) given in Fig. 8 with time results in the velocity inside the pressure vessel, see Fig. 9. Multiplying the velocity with the density ($\rho = 981$ kg/m³) and the cross section area of the pressure vessel (0.158 m²) result in the mass flow $\dot{M}$.

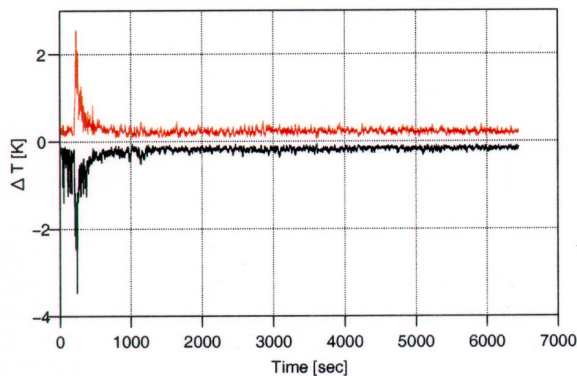The vertical temperature profiles are given in Fig. 10.

FIG. 5. Temperature deviations from the mean temperature for the lower grid.
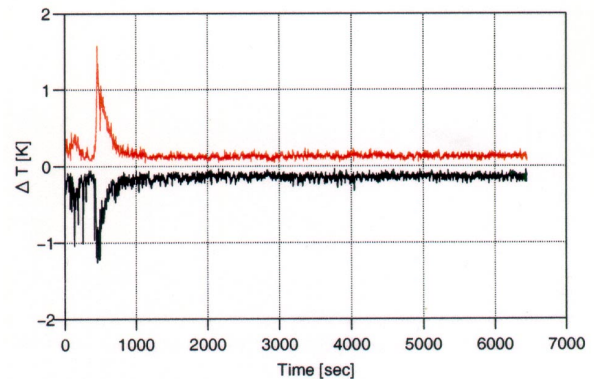

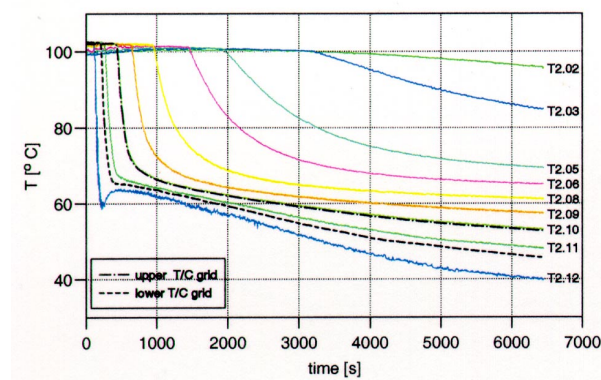FIG. 6. Temperature deviations from the mean temperature for the upper grid.

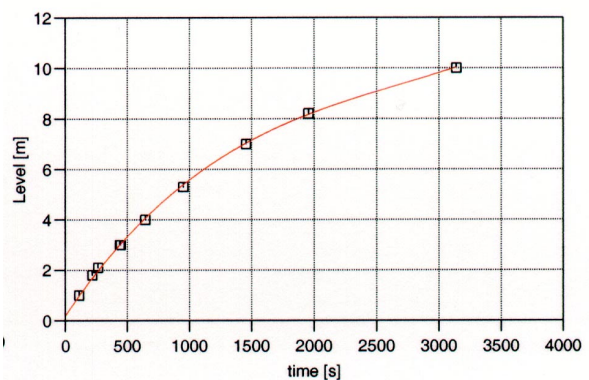FIG. 7. Temperature profile in the pressure vessel.

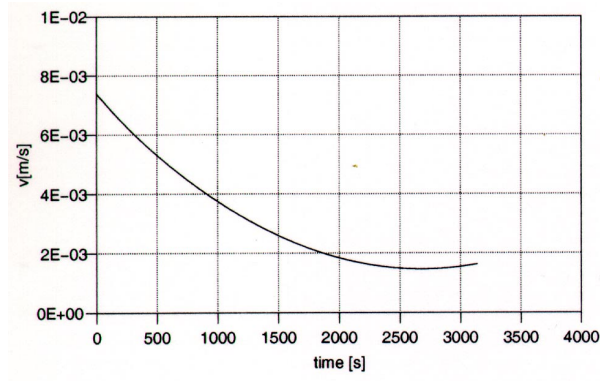FIG. 8. Time to pass for the mixture zone through the pressure vessel.

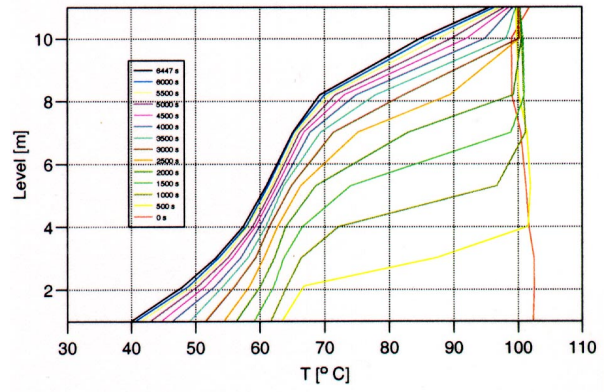FIG. 9. Velocity of the mixture zone in the pressure vessel.

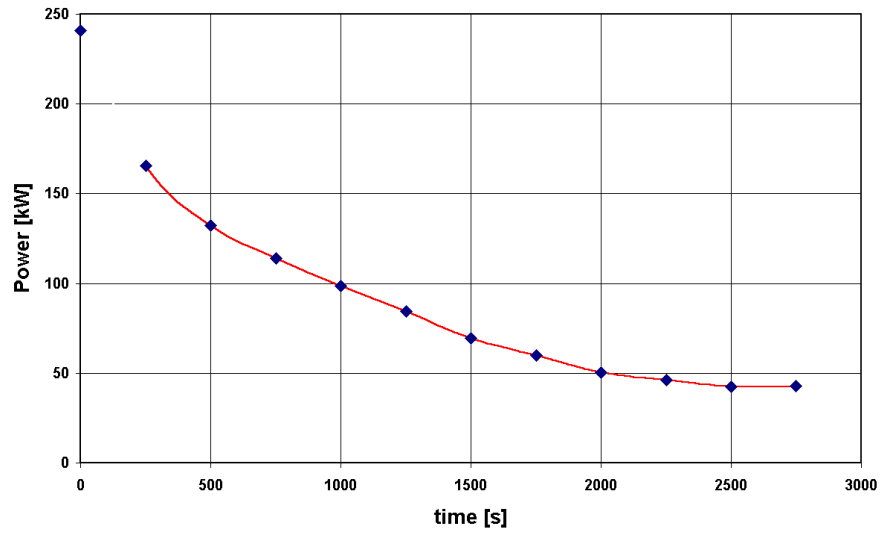FIG. 10. Vertical temperature profiles in the pressure vessel.

FIG. 11. The energy transferred by the emergency condenser.

The energy transferred from the vessel to the condenser part can be calculated from the mass flow $\dot{M}$ and the difference between the inlet and outlet enthalpies of the condenser

$$L_I = \dot{M}\left(h_{in} - h_{out}\right).$$

In Fig. 11 the transferred energy is shown. At the beginning of the natural circulation the transferred power is about 180 kW.

4. APPLICATION TO POWER PLANTS

The SWR 1000 (about 3000 MW_{th}) from SIEMENS is equipped with emergency condensers.

With the assumptions

-   same flow resistances as in the SWR 1000
-   200 tubes with the same material and geometries as used in NOKO

242

- temperature in the Reactor Pressure Vessel about 100 C
- temperature of the outside pool 30°C

a total power of about 12 MW could be transferred.

This corresponds to a decay heat at about two days after scram.

A change in flow resistances, number of tubes and pool temperature would change the amount of energy transferred but not the mode of heat transfer.

For long periods it has to be considered that the water pool has to be cooled.

Another possibility would be to bring the Reactor Pressure Vessel to a pressure below 1 MPa and allow boiling of the water pool. Then energy would be removed from the water pool via the building condensers to a pool outside the containment.

5.   CONCLUSIONS

A test with the NOKO facility has confirmed that the Emergency Condensers as proposed for the SWR 1000 from SIEMENS can transfer decay heat produced in the core region to an outside water pool. The capacity, however, is not high enough to cope with the total amount of decay heat immediately after scram. However, after some time – depending on the actual design – this heat transfer mode is effective.

REFERENCES

[1]   A. SCHAFFRATH; H. JAEGERS: "Allgemeine Beschreibung des NOKO-Versuchsstandes", Jül-3167, Research Center Jülich, Januar 1996.
[2]   A. SCHAFFRATH: Experimentelle und analytische Untersuchungen zur Wirksamkeit des Notkondensators des SWR 600, Abschlussbericht zum Forschungsvorhaben BMBF 15 NU 09485, Ruhr-Universität Bochum, RUB ISR-01, Bochum, März 1997.
[3]   H. JAEGERS; E. HICKEN; P. DAVID; R. KOSCHMIEDER: Decay Heat Removal during Shut-down, INNO-IPSS(00)-D-2.1.9, June 2000.

LIST OF PARTICIPANTS

Ağlar, F.

Turkish Atomic Energy Agency,
Eskisehir Yolu 9. Km, 06530 Ankara, Turkey

D'Auria, F.

DIMNP - University of Pisa,
Via Diotisalvi 2, I-56100 Pisa, Italy

de Kruijf, W.J.M.

Technical University Delft, Interfaculty Reactor Institute,
Reactor Physics Department,
Mekelweg 15, NL-2629 JB Delft, Netherlands

Delmastro, D.F.

Centro Atómico Bariloche – CNEA,
8400 - S.C. Bariloche, R.N., Argentina

Dr, P.

Gesellschaft f. Anlagen- und Reaktorsicherheit (GRS) mbH,
Forschungsgelände, D-85748 Garching, Germany

Duffey, R.B.

AECL - Chalk River Laboratories,
Bldg. 600 Station 99, Chalk River, Ontario K0J 1JO, Canada

El Shehawy, I.A. Saleh

Nuclear Power Plants Authority,
P.O. Box 108 Code No. 11381 Abbassia, Cairo, Egypt

Fil, N.

EDO Gidropress, 21 Ordzhonikidze str.,
Podolsk, Moscow Region 142103, Russian Federation

Grötzbach, G.

Forschungszentrum Karlsruhe, Technik und Umwelt,
Institut für Reaktorsicherheit,
Hermann-von-Helmoltz-Platz 1,
D-76344 Eggenstein-Leopoldshafen, Germany

Hicken, E.

Forschungszentrum Jülich,
Institut für Sicherheitsforschung und Reaktortechnik,
D-52425 Jülich, Germany

Jackson, J.D.

The Manchester School of Engineering,
The University of Manchester,
Room 1, 63, 1/F, Simon Building,
Oxford Road, Manchester M13 9PL, United Kingdom

Kendall, J.M.

International Atomic Energy Agency,
P.O. Box 100, A-1400 Vienna, Austria

Kurakov, Y.A.

Department of Nuclear Reactors, MINATOM R.F.
26 Staromonetny per, Moscow 109180, Russian Federation

Meseth, J.

Siemens AG, Unternehmensbereich KWU,
Postfach 10 10 63, D-63010 Offenbach, Germany

Vihavainen, J.   Lappeenrante University of Technology,
                        Department of Energy Technology,
                        Laboratory of Nuclear Engineering,
                        P.O. Box 20, FIN-53851 Lappeenranta, Finland

Vijayan, P.K.   Bhabha Atomic Research Centre (BARC),
                        Red, Hall-7, Mumbai - 400 085, India

Žežula, L.   NRI Řež, 28068 Řež u Prahy, Czech Republic

Zhang, S.   Nuclear Power Institute of China,
                        28 South Third Section, Yiyuan Road,
                        Chengdu 610041, China